CHEMICAL REVIEWS

Review

pubs.acs.org/CR

Structures of Metal−Organic Frameworks with Rod Secondary Building Units

Alexander Schoedel,[†,‡,§] Mian Li,[∥] Dan Li,[∥,⊥] Michael O'Keeffe,[*,@] and Omar M. Yaghi[†,‡,▽]

[†]Department of Chemistry, University of California, Berkeley, California 94720, United States

[‡]Materials Sciences Division, Lawrence Berkeley National Laboratory, Kavli Energy Nanoscience Institute, Berkeley, California 94720, United States

[§]Department of Chemistry, Florida Institute of Technology, 150 West University Boulevard, Melbourne, Florida 32901, United States

[∥]Department of Chemistry, Shantou University, Guangdong 515063, P. R. China

[⊥]College of Chemistry and Materials Science, Jinan University, Guangzhou 510632, P. R. China

[@]School of Molecular Sciences, Arizona State University, Tempe, Arizona 85287, United States

[▽]King Abdulaziz City for Science and Technology, P.O Box 6086, Riyadh 11442, Saudi Arabia

Supporting Information

ABSTRACT: Rod MOFs are metal−organic frameworks in which the metal-containing secondary building units consist of infinite rods of linked metal-centered polyhedra. For such materials, we identify the points of extension, often atoms, which define the interface between the organic and inorganic components of the structure. The pattern of points of extension defines a shape such as a helix, ladder, helical ribbon, or cylinder tiling. The linkage of these shapes into a three-dimensional framework in turn defines a net characteristic of the original structure. Some scores of rod MOF structures are illustrated and deconstructed into their underlying nets in this way. Crystallographic data for all nets in their maximum symmetry embeddings are provided.

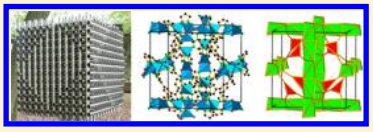

CONTENTS

Received: June 6, 2016

DOI: 10.1021/acs.chemrev.6b00346
Chem. Rev. XXXX, XXX, XXX−XXX

1. INTRODUCTION

Nothing exists except atoms and empty space; everything else is opinion.[1]

1.1. Metal−Organic Frameworks

Metal−organic frameworks (MOFs) are now a major subject of materials chemistry and are the topic of many thousands of papers annually because of their actual and potential applications.[2] Many also have beautiful and intricate crystal structures often quite unlike those seen before in chemistry. The essence of MOF chemistry is that frameworks are assembled by linking molecular units of well-defined shapes by strong bonds into periodic frameworks. The theory and practice of this is the discipline of reticular chemistry.[3] An important component of reticular chemistry is the deconstruction of such structures into their underlying nets (framework topology) to facilitate designed synthesis of materials with targeted porosity, pore size, and functionality.[4]

MOFs are composed of two or more secondary building units (SBUs). These are of two general types: (a) metal-containing units that range from having single metal atoms to infinite groups (rods and layers) and (b) polytopic organic linkers that may themselves incorporate metal atoms (as in a porphyrin). The metal-containing SBUs are most commonly finite units with points of extension (points at which they are joined to the linkers) forming a well-defined geometrical shape such as a square or an octahedron. These shapes are joined by polytopic linkers into periodic frameworks. The deconstruction of such structures containing branched polytopic linkers into underlying nets and the nature of those nets was the topic of a recent review.[5]

In some MOFs, there are finite metal-containing SBUs in which, for example, metal−oxygen polyhedra are linked into rings. There is however a second major class of MOFs in which the metal-containing SBUs are infinite in one dimension.[6] Such SBUs are generally referred to as rods, and it is with the description and deconstruction of the structures of MOFs containing them (rod MOFs) this review is concerned. It is emphasized that the topic is methods of deconstruction of structures and not an exhaustive catalog of rod MOFs themselves. Rod MOFs have attracted considerable attention because of their potentially valuable properties to gas storage, separations, and catalysis, and we note that compilations of theoretical materials[7−18] have started to include rod MOFs recently,[7,12,18] following intensive effort made on those with finite SBUs.[7−17]

1.2. Crystal Nets

Crystal nets are special kinds of graphs. The graphs are simple; the edges are undirected and there are no loops (edges that begin and end on the same vertex) or multiple edges between a pair of vertices. Also, they are connected; there is a continuous path of edges between every pair of vertices. The nets we will be concerned with are crystallographic: they have an automorphism group (the group of permutations of vertices that leaves the connectivity pattern of the graph unchanged) that is isomorphous with a crystallographic space group.[19] This space group is the maximum possible symmetry of a realization (i.e., embedding) of the net, and we refer to it here simply as the symmetry of the net.

It is useful to distinguish between the abstract graph, which consists of vertices and edges, and an embedding. In an embedding (sometimes called a realization) the vertices of the abstract graph are assigned coordinates and now referred to as links or branch points. Edges are now referred to as nodes. This distinction is necessary as, for example, we sometimes want to refer to the length of a link, but an edge of an abstract graph obviously cannot have a "length". In an embedding of a crystallographic graph, a unit cell is assigned, usually of the maximum possible symmetry, and the nodes have coordinates usually chosen for unit link length and for minimum density subject to that constraint. Embeddings of nets of interest to crystal chemistry are collected in a searchable database, the Reticular Chemistry Structure Resource (RCSR).[20] There they are assigned symbols, generally three letters lower case bold as **xyz**. The symbols may have extension as in **xyz-a**. The extension **−a** refers to the augmented net in which the original vertices are replaced by the vertex figure (coordination figure) which will be a simple shape such as a square or octahedron. Note that one can only identify a vertex figure for an embedded net (not for a graph). The reader is warned that unfortunately one sometimes finds three-letter symbols or three-letter plus number symbols that are not RCSR symbols in papers. Sometimes RCSR symbols are given incorrectly in italics.

If a net has just one topological type of vertex (edge), it is said to be vertex (edge)-transitive. In a maximum-symmetry embedding of a vertex (edge)-transitive net, all nodes (links) are related by symmetry. More generally, a graph has a transitivity p q, which says that there are p topological kinds of vertex and q kinds of edge.

We use the notation k-c for a vertex that has k edges incident on that vertex. It is common to refer to such a vertex as k-connected, but we try to avoid that term as connectivity has a

DOI: 10.1021/acs.chemrev.6b00346
Chem. Rev. XXXX, XXX, XXX−XXX

meaning quite distinct from coordination in graph theory. In nets with mixed coordination k_1, k_2, ..., we use the notation (k_1, k_2, ...)-c to describe the net.

We proposed a principle of minimal transitivity, which states that the transitivity of the underlying nets of crystal structures is usually (there are exceptions) the minimum possible consistent with the number and structure of the SBUs.[5] We find this principle also holds generally for rod MOFs. The most important nets in MOF chemistry are edge transitive (transitivity 1 1 or 2 1). An account of these and their importance to designed synthesis has been given.[21]

1.3. SBUs, Points of Extension, and Deconstructing Rod MOFs

A commonly used metal SBU is the $Cu_2(-COO)_4$ cluster (paddle wheel) that appears in copper acetate. The four carboxylate carbon atoms are the points of linking to the organic linker (the points of extension), for example, the tritopic trimesate (1,3,5-benzene tricarboxylate = BTC) in the MOF HKUST-1 (Figure 1).[22] The carboxylate C atoms are at the

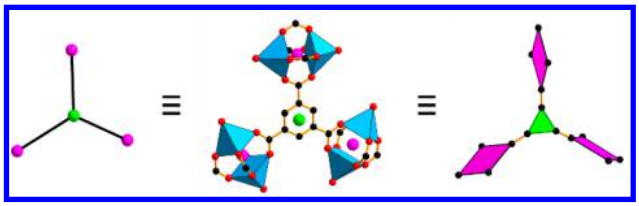

Figure 1. Center: the linker in HKUST-1 joined to three $Cu_2(-COO)_4$ paddle wheel SBUs.[22] Left: the 3-c (green) and 4-c (magenta) nodes of the underlying net. Right: A fragment of the augmented net with nodes at the points of extension. Color code: black, C; red, O; blue polyhedra, metal.

vertices of a square, so we consider the SBU to correspond to a square 4-c node at the center. Likewise, we consider the BTC to correspond to a 3-c node as shown. The resulting (3,4)-c net is **tbo**. To illustrate the net, it is informative to use the augmented net, **tbo-a**, in which the nodes are replaced by their coordination figures (in this case squares and triangles). Note that the points of extension of the metal SBU correspond to nodes in the augmented net. The augmented net directly illustrates the shapes that are linked.

A metal SBU consists of groups of metal atoms (M) joined to one or more other metal atoms in the same SBU either by M-X-M links (here X is a non metal such as N or O) or through a common point of extension (for example by M−O−C−O−M carboxylate). In the MOFs of this paper, metal atoms are thus linked into infinite rods.

There is a large family of isoreticular (having the same underlying net) rod MOFs generally known as MOF-71,[6] MIL-47,[23] and MIL-53.[24] We use the structure of MOF-71 with rod of composition $[Co_2O(-COO)_4]_\infty$ to illustrate how simple rod MOF structures are deconstructed (Figure 2). Note that now we keep the pattern of points of extension (carboxylate C atoms in this case) as defining the shape of the metal SBU. In these MOFs, the linker is ditopic, in MOF-71 terephthalate = 1,4 benzenedicarboxylate (BDC), so we link these shapes, zigzag ladders, by single linkers into a 3-periodic network. The net in this case has RCSR symbol **sra** and is shown in Figure 2. This procedure is very like using the augmented net in the example of a finite SBU. Now however there is no "un-augmented" version as the rod pattern does not have a well-defined center point. So, when possible, with rod SBUs linked by ditopic linkers,

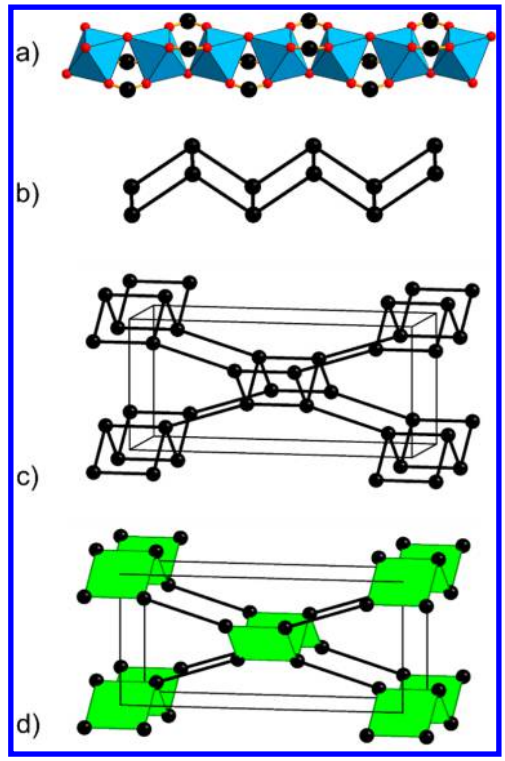

Figure 2. (a) One rod of MOF-71 of composition $[Co_2O(-COO)_4]_\infty$;[6] (b) the points of extension forming a zigzag ladder; (c) the linkage of the ladders in the crystal structure forming the **sra** net; and (d) the same net with the ladder colored. Color code: black, C; red, O; blue polyhedra, metal.

we define the underlying net to be the pattern of rod SBU points of extension joined together and then linked into a 3-periodic network.

A similar structure is found in a chromium azolate.[25] The rod has composition $[Cr_2O(\text{-}TZ)_4]_\infty$, here TZ stands for tetrazolate with a CN_4 ring (Figure 3). We could take the tetrazole C atoms

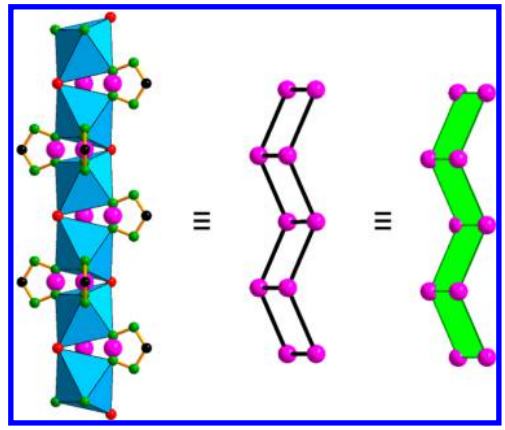

Figure 3. Zigzag ladder of formula $[Cr_2O(\text{-}TZ)_4]_\infty$, and its simplification.[25] Color code: black, C; red, O; green, N; blue polyhedra, metal; pink, points of extension.

as the points of extension, but it is more consistent with the previous case to take as point of extension a fictive atom located between the two N atoms that are directly bonded to the metal atom. This choice of fictive atom is helpful in considering the structures of mixed carboxylates/azolates. Their pattern of points of extension, a zigzag ladder, is similar to that in the previous

DOI: 10.1021/acs.chemrev.6b00346
Chem. Rev. XXXX, XXX, XXX−XXX

example. The linker is again ditopic (benzene ditetrazole) so one gets again the **sra** pattern as the underlying net.

The 4-c **sra** net is one of the most-commonly occurring in MOF chemistry. The symbol comes from the fact that it is the Al net in $SrAl_2$. The same topology occurs as the zeolite framework type **ABW**. Clearly a zigzag ladder rod must have at least two kinds of link (rungs and risers); there must be a third kind of link to join the rods into nets. Accordingly, the minimal transitivity for a net of linked ladders is 1 3. This is indeed the transitivity of the **sra** net.

It should be remarked that there is occasionally a very different mode of deconstructing MOF structures advocated. This is to identify the nodes of the net as the metal atoms and the centers of the linkers. This is the so-called standard representation of the program TOPOS.[26,27] But this procedure is never used in practice for MOFs with finite multimetal-atom SBUs (recall the example of HKUST-1 above).

We show here a rod that has a different, but related, ladder SBU. The compound is a Tb terephthalate and an early example of a rod MOF.[28] The carboxylate C atoms on the rod again define ladders, but now they are "twisted" (rungs not parallel) and they are linked into a different net, **irl** (Figure 4) with symmetry

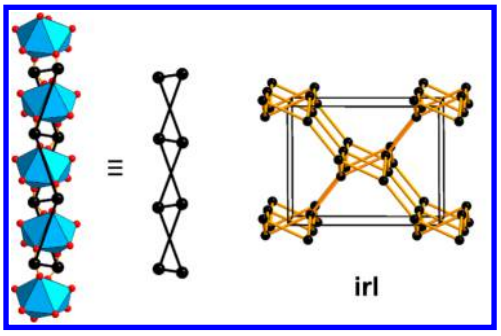

Figure 4. Twisted ladder rod SBU and the resulting **irl** topology. Color code: black, C; red, O; blue polyhedra, metal.[28]

Cmcm, but again with minimal transitivity 1 3. It is interesting that in the original paper, the rod nature of the SBU was not emphasized nor was the **irl** topology recognized. Instead the "standard representation" in which the nodes of the net were taken as the metal atoms and the centers of the linkers were used. The resulting net is the tetragonal net **pts** which in no way reflects that the salient feature of the structure is parallel rods of metal−oxygen polyhedra. Likewise, the "standard representation" of the **sra** MOFs leads to another tetragonal net **lvt** in which again there are no parallel rods of vertices. The **irl** topology was first recognized a little later in MOF-75[6] which has the same Tb rod but a different ditopic linker.

When deconstructing the structure of rod MOFs with polytopic linkers, to be consistent, one should also use the "augmented" form, specifically replacing each branch point of the linker by the coordination figure (usually a triangle, square, or tetrahedron). Figure 5 illustrates a rod MOF (UTSA-30) with tritopic linker that was recently described in this way.[29] The underlying net is **hyb**. The net must have at least two kinds of vertices, one each on the rod and the linker. Likewise, there must be at least two edges on the rod and two on the linker, so the minimal transitivity is now 2 4, which is that of **hyb**. Generally, when considering the complexity of a rod net, as measured by its transitivity, it should be compared with the augmented version of the net of a MOF composed of finite SBUs. Thus, the transitivity of **tbo-a** (the augmented net of HKUST-1) is also 2 4.

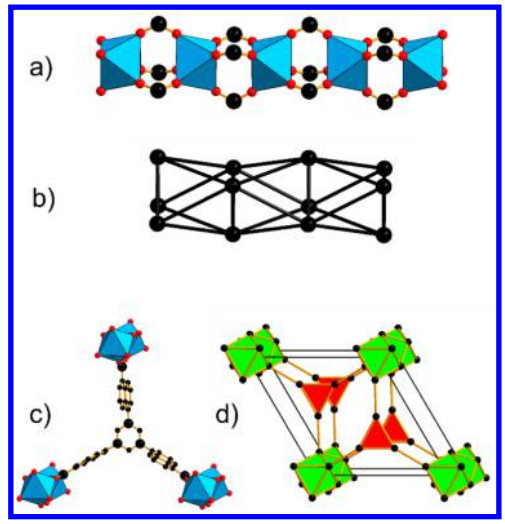

Figure 5. (a) $[Yb(-COO)_3]_\infty$ rod in UTSA-30; (b) the pattern of points of extension (carboxylate C atoms);[29] and (c) one linker in UTSA-30. The large black spheres are identified as nodes of the net; and (d) the net **hyb** formed by the nodes in (c) shown as rods of face-sharing octahedra (green) linked to triangles (red). Color code: black, C; red, O; blue polyhedra, metal.

However, some rod MOF structures have nets of considerable complexity. A striking example is the recently reported structure of the chemically simple bismuth trimesate.[30] This MOF has rod SBUs that are in themselves the same topologically but are linked into a structure of unprecedented topological complexity (section 13.2): the net has transitivity 54 135. Indeed, this rod MOF is a rare example in which the rods of the crystal structure are not related by symmetry.

We recognize that, in some instances at least, the choice of location of points of extension is arbitrary (it may not be at an atom site). Further, the choice of links between these points of extension may also not be obvious. Thus, an inevitable element of subjectivity enters; see the quotation at the beginning of this review. But this ambiguity is part of the fabric of structural chemistry: people can, and often do, argue about such matters as the very existence of a bond between a pair of atoms or about the appropriate description of a coordination polyhedron.[31,32] We return to this topic in section 14.

Some further examples of assignment of points of extension are given here. In tetrazolates with three or four N atoms linked to metals, we use a fictive atom at the center of the group of three (see e.g., Figure 10). For phenolic −OH, we take the C atom to which it is joined (e.g., the MOF-74 related compounds of section 13.2). For pairs of such −OH on adjacent C atoms, we take a fictive atom between that pair as for MOF-910 (Figure 66). For three adjacent −OH, we take a fictive atom between the three C atoms as in pyrogallate (Figure 26). For phosphonate/sulfonate, points of extension are P/S atoms (Figure 10, top; Figures 34, 53, and 58). For pyridine, we take the N atom in the ring (Figure 10, bottom).

The analysis of rod MOFs sometimes leads to underlying topologies that are quite complicated and would not serve the purpose of RCSR. The database contains mainly structures of interest for designing new materials as well as structures of special interest to the theory of periodic graphs and tilings. This in turn means that only simple structures can be added that are, in principle, amenable to reticular chemistry.[3] Nevertheless, some frameworks, SBUs, or topologies that we have encountered are worth describing even if they most likely remain isolated

DOI: 10.1021/acs.chemrev.6b00346
Chem. Rev. XXXX, XXX, XXX−XXX

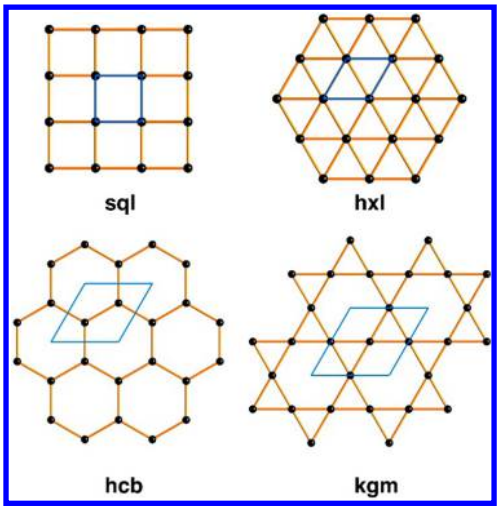

Figure 6. Invariant 2-periodic patterns.

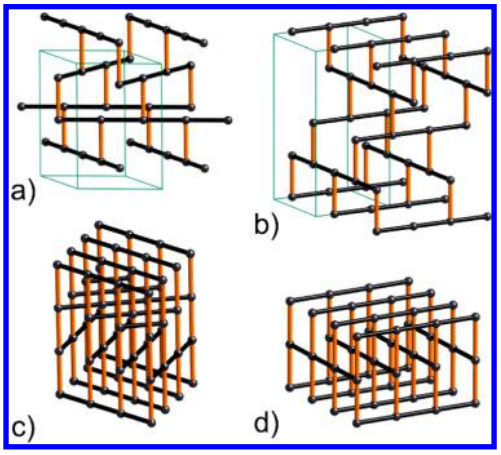

Figure 7. Nets illustrating the invariant rod patterns with rod axes in parallel layers. The nets and symmetries are (a) **bto-z**, $P6_222$ (b) **ths-z**, $I4_1/amd$, (c) **qzd**, $P6_222$, and (d) **cds**, $P4_2/mmc$.

examples. In this review, we therefore decided to name them rod nets, together with a unique number (e.g., **rn-1**). The maximum symmetry embedding of such nets, as Systre output files,[33] can be found in the Supporting Information.

1.4. Cylinder and Sphere Packings

Sphere packings play a central role in descriptive crystal chemistry. We refer specifically to packings of spheres of equal diameter. Periodic structures of this sort have nets with embeddings in which the links (defined by sphere contacts) are all of equal length and are the shortest distances between nodes. The basic uninodal and binodal nets of prime importance in describing the topology of MOFs with finite SBUs are nearly all sphere-packing nets.

The importance of rod structures in crystal chemistry was described some time ago.[34,35] The most symmetrical rods are cylinders, and the structures of periodic packings of symmetry-related cylinders are of relevance to crystal chemistry (just as are sphere packings). The most important, but perhaps the most difficult to appreciate, are those with cubic symmetry and these have been systematically enumerated.[36−38] Of more interest (so far!) to MOF chemistry are the invariant cylinder packings. In these structures, the positions of the cylinder axes are fixed by symmetry. There are 14 of them and their structures and symmetries have been described.[6]

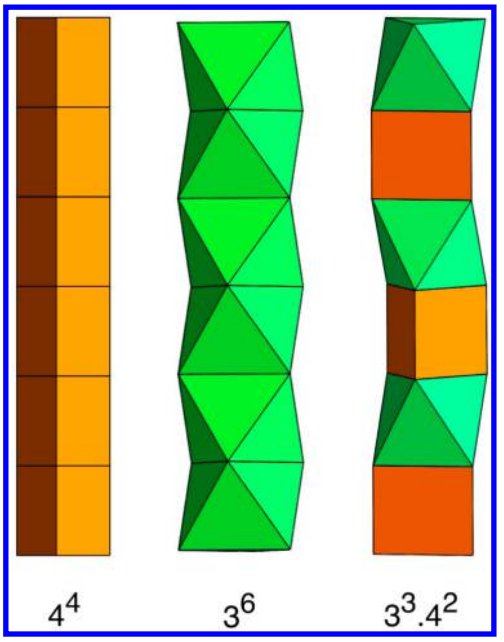

Figure 8. Examples of rods that are cylinder tilings.

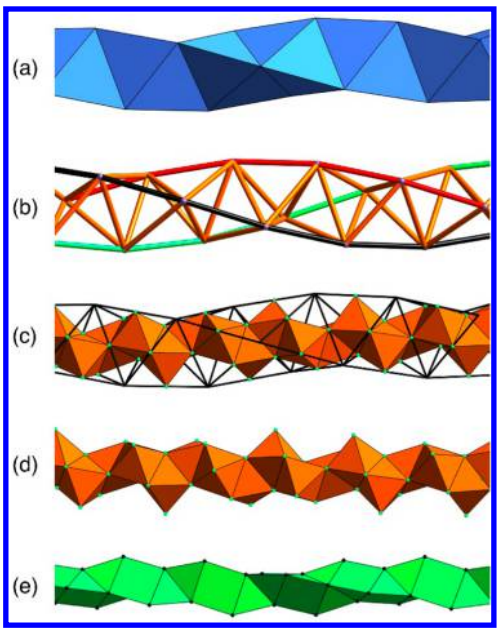

Figure 9. (a) Boerdijk-Coxeter (BC) helix as a rod of face-sharing tetrahedra; (b) the same showing the triple helix; (c) the pattern of the point at the mid points of the edges of the BC helix; (d) the same as a rod of face-sharing octahedra, the Lidin-Andersson (LA) helix; and (e) the rod of face-sharing square pyramids obtained by removing the outer vertices of the LA helix.

Structures with rods all parallel are easiest to visualize and are most common in rod MOFs. The rod axes intersect a perpendicular plane in a pattern of the nodes of a 2-periodic net. By far the most important are three of the four invariant structures: the square lattice, **sql**, the hexagonal lattice, **hxl**, and the honeycomb pattern, **hcb**. The fourth (least commonly occurring) is the kagomé pattern, **kgm** (Figure 6). Indeed we know of only two examples of rod MOFs with parallel rods in which the rod pattern is not one of these four invariant structures. In these, parallel rods intersect the plane in a uninodal 2-periodic pattern $3^2.4.3.4$ (**tts**) (section 10) or 3.4.6.4 (**htb**) (section 13.2).

DOI: 10.1021/acs.chemrev.6b00346
Chem. Rev. XXXX, XXX, XXX−XXX

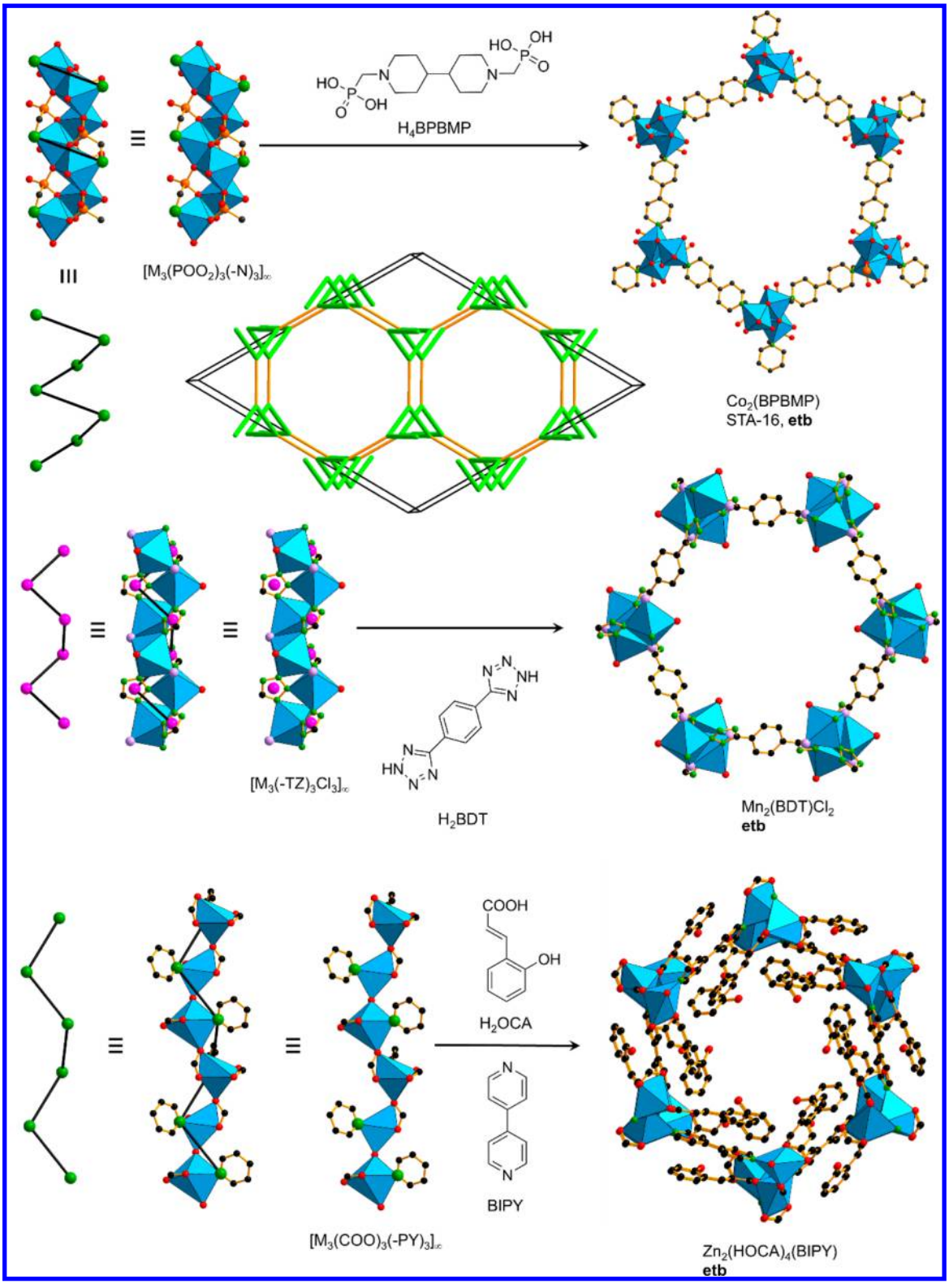

Figure 10. MOFs, showing **etb** topology, formed by rod, simple helical SBUs. Each node, marked as a large sphere, is 3-c, with 2 coordination within the trifold helix and one to the linker.[88−90] Color code: black, C; red, O; green, N; orange, P; lavender, Cl; blue polyhedra, metal; pink, points of extension.

Structures with nonparallel rods in parallel layers also occur, and invariant rod patterns are briefly described here. There are four: two with hexagonal symmetry (both $P6_222$ or $P6_422$) and two with tetragonal symmetry ($P4_2/mmc$ and $I4_1/amd$). They can be illustrated by the structures of common nets: two 3-c and two 4-c. They are shown in Figure 7. So far we have only recognized the tetragonal patterns in rod MOFs.

We know of just one example of rod MOFs with a cubic 3-way pattern (Section 4.3).[39] It is easy to see why they are rare. The crystal dimensions are completely determined by the

DOI: 10.1021/acs.chemrev.6b00346
Chem. Rev. XXXX, XXX, XXX−XXX

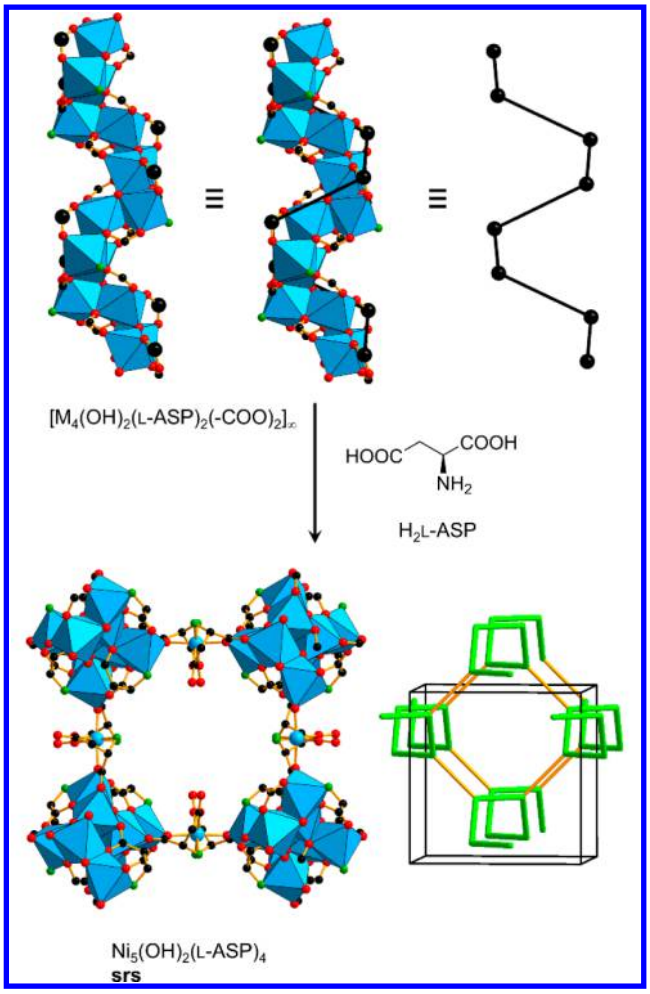

Figure 11. Rod of $Ni_5(OH)_2(L\text{-}ASP)_4$ consists of a chiral 4-fold helix that, when combined with a ditopic metallo-linker $[Ni(L\text{-}ASP)_2]^{2-}$, produces a 3-c **srs** topology net.[93] Color code: black, C; red, O; green, N; blue polyhedra, metal.

periodicity of the rods, so the linker must have exactly the right dimensions to fit.

1.5. Some Simple Rods

The simplest periodic rod is just equally spaced points on a straight line. Simple variations of this are helices. The crystallographic restriction in three dimension limits helices to those of type 2_1 (better called a zigzag), and the enantiomorphous pairs 3_1 and 3_2, 4_1 and 4_3, and 6_1 and 6_5. In one dimension there is no crystallographic restriction and any order of rotation or screw axes is allowed for the rod. In Section 10, we describe rods with 5_1 and 5_4 axes. Of course in such 3-periodic structures the symmetries act only on the rod, not the crystal as a whole.[40]

Next in complexity are ladders.[41] Their shapes are determined by the manner of linkage into a 3-periodic net. The two most common are zigzag ladders (already seen in Figure 2) and twisted ladders (Figure 4).

Many of the rods we meet in deconstructing rod MOF structures can be described as rods of polyhedra sharing edges or faces. Most of these are easy to visualize and have been described in a systematic account of 1-periodic sphere packings.[42] Perhaps most common are (a) rods of octahedra, (or more generally antiprisms) sharing opposite faces (3^6 cylinder tiling), (b) rods of trigonal prisms (or prisms in general) sharing opposite faces

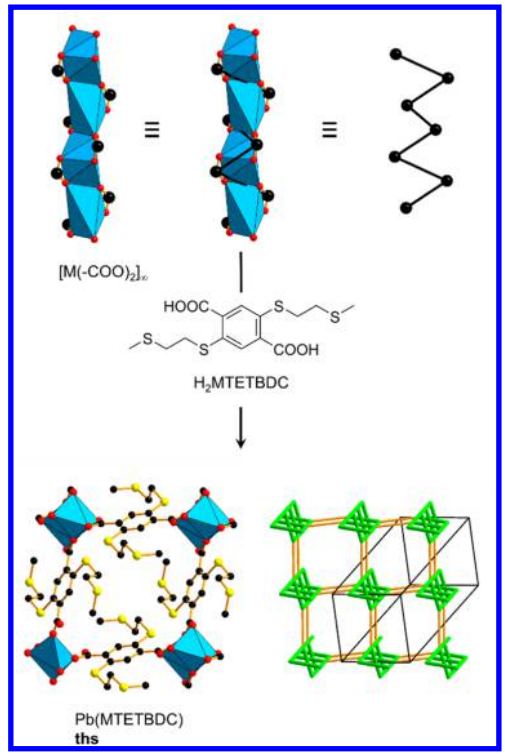

Figure 12. Single crystal structure of Pb(MTETBDC). The 4-fold helices form an overall **ths** net.[96] Color code: black, C; red, O; yellow, S; blue polyhedra, metal.

(4^4 cylinder tiling), and (c) alternating octahedra and trigonal prisms (prisms and antiprisms) sharing opposite faces ($3^3.4^2$ cylinder tiling). These are illustrated in Figure 8.

There are two special structures that we meet that are worth mentioning. The first is formed by a rod of face-sharing tetrahedra, Figure 9. The structure is chiral and, if the tetrahedra are regular, aperiodic. It is generally known as the Boerdijk-Coxeter (BC) helix or the Bernal spiral after early describers[43,44] and arises in several different contexts in chemistry.[45−52] It is a special case, symbol (1,2,3), of the 3^6 tilings of a cylinder by equilateral triangles described in detail some time ago.[53] The dual structures are those of single-wall carbon nanotubes whose structures and symmetries are well documented.[54]

A second structure we call the Lidin-Andersson (LA) helix after its early describers.[48] This is a rod of face-sharing octahedra and is similarly aperiodic for regular polyhedra. It was noted by Lord[50] that the centers of the edges of a regular tetrahedron define a regular octahedron and the centers of the edges of the BC helix define the LA helix. As there are three kinds of edge on the BC helix, there are three kinds of vertices in the LA helix with vertex symbols 3^4, 3^6, and 3^8.

It appears that all chiral 3^6 cylinder tilings with equilateral triangles (deltahedra) are aperiodic so that periodic nets derived by linking such structures cannot be made with equal edges. We note here that the rods in the extraordinary bismuth trimesate (CAU-17)[30] referred to above have points of extension in the LA helix.

Removing the outer points of the LA helix leaves a rod of square pyramids sharing triangular faces as shown in the figure. Now there are two kinds of vertices: 3.4.3.4 and $3^2.4.3^2.4$. We identify this rod in the structure of MOF-74 which is perhaps the most-important rod MOF (certainly the most-studied).[55−67]

DOI: 10.1021/acs.chemrev.6b00346
Chem. Rev. XXXX, XXX, XXX−XXX

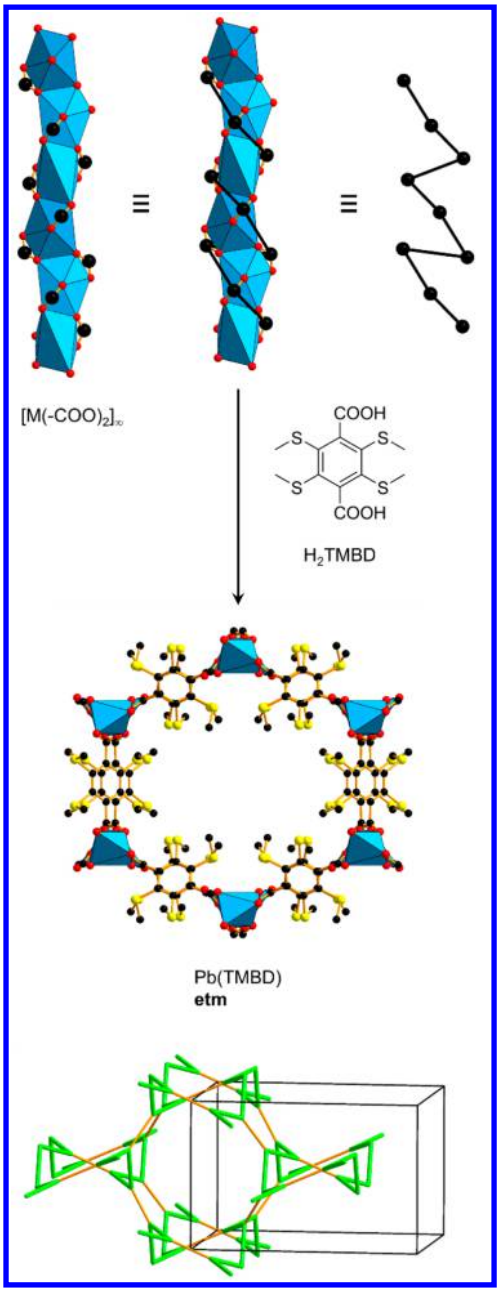

Figure 13. Single crystal structure of Pb(TMBD) that shows an underlying **etm** topology net.[97] Color code: black, C; red, O; yellow, S; blue polyhedra, metal.

The vertices of the BC helix lie on a cylinder. For unit edge, the radius of the cylinder is $1/\sqrt{10}$ and one vertex is related to the next by translation $3\sqrt{3}/10$ and rotation by $\cos^{-1}(-2/3)$ = 131.8°. This angle is not a rational fraction of 360°, so the helix is aperiodic. However, a small change in the rotation angle to (3/8)360° = 135° gives a periodic structure, now with unequal edges, with 8 vertices in the repeat unit related by an 8_3 screw axis.[68] The rod symmetry is $\mathbf{p}8_322$ (or $\mathbf{p}8_522$ depending on the sense of the rotation). Here **p** is the symbol for the one-dimensional lattice. 8-Fold symmetry is not possible in a 3-periodic structure, and in nets based on the BC helix, the rods have $\mathbf{p}4_322$ (or have $\mathbf{p}4_122$) symmetry. The same rods also occur in the structure of β-Mn,[47] in which the local 8-fold symmetry was explicitly recognized.[69]

In the LA helix, there are three kinds of vertices and 8-fold rod symmetry is not possible. Vertices of each kind are again related

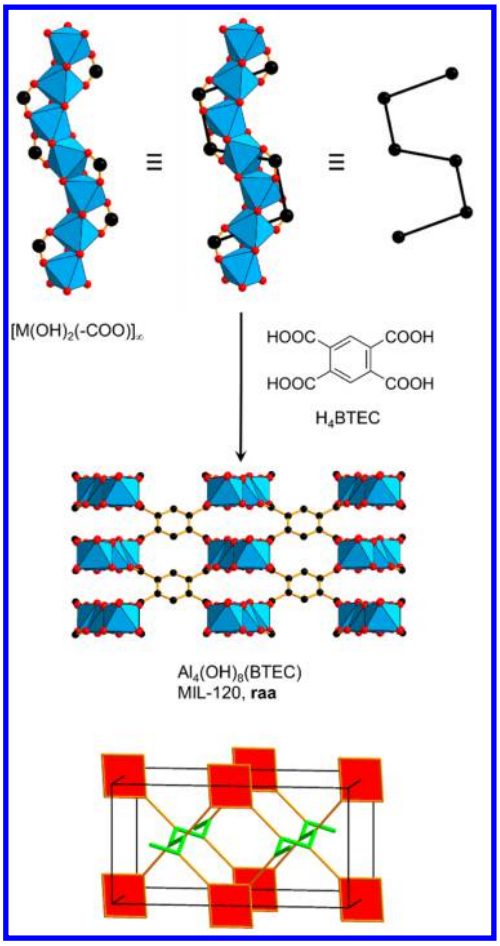

Figure 14. Single crystal structure of $Al_4(OH)_8(BTEC)$, MIL-120. The helical rod SBUs are connected by tetratopic organic linkers yielding a (3,4)-c **raa** net.[100] Color code: black, C; red, O; blue polyhedra, metal.

by 131.8° rotations, and the simplest periodic approximation is to distort to 120° rotation which results in rods with $\mathbf{p}3_12$ or $\mathbf{p}3_22$ symmetry. All the nets in this work based on the LA helix or on its diminished form are indeed trigonal with chiral rods.

1.6. Special Properties of Rod MOFs: Breathing and Forbidden Catenation

Although this review is concerned with structure rather than properties, we would be remiss if we fail to mention two properties of rod MOFs that are intimately related to their structures. These were both noted in the earliest rod MOF papers.

The first is "forbidden catenation". This term was first applied at the outset of rod-MOF chemistry.[70] It means that for rod MOFs, no matter how large the pores, there can be no multiple intergrowths of the same structure. This simply results from the fact that the periodicity along the rods is at most a few ångströms, generally insufficient to allow intercalation of a second copy of the structure. This property has recently been used to make a large suite of isoreticular rod MOFs with pore diameters ranging from 14 to 98 Å.[71] For a rare example of interpenetration (catenation) in a rod MOF see section 13.1.

The second property that has been the subject of considerable interest is that rod MOFs, particularly of the MIL-53[24] types, is that they have flexible frameworks and can "breathe" (change volume) with uptake or desorption of guests. This property has been the subject of considerable theoretical study.[72−86] It should be remarked, however, that not all rod MOF structures breathe,

DOI: 10.1021/acs.chemrev.6b00346
Chem. Rev. XXXX, XXX, XXX−XXX

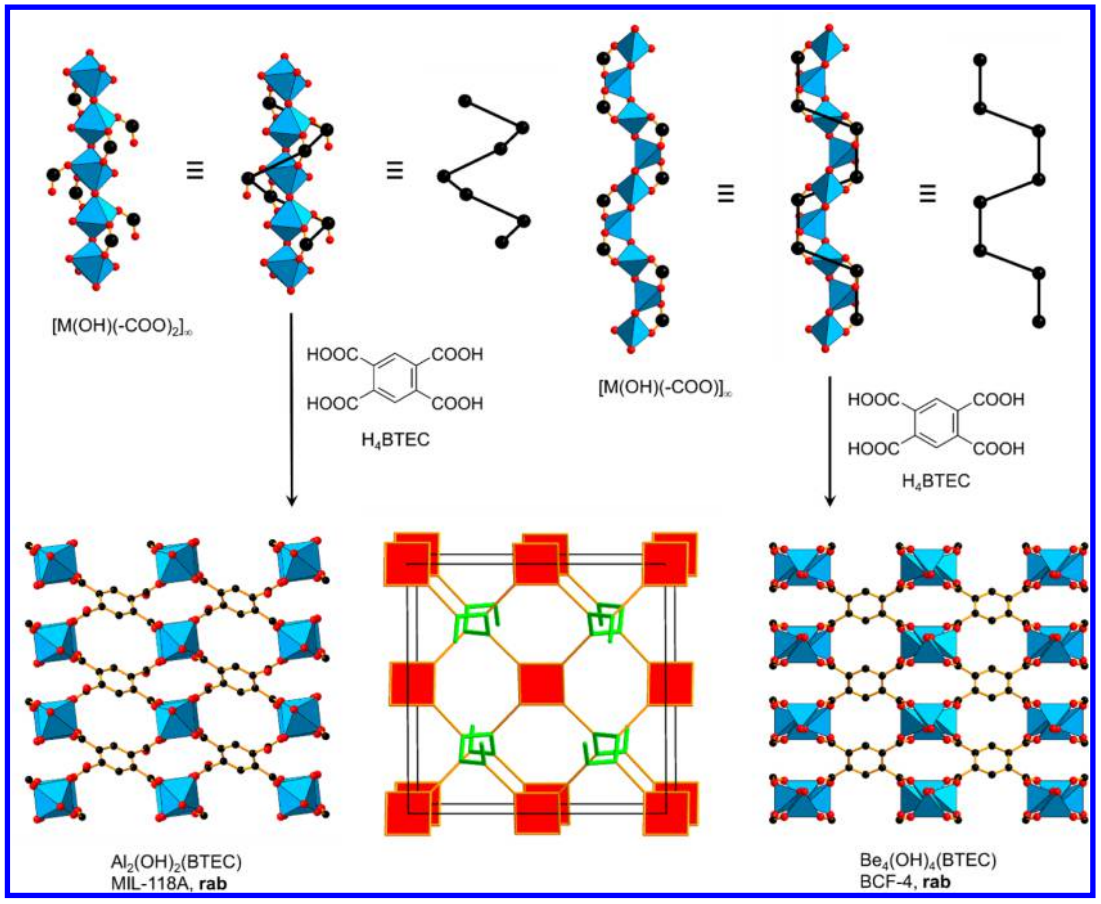

Figure 15. Two structurally different MOFs that show an underlying **rab** net topology. The 4-fold helices are connected through tetratopic linkers.[101,102] Color code: black, C; red, O; blue polyhedra, metal.

and some breathing structures are not rod MOFs. A recent paper has shown that the flexibility of a framework is determined by its topology, an important factor in theoretical studies of the properties of hypothetical MOFs.[87]

2. MOFS WITH SIMPLE HELICAL SBUS

We herein describe MOFs that have rod SBUs that can be deconstructed to simple helices. Such helices can be further linked into 3-dimensional MOFs through either ditopic or polytopic linkers and contain many early examples of rod MOFs. For each topology, we highlight just one or two examples. Nodes in helical SBUs are regularly 3-c, where 2-c are within the SBU and one coordination is provided to the linker.

2.1. MOFs with Simple Helical SBUs and Ditopic Linkers

A long-known and large group of MOFs are those with structures based on the **etb** topology, a deconstruction that was initially also applied to the popular MOF-74 structure.[6] However, from our perspective, there are more appropriate ways to describe this particular structure, which we detail in section 13.2. In general, there are only two ways of linking trifold helices with one kind of vertex: all helices are of same hand to give **eta** nets, or of a different hand to give **etb** with symmetry $R\bar{3}m$. The latter is a 3-c net with transitivity 1 2. The MOFs with **etb** topology are therefore all composed of ditopic linkers with a diversity of coordinating groups, including but not limited to phosphonates,[88] azolates,[89] and pyridines[90] (Figure 10).

An isoreticular (same net topology) class of phosphonate MOFs were first explored in 2006 and are composed of $[M_3(PO_2)_3(\text{-}N)_3]_\infty$ SBUs, where the metal cations are octahedrally coordinated by phosphonate O and nitrogen moieties of the central piperidine.[91] The latter also serves as the points of extension to the neighboring rods to form an overall framework with hexagonal channels. An isostructural compound was later developed for the adsorption of fuel-related gases and has been termed Ni-STA-12 (STA: St. Andrews porous material).[92] Isostructural MOFs containing Fe and Co were also reported.[91] Reticular chemistry has then enabled the expansion of this structure by introducing a longer linker H_4BPBMP (H_4BPBMP = *N*,*N*′-4,4′-bipiperidinebis(methylenephosphonic) acid) to produce STA-16, Co_2(BPBMP) (Figure 10, top).[88]

Another structure with **etb** topology is provided by the TZ containing linker BDT [H_2BDT = 5,5′-(1,4-phenylene)bis-(1*H*-tetrazole)] that links a $[M_3(\text{-}TZ)_3Cl_3]_\infty$ SBU into a 3-dimensional framework.[89] The SBU is composed of octahedrally coordinated metal cations, and the points of extension are selected as the centers of the tridentate TZ moieties. We have inserted pseudoatoms at such centers as pink spheres (Figure 10, middle). The overall structure contains hexagonal channels and was investigated for hydrogen storage.

Another framework is composed of mixed coordination environments containing carboxylates and pyridines to produce the helical SBU, however only the pyridyl moieties serve as points of extension, whereas the carboxylates are just simple monotopic ligands (Figure 10, bottom). The reaction of zinc salts with BIPY (BIPY = 4,4′-bipyridine) and HOCA [HOCA = (*E*)-3-(2-hydroxyphenyl)acrylic acid] produces $Zn_2(HOCA)_4$-(BIPY) that is composed of $[M_3(COO)_3(\text{-}PY)_3]_\infty$ SBUs.

DOI: 10.1021/acs.chemrev.6b00346
Chem. Rev. XXXX, XXX, XXX−XXX

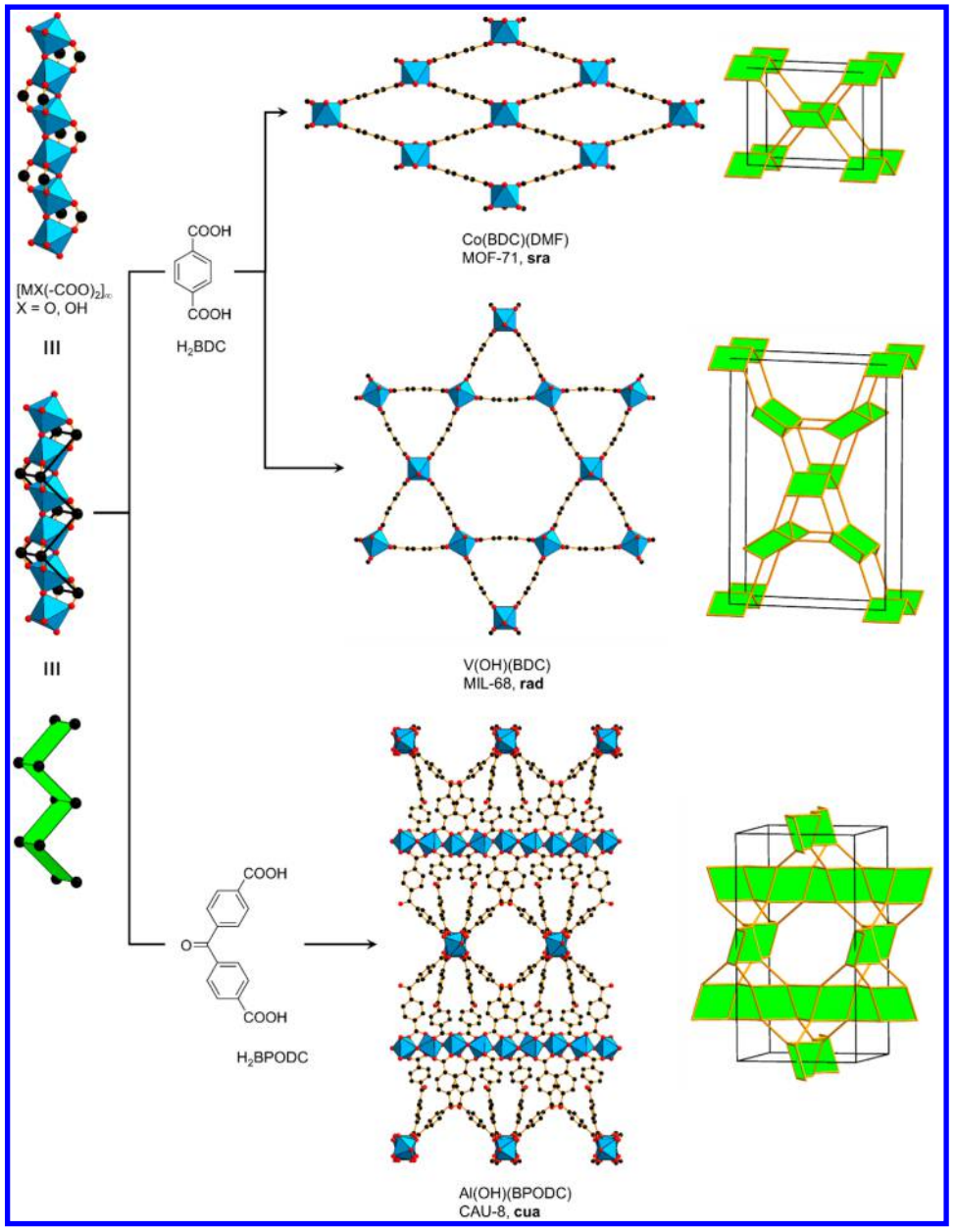

Figure 16. Three topologically different frameworks formed by zigzag ladders of general formula $[MX(-COO)_2]_\infty$ (X = O, OH). Various angles subtended either at the SBU or the linkers facilitate different orientation of rod SBUs in 1-dimension (**sra**, **rad**) or in 2-dimensions (**cua**).[6,114,116] Color code: black, C; red, O; blue polyhedra, metal.

The OCA moieties are part of the SBU; however, they do not link them together. The resulting hexagonal framework was described correctly as **etb** topology, particularly as MOF-74 analog, and was investigated toward luminescent properties.

In contrast to the 3-fold symmetric helix, as observed in **etb** nets, a 4-fold symmetry occurs in a tetragonal structure based on the **srs** net. All helices are of the same hand in **srs**, a chiral net, showing symmetry $I4_132$. The 3-c net has minimal transitivity 1 1. The edge is represented by a ditopic linker (e.g., a dicarboxylate). The compound illustrated herein (Figure 11), $Ni_5(OH)_2(L\text{-ASP})_4$ is a combination of a relatively complicated $[M_4(OH)_2(L\text{-ASP})_2(-COO)_2]_\infty$ SBU linked together with ditopic $[Ni(L\text{-ASP})_2]^{2-}$ (H_2L-ASP = L-aspartic acid).[93] The latter can also be referred to as metallo-linker.[94] The Ni atoms in the rod are coordinated in an octahedral environment and contain additionally bound L-ASP ligands that do not act as linkers. The chiral 1D chains of nickel aspartate were previously reported and crystallize as enantiopure (helices of only one hand) or racemic (helices with both hands) compounds.[95]

Another topology that contains 4-fold symmetric rods can be found in tetragonal **ths** nets with symmetry $I4_1/amd$. The 3-c net has transitivity 1 2. The helices are linked to their four closest neighbors by linear, aromatic dicarboxylates (Figure 12). In particular, we show the MOF Pb(MTETBDC) (H_2MTETBDC = 2,5-bis((2-(methylthio)ethyl)thio)terephthalic acid) that is built from $[M(-COO)_2]_\infty$ SBUs.[96] The Pb^{2+} are each coordinated by six carboxylate groups and two S atoms of the linker. Such coordination of S is not shown here, since the bond distances are quite large. The authors described the structure as similar to MOF-70; however, we believe that the description as a **ths** net is more appropriate than a very distorted **sra** net. In terms of practical utility, the MOF was investigated for its performance in white light LEDs.

DOI: 10.1021/acs.chemrev.6b00346
Chem. Rev. XXXX, XXX, XXX−XXX

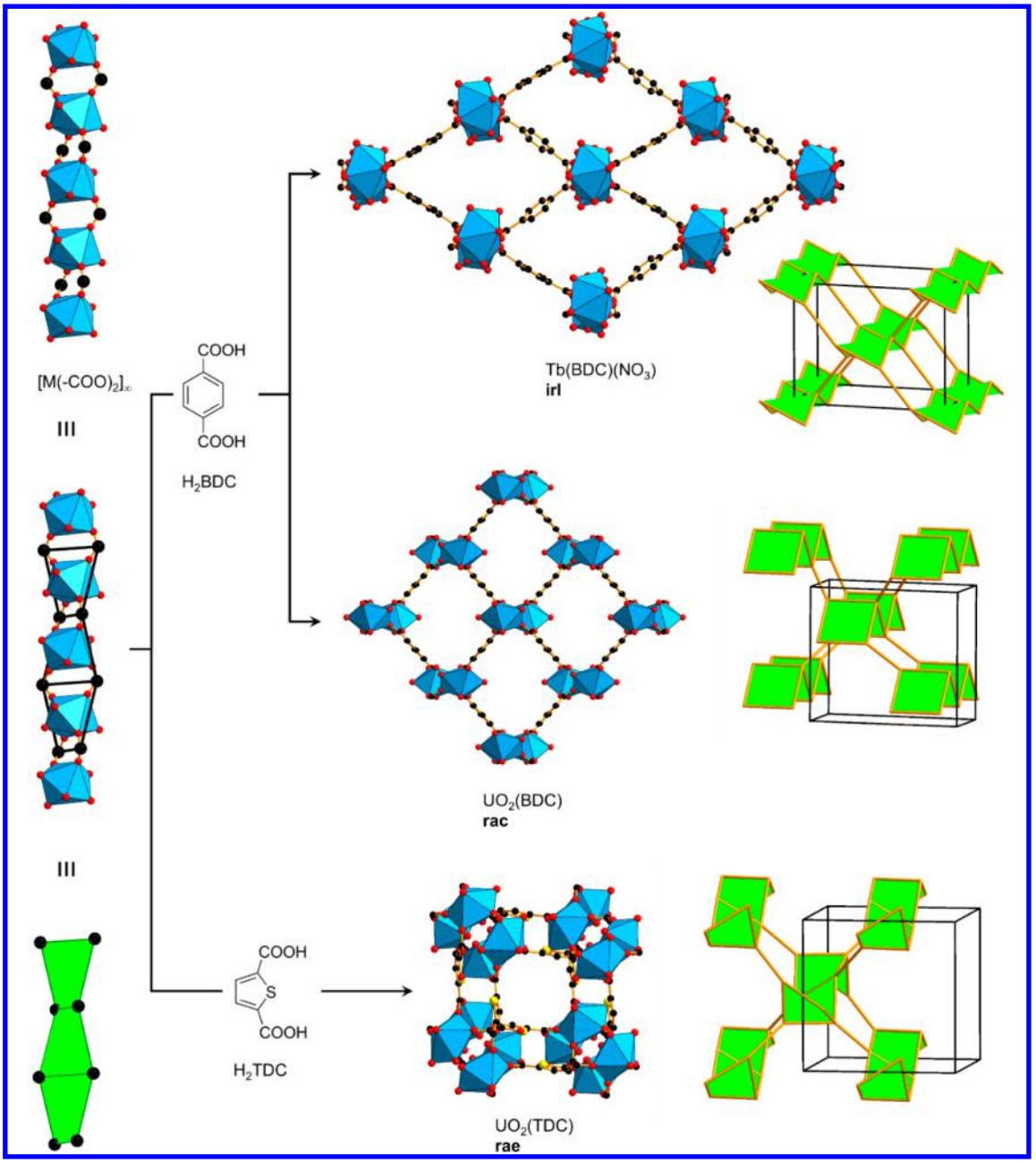

Figure 17. Single crystal structures and net topologies (**irl**, **rac**, and **rae**) of MOFs built from $[M(-COO)_2]_\infty$ twisted zigzag ladder SBUs.[28,123] Color code: black, C; red, O; yellow, S; blue polyhedra, metal.

If slightly different thiol-containing ditopic linkers are reacted with helical $[M(-COO)_2]_\infty$ SBUs of different shape, an **etm** topology net is obtained instead. In the framework with formula Pb(TMBD) (H_2TMBD = tetrakis(methylthio)-1,4-benzenedicarboxylic acid), the two crystallographically independent Pb^{2+} are each coordinated by six oxygen of the carboxylate moieties.[97] In contrast to Pb(MTETBDC), mentioned above, the thiol moieties point away from the SBU toward the inside of the channels and are therefore capable of binding $HgCl_2$ in a reversible manner. The underlying **etm** net has orthorhombic symmetry *Ibam*. The net has transitivity 2 4. Each helix is linked to their three closest neighboring helices by dicarboxylates linkers (Figure 13).

We note that in such Pb rod MOFs,[96,97] the rod SBUs are rather irregular,[98] leading to nets with nonminimal transitivity (e.g., **etm**) or other novel topology. This result may be related to the preferred noncentrosymmetric coordination geometries of post-transition metal ions (e.g., Tl^{I}, Pb^{II}, and Bi^{III}) due to the lone pair effect,[99] which should be considered in reticular synthesis of MOFs.

2.2. MOFs with Simple Helical SBUs and Polytopic Linkers

In Figure 14, we illustrate the structure and topology of a framework that was termed MIL-120 (MIL: Material Institute Lavoisier) and is composed of $[M(OH)_2(-COO)]_\infty$ SBUs, that when combined with tetratopic BTEC linkers (H_4BTEC = benzene-1,2,4,5-tetracarboxylic acid) produce $Al_4(OH)_8$(BTEC).[100] Both independent Al^{3+} have an octahedral coordination environment, containing four carboxylate O and two μ_2-OH groups. The rod SBU is composed of edge-sharing octahedra, in terms of coordination which the authors describe as zigzag inorganic wires. The points of extension (i.e., all carboxylate C in the structure) form helices as previously observed in **ths** nets;

DOI: 10.1021/acs.chemrev.6b00346
Chem. Rev. XXXX, XXX, XXX−XXX

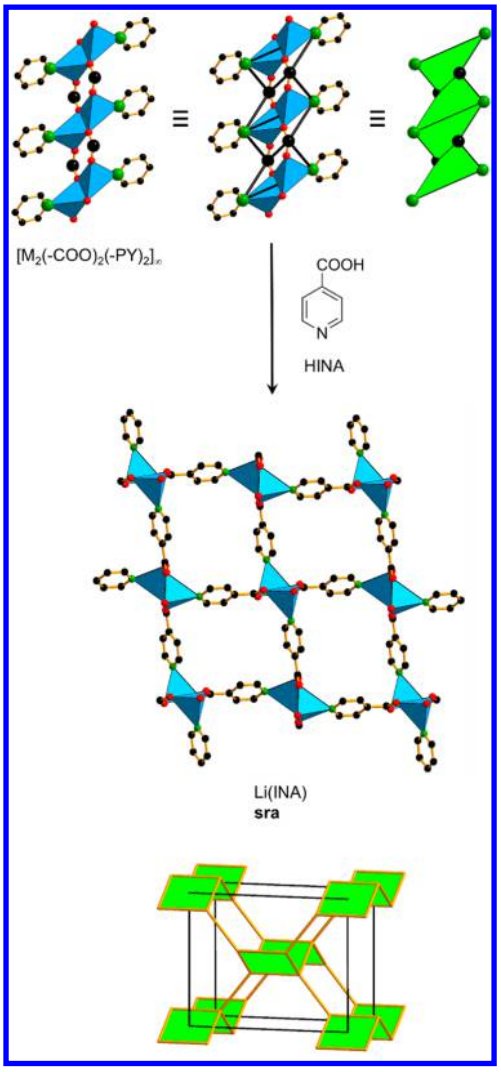

Figure 18. Crystal structure of Li(INA) formed by a bifunctional and distorted zigzag ladder SBU. The underlying topology is a regular **sra** net.[113] Color code: black, C; red, O; green, N; blue polyhedra, metal.

however, they show both hands and are in turn connected to and separated by squares. The binodal (3,4)-c net, symbol **raa**, has transitivity 2 5 and symmetry *C*2/*m*.

Another (3,4)-c net, **rab**, is observed in at least two chemically different MOFs (Figure 15). First, MIL-118A of formula $Al_2(OH)_2(BTEC)$ that is composed of $[M(OH)(-COO)_2]_\infty$ SBUs joint by BTEC linkers.[101] Each Al^{3+} is octrahedrally coordinated by three carboxylate O and two μ_2-OH groups. The remaining coordination site is occupied by a water molecule in MIL-118A, that in turn forms a hydrogen bond interaction to one of the uncoordinated carboxylate oxygens. This water molecule can be removed through heating to yield activated MIL-118B, which therefore represents a material suitable for reversible water adsorption. The other framework with **rab** topology was termed BCF-4 (BCF = beryllium carboxylate framework) $Be_4(OH)_4(BTEC)$ and consist of $[M(OH)(-COO)]_\infty$ SBUs, also linked through BTEC.[102] In the rod SBU, each beryllium is coordinated tetrahedrally, as commonly observed in beryllium chemistry, by two oxygens of bridging carboxylate groups and two μ_2-OH groups. The authors have described the topology as a new zeolitic type, evaluated through the program package TOPOS and taking into account the

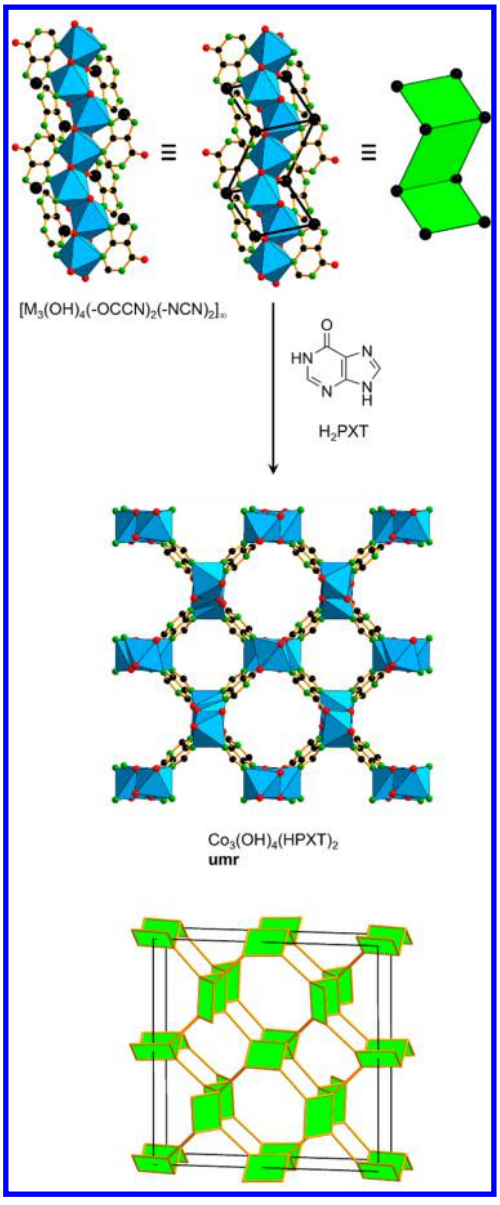

Figure 19. Crystal structure and net topology (**umr**) of $Co_3(OH)_4(HPXT)_2$.[128] Color code: black, C; red, O; green, N; blue polyhedra, metal.

tetrahedral coordination of beryllium. However, we believe that M−OH−M does not represent an appropriate edge of the net, and only carboxylate C should be considered as points of extension. Accordingly, the points of extension form a helix that can also be observed in **srs** nets, where they occur only in one hand. However, in **rab** nets both hands are present and therefore render it into an achiral net. The (3,4)-c net has transitivity 2 5 and symmetry *Cccm*.

3. MOFS WITH ZIGZAG LADDER SBUS

A versatile and often studied group of MOFs has SBUs that can be described as zigzag ladders (also called "double zigzag") and nets with 4-c nodes. Three of the four links between nodes belong to the zigzag ladder, and the remaining one linking them together, into the 3D MOF, through either ditopic or polytopic linkers. The SBU can either be fairly regular in shape or considerably twisted and, together with variable linker geometries, lead to different nets as discussed below.

DOI: 10.1021/acs.chemrev.6b00346
Chem. Rev. XXXX, XXX, XXX−XXX

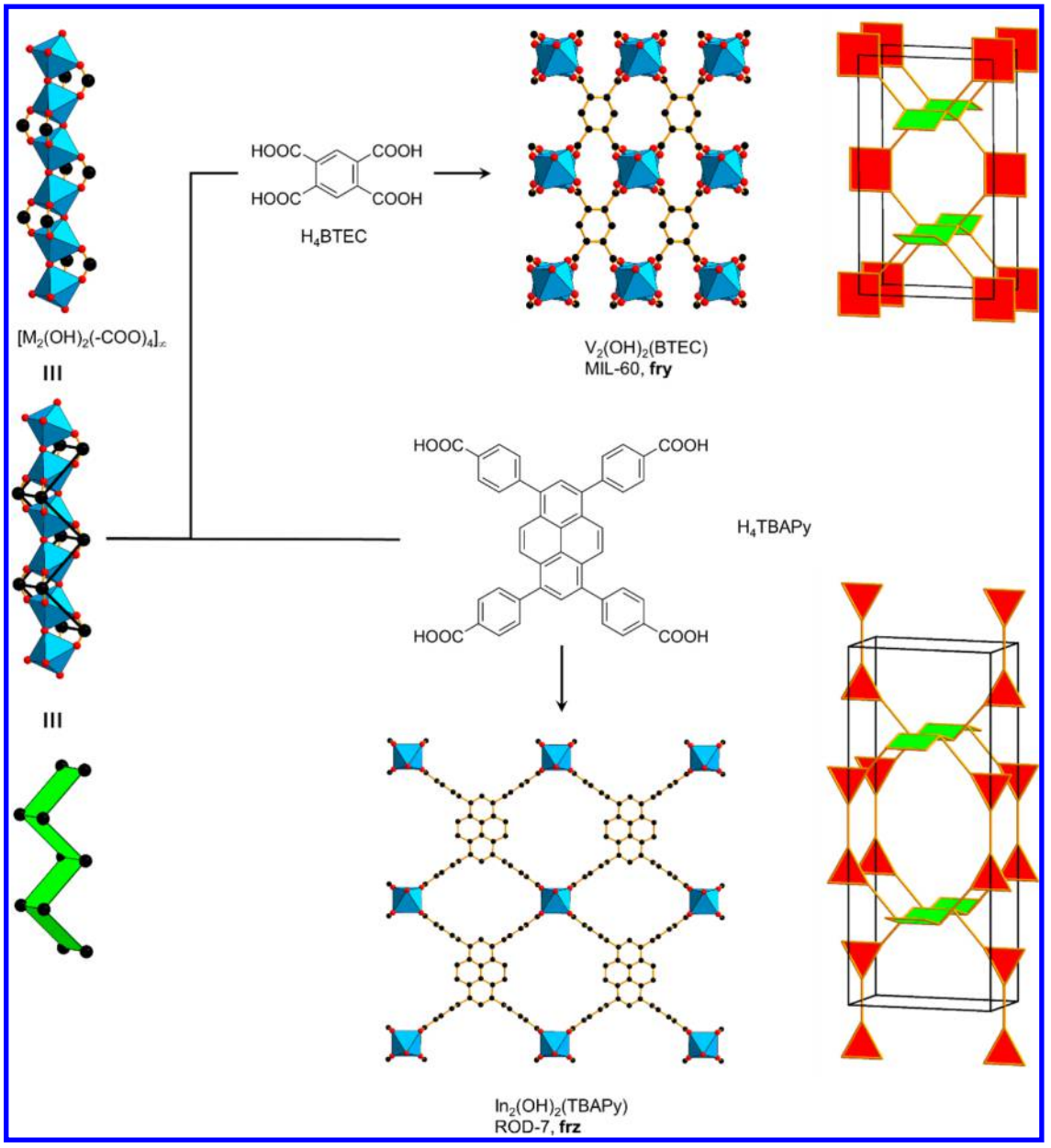

Figure 20. Zigzag ladder rod SBUs combined with tetratopic linkers. Symmetric linkers lead to a binodal (3,4)-c **fry** topology, asymmetric linkers to a trinodal (3,4)-c **frz** topology.[129,134] Color code: black, C; red, O; blue polyhedra, metal.

3.1. MOFs with Zigzag Ladder SBUs and Ditopic Linkers

Probably the most-frequently observed group of MOFs is that containing SBUs that consist of a rod of MO_6 octahedra sharing opposite corners with formula $[MX(-COO)_2]_\infty$ (X = O, OH), as detailed in Figure 16. If such building units are combined with simple, rigid ditopic linkers [e.g., BDC (H_2BDC = benzene-1,4-dicarboxylic acid)], MOF-71, Co(BDC) (DMF) (DMF = *N*,*N*-dimethylformamide) is produced.[6] We intentionally left the DMF in this particular formula since it provides a μ_2-O that is part of the framework and cannot be removed without disturbing its integrity. The net, symbol **sra**, consists of simply linked zigzag ladders. The net has transitivity 1 3 and symmetry *Imma*. Each rod is linked to four others through a ditopic linker and thus generates rhombic-shaped pores. The linker functionality is highly variable in **sra** nets and frameworks, containing carboxylates,[24,70,103−107] phosphonates,[108,109] azolates,[110,111] and even mixed functionalities[112,113] were observed. A striking feature of many **sra** nets is their flexibility which allows for structural changes upon solvent exchange or drying, a phenomenon detailed in the introduction and also described as "breathing".[24]

If $[MX(-COO)_2]_\infty$ rod SBUs are connected with BDC and subtend different angles at the SBU and with respect to each other then the framework V(OH) (BDC) (MIL-68) was produced (Figure 16).[114] In contrast to MOF-71, this framework contains both triangular and hexagonal channels running along [001]. The authors initially classified the topology as related to ReO_3 (**reo**) by considering each vanadium ion as the node, and OH as well as BDC as the linkers. Later, it was also interpreted as a linked kagomé (**kgm**) pattern owing to the triangular and hexagonal windows observed in **kgm**. This pattern distinguishes it clearly from MIL-47,[115] that we have unambiguously determined as an **sra** topology. However, in our deconstruction approach, only the carboxylate C atoms should be considered as points of extension which therefore renders MIL-68 into

DOI: 10.1021/acs.chemrev.6b00346
Chem. Rev. XXXX, XXX, XXX−XXX

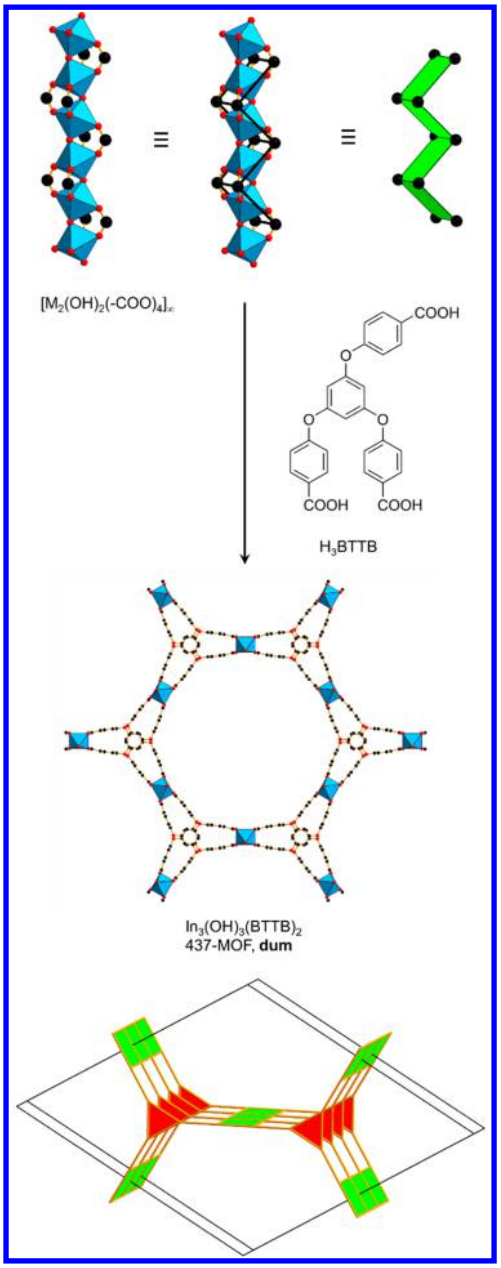

Figure 21. Zigzag ladder rod SBUs combined with flexible, tritopic linkers, leading to a framework with (3,4)-c **dum** topology.[136] The zigzag ladder becomes straight in the ideal embedding of the net. Color code: black, C; red, O; blue polyhedra, metal.

a **rad** net. In contrast to **sra**, half of the SBUs are tilted with respect to each other and do not support an overall hexagonal symmetry. The net has transitivity 3 6, and its symmetry is *Cmcm*.

In contrast, if an angular linker, such as BPODC (H_2BPODC = 4,4′-benzophenonedicarboxylic acid) is combined with the same zigzag ladder SBU, a framework termed CAU-8, Al(OH)(BPODC), was obtained (Figure 16, bottom).[116] This compound was referred to as the first keto-functionalized microporous Al-based MOF. The special feature in this context is that CAU-8 contains AlO_6 rod SBUs that propagate in two directions (90° to each other) along [100] and [010] in an ABCDA stacking [compare Figure 7 (b)]. This motif is caused by the angle subtended at the keto moiety of the BPODC linker and is also responsible for creating a rigid, rather than a flexible structure as observed in **sra** nets. The authors classified the topology using Systre and TOPOS, by reducing the rod SBU not into a zigzag ladder, but into a zigzag line with metal centers as nodes. We have previously pointed out (section 1.3) the disadvantage of this approach, which in this case results in a uninodal 4-c net with the point symbol $5^4.8^2$. In contrast, we use the deconstruction into a zigzag ladder, taking the actual points of extension (carboxylate C atoms) into account. The resulting net, symbol **cua**, has transitivity 2 5, and symmetry $I4_1/a$.

There are more zigzag ladders that do not necessarily contain parallel rungs (i.e., they may be twisted and therefore facilitate formation of different nets). MOFs that consist of such twisted zigzag ladder SBUs can be seen in Figure 17 and consist of $[M(-COO)_2]_\infty$ building units, where each metal cation is 7- or 8-coordinated through four oxygen from carboxylate groups and the remaining coordination sites are either occupied by water or charge balancing oxides.

A combination of the twisted $[M(-COO)_2]_\infty$ building unit with rigid ditopic BDC produces a MOF with formula Tb(BDC)(NO_3) (Figure 17, top).[28] The structure of Tb(BDC) contains rhombic-shaped channels that are partially occupied by charge-balancing NO_3^- counterions; however, the structure is still accessible to CO_2 gas. As pointed out earlier, the structure is best described as an **irl** net, based on twisted zigzag ladder SBUs, where each rod SBU is linked to four neighboring SBUs. The **irl** net has transitivity 1 3 and symmetry *Cccm*. In similarity to the previously discussed **sra**, **irl** nets are observed in many examples in the literature, build mainly from carboxylates,[117−120] as well as phosphonates.[121,122]

Two other structures with the same rod are based on 7-coordinated uranium(VI) or 5-coordinated uranyl cations $[UO_2]_2^+$, respectively.[123] We note here, that uranyl MOFs are special in crystal chemistry because U(VI) ion can adopt high coordination numbers and unusual coordination geometries (e.g., pentagonal bipyramid and hexagonal bipyramid). Such versatility gives rise to a range of oxo- and hydroxo-clusters that can act as SBUs in MOFs, many of which are rod MOFs.[124−126]

Reaction of uranyl nitrate with H_2BDC produces a MOF with formula UO_2(BDC) that contains rhombic-shaped pores (Figure 17, middle). Each uranium cation is coordinated by four carboxylate O, two oxides, and a solvent molecule. The underlying net, was assigned to **rac** and appears to be similar to the previously discussed **sra**. However, there is a subtle difference in connectivity of the zigzag ladders, being parallel up and down in **sra**, and antiparallel up and down in **rac**. The latter net has transitivity 1 4 and symmetry *Pnna*.

If the same uranyl rod SBU is reacted with TDC (H_2TDC = thiophene-2,5-dicarboxylic acid) instead, UO_2(TDC) is obtained, that shows narrow channels of around 6 × 6 Å (Figure 17, bottom).[123] The coordination geometry at the metal ions is identical to UO_2(BDC); however, the nonlinear nature of the TDC linker facilitates a **rae** net resulting in a twisted zigzag ladder. The connectivity between the SBUs is also antiparallel up and down, similar but not the same as in **rac**. The **rae** net has transitivity 2 5 and symmetry *Pbcn*.

Another **sra** net is found in a $[M_2(-COO)_2(\text{-PY})_2]_\infty$ SBU that contains mixed functionalities (i.e., carboxylates and pyridines). If this SBU is combined with INA linkers (HINA = isonicotinic acid), a framework with composition Li(INA) was produced (Figure 18).[113,127] Each Li^+ shows the usual tetrahedral coordination, in particular by three oxygen from carboxylate groups and one nitrogen from pyridine. These carboxylates and pyridines also both serve as points of extension to build the zigzag ladder and link to the four nearest neighboring SBUs.

DOI: 10.1021/acs.chemrev.6b00346
Chem. Rev. XXXX, XXX, XXX−XXX

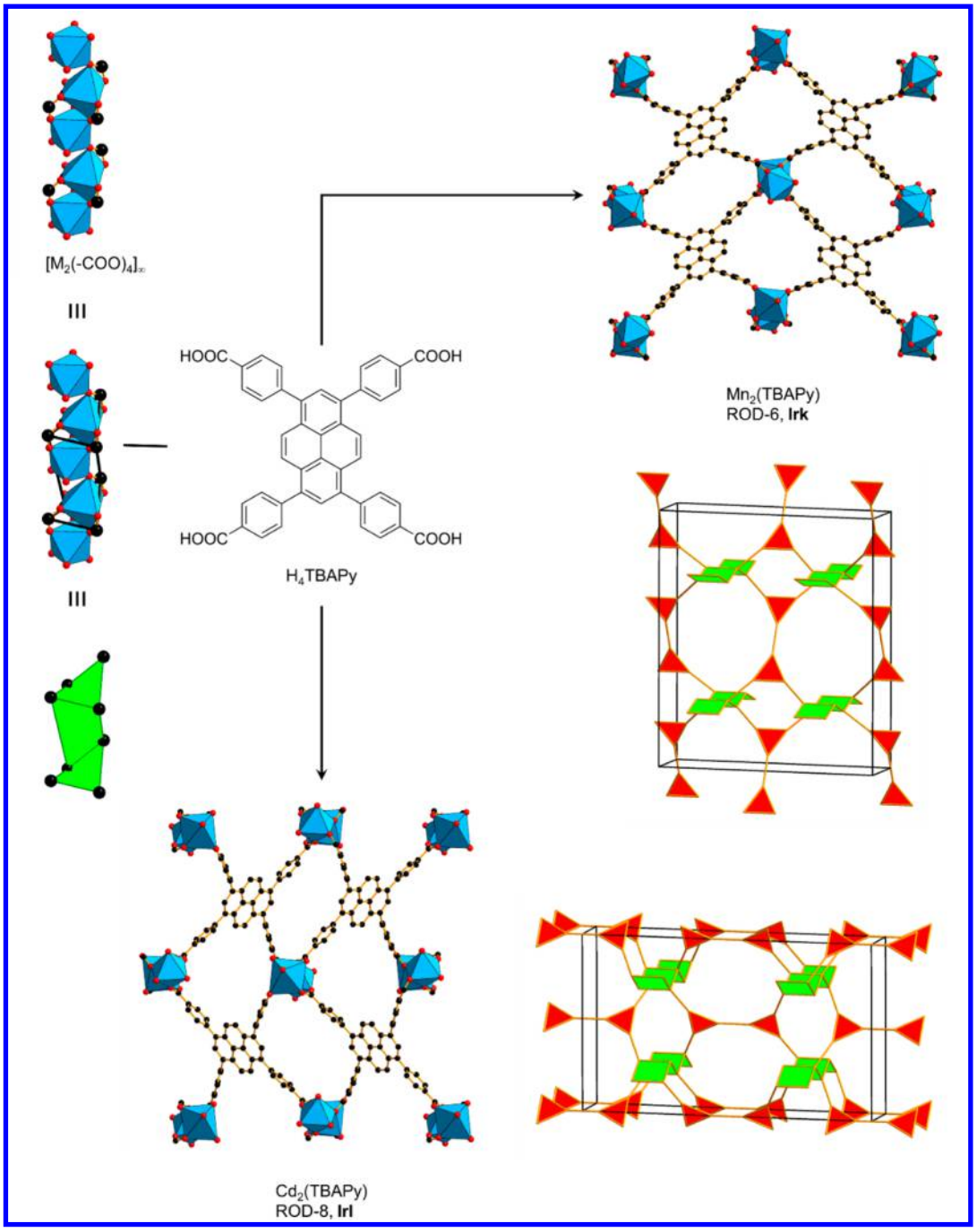

Figure 22. Single crystal structures of ROD-6 and ROD-8. ROD-6 crystallizes in the **lrk** topology, whereas ROD-8 shows positional disorder and is best described as an average between **lrl** (shown here) and **lrk** topology.[137] Color code: black, C; red, O; blue polyhedra, metal.

We would like to emphasize here that, even if the zigzag ladder appears strongly twisted in the crystal structure, in the symmetry embedding of **sra** net, the ladder becomes regular.

As previously detailed, the arrangement of zigzag ladders with respect to each other can facilitate different nets than **sra**. In Figure 19, we highlight the structure and topology of a framework composed of quite complicated $[M_3(OH)_4(-OCCN)_2(-NCN)_2]_\infty$ SBUs, that when combined with H_2PXT linkers (H_2PXT = 6-hydroxypurine) produce $Co_3(OH)_4(HPXT)_2$.[128] The two types of channels have different diameters, and interestingly only the large channel is occupied by solvent molecules. Both independent Co^{2+} have an overall octahedral coordination, one cobalt is bound to two μ_2-OH groups, two N and two O from four HPXT, the other to three μ_2-OH groups, and two N and one O from three HPXT. The assigned points of extension lie either on the −OCCN− or on the −NCN− fragment of HPXT, in an alternating fashion. The rod SBU is therefore composed of a zigzag ladder, and the correct topology **umr** was assigned in the original contribution. The **umr** net is different from **sra**, since it contains alternating layers of zigzag ladders, which are rotated by 90° with respect to each other (ABCDA packing). The 4-c net has transitivity 1 3 and symmetry $I4_1/acd$, and each rod is linked to its four nearest neighbors.

3.2. MOFs with Zigzag Ladder SBUs and Polytopic Linkers

In this section, we focus on the combination of zigzag ladder SBUs with polytopic linkers, in particular, tri- and tetratopic

DOI: 10.1021/acs.chemrev.6b00346
Chem. Rev. XXXX, XXX, XXX−XXX

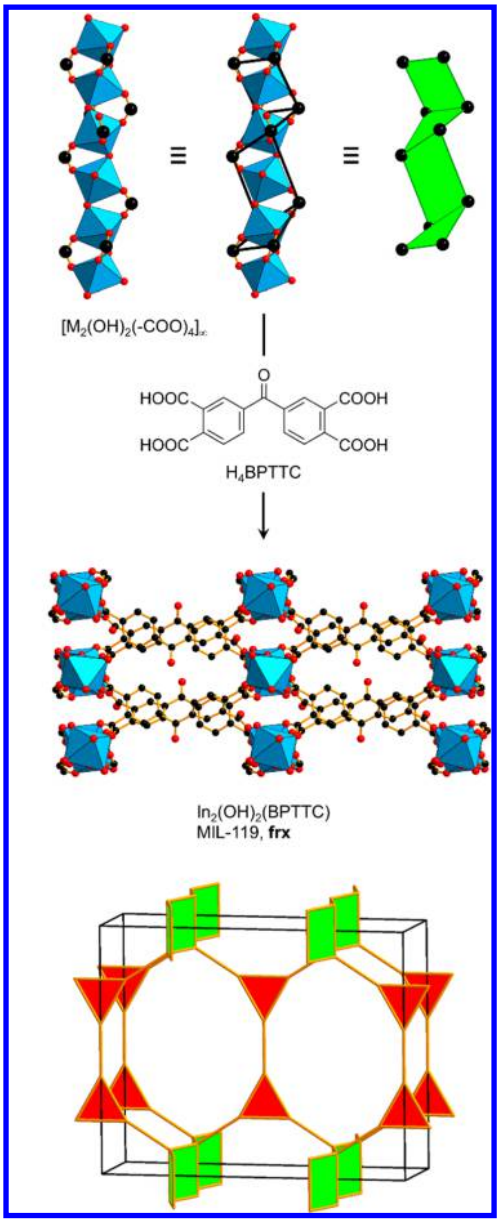

Figure 23. Single crystal structure of MIL-119 and its underlying **frx** net.[138] Color code: black, C; red, O; blue polyhedra, metal.

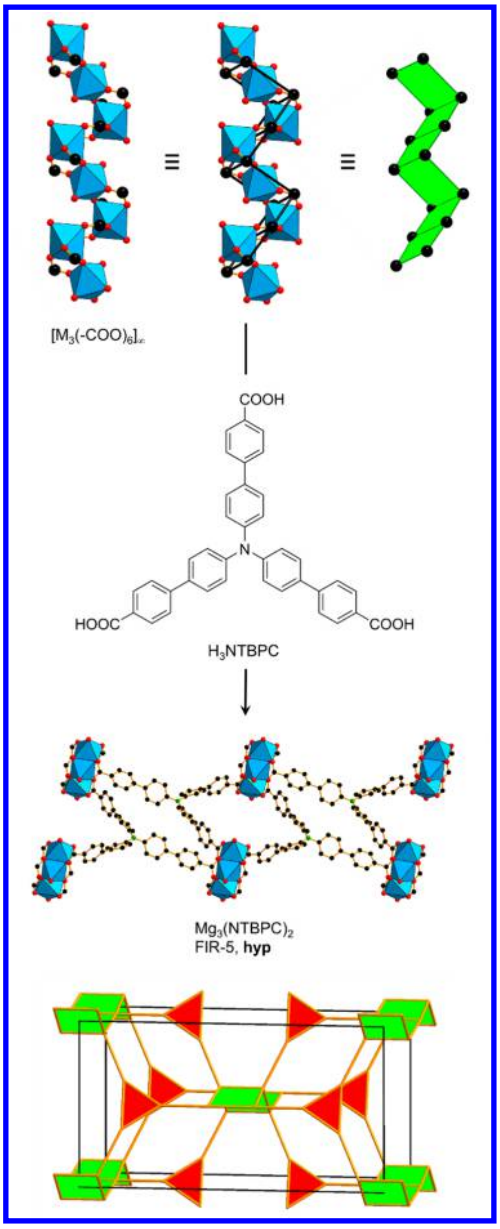

Figure 24. Single crystal X-ray structure of FIR-5 and the underlying (3,4)-c **hyp** net.[139] Color code: black, C; red, O; green, N; blue polyhedra, metal.

carboxylates. Unsymmetrical tetratopic linkers are split into connected triangles according to the previously reported deconstruction approach.[4,5] Figure 20 shows the structure of two related MOFs, termed MIL-60 and ROD-7 (ROD = rod metal−organic framework), which are both composed of $[M_2(OH)_2(-COO)_4]_\infty$ SBUs. Combination of this SBU with tetratopic BTEC linkers produces $V_2(OH)_2(BTEC)$, a material first synthesized in 2003.[129] Each rod is isolated from the others and exclusively linked to squares. The topology was initially interpreted by the authors as a linked, interpenetrated MIL-47[23] (**sra**), which can be obtained, if half of the rod SBUs are removed. In contrast to MIL-47, MIL-60 is densely packed and shows no accessibility for small molecules. The topology generally consists of simply linked zigzag ladders connected through squares, yielding a **fry** net. This net has transitivity 2 5 and symmetry *Cmmm*. Other compounds that were identified as **fry** nets include MIL-62,[130] MIL-66,[131] MIL-122 (Al, Ga, In),[132] MIL-118B/118C,[101] and an aluminum-based porphyrin MOF $Al_2(OH)_2(H_2TCCP)$[133] (H_6TCCP = meso-tetra(4-carboxyl-phenyl) porphyrin).

In contrast to symmetrical square-shaped linkers in **fry** nets, the use of asymmetric tetratopic linkers lead to its related **frz** nets (Figure 20, bottom). We describe the structure and topology of $In_2(OH)_2(TBAPy)$ (H_4TBAPy = 1,3,6,8-tetrakis(*p*-benzoic acid)pyrene), first synthesized in 2010,[134] and later termed ROD-7.[135] In this structure, that contains rhombic-shaped pores, accessible to solvents as well as gases, the tetratopic TBAPy linker can be deconstructed into two linked triangles, yielding to **frz** nets with symmetry *Cmmm* and transitivity 3 6. The edges between the zigzag ladder and the triangles all run parallel to each other.

If the same $[M_2(OH)_2(-COO)_4]_\infty$ SBUs are combined with a flexible, tritopic linker BTTB (H_3BTTB = 4,4′,4″-(benzene-1,3,5-triyltris(oxy))tribenzoic acid), a framework of composition $In_3(OH)_3(BTTB)_2$ is produced, termed 437-MOF (Figure 21).[136] The flexibility of the linker that adopts a unique conformation and trigonal symmetry facilitates the formation of large mesopores along [001]. The topology of 437-MOF was determined by

DOI: 10.1021/acs.chemrev.6b00346
Chem. Rev. XXXX, XXX, XXX−XXX

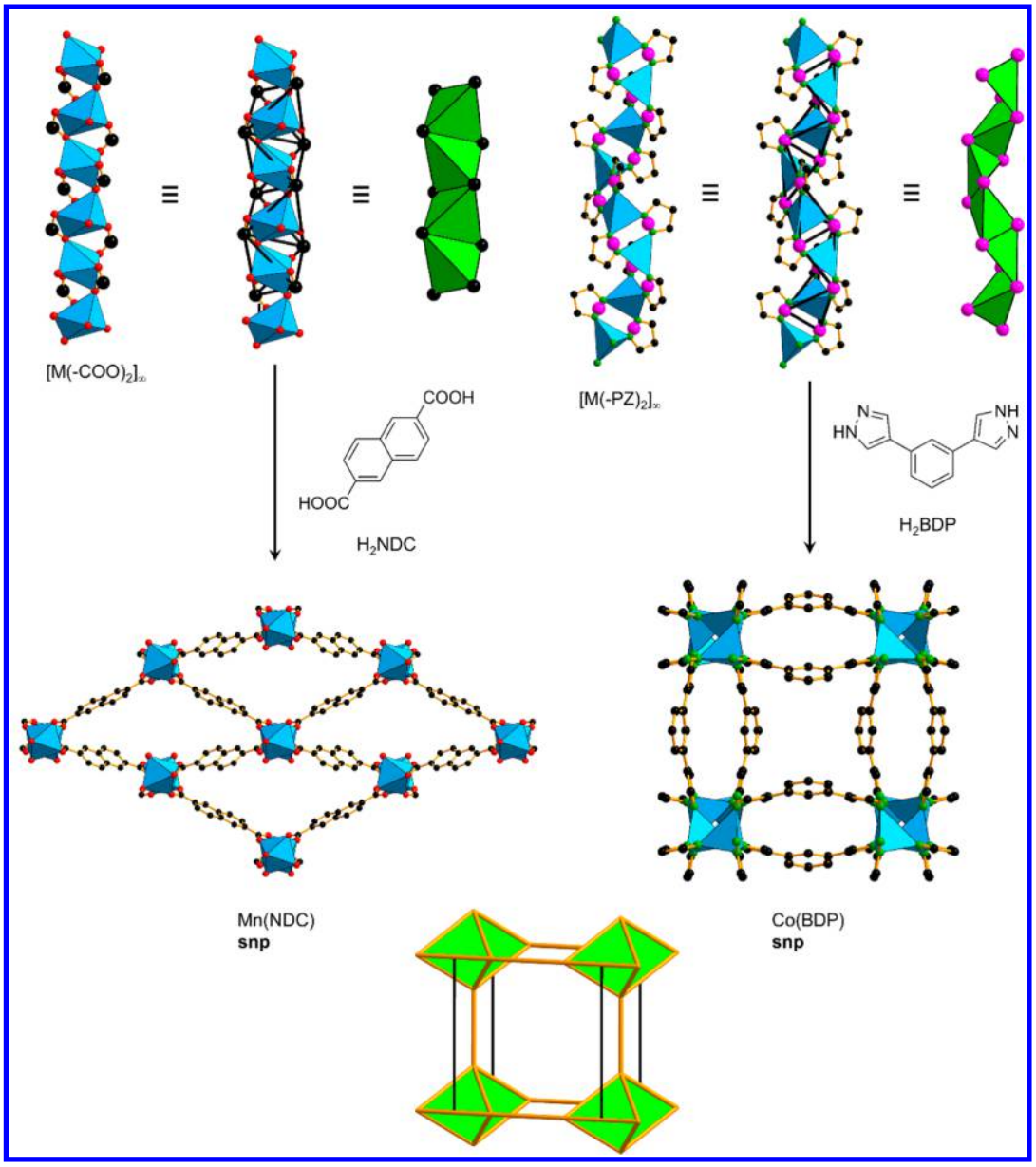

Figure 25. snp Net composed of opposite edge-sharing tetrahedra. Examples of rod SBUs composed of carboxylates and azolates are highlighted.[140,142] Color code: black, C; red, O; green, N; blue polyhedra, metal; pink, points of extension.

taking carboxylate C as points of extension and assigned the symbol **dum** in RCSR. This (3,4)-c net has transitivity 2 4 and symmetry *P6/mmm*. We note that the zigzag ladder becomes straight (a real ladder) in the ideal embedding of the net.

The linkage of tetratopic TBAPy with a slightly different zigzag ladder SBU $[M_2(-COO)_4]_\infty$ leads to the formation of two related frameworks, termed ROD-6, Mn_2(TBAPy) and ROD-8, Cd_2(TBAPy), with **lrk** and **lrl** topology, respectively (Figure 22).[135,137] In detail, both structures contain two crystallographically independent metal ions, one of them coordinated in a pentagonal bipyramidal geometry by seven carboxylate O, the other in a distorted octahedral geometry by four carboxylate O and two water ligands. The topology of ROD-6 was assigned **lrk** and appears similar to aforementioned **frz**; however, in the latter, the edges run antiparallel, with the triangular nodes being tilted with respect to the normal of the zigzag ladder. This net has transitivity 3 7 and symmetry *Cccm*. The structurally similar framework ROD-8 in turn displays a positional disorder of the TBAPy linker that can be regarded as an average between the **lrk** and an **lrl** topology. The latter can be described as similar to **lrk**, the only difference being the rotation of the triangular SBUs by 90° (Figure 22, bottom). Since ROD-8 is a disordered structure, the average of both **lrk** and **lrl** nets yields to the parent net **lrj**, a binodal net (transitivity 2 6) containing a square SBU instead of linked triangles. It also has a symmetry *Cccm*.

Figure 23 shows the structure and topology of a MOF, MIL-119, $In_2(OH)_2$(BPTTC) (H_4BPTTC = 3,3′,4,4′-benzophenonetetracarboxylate) which is built from $[M_2(OH)_2(-COO)_4]_\infty$ rod SBUs together with an asymmetrical tetracarboxylate linker.[138] The rod is composed of trans corner-sharing octahedra, in which the metal center is coordinated by two μ_2-OH groups and four carboxylate O. MIL-119 is a densely packed structure and therefore nonporous. The net, symbol **frx**, consists of zigzag ladders, each four of them connected through two triangles. The net has transitivity 3 6 and symmetry *Cmmm*. The **frx** net is

DOI: 10.1021/acs.chemrev.6b00346
Chem. Rev. XXXX, XXX, XXX−XXX

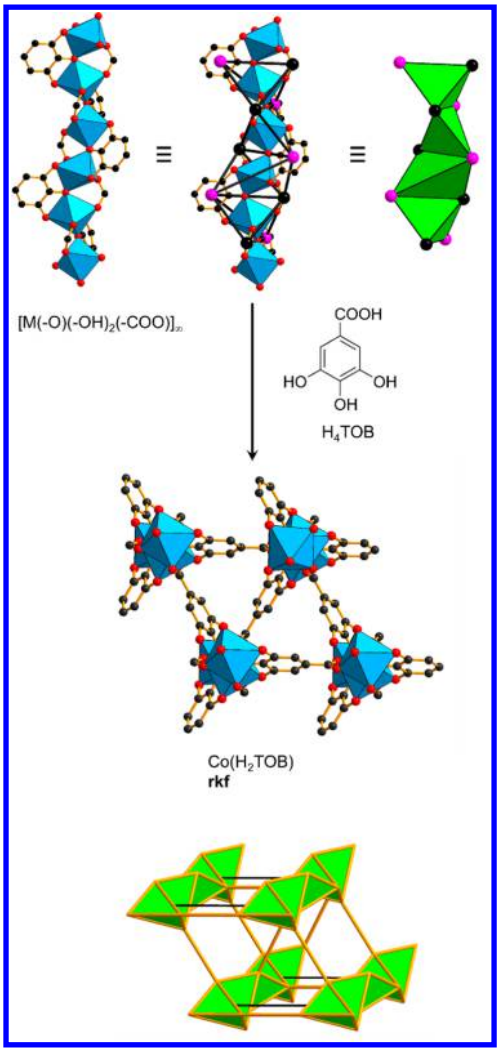

Figure 26. Combination of gallic acid with $[M(-O)(-OH)_2(-COO)]_\infty$ SBUs leads to a family of chiral frameworks $M(H_2TOB)$ with **rkf** topology.[152] Color code: black, C; red, O; blue polyhedra, metal; pink, points of extension.

derived from aforementioned **fry**, by replacing the central square SBU with two linked triangles, taking into account the asymmetric nature of the linker.

A slightly different zigzag ladder $[M_3(-COO)_6]_\infty$ is shown in Figure 24, and when combined with triangular NTBPC [H_3NTBPC = 4′,4‴,4⁗′-nitrilotris(([1,1′-biphenyl]-4-carboxylic acid))], produces a MOF, termed FIR-5 (FIR = Fujian Institute of Research on the Structure of Matter) with formula $Mg_3(NTBPC)_2$.[139] Each magnesium is coordinated in a distorted octahedral environment by five carboxylate O and one solvent molecule. The topology of the structure was initially described by the authors using TOPOS, as a (3,8)-c **tfz** net that could be derived from the well-known 2D kagomé dual net (**kgd**). This classification was made based on the assumption of a binuclear SBU formed by adjacent Mg centers. However, we believe that the rod SBU should be deconstructed differently, as seen in Figure 24, and assigned a 4-nodal **hyp** net with transitivity 4 8 and symmetry *I*2/*m*.

4. MOFS WITH SBUS OF EDGE-SHARED TETRAHEDRA

In contrast to ladders in which rungs fall on (almost) parallel lines, patterns in which rungs are on lines at 90° to their neighbors are really rods of tetrahedra sharing opposite edges. In such a rod,

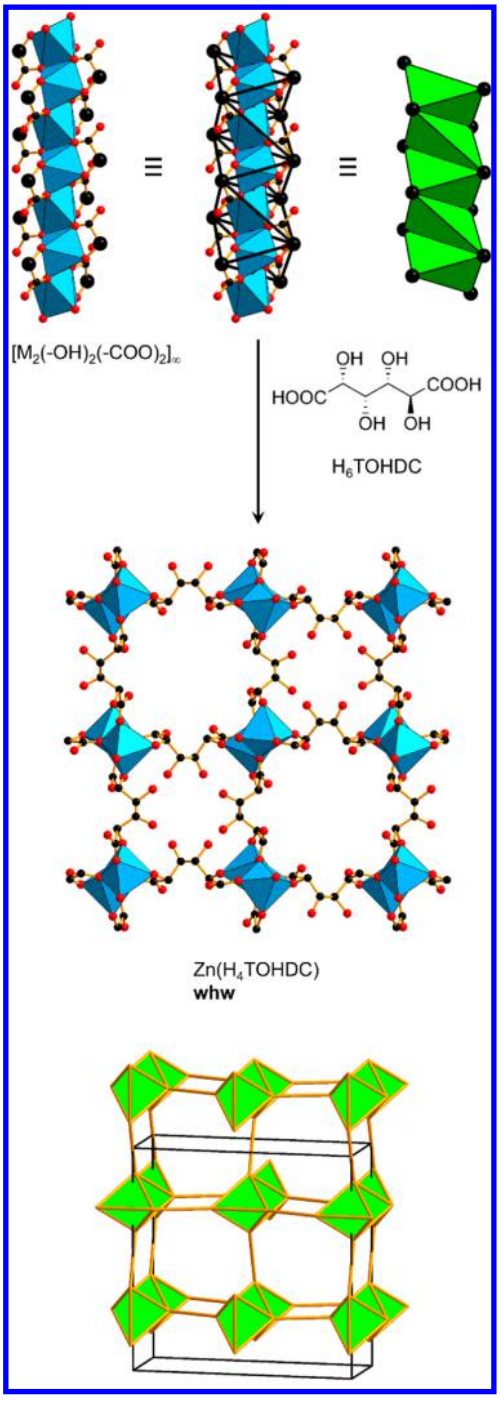

Figure 27. Chiral $Zn(H_4TOHDC)$ frameworks, showing hydrophilic and hydrophobic channels. The underlying net is **whw**.[153] Color code: black, C; red, O; blue polyhedra, metal.

which we discuss next, there must be at least two kinds of edge and each vertex is connected to five others on the net, formed with ditopic linkers will be 6-c and have minimal transitivity 1 3. We indeed find such a net.

Tetrahedra can also form rods by sharing faces. The structure is then related to the BC helix described in section 1.5. We discuss MOFs with such SBUs in section 13.1.

4.1. MOFs with SBUs of Edge-Shared Tetrahedra and Ditopic Linkers

Linked tetrahedra can be composed of many different multidentate linkers. First, we tend to introduce carboxylates or pyrazolates, that

DOI: 10.1021/acs.chemrev.6b00346
Chem. Rev. XXXX, XXX, XXX−XXX

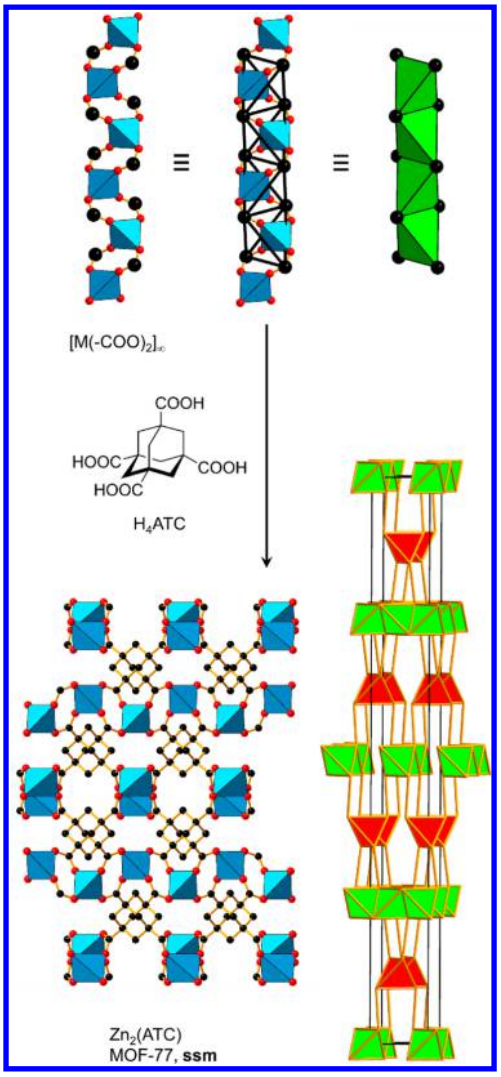

Figure 28. Crystal structure of MOF-77 and the underlying **ssm** net. The opposite edge-sharing tetrahedra rod SBUs are running in two directions.[6] Color code: black, C; red, O; blue polyhedra, metal.

form $[M(-COO)_2]_\infty$ and $[M(\text{-}PZ)_2]_\infty$ SBUs, respectively. The former contains manganese in an octahedral coordination environment with five carboxylate oxygen and one solvent molecule. The latter contains tetrahedrally coordinated zinc, surrounded by four pyrazolate nitrogen. Combination of $[M(-COO)_2]_\infty$ SBUs with linear NDC (H_2NDC = naphthalene-2,6-dicarboxylic acid) produces Mn(NDC),[140] and combination of $[M(\text{-}PZ)_2]_\infty$ with the angular (120°) BDP linker (H_2BDP = 1,4-benzenedipyrozolate) yields Co(BDP) (Figure 25).[141,142] Although both structures are quite different and their SBUs are either straight or helical, the underlying topology is the same: a **snp** net. This 6-c net was originally introduced in 2012[4] and has transitivity 1 3 (the minimum possible), with a symmetry $P4_2/mmc$. Such **snp** nets have since been frequently observed when utilizing diazolates with different length and functional groups,[111,143−149] sterically hindered dicarboxylates,[150] or linkers containing different functionalities.[151]

A framework, Co(H_2TOB) (H_4TOB = 3,4,5-trihydroxybenzoic acid, gallic acid), of opposite edge-sharing tetrahedra SBUs, $[M(\text{-}O)(-OH)_2(-COO)]_\infty$, that are found for different functional groups, a carboxylate and a pyrogallate group, are shown in Figure 26.[152] The isostructural compounds can also be obtained by using Fe, Ni, or Mn, and the metal centers are octahedrally coordinated by four phenolic O and two carboxylate O.

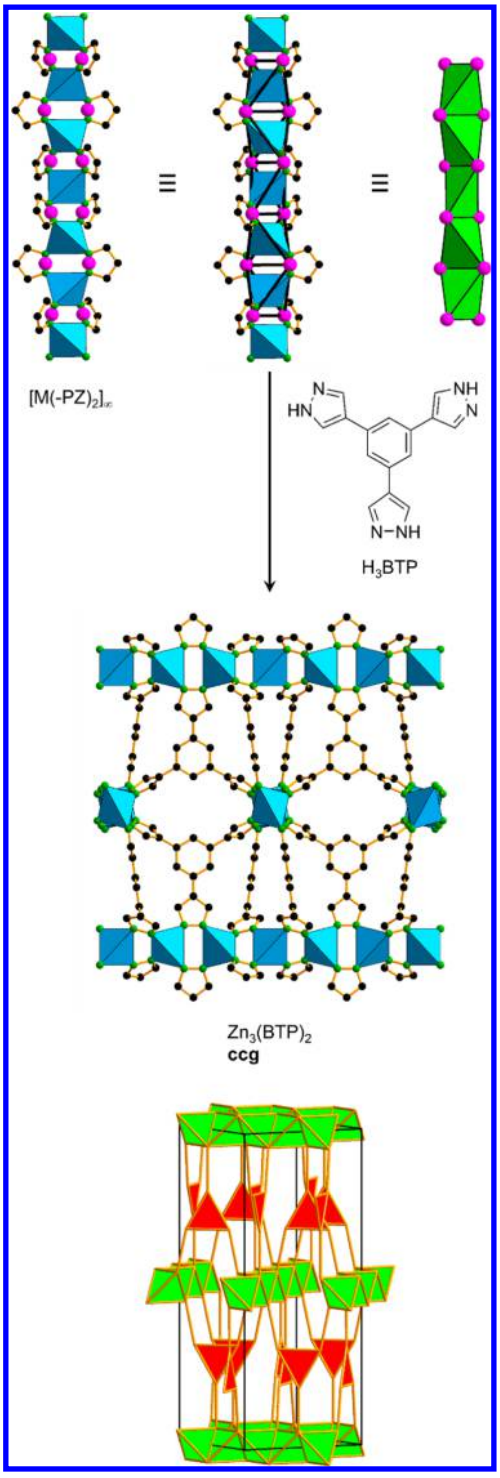

Figure 29. Rod SBUs formed by edge-sharing $[M(\text{-}PZ)_2]_\infty$ tetrahedra. The **ccg** net contains rod SBUs forming a tetragonal ABA packing.[39] Color code: black, C; red, O; green, N; blue polyhedra, metal; pink, points of extension.

The assigned points of extension are represented by the carboxylate C as well as the center of the pyrogallate moiety (shown as pink sphere), resulting in an overall chiral, 6-c **rkf** net with transitivity 1 4. The symmetry is $P6_222$.

Another chiral MOF, Zn(H_4TOHDC), (H_6TOHDC = (2*R*,3*S*,4*S*,5*S*)-2,3,4,5-tetrahydroxyhexanedioic acid, D-saccharic acid) built by edge-sharing tetrahedra $[M_2(-OH)_2(-COO)_2]_\infty$ SBUs is produced by reacting zinc salts together with D-saccharic

DOI: 10.1021/acs.chemrev.6b00346
Chem. Rev. XXXX, XXX, XXX−XXX

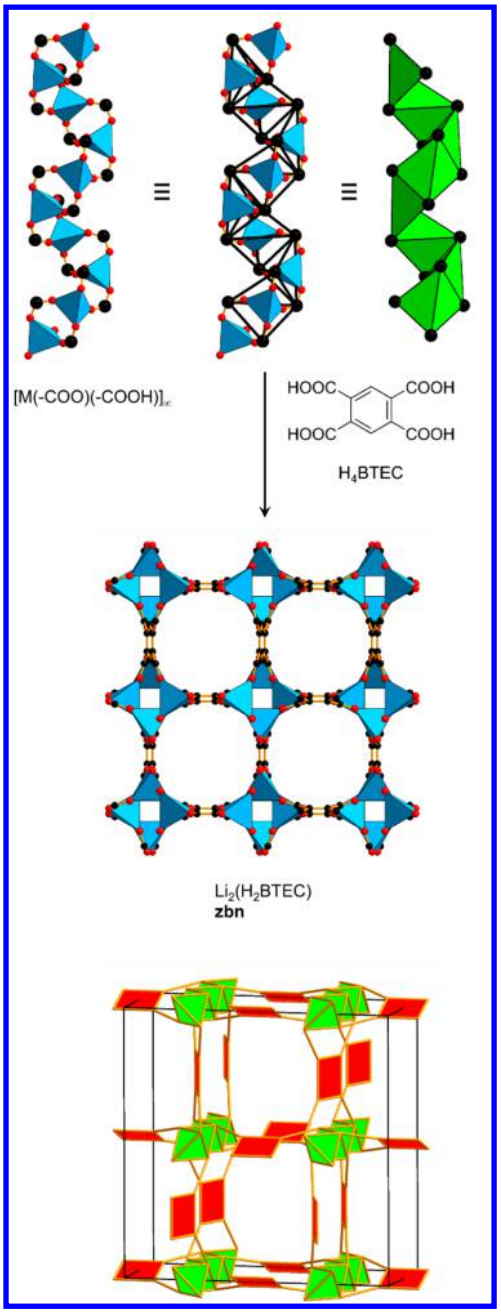

Figure 30. Combination of helical $[M(-COO)(-COOH)]_\infty$ SBUs with tetratopic BTEC produces $Li_2(H_2BTEC)$. It is best described as a binodal (3,6)-c **zbn** net.[154] Color code: black, C; red, O; blue polyhedra, metal.

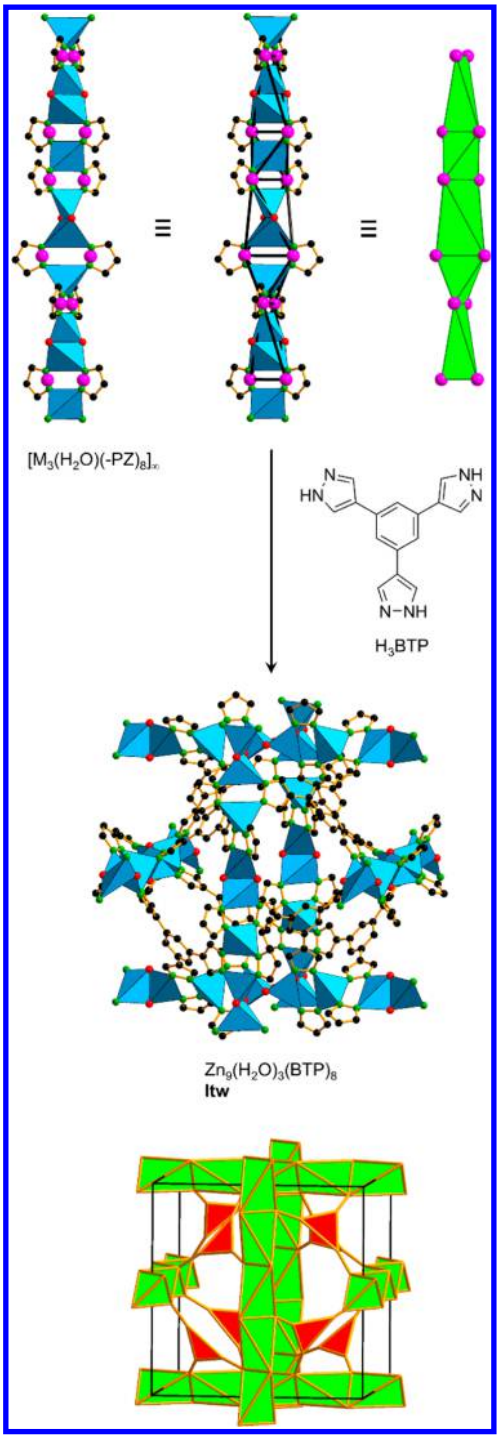

Figure 31. Idealized crystal structure of $Zn_9(H_2O)_3(BTP)_8$, the only cubic 3-way pattern in rod MOFs. The underlying topology is a binodal (3,6)-c **ltw** net.[39] Color code: black, C; red, O; green, N; blue polyhedra, metal; pink, points of extension.

acid in water (Figure 27).[153] The chiral framework contains square channels, half of them hydrophobic, the other half hydrophilic, in an alternating arrangement. The two distinct Zn^{2+} form edge-sharing octahedra, that are in turn slightly distorted, coordinated by four μ_2-oxygen (from carboxylate groups) and two oxygen from OH groups. The other two OH groups of the linker remain free and decorate the interior of the hydrophilic pore. The underlying topology is **whw**. This 6-c net has transitivity 1 4. The symmetry is $I4_1/amd$, so the net is not inherently chiral.

4.2. MOFs with SBUs of Edge-Shared Tetrahedra and Polytopic Linkers

In this section, we describe differently linked tetrahedra SBUs with polytopic organic linkers. Figure 28 shows the structure and topology of MOF-77, $Zn_2(ATC)$ (H_4ATC = adamantane-1,3,5,7-tetracarboxylic acid).[6] The rod SBU of this MOF $[M(-COO)_2]_\infty$ is composed of opposite edge-sharing tetrahedra, where each zinc is coordinated by four carboxylate O. The tetrahedral nature of the ATC linker facilitates rods that propagate in the [100] and [010] directions. The tetragonal layer packing (ABCDA) of such rods was previously described as related to the **ths-z** net (Figure 7b). We now prefer the description as a **ssm** net, related to the nonaugmented (linker as one 4-c node) **mss** that has

DOI: 10.1021/acs.chemrev.6b00346
Chem. Rev. XXXX, XXX, XXX−XXX

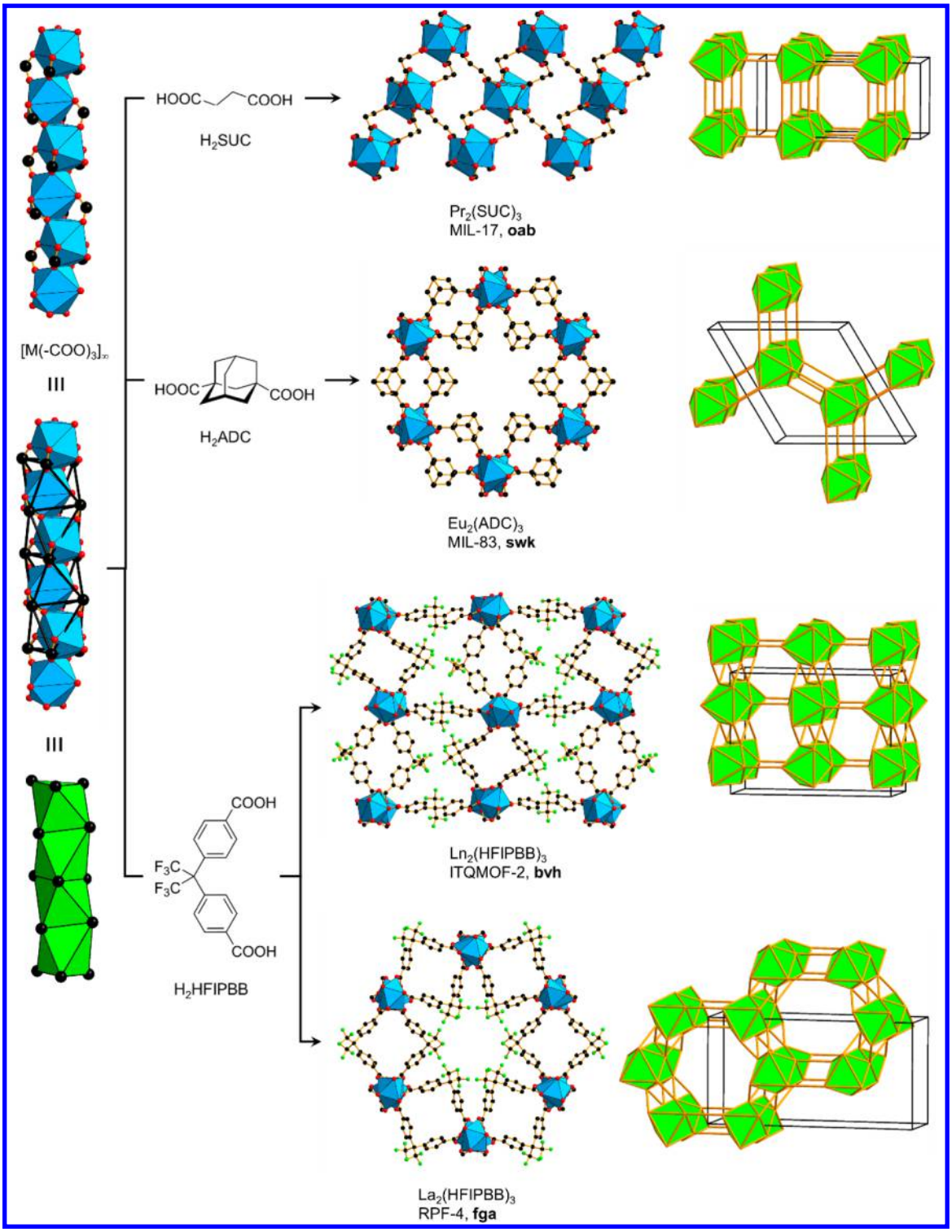

Figure 32. Linking of face-sharing octahedral SBUs, $[M(-COO)_3]_\infty$, with rigid and flexible dicarboxylates leads to a large structural diversity exemplified by **oab**,[155] **swk**,[160] **bvh**,[164] and **fga** nets,[165] respectively. Color code: black, C; red, O; green, F; blue polyhedra, metal.

previously been discussed.[4] The (4,6)-c **ssm** net has transitivity 2 7 and symmetry $I4_1/a$.

Opposite edge-sharing tetrahedra rod SBUs might also be composed of pyrazolates, as in $[M(\text{-}PZ)_2]_\infty$, that when combined with triangular BTP (H_3BTP = 1,3,5-tris(1H-pyrazol-4-yl)-benzene) produces $Zn_3(BTP)_2$ (Figure 29).[39] In the rod, each zinc is coordinated by four N of the pyrazolate moiety, and the dihedral angle (around 64°) of the triangular linker causes the rods to run perpendicular to each other, along [110] and equivalent. The tetragonal layer packing of rods in this **ccg** net is ABA (Figure 7d). The net has transitivity 4 10 and symmetry $P4_2/ncm$.

If the same linked edge-sharing tetrahedra moiety propagates along a 4_1 axis, a helical $[M(-COO)(-COOH)]_\infty$ SBU was obtained (Figure 30). Linking of such SBUs with BTEC produces $Li_2(H_2BTEC)$ that contains square-shaped channels

DOI: 10.1021/acs.chemrev.6b00346
Chem. Rev. XXXX, XXX, XXX−XXX

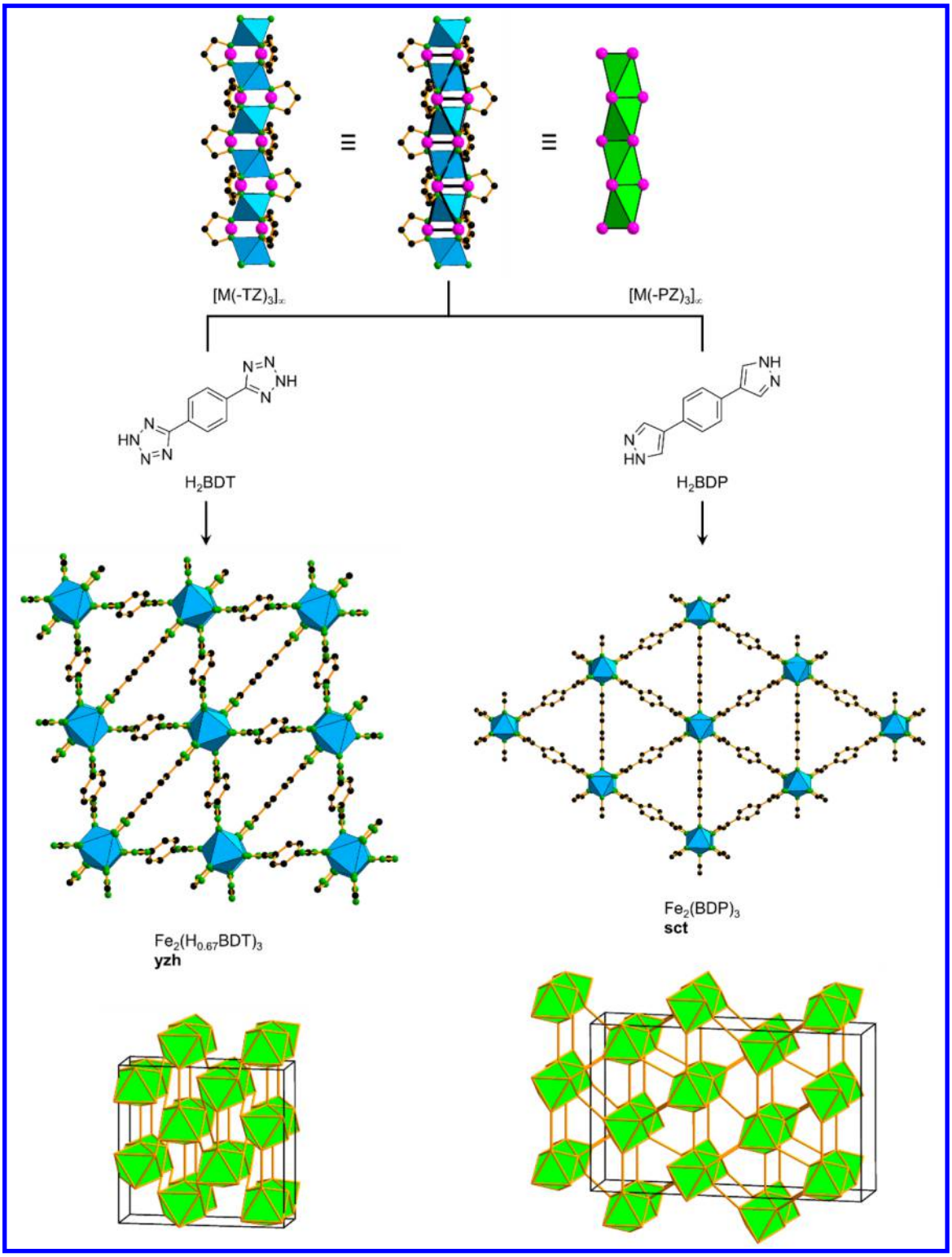

Figure 33. Linking of face-sharing octahedral SBUs, $[M(\text{-}PZ)_3]_\infty$ and $[M(\text{-}TZ)_3]_\infty$, with rigid, ditopic azolates. The resulting 7-c nets have the symbols **sct** and **yzh**, respectively.[159,166] Color code: black, C; green, N; blue polyhedra, metal; pink, points of extension.

of 4.5 × 4.5 Å.[154] Each lithium is coordinated by four carboxylate O in a tetrahedral environment, as commonly observed in lithium chemistry. The authors identified the topology of the structure as a "complicated" (4,8)-c binodal net, without taking the rod SBU into account. Following our approach, we describe the net as **zbn** with transitivity 2 7 and symmetry $I4_1/amd$.

4.3. MOF with Rod SBUs Arranged in Three Directions

A special example of a rod MOF is one with SBUs in a cubic 3-way rod-packing pattern.[39] We believe only one such compound has been reported so far. The framework in question has the formula $Zn_9(H_2O)_3(BTP)_8$ and is obtained from $Zn_3(BTP)_2$ under aqueous, basic conditions (Figure 31). In the $[M_3(H_2O)(\text{-}PZ)_8]_\infty$ SBU, one Zn^{2+} is tetrahedrally coordinated by four nitrogen

DOI: 10.1021/acs.chemrev.6b00346
Chem. Rev. XXXX, XXX, XXX−XXX

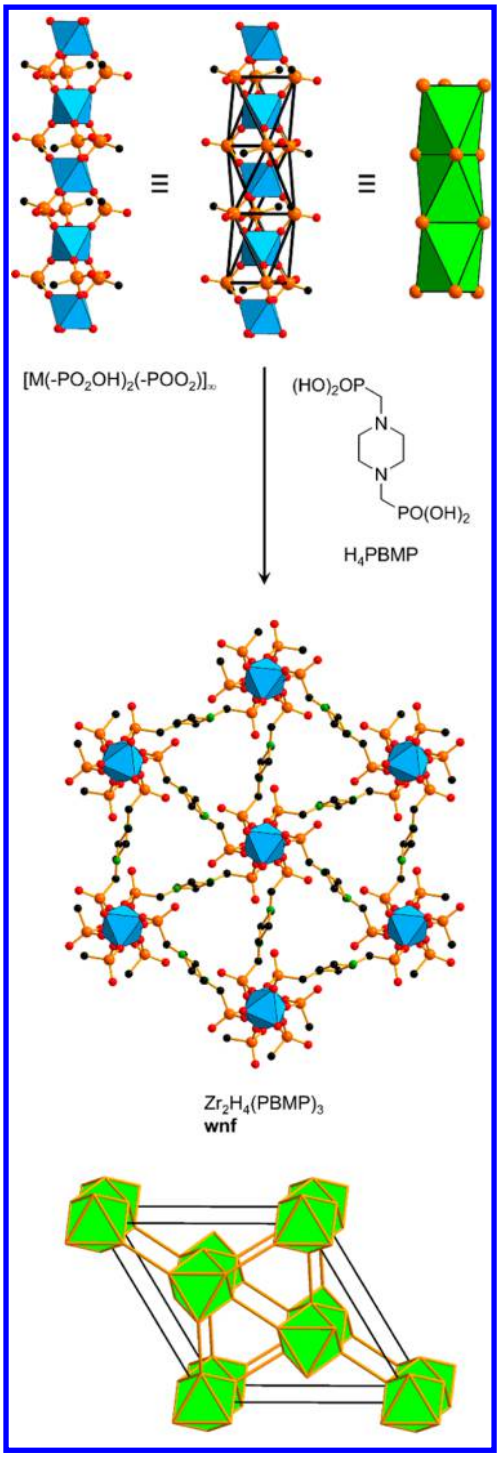

Figure 34. Crystal structure of $Zr_2H_4(PBMP)_3$ and its underlying uninodal 7-c net **wnf**.[169] Color code: black, C; red, O; green, N; orange, P; blue polyhedra, metal.

of two BTP linkers, the other by two nitrogen from two BTP linkers and two μ_2-H_2O molecules. If points of extension (pink spheres) are placed between two nitrogen atoms of BTP, we obtain an overall rod SBU composed of tetrahedra sharing opposite edges. Such rods propagate in all three dimensions and are linked by triangles, yielding to an overall binodal (3,6)-c **ltw** topology. This net has transitivity 2 6 and cubic symmetry $P\bar{4}3n$. We note that the authors reported a disordered structure with symmetry $Pn\bar{3}n$, but we found that an ordered structure with acceptable interatomic distances was obtained using coordinates identical to those in the original report (except for origin shift) in $P\bar{4}3n$. See also the Supporting Information. The rod pattern, symbol $\Pi^{\bullet}$, is one of the invariant cubic rod patterns sometimes named for the β-W (A15) structure.[34]

5. MOFS WITH SBUS OF EDGE- OR FACE-SHARED OCTAHEDRA

Rod SBUs composed of octahedra rely primarily on edge- or face-sharing. This in turn means that every vertex is at least 7-c or 6-c, respectively. We note that in some cases the distinction between distorted octahedral and distorted trigonal prismatic rods is rather difficult.

5.1. MOFs with SBUs of Edge- or Face-Shared Octahedra and Ditopic Linkers

Linked octahedra can have different ditopic linkers, and we first discuss those based on dicarboxylates. A large group of rod MOFs are composed of face-sharing $[M(-COO)_3]_\infty$ octahedra, where each lanthanide ion is in principle coordinated by eight oxygen from six carboxylate groups. Combination of this rod SBU with flexible succinic acid (H_2SUC) produces MIL-17, $Pr_2(SUC)_3$.[155] The underlying topology is a 7-c **oab** net with transitivity 2 6 and symmetry *Cmmm* (Figure 32, top). Since the discovery of MIL-17, a number of compounds based on **oab** nets have been reported, composed of different lanthanide carboxylates[156,157] and transition metal azolates.[158,159]

As previously detailed, different linker geometries can lead to differences in connectivity of rod SBUs. This is exemplified by linking $[M(-COO)_3]_\infty$ SBU through ADC (H_2ADC = 1,3-adamantanedicarboxylic acid) to produces MIL-83, $Eu_2(ADC)_3$.[160] This framework was first reported in 2004 and has the 7-c **swk** net with transitivity 1 4 and symmetry $P6_3/mcm$ (Figure 32, middle). MOFs with **swk** nets have also been obtained by linking face-sharing octahedral rod SBUs with rigid,[161] and flexible carboxylates,[162,163] as well as phosphonates.[91]

The use of angular, fluorinated linkers such as HFIPBB [H_2HFIPBB = 4,4′-(hexafluoroisopropylidene)-bis(benzoic acid)] leads to further structural diversity as exemplified by ITQMOF-1, $Ln_2(HFIPBB)_3$ (Ln = all lanthanides, except Pm)[164] and the polymorphic RPF-4 (RPF = rare-earth polymeric framework), $La_2(HFIPBB)_3$.[165] Both frameworks show the same rod SBUs but contain linkers with different angles, subtended at the $-C(CF_3)_2-$ moiety. These structural differences lead to different connectivity and therefore ITQMOF-2 has a **bvh** net and RPF-4 has a **fga** net, respectively (Figure 32, bottom). The 7-c **bvh** net has transitivity 2 7 and symmetry *Ccca*. In contrast, the **fga** net has transitivity 3 11. The symmetry is also orthorhombic, however *Pnna*.

Linear linking of related $[M(-PZ)_3]_\infty$ and $[M(-TZ)_3]_\infty$ face-sharing octahedra SBUs lead to different structures. In such SBUs, each metal is coordinated by six N of six pyrazolate or tetazolate moieties, respectively. Combination of this rod SBU with BDP (H_2BDP = 1,4-benzenedipyrazole) produces a framework with formula $Fe_2(BDP)_3$.[166] The authors described the beneficial effect of triangular channels on selective hexane isomer separation. The underlying topology of this framework is a 7-c **sct** with transitivity 2 8 and symmetry *Fddd* (Figure 33, right). This net has previously been obtained using carboxylates,[167] and structural changes have recently been studied under extremely high pressures.[168] If linking of the rod SBU is facilitated by BDT, instead of BDP, a different framework $Fe_2(H_{0.67}BDT)_3$ is obtained (Figure 33, left).[159] The

DOI: 10.1021/acs.chemrev.6b00346
Chem. Rev. XXXX, XXX, XXX−XXX

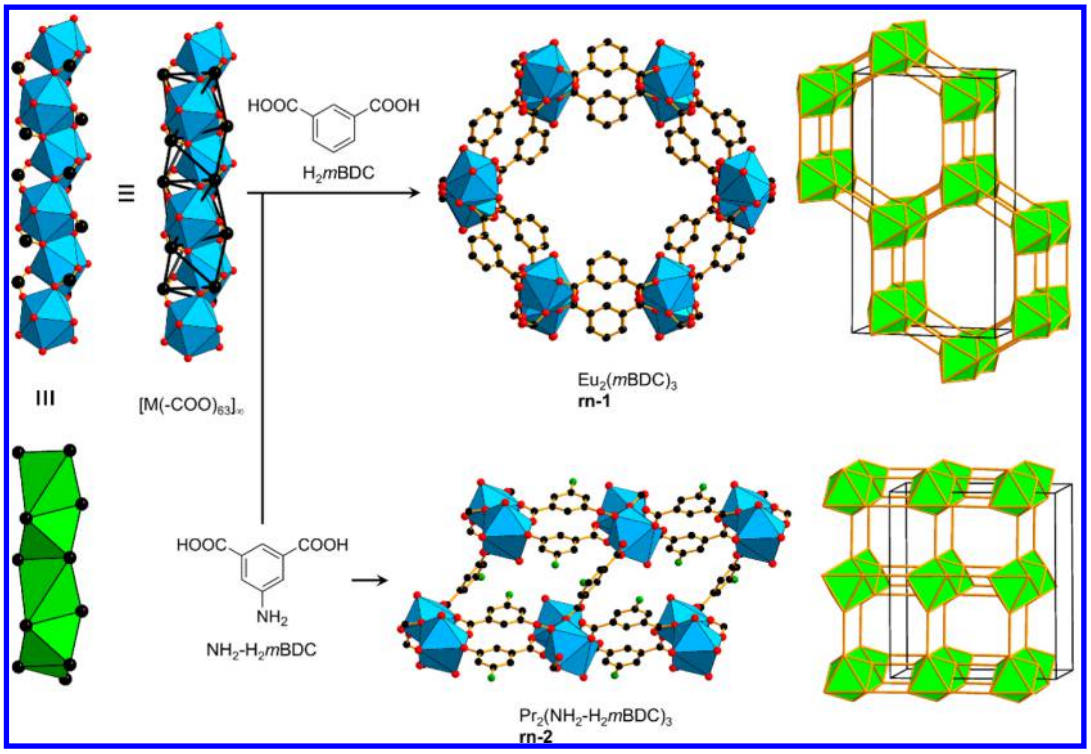

Figure 35. Linking of face-sharing octahedral SBUs, $[M(-COO)_3]_\infty$, with angular dicarboxylates leading to different nets.[171,172] Color code: black, C; red, O; green, N; blue polyhedra, metal.

structure shows what has been described as a "squashed rhombohedral pattern" with a new topology and the symbol **yzh**. This binodal net has transitivity 2 8. The symmetry is also *Fddd*. We point out that **sct** and **yzh** are quite similar; however, the subtle difference lies in the connectivity between the rods which are parallel for **sct** and antiparallel (crisscross) for **yzh**, when viewed along [010].

Face-sharing octahedra SBUs can also be formed by coordination of flexible phosphonate linkers, very similar to those utilized in the synthesis of Ni-STA-12.[91] The rod SBU with formula $[M(\text{-}PO_2OH)_2(\text{-}POO_2)]_\infty$ produces $Zr_2H_4(PBMP)_3$, when combined with PBMP [H_4PBMP = piperazine-*N*,*N*′-bis(methylenephosphonic acid)] linkers (Figure 34).[169] In this framework, each Zr^{4+} has octahedral coordination, bound by six oxygen of the phosphonate groups, and in contrast to Ni-STA-12, the nitrogen moieties of the linker remain unbound. The underlying topology is a 7-c **wnf** net with transitivity 1 4 and symmetry $R\bar{3}m$. Frameworks of the same **wnf** topology can also be obtained through the diverse chemistry of azolates.[159,170]

Some materials based on rods of face-sharing octahedra $[M(-COO)_3]_\infty$, as previously described, have more complicated rod nets. Figure 35 (top) shows the linking of this rod SBU with angular *m*BDC (H_2*m*BDC = benzene-1,3-dicarboxylic acid) to produce $Eu_2(mBDC)_3$.[171] The underlying topology, identified as **rn-1**, has transitivity 3 10 and symmetry *Pnna*. When the same rod SBU is linked through the similar NH_2−*m*BDC (NH_2−H_2*m*BDC = 5-amino-benzene-1,3-dicarboxylic acid), a framework of similar composition $Pr_2(NH_2\text{−}H_2mBDC)_3$ is obtained (Figure 35, bottom).[172] The net **rn-2** also has transitivity 3 10. However, the symmetry is monoclinic *A*2/*n*. The difference between both nets are the angles subtended at the rod SBU, leading to quasi-hexagonal pores in **rn-1** and rectangular-shaped pores in **rn-2**, respectively.

Bifunctional linkers, containing carboxylate and pyridyl moieties lead to different edge-sharing octahedral SBUs of formula $[M(-COO)_2(-PY)_2]_\infty$. Each metal center is coordinated in an octahedral environment by four oxygen of bridging carboxylates and two pyridines. The use of a rigid, linear linker PBA (HPBA = 4-(pyridin-4-yl)benzoic acid) produces a framework, termed MCF-44 (MCF = metal-carboxylate framework), $Fe(PBA)_2$, that consists of an SBU of only opposite edge-sharing octahedra (Figure 36).[173] In the original contribution, the authors described the net as (3,6)-c **rtl**, assuming a 6-c metal center and a triangular linker. They also utilized the approach detailed herein and obtained a new (5,8)-c binodal net, **hlz**, with transitivity 2 4 and symmetry $P4_2/mnm$. Frameworks of the same **hlz** topology have previously been reported based on different linker length but have always been described as binodal **rtl** nets (**rtl** is the net of the rutile form of TiO_2).[174−176] Such deconstruction is misleading since it suggests the existence of discrete, rather than rod SBUs.

The use of an angular linker can instead result in a differently shaped rod SBU of the same formula, $[M(-COO)_2(-PY)_2]_\infty$. Figure 37 details the framework $Mn(mPBA)_2$ (H*m*PBA = 3-(pyridin-4-yl)benzoic acid), termed MCF-34, and the SBU that contains alternating opposite and adjacent edge-sharing octahedra.[173] It was demonstrated that this framework undergoes deformation on the incorporation and release of guest molecules.[177] The (5,8)-c **zhl** net is therefore different with transitivity 2 8. The symmetry of **zhl** (*I*2/*a*) is lower than that of **hlz** ($P4_2/mnm$).

5.2. MOFs with SBUs of Edge- or Face-Shared Octahedra and Polytopic Linkers

The combination of face-sharing octahedra SBUs, $[M(-COO)_3]_\infty$, with a triangular BTTN linkers [H_3BTTN = 5,5′,5″-(benzene-1,3,5-triyl)tris(1-naphthoic acid)] produces a hexagonal framework termed UTSA-30, with the formula Yb(BTTN).[29] In this structure

DOI: 10.1021/acs.chemrev.6b00346
Chem. Rev. XXXX, XXX, XXX−XXX

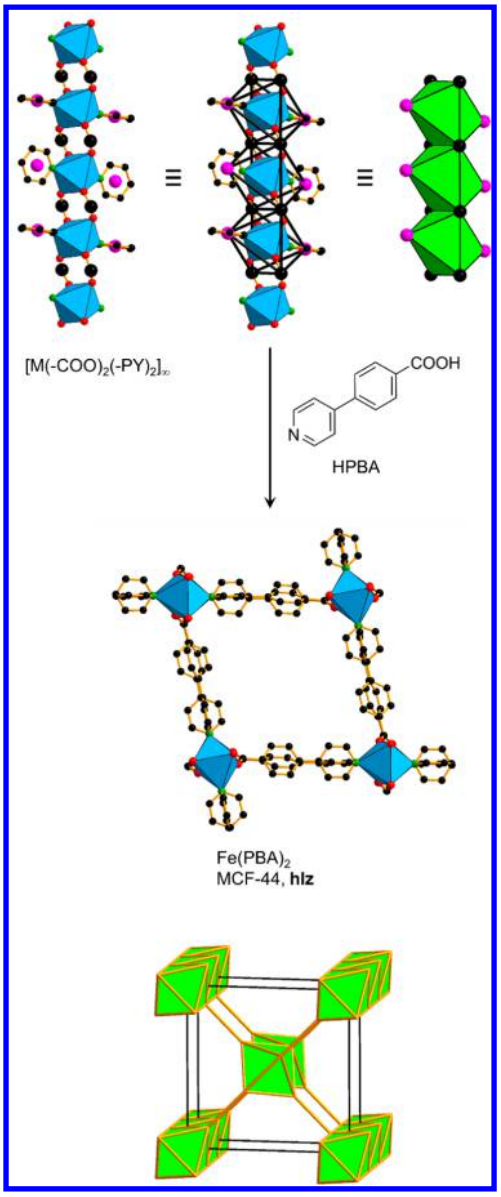

Figure 36. Combination of opposite edge-sharing octrahedral SBUs $[M(-COO)_2(-PY)_2]_\infty$ and the underlying **hlz** net.[173] Color code: black, C; red, O; green, N; blue polyhedra, metal; pink, points of extension.

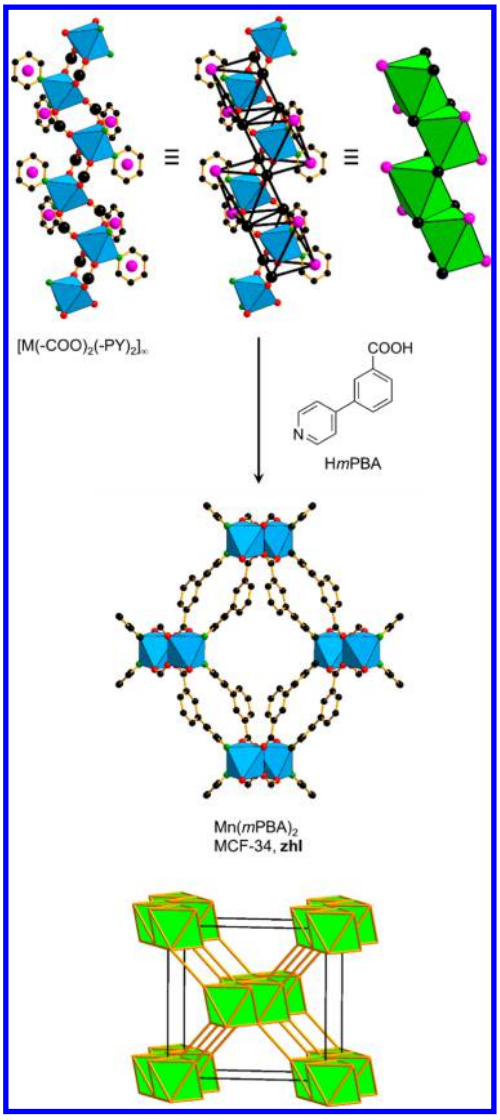

Figure 37. Combination of opposite and adjacent edge-sharing octrahedral SBUs $[M(-COO)_2(-PY)_2]_\infty$ and the underlying **zhl** net.[173] Color code: black, C; red, O; green, N; blue polyhedra, metal; pink, points of extension.

(Figure 38), each Yb^{3+} has octahedral coordination environment, bound by six carboxylate O that are bridging to adjacent metal centers along the rod. For lanthanide ions, this relatively low coordination number is rather uncommon. The hexagonal symmetry is caused by the orientation of the octahedra with their 3-fold axis along [001]. The underlying topology is a (3,7)-c **hyb** net with transitivity 2 4 and symmetry $P6_3/mmc$.

When face-sharing octahedra, $[M(-COO)_3]_\infty$, are joined together with other tri- or hexatopic linkers, the resulting structures are different. The SBU is composed of lanthanide centers that are nine-coordinated by six distinct carboxylates to provide an overall octahedral shape. A compound of formula Ce(NTBPC) [H_3NTBPC = 4′,4‴,4⁗′-nitrilotris(([1,1′-biphenyl]-4-carboxylic acid))], termed FIR-8, is produced by reaction with the symmetrical, tritopic H_3NTBPC linker (Figure 39, top).[178] In the original contribution, the structure was correctly identified as a rod MOF; however, a topological analysis was not provided. We identify the underlying topology as net **hyc** with transitivity 4 9 and symmetry *Ima*2. Joining of the same face-sharing octahedra with an unsymmetrical linker [i.e., CMPDB (H_3CMPDB = 4,4′-((2-((4-carboxyphenoxy)methyl)-2-methylpropane-1,3-diyl)bis(oxy))dibenzoic acid)], a framework of formula Er(CMPDB) was produced (Figure 39, middle).[179] The triangular pyramid-shaped linker therefore leads to a different topology **hyd**. This net has transitivity 4 9 and symmetry $Cmc2_1$. The subtle difference to **hyc** lies in the connection of triangles to the rod SBUs and the chiral axis. Isostructural compounds using other lanthanide salts have also been reported and were investigated toward luminescence properties.[180] If hexatopic linkers, such as H_6L (Figure 39, bottom) are used to join $[M(-COO)_3]_\infty$ SBUs, frameworks with composition Ln_2(L) (Ln = La, Eu, Tb) were obtained.[181] The underlying topology (**rn-3**, see Supporting Information) is complicated with transitivity 7 19. The symmetry is $I2_1$.

The combination of adjacent edge-sharing octahedra SBUs, $[M(-COO)_3]_\infty$, together with DDPP linkers (H_4DDPP = 2,5-di(2′,4′-dicarboxylphenyl)pyridine acid) produces a MOF with formula Eu(DDPP).[182] In this framework (Figure 40),

DOI: 10.1021/acs.chemrev.6b00346
Chem. Rev. XXXX, XXX, XXX−XXX

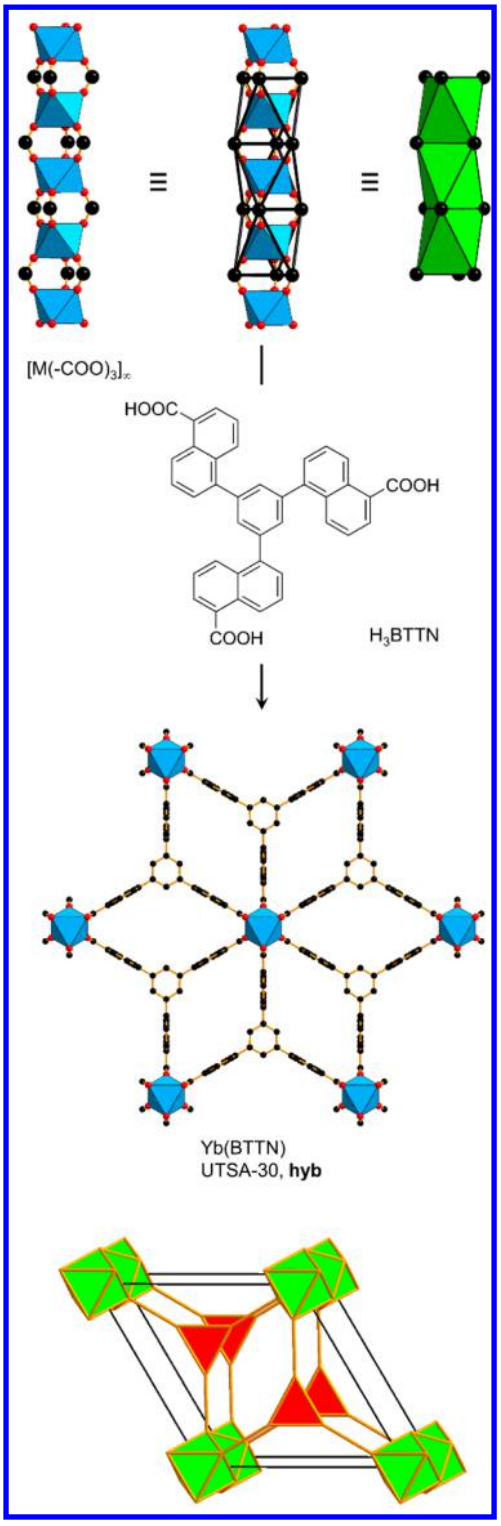

Figure 38. Linking of face-sharing octahedra with a triangular tricarboxylate produces UTSA-30, a framework with **hyb** topology.[29] Color code: black, C; red, O; blue polyhedra, metal.

the octahedral SBUs are arranged in a zigzag fashion; however, different to the rods in the aforementioned **zhl** net. In the original contribution, the authors performed the correct deconstruction of the net into edge-sharing octahedra rod SBUs and two linked triangles. However, determination of the topology using TOPOS was done incorrectly and resulted in a uninodal 6-c **msw** net. In contrast, we find the net (**rn-4**) to be rather complicated (transitivity 5 13) and symmetry *I*2/*a*.

6. MOFS WITH SBUS OF EDGE- AND/OR FACE-SHARED TRIGONAL PRISMS

Deconstruction of rod SBUs into rods of trigonal prisms usually yields edge- and face-sharing polyhedra. In contrast to the octahedron, the trigonal prism contains different faces, two triangles and three rectangles, which facilitates different connectivity between them. This in turn means that every vertex is either 5-c, in the case of face-sharing, or 6-c in the case of edge-sharing.

6.1. MOFs with SBUs of Edge- and/or Face-Shared Trigonal Prisms and Ditopic Linkers

First, we introduce rod SBUs composed of triangular face-sharing trigonal prisms. When such $[M(-COO)_3]_\infty$ SBUs are joined together with linear linkers, the structures are different depending on linker geometry as well as flexibility. The SBU is composed of lanthanide centers that are seven coordinated by six different carboxylates that form the overall trigonal prismatic geometry. The remaining oxygen is provided by a solvent molecule (DMF). A compound of formula $Er_2(m\text{PYDC})_3$ (H_2mPYDC = pyridine-3,5-dicarboxylic acid) is produced through reaction with angular *m*PYDC, where the pyridyl-moiety remains uncoordinated (Figure 41, top).[161] The authors have not determined the topology; however, a simplification was carried out by considering only metal centers, leading to a 5-c **bnn** net. However, we identify the underlying topology, based on linked trigonal prisms, as a uninodal 5-c net and assigned the symbol **ttw**. This net has transitivity 1 3, the minimum possible. The symmetry is *P*6/*mmm*. Other frameworks that have **ttw** topology were synthesized from linear dicarboxylates,[183,184] or different metal centers and used for sensing applications.[185] Joining of the same trigonal prism rod SBUs with the flexible linker ADIP (H_2ADIP = adipic acid) produced a framework of formula $Pr_2(ADIP)_3$, termed GWMOF-6 (GWMOF = George Washington University MOF, (Figure 41, bottom).[186] The underlying trinodal net (**rn-5**, see Supporting Information) has transitivity 3 8. The symmetry is *Pbcn*. Isostructural compounds were reported with different lanthanide centers and investigated toward luminescence properties.[187]

Another class of frameworks is based on edge- and face-sharing trigonal prisms of the general formula $[M_2(-COO)_6]_\infty$, that are joined together with ditopic carboxylate linkers. In detail, the rod SBU is composed of lanthanide centers, each of them eight-coordinated by five carboxylate O and a terminal water ligand. In addition, two Ln^{3+} are bridged by two μ_2-oxygen from carboxylates. The so-obtained trigonal prisms are face- and edge-sharing in an alternating fashion. A compound of formula $Nd_2(CHDC)_3$ (H_2CHDC = cyclohexane-1,4-dicarboxylic acid) was produced through reaction with ditopic CHDC (Figure 42, top).[188] The authors have identified the infinite rod SBUs; however, a precise topology classification was not attempted. We therefore describe the underlying topology as a (5,6)-c net **zbf**. This net has transitivity 2 6 and symmetry is *Pmmm*. Joining of the same trigonal prism SBU with the rigid ditopic linker BDC, under urothermal conditions, produced a framework of formula $Cd_3(BDC)_3$ (Figure 42, middle).[189] The rigid, linear linker therefore leads to a different, but related topology, **zbc**. The net has transitivity 3 7 and symmetry *C*2/*m*. If a longer ditopic linker [i.e., BPDC (H_2BPDC = [1,1′-biphenyl]-4,4′-dicarboxylic acid)] is used instead to join $[M_2(-COO)_6]_\infty$ SBUs, frameworks with composition $Ln_2(BPDC)_3$ (Ln = Tb, Ho, Er, Y) were obtained (Figure 42, bottom).[190] The underlying net topology (**rn-6**, see Supporting Information) has transitivity

DOI: 10.1021/acs.chemrev.6b00346
Chem. Rev. XXXX, XXX, XXX−XXX

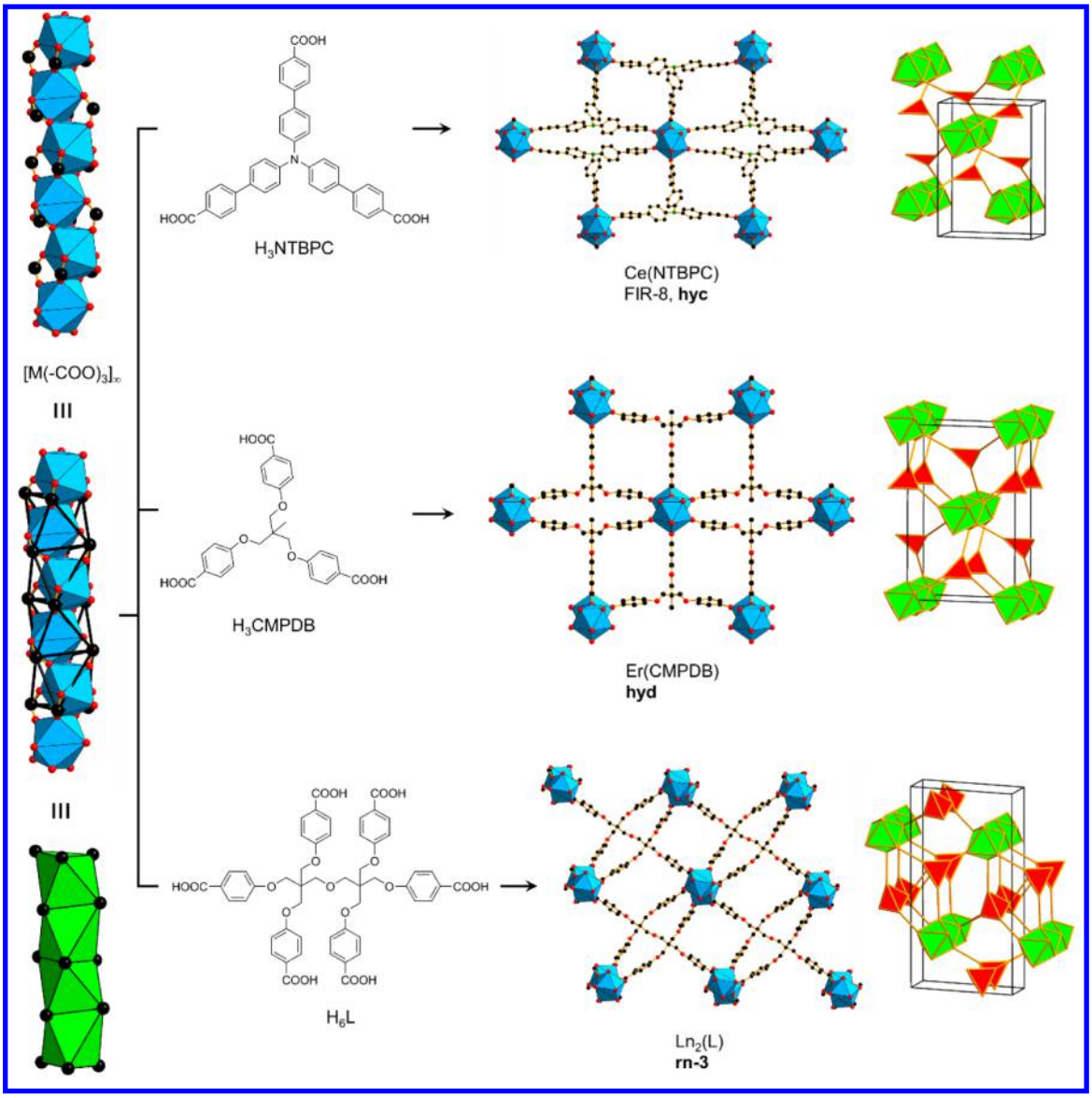

Figure 39. Linking of face-sharing octahedra with a tritopic linkers of different shape and a hexatopic linker leads to frameworks with **hyc**,[178] **hyd**,[179] and **rn-3** topologies,[181] respectively. Color code: black, C; red, O; green, N; blue polyhedra, metal.

3 9 and symmetry *C*2/*c*. Frameworks with this underlying net (**rn-6**) have been synthesized with a variety of linear and angular dicarboxylates.[189,191,192] The differences between these three nets are the orientation of the rod SBUs with respect to each other as well as their connectivity.

Edge- and face-sharing trigonal prisms of a different composition, $[M_2Cl(-COO)_6]_\infty$, produce isostructural $Ln_2Cl(1,4\text{-NDC})_3$ (H_2-1,4-NDC = naphthalene-1,4-dicarboxylic acid, Ln = La, Ce, Pr, Nd, Sm, Eu, Gd, Tb, Dy, Ho, Er, Y) when combined with ditopic 1,4-NDC linkers, in ionic liquids (Figure 43).[193] The rod SBU is particularly composed of rare earth centers, each of them seven-coordinated in a monocapped trigonal prismatic geometry by six carboxylate O and one μ_2-Cl anion. If carboxylate C are considered as points of extension, trigonal prisms in an alternating face- and edge-sharing manner are obtained. In an attempt to analyze the topology of the net, the authors took the metal centers as 7-c nodes and the linkers as 4-c nodes. We prefer the description as a rod MOF and therefore identified the underlying topology as a (5,6)-c net **zbh** with transitivity 2 7 and symmetry *Imma*.

The linking of quadrangular face-sharing trigonal prism SBUs, $[NaM(-COO)_4]_\infty$, with an angular, ditopic BPODC linker produces a framework with the formula $NaTb(BPODC)_2$.[194] In this structure (Figure 44) that contains rhombic-shaped channels, each Tb^{3+} is eight-coordinated, exclusively by carboxylate O, and the charge is balanced through coordinated sodium ions. We identified the underlying topology as a (5,7)-c **zbd** with transitivity 2 6 and symmetry *Cmcm*.

6.2. MOFs with SBUs of Edge- and/or Face-Shared Trigonal Prisms and Polytopic Linkers

The linking of triangular face-sharing trigonal prism SBUs with general formula $[M(-COO)_3]_\infty$, together with triangular BTB linkers (H_3BTB = 1,3,5-benzenetrisbenzoic acid) produces a framework, Tb(BTB), termed MIL-103 (Figure 45).[195] The SBU is composed of nine coordinated Tb^{3+}, with eight oxygen from carboxylate groups and one from a water molecule. The authors originally determined the topology as the (3,5)-c **hms** net. We identified the underlying topology as a binodal (3,5)-c **tpr** net with transitivity 2 4 (the minimum possible) and

DOI: 10.1021/acs.chemrev.6b00346
Chem. Rev. XXXX, XXX, XXX−XXX

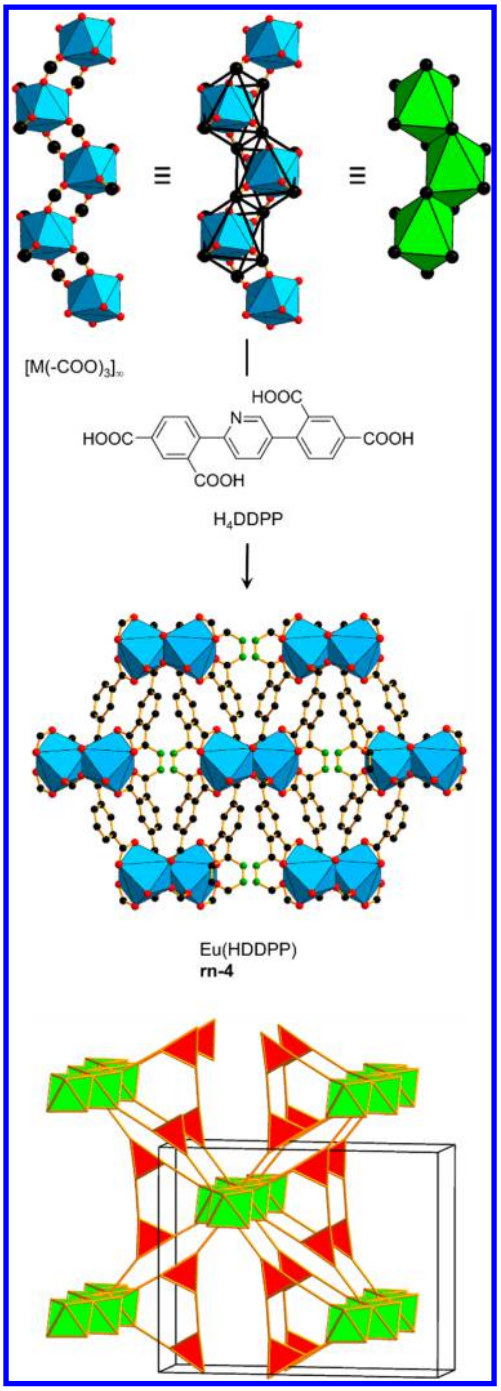

Figure 40. Combination of adjacent edge-sharing octahedra SBUs with a tetratopic linker produces a framework with a 5-nodal net.[182] Color code: black, C; red, O; green, N; blue polyhedra, metal.

symmetry $P\bar{6}m2$. After its first synthesis in 2005, numerous examples of **tpr** nets have emerged, being isostructural to MIL-103 using other lanthanides or main group elements.[196−199] However, when the benzene moiety is replaced by naphthalene in an expanded linker, different topologies are obtained.[200,201] Another way to deconstruct such **tpr** nets will be given in section 13.3.

When edge- and face-sharing trigonal prisms, $[M_2(-COO)_6]_\infty$, are joined together with tritopic linkers, such as NTB (H_3NTB = 4,4′,4″-nitrilotribenzoic acid), a framework of formula Tb(NTB) is obtained (Figure 46).[202] The SBU is the same as described for **zbf** and **zbc** nets. In the original contribution, the topology was not discussed, but we identified it as net **zbi** with transitivity 4 8 and symmetry *Immm*.

7. MOFS WITH SBUS OF EDGE-SHARED SQUARE PYRAMIDS

The rod SBUs composed of square pyramids discussed here are exclusively edge-sharing polyhedra, which have one square and four triangular faces. Such squares are often associated with open metal sites, and we therefore recommend to not dissect them into triangles, even if they could be because of relatively short distances between points of extension.

7.1. MOFs with SBUs of Edge-Shared Square Pyramids and Ditopic Linkers

We first discuss linked square pyramids based on ditopic linkers. A framework, termed GWMOF-3, $Pr_2(ADIP)_3$ was synthesized by linking $[M_2(-COO)_6]_\infty$ SBUs together with flexible ADIP (Figure 47).[186] In this structure, each lanthanide center is coordinated by ten oxygen, eight of them belonging to five carboxylate groups and the remaining two are water molecules. The authors have identified the infinite rod SBUs; however, a precise topology classification was not given. We therefore determine the underlying topology as a (5,6)-c net **zbl** with transitivity 2 5 and symmetry *Fmmm*.

Joining of a similar linked square pyramid SBU of formula $[M(-COO)_3(HCOOH)]_\infty$ with the rigid ditopic linker BPDC produced a framework of formula $Ln_2(BPDC)_3(HCOOH)_2$ (Ln = Eu, Sm, La, Ce, Gd, and Nd).[203] In Figure 48, we detail the SBU that is composed of the lanthanide center, coordinated by seven oxygen from six carboxylate groups and a terminal formic acid molecule. The points of extension that are represented by BPDC carboxylate C are depicted as large spheres, whereas formic acid is not a part of the framework. We identified this net as **zbo** with transitivity 3 9 and symmetry *C*2.

When linking $[M(-COO)_3]_\infty$ SBUs together with PDC (H_2PDC = 2,7-pyrenedicarboxylic acid), MOF-80 of formula $Tb_2(PDC)_3$ was produced (Figure 49).[6] The SBU is composed of Tb^{3+} centers that are in turn eight-coordinated by five different carboxylates that produce the overall square pyramidal geometry. Simplification of the framework, in the original contribution, revealed a **pcu** net. However, we prefer to deconstruct the topology based on rod SBUs, leading to a rather complicated net, termed **rn-7** (see Supporting Information), with transitivity 3 10. The symmetry is triclinic $P\bar{1}$. Other frameworks that show the same topology (isoreticular) were obtained from flexible[204,205] or unsymmetrical dicarboxylates.[120]

It is noted that, despite diversity of linkers, all rod MOFs based on edge-sharing square pyramids described here are composed of lanthanide (or rare earth) metals. Lanthanide ions are known to exhibit high coordination numbers and tend to form 1-periodic rod SBUs in the absence of chemical control such as water-repelling additives. Elegant examples of how to exert control over formation of discrete rare earth SBUs through the use of modulators have recently been reported, leading to **fcu** and **gea** MOFs.[206] Many lanthanide rod MOFs have also been studied for various applications, summarized in recent review articles.[207,208]

7.2. MOFs with SBUs of Edge-Shared Square Pyramids and Polytopic Linkers

The linking of edge-sharing square pyramid SBUs of general formula $[M(-COO)_3]_\infty$ or $[M_2(-COO)_6]_\infty$, respectively, with triangular linkers produced two frameworks with the same topology. MIL-112, La(BCMTPA), (H_3BCMTPA = 4-[3,5-Bis(1-carbonylmethyl-1H-[1,2,3]triazol-4-yl)-phenyl]-[1,2,3]-

DOI: 10.1021/acs.chemrev.6b00346
Chem. Rev. XXXX, XXX, XXX−XXX

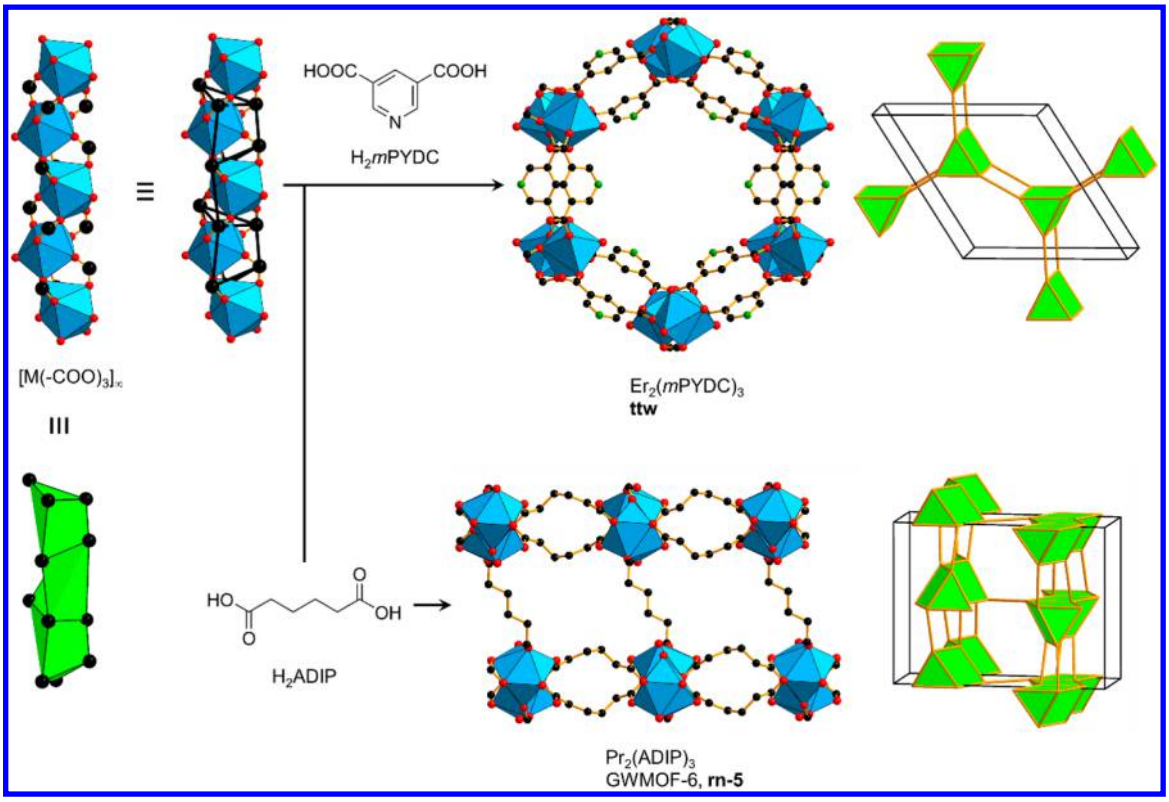

Figure 41. Linking of triangular face-sharing trigonal prisms with rigid and flexible ditopic linkers to produce frameworks with **ttw**[161] and **rn-5**[186] topology. Color code: black, C; red, O; green, N; blue polyhedra, metal.

triazol-1-yl]acetic acid) is composed of $[M(-COO)_3]_\infty$ and BCMTPA linkers (Figure 50).[209] The lanthanide centers LaO_{10} are coordinated by eight oxygen from five carboxylate groups and two terminal water molecules. Four of these eight carboxylate oxygen are bound in a μ_2-fashion and facilitate edge-sharing polyhedra. The authors described the topology as ABA staggered stacking of four (square) and eight (rectangle) membered rings. In addition, they emphasize the importance of some flexibility in the linker moiety to obtain this particular compound. We omit the description of topology here, since the 6-nodal net is complicated (transitivity 6 14) and has low symmetry $P2_1/c$.

Another framework, La(CPIA), (H_3CPIA = 5-(4-carboxyphenoxy)-isophthalic acid), contains a flexible, asymmetric linker joining $[M_2(-COO)_6]_\infty$ rod SBUs (Figure 51).[210] The La^{3+} are coordinated by nine oxygen, from two chelating and three bridging carboxylates as well as two water molecules. The authors determined the topology based on a La_2 dimeric unit (8-c) and the linker which is bound to two La-centers and the remaining carboxylate bridges two La-centers (4-c). They described the structure as (4,8)-c net, but we prefer the assignment to be **rn-8**, a net with transitivity 4 8 and symmetry $C2/c$ (for details, see Supporting Information).

Linking of edge-sharing square pyramid SBUs in a different manner, rod SBUs with helical shapes can be obtained. First, we discuss a framework with formula Yb(BPT) (H_3BPT = biphenyl-3,4′,5-tricarboxylic acid) built from $[M(-COO)_3]_\infty$ and H_3BPT linkers (Figure 52).[211] The Yb^{3+} centers are coordinated by six oxygen from five carboxylate groups and one terminal water molecule. The topology was determined as a 4-nodal **rnc**.[4] However, we obtained the **zcd** net with transitivity 6 13 and symmetry $P4_3$. By looking at several structures, it seems that the introduction of 1,3-BDC moieties, where carboxylates bind to the same SBU, could be a design element to obtain helical rod, rather than straight SBUs. We will summarize this observation later and exemplify it on our recently synthesized MOF-910 (**tto**) in section 9.

Flexible, tritopic phosphonate linkers [i.e., TTTP (H_6TTTP = 2,4,6-trimethylbenzene-1,3,5-triyl)tris(methylene)triphosphonic acid) can also facilitate the formation of rod SBUs $[M_3(-PO_2OH)_3]_\infty$ (Figure 53].[212] The resulting framework with formula Al(H_3TTTP) contains hexagonal channels running along [001]. Each Al^{3+} is octahedrally coordinated (AlO_6) by six oxygen of five phosphonate groups and contains an additional water ligand. Considering the phosphorus as points of extension, similar to carbon in the case of carboxylates, we obtained a net composed of linked square pyramids connected through triangles. This 6-nodal net was assigned as **zbq**, which has 13 kinds of edges and symmetry $R\bar{3}$. Since the 1,3-phosphonate moieties bind to the same rod, we also observe helix formation here.

A remarkably beautiful net is obtained by linking of edge-sharing square pyramid SBUs with bifunctional, triangular *m*PYDC, containing two carboxylate and one pyridyl moiety (Figure 54).[213,214] The SBU is composed of $[M(-COO)_2(-PY)]_\infty$, where each Mg^{2+} is octahedrally coordinated by four carboxylate O, one pyridine N, and an additional water molecule. Rod SBUs composed of square pyramids are obtained when carboxylate C and pyridine N are considered as points of extension and form a 6-fold helix along [001]. The resulting framework with formula Mg(*m*PYDC) is chiral, and the authors determined the topology based on the coordination of metal and linker, leading to a 5-c net. From our viewpoint, this description omits important properties of the net. We therefore describe the underlying topology as a net with symbol **zbp**, with transitivity 4 8 and symmetry $P6_122$.

DOI: 10.1021/acs.chemrev.6b00346
Chem. Rev. XXXX, XXX, XXX−XXX

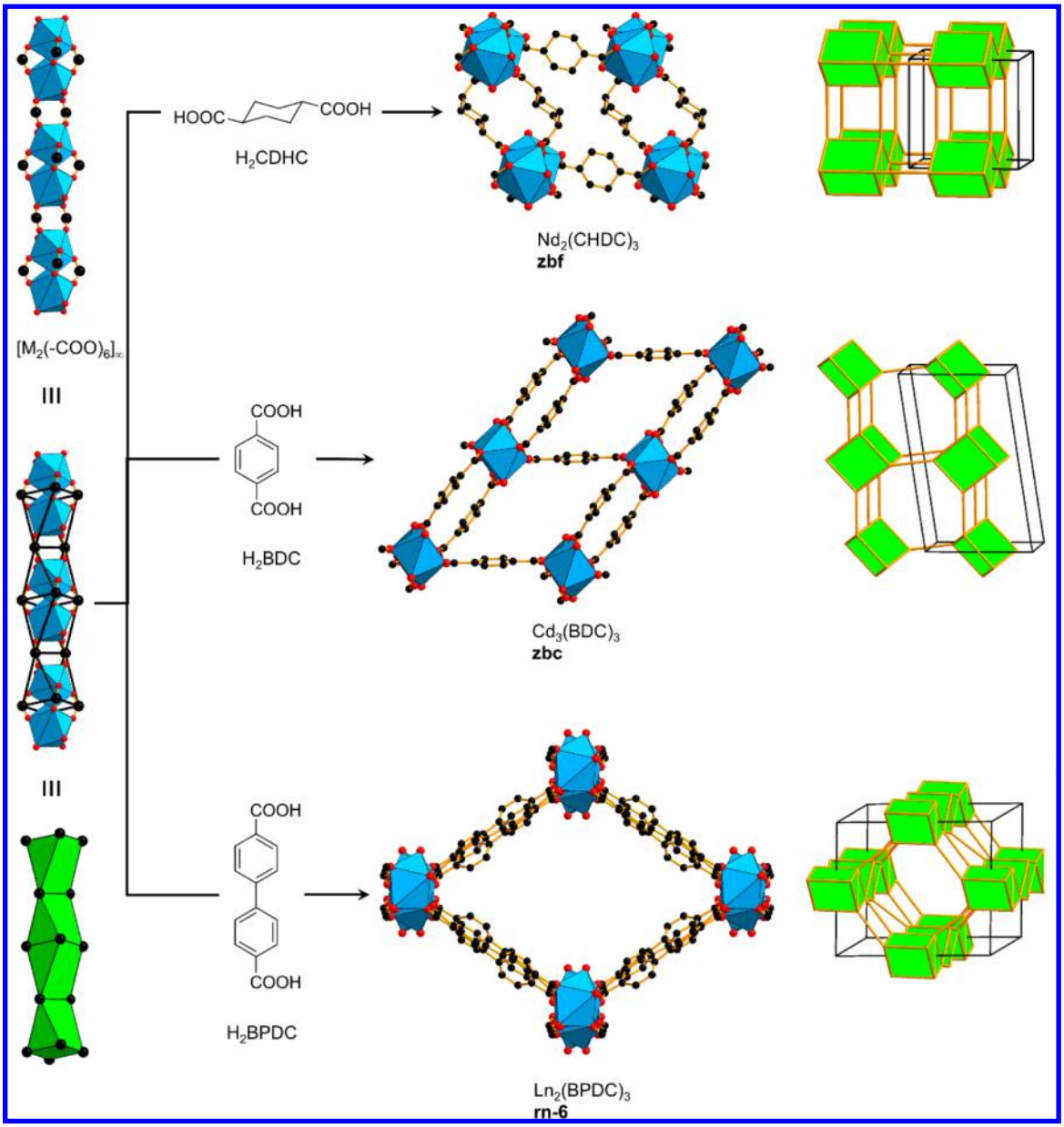

Figure 42. Linking of face- and edge-sharing trigonal prisms with ditopic linkers, leading to frameworks with **zbf**,[188] **zbc**,[189] and **rn-6** topology.[190] Color code: black, C; red, O; blue polyhedra, metal.

8. MOFS WITH SBUS OF FACE-SHARED TETRAGONAL PRISMS

Rod SBUs in this category are composed of either linked tetragonal prisms or antiprisms and are all connected by face-sharing. They can be found in carboxylates as well as sulfonates and are usually 5-c in the case of regular prisms or 7-c in the case of antiprisms.

8.1. MOFs with SBUs of Face-Shared Tetragonal Prisms and Ditopic Linkers

Face-sharing tetragonal prism SBUs of formula $[M_2O_2(-COO)_4]_\infty$ linked by simple ditopic BDC produced a framework, termed MIL-140A, ZrO(BDC).[215] Other isoreticular variants were obtained by replacing BDC through longer linkers (MIL-140B-D). Figure 55 shows the rod-SBU, where each Zr^{4+} is seven coordinated with three μ_3-oxygen and four carboxylate oxygen. The higher hydrolytic stability of this MOF, in comparison to UiO-66,[216] was attributed to the inorganic rod Zr oxide chains versus the isolated $Zr_6O_4(OH)_4$ clusters. The SBU was described as either a corner-sharing double chain or chains of edge-sharing dimers of zirconium-polyhedra, which the authors simplified to a uninodal 6-c β-Sn topology, **bsn**.[217] In accordance with our approach, the SBU is deconstructed differently, leading to a 5-c **gui** net with transitivity 3 6 and symmetry *Imma*. The face-sharing tetragonal prisms run along [010] in undulating fashion and are linked through their shortest inter-rod distances.

In contrast, face-sharing tetragonal antiprism SBUs of the same formula, $[M_2O(-COO)_4]_\infty$, were formed when angular *m*BDC was used instead of linear BDC (Figure 56).[218] The so-produced framework with formula $In_2O(mBDC)_2$ contains In^{3+} that are coordinated in a distorted octahedral environment with four oxygen from four different carboxylate groups and two μ_3-oxygen. The carboxylate C atoms form tetragonal antiprism SBUs. The authors have also discussed the structure as double-chains, similar to what was detailed above for the **gui** net. After deconstruction of this framework in the same manner, we

DOI: 10.1021/acs.chemrev.6b00346
Chem. Rev. XXXX, XXX, XXX−XXX

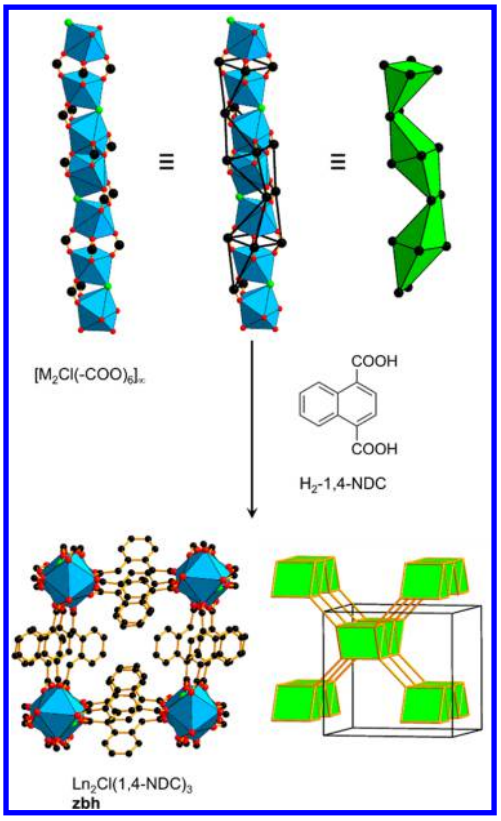

Figure 43. Linking of face- and edge-sharing trigonal prisms with ditopic linkers, leading to an anionic framework with **zbh** topology.[193] Color code: black, C; red, O; green, Cl; blue polyhedra, metal.

determined a 7-c **svq** net, with transitivity 1 4 and symmetry $I4_1/mcm$.

Face-sharing tetragonal prism SBUs can also be composed of other functional groups such as sulfonates, or bifunctional linkers containing carboxylate and pyridyl moieties. First, we introduce framework of formula Ln(OH) (NDS) (Ln = La, Pr, Nd, H_2NDS = 1,5-naphthalenedisulfonic acid), termed LnPF-1 (LnPF = lanthanide polymeric framework), that is built of $[M_2(OH)_2(-SO_2)_4]_\infty$ rod SBUs (Figure 57, left).[219] In such structures, each Ln^{3+} is eight-coordinated (LnO_8) by two μ_2-OH groups, five sulfonate O, and one water molecule. If a dimer is considered, the points of extension are represented by the sulfur moieties of the $[M_2(OH)_2(-SO_2)_4]_\infty$ building unit and thus produce a tetragonal prism SBU. Linear linking through a naphthalene core then leads to an underlying **fee** net with transitivity 1 3 and symmetry $P4/mmm$. Another framework, $Co_3(OH)_2$(*o*PYDC)$_2$ (H_2*o*PYDC = pyridine-2,4-dicarboxylic acid) with the same topology was produced through combination of mixed linkers with $[M_3(OH)_2(-COO)_4(-PY)_2]_\infty$ SBUs (Figure 57, right).[220] In this compound, termed CUK-1 (CUK = Cambridge University-KRICT), both Co^{2+} are coordinated in a distorted octahedral environment by two carboxylate O, two μ_3-OH, one pyridine N, and one water ligand. The SBU itself is also slightly undulated; however, the angular nature of the linker compensates for that and leads to the overall **fee** topology. Isostructural frameworks, obtained from different metal sources,[221] as well as the use of mixed linkers have also resulted in **fee** nets.[222]

8.2. MOFs with SBUs of Face-Shared Tetragonal Prisms and Polytopic Linkers

There are only very few examples of tetragonal prism SBUs linked through polytopic sulfonates, and they are based on

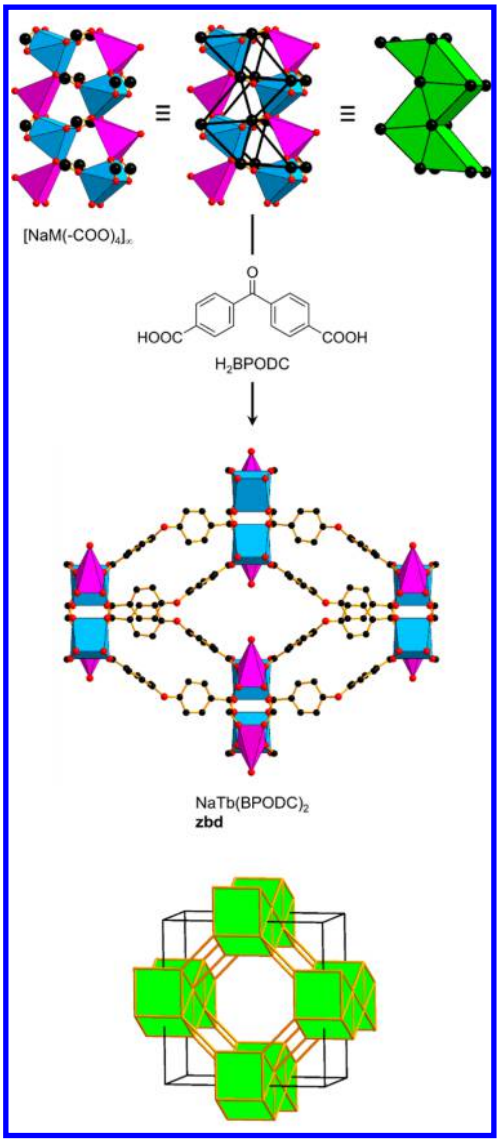

Figure 44. Linking of quadrangular face-sharing trigonal prism SBUs with an angular ditopic linker to produce NaTb(BPODC)$_2$, showing **zbd** topology.[194] Color code: black, C; red, O; blue polyhedra, metal; pink polyhedra, Na.

face-sharing units of formula $[M(-SO_2)_4]_\infty$ linked through tetratopic V−H_4TPPS (V−H_4TPPS = vanadium-tetra(4-sulfonatophenyl)porphyrinate).[223] Figure 58 shows the rod SBU of Sm(V-HTPPS), in which each Sm ion is coordinated by eight oxygen from eight different sulfonate groups. The authors also discuss weak V═O···V interactions (4.957 Å) indicating another 1D chain along the porphyrins. However, due to the weakness of this interaction and the disorder of the vanadium ion, we only consider V-HTPPS as a 4-c node, leading to an overall (3,5)-c **zbs** net with transitivity 2 4 and symmetry $P4/mmc$. Other frameworks with the same topology have been reported by using different metal cations in the porphyrin moiety as well as different lanthanides.[224,225]

Another framework that falls into this category is $Co_3(OH)_2(DOCBD)_2$ (H_2DOCBD = 3,4-dihydroxycyclobut-3-ene-1,2-dione) as shown in Figure 59.[226] The SBU is composed of corner-sharing octahedra with general formula $[M_3(OH)_2(-O)_8]_\infty$, where each Co^{2+} is coordinated by four carboxylate O and two μ_3-OH groups. Such SBUs are then

DOI: 10.1021/acs.chemrev.6b00346
Chem. Rev. XXXX, XXX, XXX−XXX

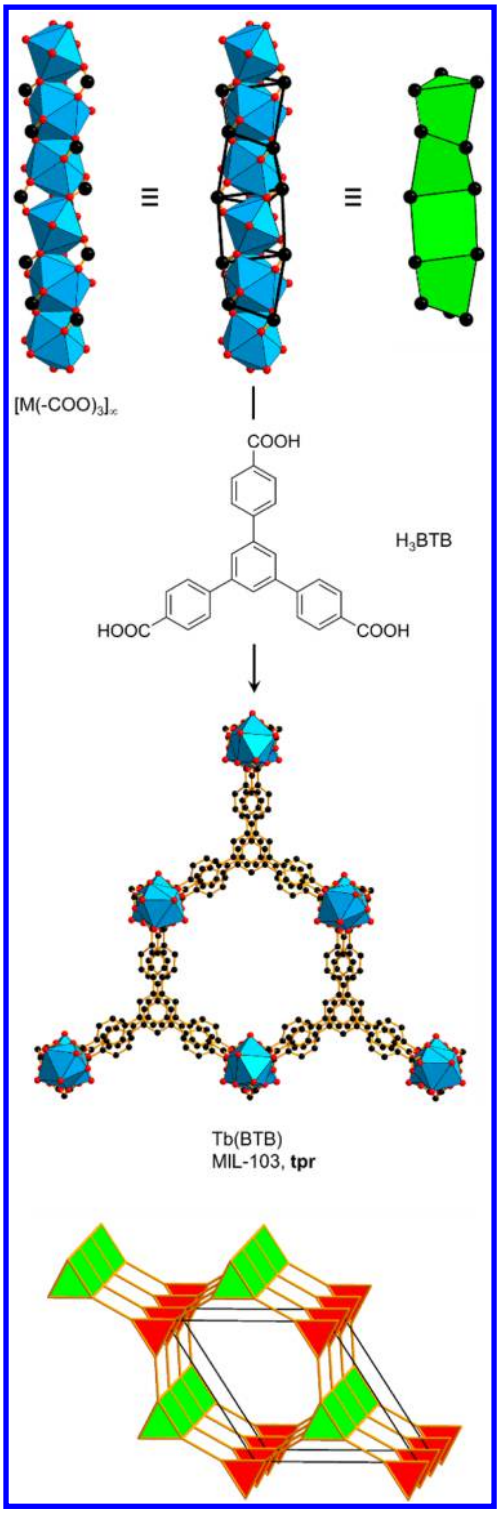

Figure 45. Linking of triangular face-sharing trigonal prism SBUs with tritopic BTB to produce MIL-103, showing **tpr** topology.[195] Color code: black, C; red, O; blue polyhedra, metal.

linked together by DOCBD into a framework with rectangular channels. The deconstruction of the framework is in this case not obvious, and we therefore do not describe the topology in detail. If all the carbon atoms are selected as points of extension then this would lead to a (3,5)-c **zbr** topology; however, we point out that other ways of deconstruction are also feasible.

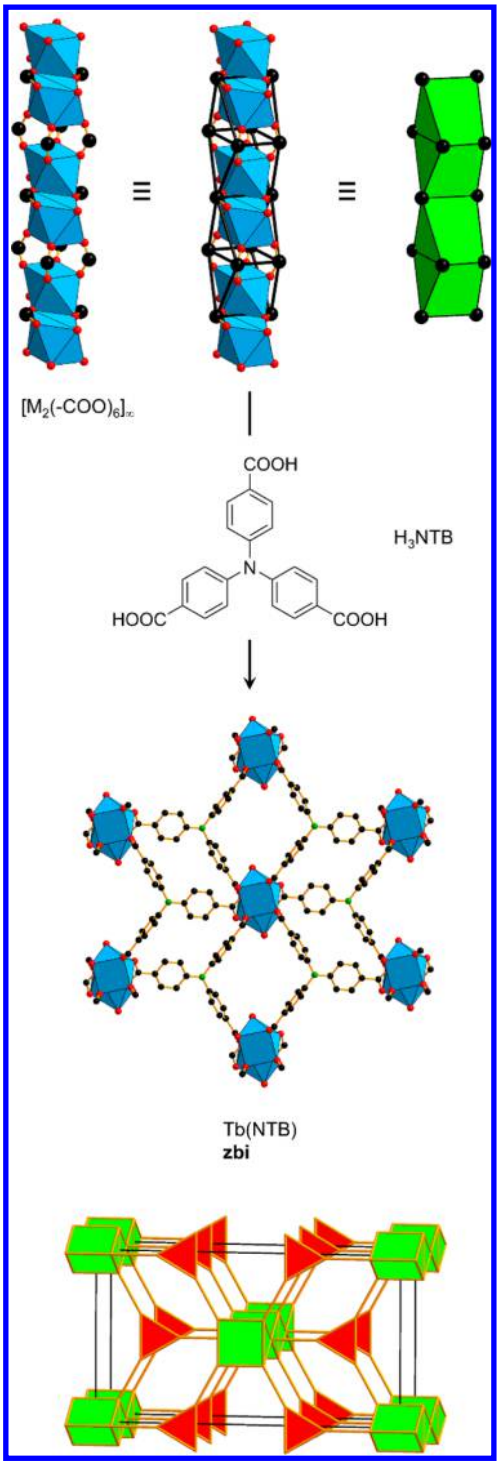

Figure 46. Edge- and face-sharing trigonal prism SBUs together with tritopic NTB produce Tb(NTB), a 4-nodal **zbi** net.[202] Color code: black, C; red, O; green, N; blue polyhedra, metal.

9. MOFS WITH SBUS OF EDGE- OR FACE-SHARED MIXED POLYHEDRA

Frameworks in this category are composed of two linked polyhedra SBUs being either squares, tetrahedra, octahedra, or tetragonal prisms. They are mostly found in carboxylates, but also by mixed functionality linkers.

First, we discuss a class of rod MOFs based on edge-sharing tetrahedra and squares in a 2:1 ratio composed of $[M_2(-COO)_4M(-COO)_2]_\infty$ SBUs joined together by BPT linkers. The two

DOI: 10.1021/acs.chemrev.6b00346
Chem. Rev. XXXX, XXX, XXX−XXX

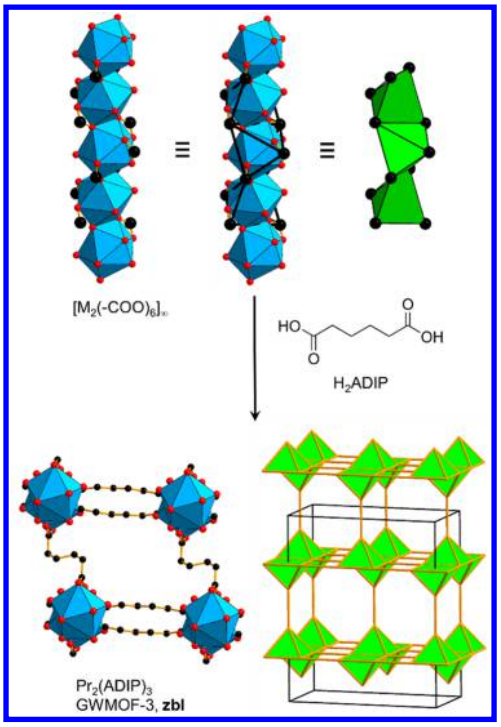

Figure 47. Linking of edge-sharing square pyramid SBUs with a flexible dicarboxylate. The resulting **zbl** net shows alternating layers of square pyramids that are interconnected.[186] Color code: black, C; red, O; blue polyhedra, metal.

polymorphic structures of formula $Cd_3(BPT)_2$, shown in Figure 60, are generated by different binding sites of the asymmetric BPT linker to the SBUs.[227] The coordination geometry in both structures is similar in terms of bound carboxylates, and only the number and nature of solvent molecules are different. The tetrahedral SBU $M(-COO)_2$ is formed from a seven-coordinated Cd^{2+}, particularly by six oxygen from four carboxylate groups and one solvent molecule. The square-shaped SBU $M(-COO)_2$ contains Cd^{2+} in an octahedral geometry with four carboxylate O and two solvent molecules. The authors have described their nets as 2D layer networks, but a complete determination of the topology was not done. If carboxylate C are considered as points of extension, the topology of the nets is quite different, and nets **zbu** and **zbv** are found. The **zbu** net has transitivity 4 9 and symmetry *I*2/*m*. On the other hand, the **zbv** net has transitivity 6 13 and symmetry *C*2/*c*. The difference between the nets is the connectivity of the asymmetric 4′-benzoate moiety that forms the face-sharing tetrahedra in the case of **zbu** and connects the tetrahedra and the square in case of **zbv**, respectively. In the **zbv** net, the rod SBUs propagate in two ways, a property similar to what has been described earlier for **cua** (CAU-8), containing zigzag ladder SBUs (section 3.1).

Other rod MOFs are based on alternating octahedra and quadrangles in a 1:1 ratio forming $[M(-COO)_2M(-COO)_2(-C_2O_2)_2]_\infty$ SBUs joint together by OX (H_2OX = oxalic acid) and TDC linkers to yield a framework with formula $Dy_2(TDC)_2(OX)$, shown in Figure 61.[228] In the particular SBU, the $M(-COO)_2$ quadrangle, the Dy^{3+} is coordinated by four carboxylate O and two water molecules, whereas in the $M(-COO)_2(-C_2O_2)_2$ octahedron, the Dy^{3+} is coordinated by four carboxylate O and four oxalate O. The authors used TOPOS to determine the topology and reported a (4,6)-c trinodal net, where TDC represents a 4-c node together with 4-c and 6-c metal centers.

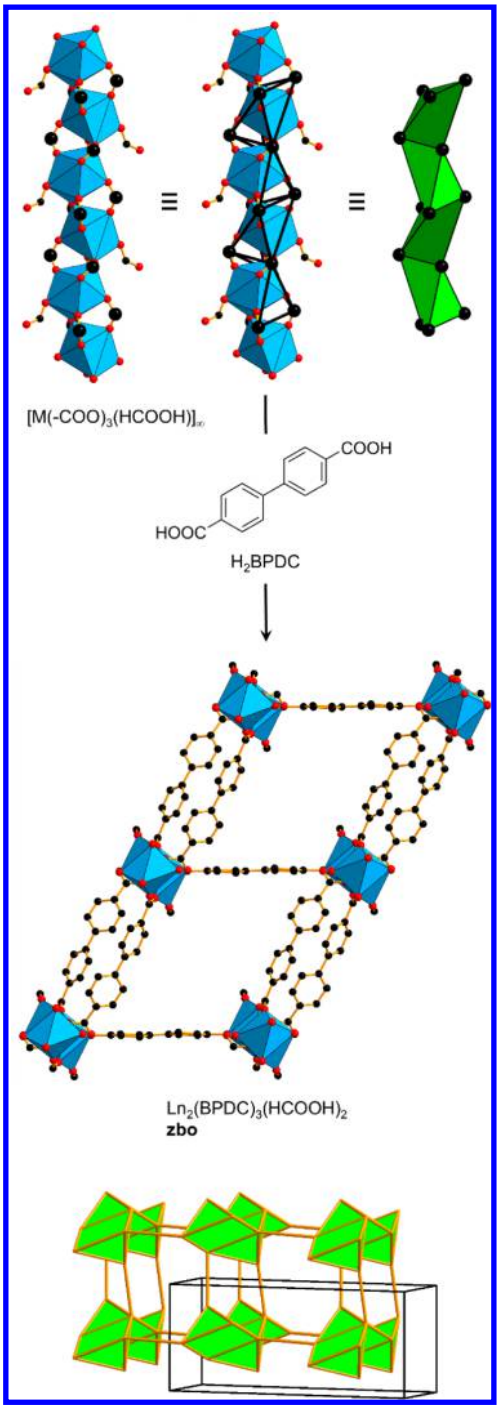

Figure 48. Joining of linked square pyramid SBUs into a framework with underlying **zbo** topology.[203] Color code: black, C; red, O; blue polyhedra, metal.

We assigned a different topology, by taking carboxylate C of TDC as well as centers of OX (shown as pink spheres) as points of extension. The resulting **zbt** topology is a (5,6)-c net with transitivity 2 6 and symmetry *Cmmm*.

When quadrangles are in turn linked with tetragonal prisms into the mixed rod SBU $[M_3(-COO)_6M(-COO)_2]_\infty$ and this one is combined with HPDC linkers (H_2HPDC = 4,5,9,10-tetrahydropyrene-2,7-dicarboxylic acid), a framework termed MOF-79 is obtained (Figure 62).[6] In this structure of formula $Cd_2(HPDC)_2$, the two Cd^{2+} centers are either 6- or 7-coordinated but the individual coordination environments were described as

DOI: 10.1021/acs.chemrev.6b00346
Chem. Rev. XXXX, XXX, XXX−XXX

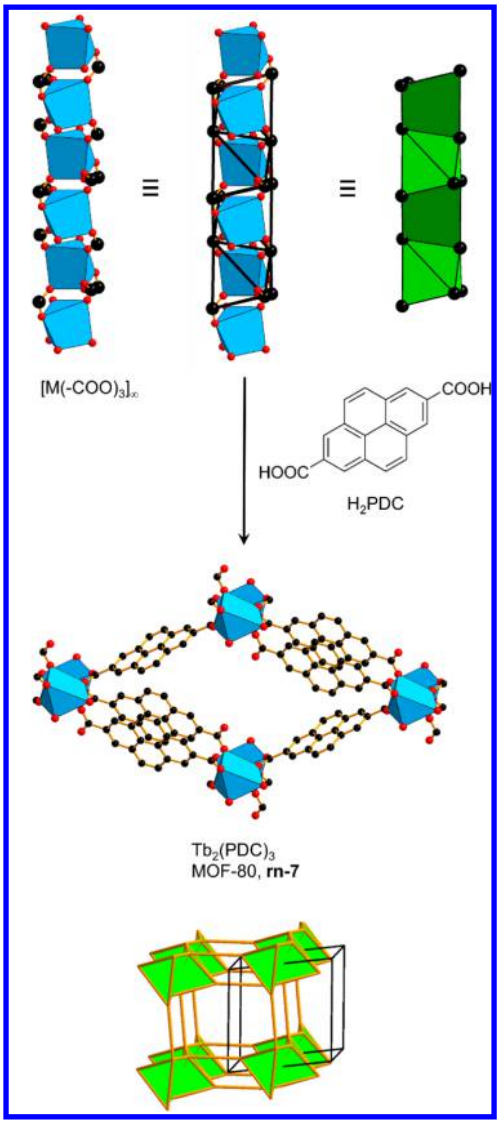

Figure 49. Combination of edge-sharing square pyramidal SBUs with a ditopic linker produce MOF-80 with a trinodal net topology.[6] Color code: black, C; red, O; blue polyhedra, metal.

complex. However, if we consider the carboxylate C atoms as points of extension, the SBU could be clearly dissected into one $M_3(-COO)_6$ tetragonal prism and one $M(-COO)_2$ quadrangle. The classification in the original contribution yielded a **pcu** type net, that we consider now an oversimplification. The underlying topology (**rn-9**, see Supporting Information) is relatively low in symmetry *I*2/m and has intransitivity 2 6.

Octahedra that are linked to tetrahedra in a face-sharing fashion are observed in the framework $(NH_2CH_3)_2[NaZn(mBDC)_2]$, termed MOF-CJ2 (Figure 63).[229] The overall SBU, $[Na_3(-COO)_7M_3(-COO)_5]_\infty$, can be dissected into an octahedron, $Na_3(-COO)_7$, formed by Na^+ which is six coordinated by six carboxylate O, whereas the tetrahedron, $M_3(-COO)_5$, is formed by Zn^{2+}, coordinated to four carboxylate O. The authors identified the structure as a rod MOF; however, the determination of topology was carried out based on the metal centers, leading to a **pcu** net. We deconstruct the framework by taking carboxylate C as points of extension yielding to the aforementioned octahedra and tetrahedral building units of the rod SBU. The net, **zbw**, has transitivity 2 8 and symmetry *C*2/*c*. An iron variant of the same net has been reported in 2012.[230]

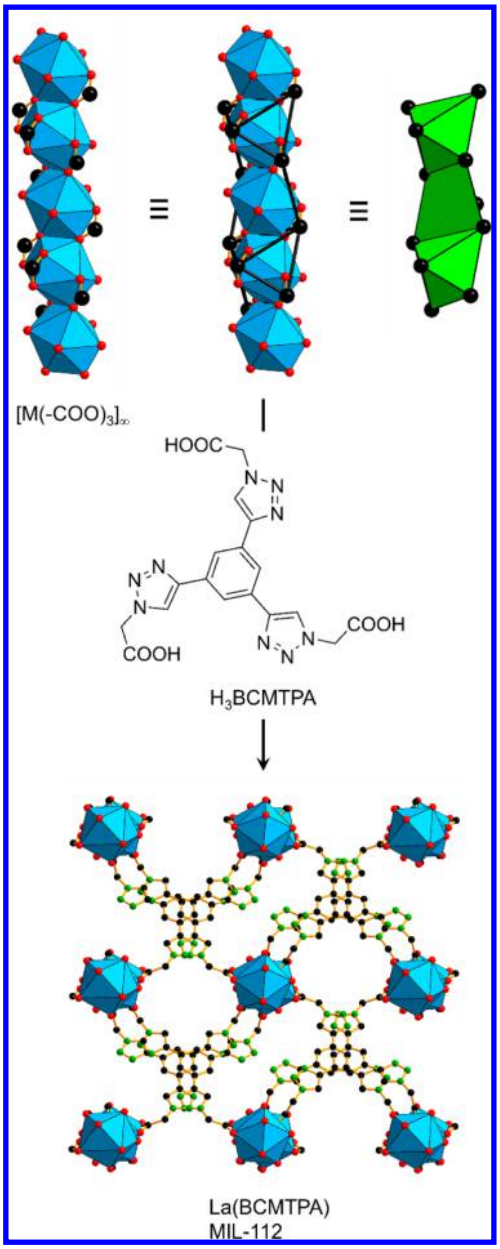

Figure 50. Flexible, tritopic linkers together with linked square pyramid SBUs produce MIL-112.[209] Color code: black, C; red, O; green, N; blue polyhedra, metal.

The linking of octahedra and tetrahedra in different ways leads to different structural and topological outcomes, as exemplified by $Mn_3(BDC)_3$, termed MOF-73 (Figure 64).[6] The $[M_3(-COO)_8M_6(-COO)_{10}]_\infty$ SBU is composed of $M_3(-COO)_8$ octahedra and $M_3(-COO)_5$ tetrahedra in a ratio of 1:2. All Mn^{2+} centers are 6-coordinated and in particular one manganese by four carboxylate groups and one solvent molecule, whereas the other manganese is only coordinated by six different carboxylates. The topology in the original contribution was determined to be **pcu**; however, according to our approach, we determined a **zbx** net, with transitivity 3 12 and a symmetry *I*2/*a*.

The topology of the rod in MOF-73, although chemically different, is found in a framework of formula Fe(BDC), reported in 2005 (Figure 65).[231] The overall SBU $[M(-COO)_3M_2(-COO)_3]_\infty$ can be divided into octahedral $M(-COO)_3$ building units in which each Fe^{2+} is coordinated

DOI: 10.1021/acs.chemrev.6b00346
Chem. Rev. XXXX, XXX, XXX−XXX

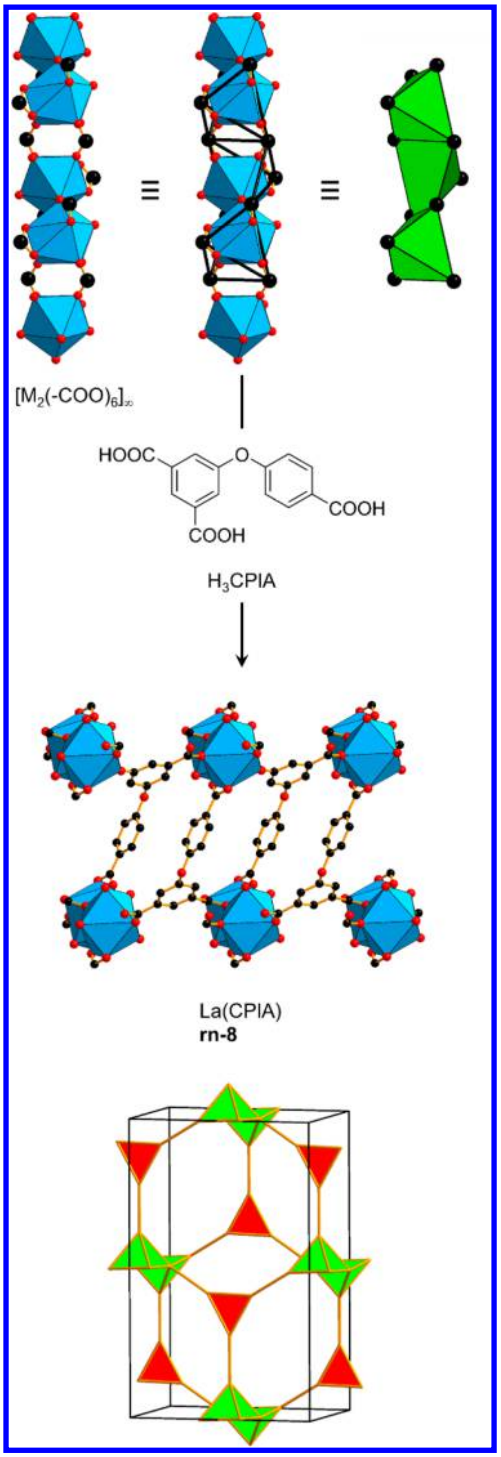

Figure 51. Flexible, asymmetric linker together with alternating, linked square pyramid SBUs produce La(CPIA).[210] Color code: black, C; red, O; blue polyhedra, metal.

by six carboxylate O and tetrahedral $M_2(-COO)_3$ building units in which each Fe^{2+} is also octahedrally coordinated by five carboxylate O and one pyridine N. The underlying net, **zce** has thus transitivity 3 10 and symmetry $P2_1/n$.

The recently reported MOF-910, $Zn_3(PBSB)_2$, ($PBSP^{3-}$ = phenylyne-1-benzoic acid, 3-benzosemiquinonate, 5-oxidopyridine) also contains a rod SBU composed of octahedra and tetrahedra in a 1:2 ratio (Figure 66, see Note Added in Proof). PBSP refers to a one-electron oxidation of deprotonated H_4PBCB (phenylyne-1-benzoic acid, 3-catechol, 5-pyridone)

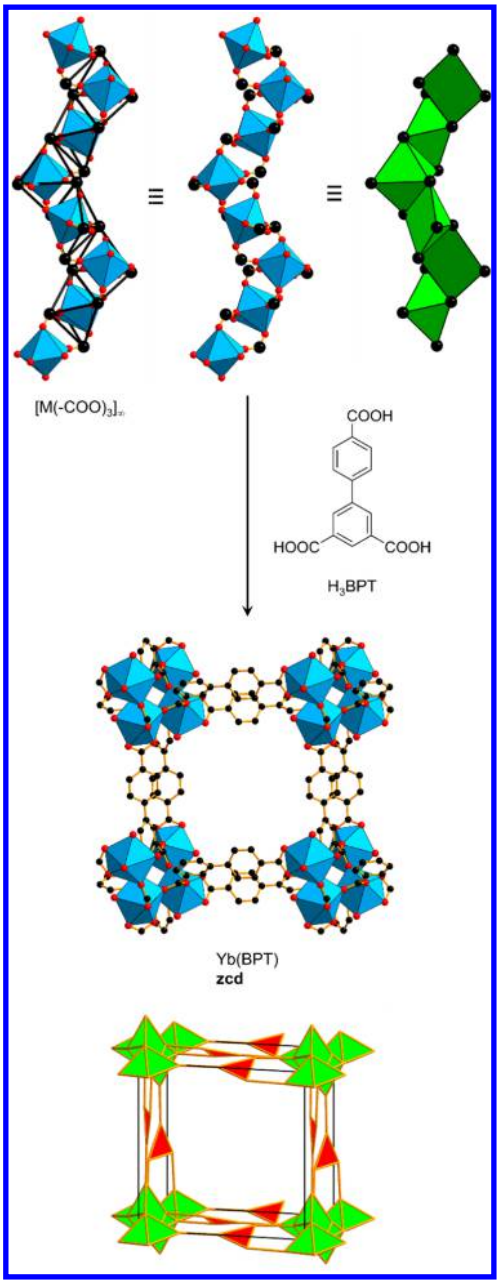

Figure 52. Combination of edge-sharing square pyramidal SBUs with tritopic BPT to produce Yb(BPT) showing a 6-nodal **zcd** topology.[211] Color code: black, C; red, O; blue polyhedra, metal.

from a catechol to a semiquinonate, that occurs during synthesis, and changes the overall charge of the linker to −3. In the quite unique rod SBU of formula $[M_2(-COO)(-C_2O_2)(-OPY)]_\infty$, the presence of three distinct bidentate coordinating groups facilitate different types of coordination environments. The Zn^{2+} ions adopt two configurations distinct in the metal−ligand bonds involved. In two-thirds of the cases, the zinc ion is bound to three benzosemiquinonate O, a carboxylate O, and a pyridonate N. The other third are bound by a pair of benzosemiquinonate O, a pair of carboxylate O, and a pair of pyridonate O. The low symmetry of the linker is herein responsible that the three coordinating groups are not interchangeable in the MOF structure. There are several structural features, unique to the asymmetrical tritopic linker, responsible for the formation of this particular rod MOF. The angular portion of the linker that coordinate to the same rod (i.e., the semiquinonate and the

DOI: 10.1021/acs.chemrev.6b00346
Chem. Rev. XXXX, XXX, XXX−XXX

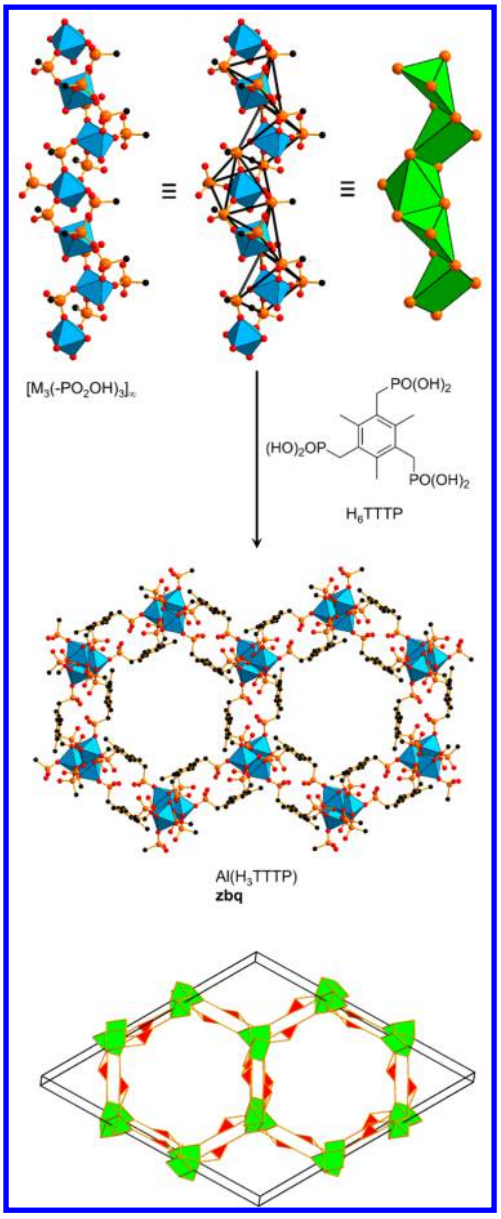

Figure 53. Linking of edge-sharing square pyramidal SBUs with tritopic TTTP to produce Al(H_3TTTP) showing a 6-nodal **zbq** topology.[212] Color code: black, C; red, O; orange, P; blue polyhedra, metal.

pyridonate moiety) are responsible for the formation of a helix rather than a straight rod or zigzag ladder. This situation is in turn comparable to that for 1,3-BDC moieties of BPT (H_3BPT = biphenyl-3,4′,5-tricarboxylic acid), that either coordinate to one rod and facilitate helix formation[211] or to different rods that are indeed nonhelical.[227] This observation is supported by other structures that contain symmetrical BTB linkers and form straight rods, when connected to three different helices.[195] We also observed that the distance between the functional groups define the pitch of the helix (here 27.12 Å), when compared to, for example, 1,3-BDC-derived linkers. In this context, the "double-walled" nature of the framework might arise from the long intramolecular distance between catecholate and pyridone that requires a second linker molecule to complete the helix. The rod SBU of MOF-910 forms are 3-fold helix since one pitch contains 12 coordinating groups, from six different linkers and therefore propagate in three directions. Longer distances could therefore lead to 4-fold symmetry helices that might

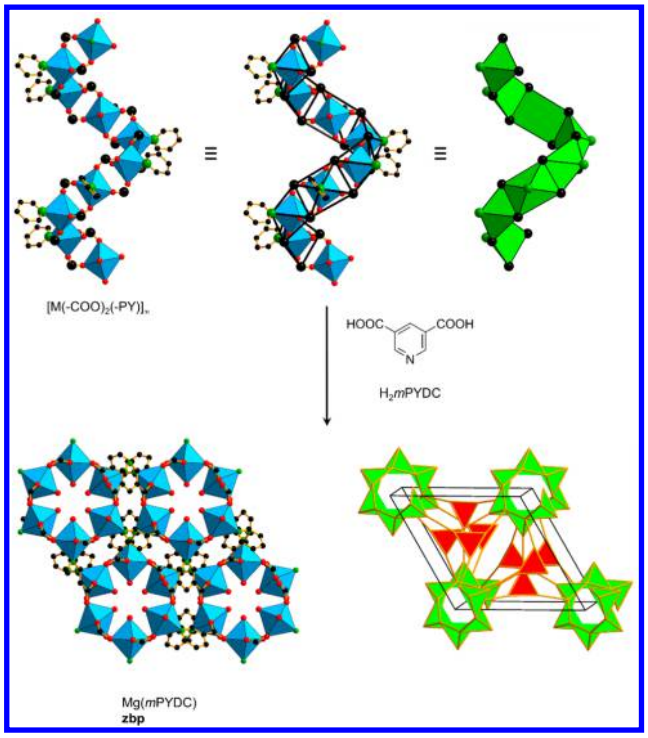

Figure 54. Linking of edge-sharing square pyramidal SBUs with bifunctional, tritopic *m*PYDC to produce Mg(*m*PYDC), a chiral framework with 4-nodal **zpb** topology.[213,214] Color code: black, C; red, O; green, N; blue polyhedra, metal.

crystallize as tetragonal frameworks, whereas shorter distances might lead to "single-walled" frameworks of either 3- or 4-fold symmetry. The different nature of coordinated linker functionalities has a profound effect on the formation of this helical rod MOF that would be unattainable with one or two kinds of functional groups. In particular, the semiquinonate provides the M-O-M infinite metal-oxide unit of the rod through coordination by two μ_2-oxygen. Such coordination polyhedra are bridged on the opposite corners by a carboxylate, or pyridonate group, that have longer distances and therefore cause a turn in the rod to facilitate the helix. In this context, the angle subtended at the pyridonate moiety is important to coordinate the metal cation, an angle that cannot be provided by a carboxylate group. In addition, these different functional groups would allow for reticular chemistry approaches without altering the underlying topology (**tto**). Since the semiquinonate/pyridonate portion of the linker is crucial for the formation of the rod SBU, MOF-910 is amenable to fine-tuning of pore size by expanding the benzoate moiety. The **tto** net is complex with transitivity 6 16 but high symmetry $R\bar{3}c$.

10. MOFS WITH HELICAL RIBBON SBUS OF EDGE-SHARED TRIANGLES

In this section, we focus on SBUs that are composed of helical ribbons formed by edge-sharing triangles. They are either carboxylates or azolates and vary in symmetry and shape depending on the nature of the linker.

A class of scandium carboxylate MOFs is particularly important in this context and demonstrates the amenability of linker size and geometry to form frameworks with triangular helical ribbon SBUs. Such nets were first explored in 2011, when $[M(OH)(-COO)_2]_\infty$ helical ribbon SBUs were linked with TDC and yielded a framework termed NOTT-401, Sc(OH)(TDC).[232] Figure 67 shows the SBU in which each Sc^{3+} is

DOI: 10.1021/acs.chemrev.6b00346
Chem. Rev. XXXX, XXX, XXX−XXX

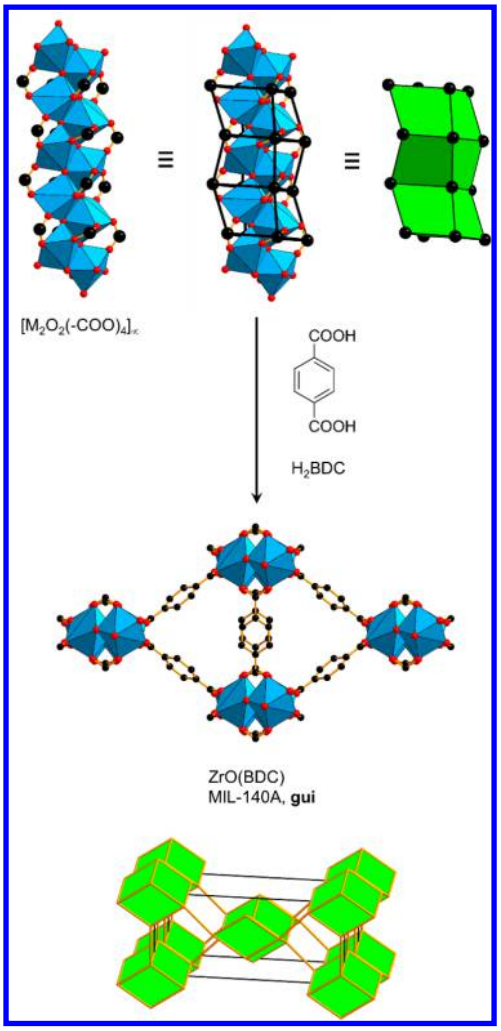

Figure 55. Linear linking of face sharing tetragonal prism SBUs with rigid, ditopic BDC to produce MIL-140A showing an underlying **gui** net.[215] Color code: black, C; red, O; blue polyhedra, metal.

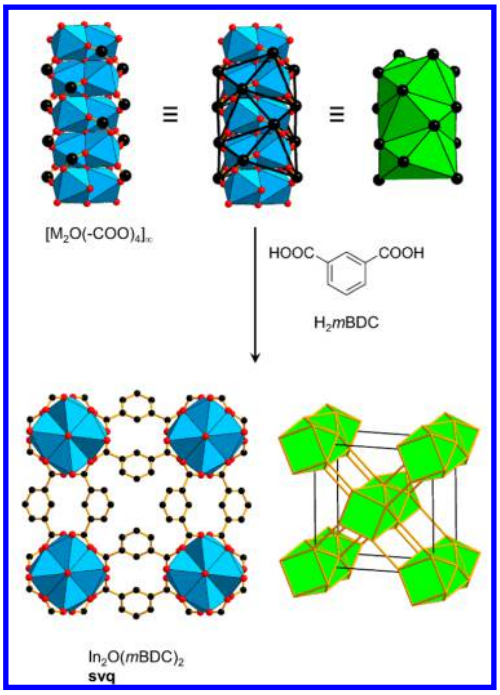

Figure 56. Linking of face-sharing tetragonal antiprism SBUs with angular, ditopic *m*BDC to produce $In_2O(mBDC)_2$ showing an underlying uninodal **svq** net.[218] Color code: black, C; red, O; blue polyhedra, metal.

octahedrally coordinated by four carboxylate O and two μ_2-OH groups. The underlying topology based on linear linking of triangular helical ribbons is a 5-c **yfm** net with minimal transitivity 1 4 and symmetry $I4_1/amd$. Such **yfm** nets have later been found using *m*BDC derivatives together with aluminum SBUs to give frameworks of general formula Al(OH)(X-*m*BDC) (X = H, CH_3, OCH_3, NO_2, NH_2, and OH).[233] When the same helical SBUs are in turn linked with tetratopic carboxylates, a framework $Sc_2(OH)_2$(BPTC) (H_4BPTC = biphenyl-3,3′,5,5′-tetracarboxylic acid), termed NOTT-400, was isolated (Figure 67, bottom).[232] This framework is chiral and possesses square-shaped channels along [001]. The net is related to **yfm** and has symbol **nti**. The **nti** nets have transitivity 3 7 and symmetry $I4_122$. The frameworks with **nti** topology have since been derivatized based on indium and aluminum SBUs.[234,235]

Helical ribbon SBUs can also be produced by pyrazolate linkers, as observed in Cd(BPZ) (H_2BPZ = 4,4′-bipyrazole), shown in Figure 68.[147] This framework crystallizes in the chiral space group $P6_122$ and contains $[M(\text{-}PZ)_2]_\infty$ SBUs and BPZ linkers. In particular, each Cd^{2+} shows an octahedral coordination environment, composed of four pyrazolate N and two μ_2-oxygen of DMF. These DMF molecules were not included in the formula; however, they are necessary to some extent in forming the helical SBU. Deconstruction of this framework was performed by creating the points of extension between the two pyrazolate N atoms (shown as pink spheres). The underlying topology is also based on linear linking of such hexagonal chains (6_1 or 6_5 helices, respectively) yielding the 5-c **wjp** net with transitivity 1 4 and symmetry $P6_122$. There are only two minimal transitivity nets when linking hexagonal ribbons, **wjp** and **fna**. An isoreticular framework with **wjp** topology has later been obtained through the use of a BPZ derivative.[148]

Another interesting compound is In(OH)(BCIm)(NO_3) (H_2BCIm = 1,3-bis(4-carboxyphenyl)imidazolium) because it is composed of 5-fold $[M(OH)(-COO)_2]_\infty$ helical rod SBUs (Figure 69).[236] Each of the five crystallographically independent In^{3+} is coordinated in an octahedral environment by two μ_2-OH groups and four carboxylate O. The underlying net, **sbq** has transitivity 10 25 and symmetry $P2_1/n$. It was shown that this high transitivity is in fact minimal and arises because the rods have noncrystallographic symmetry (5_1 or 5_4 axes).[40] In this MOF, the rod axes are arranged in the 5-c 2-periodic net **tts**, a pattern never otherwise found. This net is the simplest and highest-symmetry way of linking pentagonal rods.

Helical ribbon SBUs of formula $[CaM(-COO)_4]_\infty$ can also be composed of heterometallic carboxylates, as observed in the framework CaPb(OH-*m*BDC)$_2$ (OH−H_2*m*BDC = 5-hydroxybenzene-1,3-dicarboxylic acid).[237] Figure 70 shows such SBUs, in which each Pb^{2+} is coordinated by six oxygen from four carboxylate groups (d < 2.88 Å), whereas each Ca^{2+} is coordinated by four oxygen from four carboxylate groups and two methanol molecules. Both metal centers have a distorted octahedral coordination environment. In our illustration, the Pb center is nine-coordinated and the calcium centers were found to be unnecessary to keep the integrity of the rod. The authors have initially determined the topology as a uninodal 6-c **sne** net by deconstructing the framework with Pb centers as nodes. If the carboxylate C are taken as points of extension, the

DOI: 10.1021/acs.chemrev.6b00346
Chem. Rev. XXXX, XXX, XXX−XXX

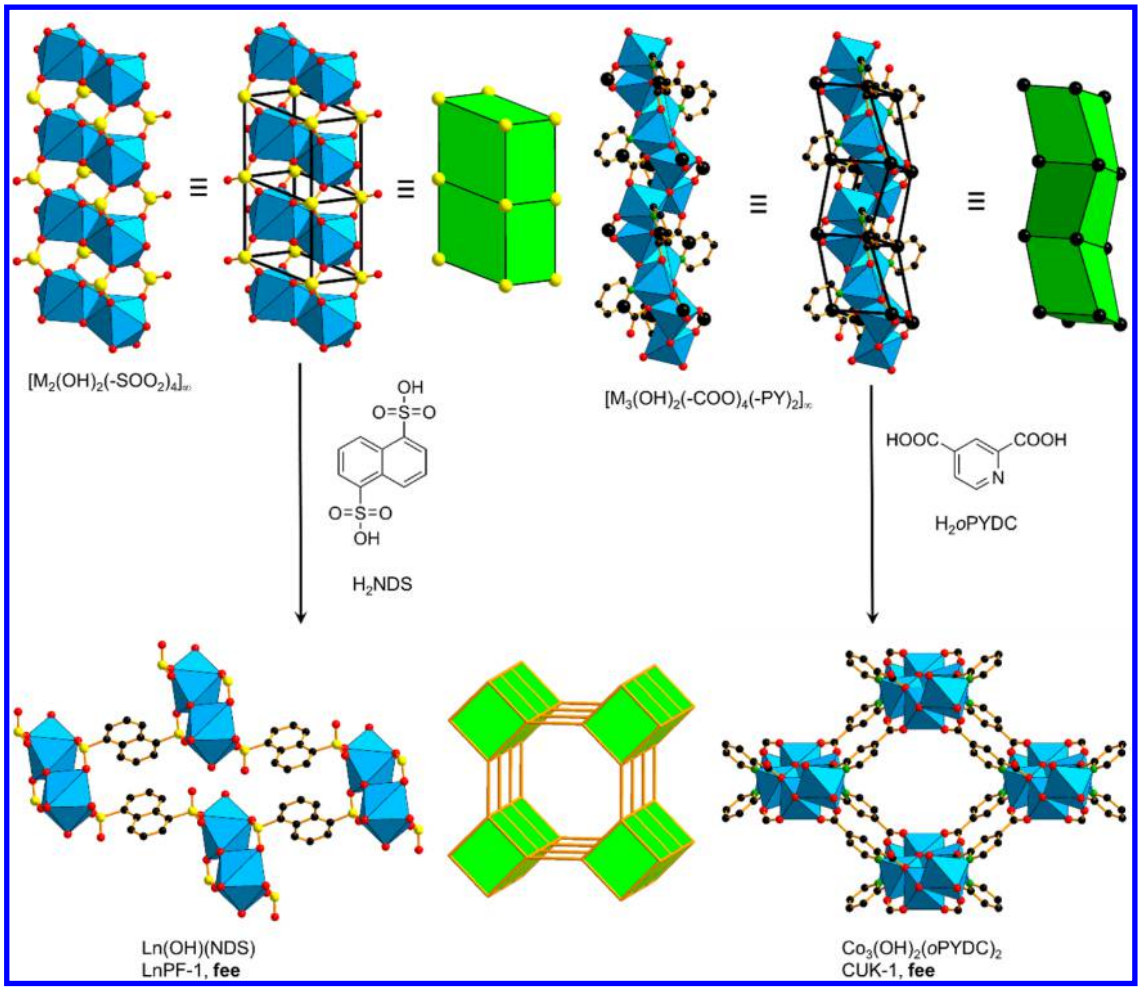

Figure 57. Two examples of **fee** topology nets, formed by ditopic sulfonate linkers (left) or pyridine dicarboxylates (right).[219,220] Color code: black, C; red, O; yellow, S; green, N; blue polyhedra, metal.

underlying topology was determined to be a (4,6)-c **zba** net with transitivity 2 6, and symmetry is $I\bar{4}2d$.

In contrast to all helical ribbons detailed so far, we show one framework that is based on helices containing both triangles and quadrangles. A framework, Co(BDC) contains SBUs of general formula $[M(-COO)_2]_\infty$ being composed of triangles and quadrangles in a ratio of 2:1 (Figure 71).[238] The Co^{2+} centers are octahedrally coordinated by four carboxylate O and two μ_2-oxygen from e-urea. The e-urea is not shown in our illustration. The authors have originally described the topology as a trinodal net by considering BDC as 4-c and Co as 6-c nodes, forming a 4_1 helix. However, we assign the carboxylate C as points of extension and therefore obtain a (4,5)-c **zbz** net with transitivity 2 6 and symmetry $P4_122$.

11. MOFS WITH SBUS OF EDGE-SHARED QUADRANGLES

In contrast to zigzag ladders, we discuss here MOFs that are based on differently linked quadrangle SBUs. Linked quadrangles can be composed of many different linker functionalities, such as carboxylates and pyridine-2-thiols as observed in the framework CUK-2, Co_2(MNA), (H_2MNA = 6-mercaptonicotinic acid), shown in Figure 72.[220] This compound contains $[M_2(-COO)_2(-CNS)_2]_\infty$ SBUs, in which each of the two independent Co^{2+} is coordinated in a distorted octahedral environment by two carboxylate O, two pyridyl N, and two μ_2-thiolate. The framework possesses square-shaped pores along [001], and the authors highlight the formation of cobalt-thiolate helical chains. In accordance with our deconstruction approach, we selected the carboxylate C, as well as the carbon adjacent to sulfur and nitrogen, by analogy to a carboxylate, as the points of extension. This leads to the 4-c **pcl** net, with transitivity 1 4 and symmetry *Cmcm*. This net named for paracelsian represents a way of cross-linking "double-crankshaft" chains into a framework related to that of the mineral feldspar.

Slightly different "double-crankshaft" chains are found in $Cd_4(OH)_2(TPTC)_2$ (H_3TPTC = [1,1′:2′,1″-terphenyl]-4,4′,4″-tricarboxylic acid) that is produced by linking $[M_4(OH)_2(-COO)_6]_\infty$ SBUs together with tritopic TPTC (Figure 73).[239] The structure contains four crystallographically independent Cd^{2+} that are coordinated as follows: Cd1 shows a slightly distorted octahedral environment with four oxygen from four carboxylate groups and two μ_3-OH. Cd2 and Cd3 are six-coordinated by four carboxylate O, one μ_3-OH and one water ligand, whereas Cd4 shows a distorted square pyramidal environment with three carboxylate O and two μ_3-OH. The authors identified the rod SBU correctly and termed it a zigzag ladder (however different to what we have herein termed zigzag ladder), but determination of the topology using TOPOS led to a (4,10)-c net. We prefer our deconstruction approach, however,

DOI: 10.1021/acs.chemrev.6b00346
Chem. Rev. XXXX, XXX, XXX−XXX

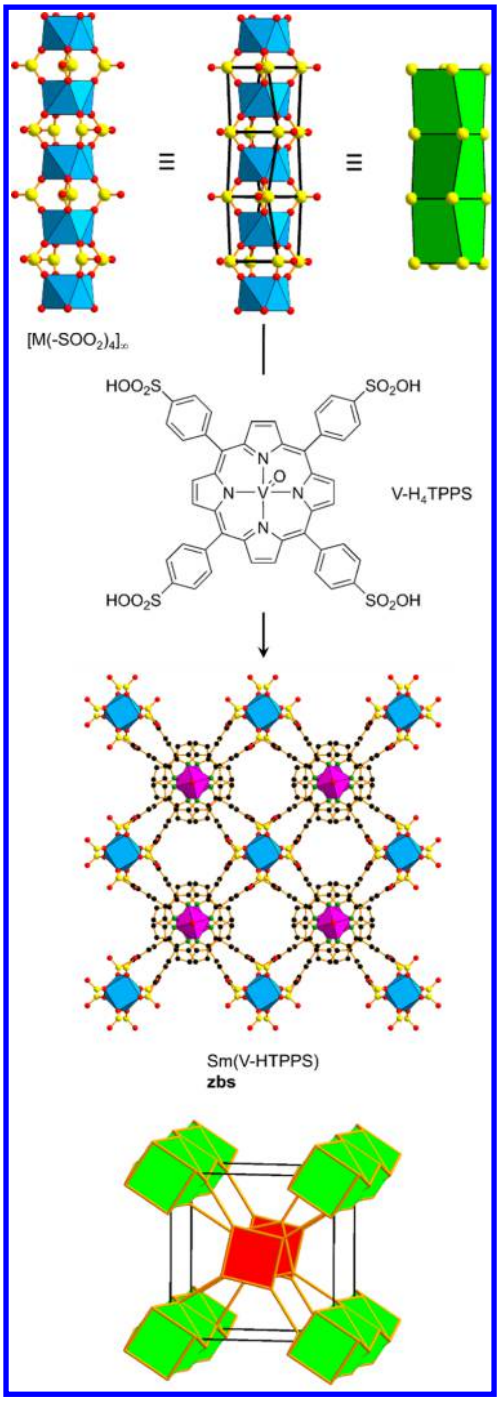

Figure 58. Linking of face-sharing tetragonal antiprism SBUs with a tetratopic porphyrin linker to produce Sm(V-HTPPS) showing an underlying (3,5)-c **zbs** net.[223] Color code: black, C; red, O; yellow, S; green, N; blue polyhedra, metal; pink polyhedra, V.

through selection of carboxylate C as points of extension led to a (3,4)-c **shf** net with transitivity 4 8 and symmetry *Imma*.

There are also different double zigzag ladders that are composed of $[M_2(-COO)_6]_\infty$ SBUs that when linked with TDC produce frameworks of composition $Ln_2(TDC)_3$ (Ln = Gd, Dy).[240] Figure 74 shows the SBU in which each Ln^{3+} center is eight-coordinated in a distorted bicapped trigonal prism, surrounded by six oxygen from five carboxylate groups and two water ligands. Although a determination of the net topology was not performed, the authors refer to the SBU as beltlike chains.

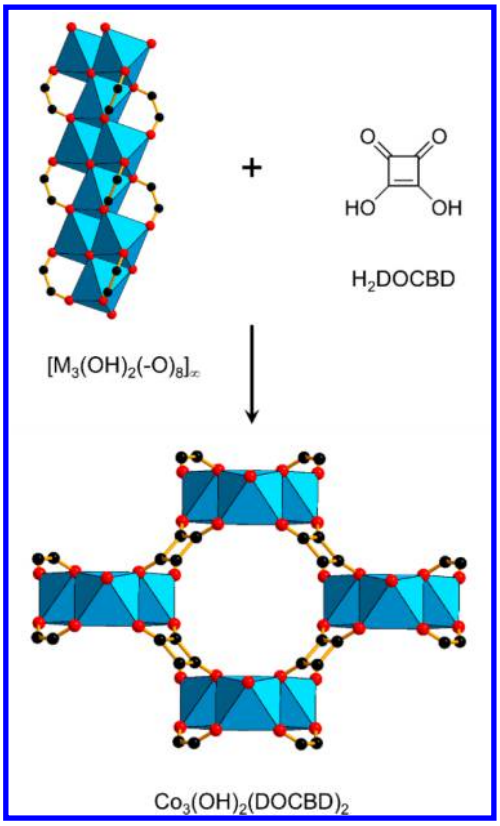

Figure 59. SBU and crystal structure of $Co_3(OH)_2(DOCBD)_2$. The deconstruction in this particular case is not obvious.[226] Color code: black, C; red, O; blue polyhedra, metal.

If the carboxylate C are used as points of extension, we obtain a net **zbb** with transitivity 3 6 and symmetry *C*2/*m*. Such double ladder frameworks have also been reported using other lanthanide centers.[191]

In Figure 75, we show a framework that also consists of double ladder SBUs, however with a different composition of $[M_5(OH)_4(-COO)_6]_\infty$.[150] When such SBUs were combined with ditopic DMBDC (H_2DMBDC = 2,5-dimethyl-benzene-1, 4-dicarboxylic acid), a framework $Zn_5(OH)_4(DMBDC)_3$ was obtained. In particular, the three crystallographically independent Zn^{2+} are also coordinated differently as follows: Zn1 shows a slightly distorted octahedral coordination by two μ_3-OH and four carboxylate O, Zn2 is also coordinated in a slightly distorted octahedral environment, by four μ_3-OH and two carboxylate O, and Zn3 shows a distorted tetrahedral environment, coordinated by two μ_3-OH and two carboxylate O. When taking the carboxylate C as points of extension, we obtained a **zca** net with transitivity 3 8 and symmetry $P2_1/c$.

12. SPECIAL ROD MOFS

12.1. MOF with SBUs of Face-Shared Large Polyhedra

We discuss here a MOF built of bicapped tetragonal prism SBU of formula $[M_5(OH)_9(-SOO_2)_6]_\infty$ (Figure 76). When this SBU is linked with NDC, a framework termed LnPF-3, $Ln_5(OH)_9(NDS)_3$ (Ln = Eu, Gd) is obtained.[221] There are three crystallographically different Ln^{3+} centers, two of them being situated in the middle of $[LnO_3(\mu_3\text{-}OH)_4(\mu_5\text{-}OH)H_2O]$ tricapped trigonal prisms to form $[Ln_4O_{12}(\mu_3\text{-}OH)_8(\mu_5\text{-}OH)(H_2O)_4]$ tetrameric units. The other lanthanide ion is coordinated in a $Ln(\mu_3\text{-}OH)_8(\mu_5\text{-}OH)$ monocapped tetragonal prism. The authors reported similarities

DOI: 10.1021/acs.chemrev.6b00346
Chem. Rev. XXXX, XXX, XXX−XXX

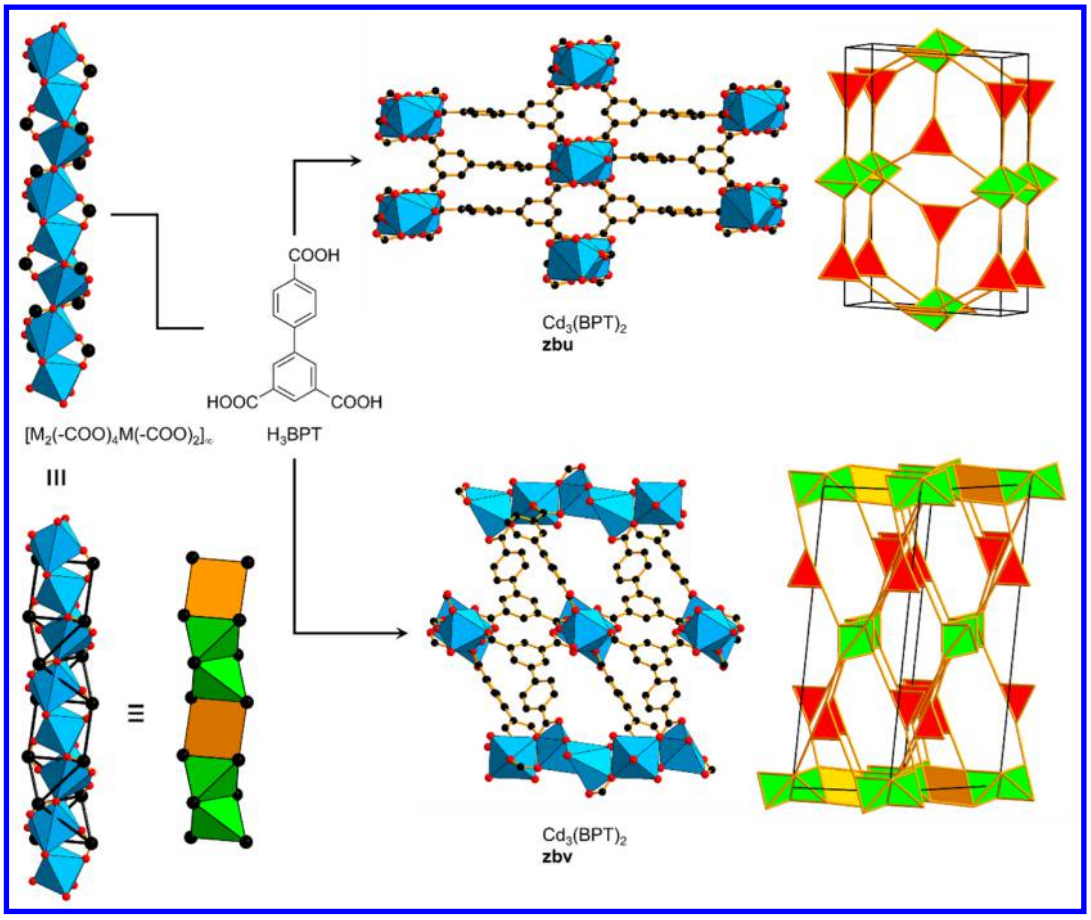

Figure 60. Crystal structures and net topology of the polymorphs with formula $Cd_3(BPT)_2$. The different **zbu** and **zbv** nets contain rod SBUs propagating in one or two dimensions.[227] Color code: black, C; red, O; blue polyhedra, metal.

of this net to the purely inorganic $Ln_8Ba_5Ni_4O_{21}$. In accordance with our approach, we deconstruct the rod SBUs, with sulfonate S as points of extension, into bicapped tetragonal prisms. A determination of topology, and an RCSR code is not given due to the complicated nature of the net.

12.2. MOF with SBUs of Edge-Shared Triangles to Make Flat Ribbons

There are other examples of rod SBUs based on triangles, that, in contrast to the helical ribbons, form straight rods. One such example can be found in the uranium-containing compound $(UO_2)_{12}O_4(OH)_8(BTEC)_3$ which has $[(MO_2)_3O(OH)_2(-COO)_3]_\infty$ rod SBUs joint with BTEC linkers (Figure 77).[241] In the SBU, there are three crystallographically independent uranium cations that are seven-coordinated in a pentagonal bipyramidal environment. It is particularly surrounded by two oxygen in the apical position, through the typical short double uranyl bond, two oxygen from carboxylate and two hydroxo and one oxo group in the equatorial plane. This cluster has previously been reported as a 1D chain.[242] When carboxylate C are considered as points of extension, the rod SBU is composed of edge-sharing triangles which when connected with squares, leads to the (3,5)-c **zcc** net with transitivity 2 4, symmetry *I*4/*mmm*.

12.3. MOFs with SBUs of Edge-Shared S-Shapes to Sinusoidal Ribbons

A special class of MOFs based on mixed polyhedra forms S-shaped (sinusoidal) SBUs. First, we discuss a framework termed MIL-45, composed of $[M(-COO)_3M_2(-COO)_4]_\infty$ SBUs joined together by BTC linkers (H_3BTC = 1,3,5-benzenetricarboxylic acid) to produce $KFe_3(BTC)_3$ (Figure 78).[243] In particular, there are $M(-COO)_3$ octahedra in which each Fe^{2+} is octahedrally coordinated by six oxygen from six different carboxylate groups. In addition, $M(-COO)_2$ tetrahedra are connected in a face-sharing fashion, and each of these metal centers is coordinated by seven oxygen from five carboxylates. The authors have identified the undulating nature of the rod SBU; however, a determination of the topology was not given. By using carboxylate C as points of extension, we obtained a **zcb** net with transitivity 6 16 and symmetry *P*2/*c*.

A complicated framework of formula $[NH_2(CH_3)_2]Fe_5(BTC)_3(OAc)_2$ is composed of both discrete and rod SBUs, the latter containing corner- and edge-sharing triangles and quadrangles, respectively (Figure 79).[244] In detail, the $[M_6(-COO)_9(COO)_2M_3(-COO)_6(COO)_2]_\infty$ rod contains $M_6(-COO)_9(COO)_2$ triangles linked to $M_3(-COO)_6(COO)_2$ quadrangles in 2:1 ratio. The metal centers are hexa-coordinated in a distorted octahedral environment, with Fe1 being surrounded by four oxygen from BTC and two oxygen from terminal acetate, whereas Fe2 is bound by three oxygen from three BTC and three oxygen from terminal acetate. In addition, there is a discrete paddle wheel $M_2(-COO)_4$ that serves as a 4-c node. Deconstruction, that takes carboxylate carbon of BTC into account, leads to a complicated net, termed **rn-10** (see Supporting Information). This net has transitivity 10 16 and symmetry $I2_1/a$. The same framework has also been reported with other cationic species (H_3O^+) to balance the anionic charge.[230]

DOI: 10.1021/acs.chemrev.6b00346
Chem. Rev. XXXX, XXX, XXX−XXX

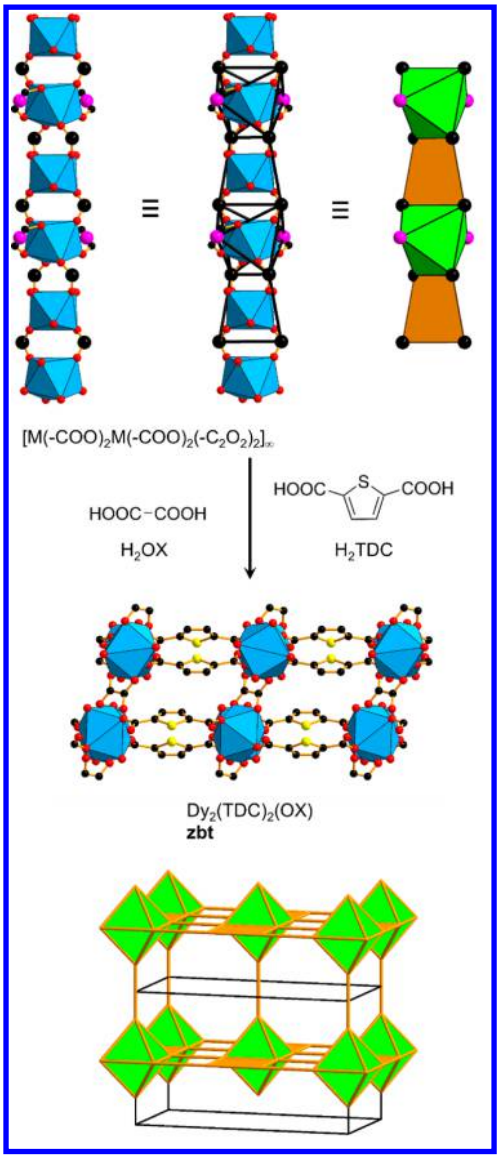

Figure 61. Crystal structure of $Dy_2(TDC)_2(OX)$ and the underlying **zbt** net.[228] Color code: black, C; red, O; blue polyhedra, metal; pink, points of extension.

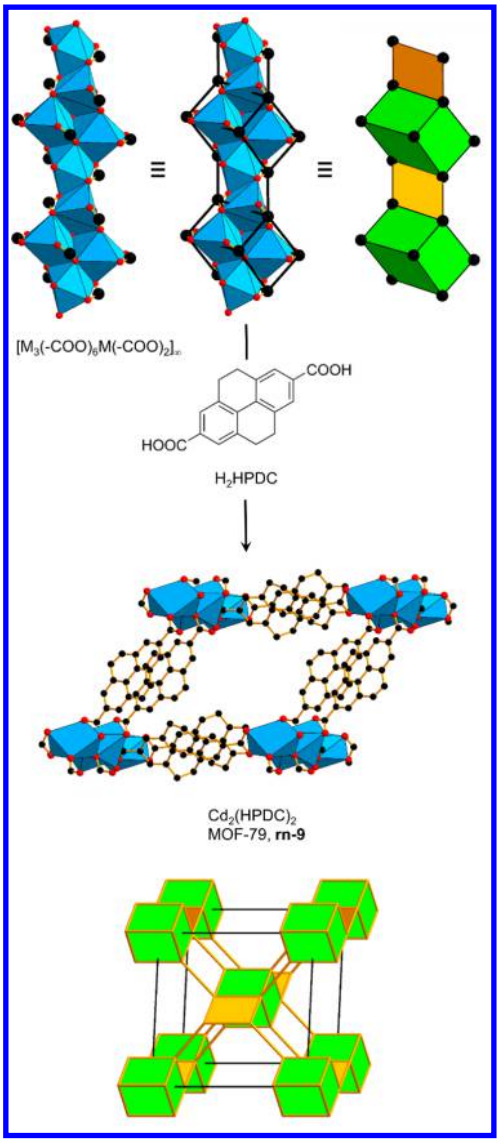

Figure 62. Crystal structure of MOF-79, $Cd_2(HPDC)_2$. The net is built from linked tetragonal prisms and quadrangles in a 1:1 ratio.[6] Color code: black, C; red, O; blue polyhedra, metal.

12.4. MOF with SBUs of Solid Columnar Structure

SBUs are here described as column shaped because they are relatively large and their exterior is only decorated with a few organic moieties. In this context, an SBU of formula $[M_{13}(OH)_{27}(-COO)_6]_\infty$ represents a column dissected into irregular hexagons and when combined with simple NH_2−BDC produces a framework $Al_{13}(OH)_{27}(NH_2-BDC)_3Cl_6$, termed CAU-6 (Figure 80).[245] The SBU has previously been reported as a discrete entity $Al_{13}(OH)_{24}(H_2O)_{24}Cl_{15}\cdot 13\ H_2O$.[246] We deconstructed this framework by considering the carboxylate C as points of extension and obtained a zeolitic, uninodal 4-c **can** net. This cancrinite net has transitivity 1 4 and symmetry $P6_3/mmc$.

13. MOFS BASED ON APERIODIC HELICAL SBUS OF FACE-SHARED POLYHEDRA

13.1. MOFs with SBUs Derived from the Boerdijk-Coxeter Helix

In contrast to the aforementioned SBUs, the tetrahedra in a rod can also be linked through their faces, yielding a cylinder tiling as discussed in the Introduction. A framework of formula Ca_2(BIPA-TC) (H_4BIPA-TC = 5,5′-(1,3,6,8-tetraoxobenzo-[*lmn*][3,8] phenanthroline-2−7-diyl)bis-1,3-benzenedicarboxylic acid) is obtained through linking of $[M(-COO)_2]_\infty$ SBUs with tetratopic BIPA-TC (Figure 81).[247] Calcium ions are all eight-coordinated, through six oxygen from carboxylates and two oxygens from solvent molecules (DMF), and form a 4_1 helix running along [001]. The authors deconstructed the structure ignoring the nodes on the linker so the 4-fold helices are joined by single links to produce the 7-c net **yan** (we describe this later in section 13.4) with transitivity 1 4 and symmetry $I4_122$.

However, the story is more complicated. Including the 3-c nodes on the linker produces the net **hqx** with transitivity 3 9 and symmetry again $I4_122$ (Figure 81). The pattern of linking means that the links joining the 3-c nodes are sufficiently widely spaced to allow a second copy of the structure with opposite hand to interpenetrate (Figure 82). The ideal symmetry of the pair of nets is $I4_1/acd$. The real structure is indeed a rare example of a rod MOF with two interpenetrating components and has symmetry $I4_1/a$.

DOI: 10.1021/acs.chemrev.6b00346
Chem. Rev. XXXX, XXX, XXX−XXX

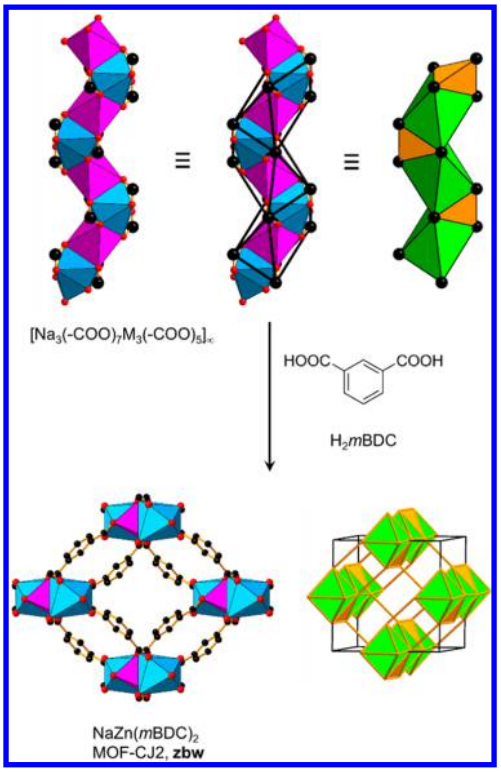

Figure 63. Crystal structure of MOF-CJ2 and its underlying **zbw** topology.[229] Color code: black, C; red, O; blue polyhedra, metal; pink polyhedra, Na.

Another example, recently obtained, also has a BC helix rod. The MOF, termed ROD-1 with formula Cd(DMPMB) (H_2DMPMB = 4-((3,5-dimethyl-1H-pyrazol-4-yl)methyl)-benzoic acid) is composed of a $[M(-COO)(-PZ)]_\infty$ rod SBU, in which each Cd^{2+} is octahedrally coordinated by three carboxylate O and three pyrazolate N (Figure 83, see Note Added in Proof). Deconstruction of this SBU, when considering carboxylate C and the center between coordinating pyrazolate N as points of extension, leads to a BC helix. The underlying topology was determined to be a uninodal 7-c net, and the symbol **wuy** was assigned in RCSR. The net contains seven kinds of edge, thus transitivity 1 6 and symmetry $I4_1/amd$. That is the simplest (minimal transitivity) possible way to link BC helices with opposite hand.

There is a unique minimal transitivity way to join such helices, all of the same hand, by links roughly normal to the helix axis, producing the 7-c net **lll** (Figure 84) with transitivity 1 6 and symmetry $I4_122$.

Such linked BC helix SBUs can also be found with mixed metals, as observed in $[NaM(-COO)_4]_\infty$, that together with octatopic Zn-OCPP (Zn−H_8OCPP = zinc−tetrakis(3,5-dicarboxyphenyl)-porphyrin), produces LnMPF-1 (LnMPF = lanthanoid−metalloporphyrin porous frameworks, Ln = Sm, Gd, Eu, Tb, Dy), Na_2Ln_2(Zn-OCPP).[248] Figure 85 shows the rod SBU, running along [001], that is composed of alternating Na^+ and Ln^{3+} centers. The latter are eight-coordinated by six oxygen from carboxylates and two additional water molecules, whereas the sodium is seven-coordinated, exclusively by carboxylate O. The rod SBUs form helices, that are of both hands and appear in an alternating fashion. The authors described the topology by deconstructing the rod into discrete $Ln(-COO)_4$ SBUs and 8-c octatopic linkers, resulting in a binodal (4,8)-c net. However, we prefer a different deconstruction approach (i.e., the octatopic linker is described as four triangles linked to a square and the rod is composed of a BC helix). The resulting net, **hqy**, has transitivity 4 10 and symmetry $I4_1/amd$.

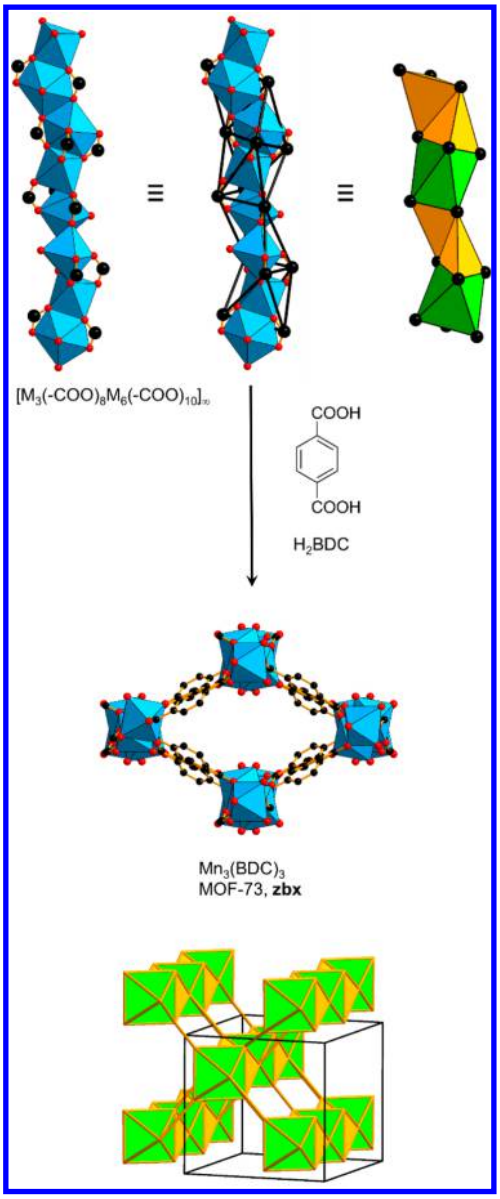

Figure 64. Crystal structure of MOF-73 and its underlying **zbx** topology.[6] Color code: black, C; red, O; blue polyhedra, metal.

13.2. MOFs with SBUs Derived from the Lidin-Andersson Helix

A recently reported, and aesthetically pleasing example of rod MOFs is Bi(BTC), termed CAU-17 (Figure 86).[30] In this structure, the asymmetric unit is quite large, containing nine Bi, nine BTC, and nine water molecules; however, the coordination around the metal center is very similar. Each Bi^{3+} is nine-coordinated by eight carboxylate O and one terminal water molecule. The $[M(-COO)_3]_\infty$ SBU can be deconstructed by considering the carboxylate C as points of extension, leading face-sharing octahedra, that in turn constitute a LA helix. In contrast to the BC helix which is always tetragonal, the LA helix is always trigonal in periodic structures. Cross-linking of the helices that are not related by symmetry through BTC leads to the formation of triangular channels, in the case of single linking, and formation of double-walled hexagonal channels, in the case of double linking.

DOI: 10.1021/acs.chemrev.6b00346
Chem. Rev. XXXX, XXX, XXX−XXX

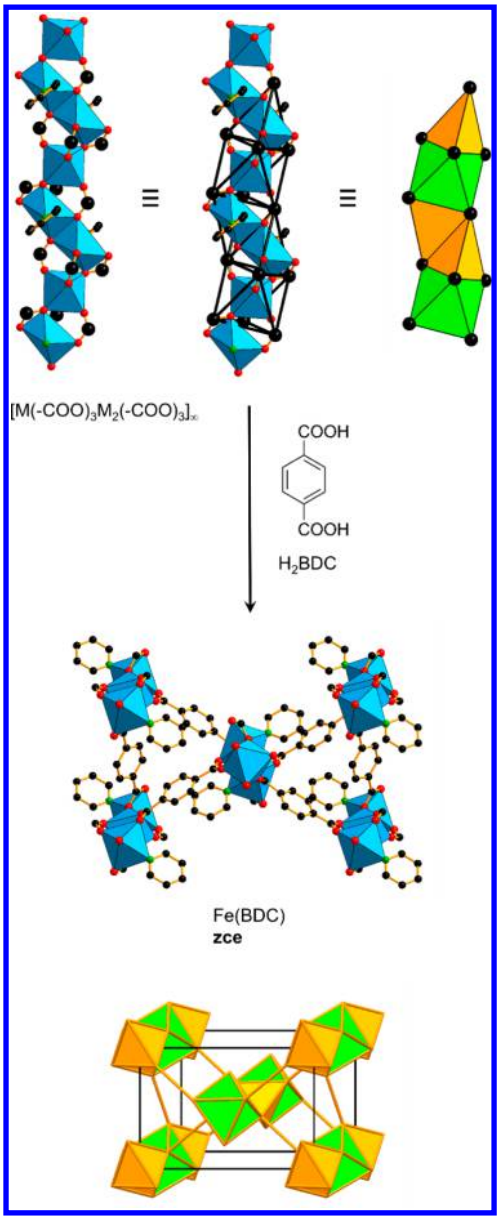

Figure 65. Crystal structure of Fe(BDC). The rod SBU is composed of linked octahedra and tetrahedra in a ratio of 1:2. The topology is a trinodal (6,7)-c **zce** net.[231] Color code: black, C; red, O; green, N; blue polyhedra, metal.

The resulting topology (**rn-11**, see Supporting Information) is of remarkable complexity and has transitivity 54 135. The symmetry is $P\bar{3}$. It therefore represents the most complicated net encountered in a MOF so far, although it is assembled from simple building units.

The most prominent example of rod MOFs is termed MOF-74 and represents the parent structure of the most studied isoreticular series in MOF chemistry. Some studies include isoreticular expansion,[71] inclusion of biomolecules, sorption of carbon dioxide[249] and hydrogen[60] and separation of various hydrocarbons[250] among others. The parent MOF-74 structure, also termed CPO-27 by its independent discoverers,[55] M_2(DOBDC) $(DMF)_2{\cdot}2H_2O$ (M= Zn, Co; H_4DOBDC = 2,5-dihydroxy-1,4-benzenedicarboxylic acid) was obtained in 2005[6] and is composed of infinite $[M_3(-O)_3(-COO)_3]_\infty$ rod SBUs that run along [001] and are linked into a hexagonal, 3-dimensional framework (Figure 87). Each Zn^{2+} is herein octahedrally coordinated by three carboxylate groups, two phenolates, and one solvent molecule. The topology was initially described as a 3-c **etb** or a 5-c **bnn** net, depending on whether the oxo-functionalities are also considered as points of extension or only the carboxylates are taken into account. According to our approach, we describe the SBU derived from a LA helix by omitting the vertices furthest from the axis to produce a rod of square pyramids sharing triangular faces (diminished LA helix). Squares (here in square pyramids) are often associated with open metal sites and could theoretically be dissected in triangles, which we do not recommend in order to keep the structural information on the open metal site. There are then two kinds of verticies: 3.4.3.4 and $3^2.4.3^2.4$, that, together with the DOBDC linkers represented by squares, lead to the 4-nodal (3,5,7)-c **msf** net. This net contains nine kinds of edges, transitivity 4 9 and symmetry $R\bar{3}$. If such MOF-74 structures are isoreticular expanded, to obtain MOFs with pore openings of up to 98 Å, the square vertex figure is deconstructed into two triangles, leading to a 5-nodal (3,5,7)-c **msg** net. Figure 87 (right) shows IRMOF-74-II, Mg_2(DOBPDC), (H_4DOBPDC = 3,3′-dihydroxy-4,4′-biphenyldicarboxylic acid).[71]

Two isomers of such structures, that in turn have different nets, are based on isomers of the linkers. In contrast to the parent MOF-74 structure, these structural isomers with formula M_2(*m*DOBDC) (M= Mg, Mn, Fe, Co, Ni; H_4*m*DOBDC = 4,6-dihydroxy-1,3-benzenedicarboxylic acid) were prepared in 2014 (Figure 88, left).[251] The rod SBU is composed of the same infinite $[M_3(-O)_3(-COO)_3]_\infty$ chains that run along [001]; however, the linker symmetry changed from 2/m = C_{2h} (H_4DOBDC) to *mm*2 = C_{2v} (H_4*m*DOBDC). This in turn causes a change in the space group to *R*3*m*. Deconstruction of this framework leads to an SBU derived from a LA helix, with different connectivity than the 4-nodal **msf** net. We have assigned the symbol **msh** in RCSR to this net having transitivity 4 10 and symmetry is *R*3*m*. The derived structure M_2(*m*DOBPDC) (M= Mg, Zn; H_4*m*DOBPDC = 4,4′-dihydroxy-3,3′-biphenyldicarboxylic acid), that has been discovered earlier, can be deconstructed similarly (Figure 88, right).[252] In addition to the LA helix, the square vertex figure is split into two triangles, leading to a 5-nodal (3,5,7)-c **msi** net with transitivity 5 11 and symmetry $P3_221$.

In Figure 89 (left), we show a framework that also consists of a diminished LA helix SBU, however with different connectivity. When such $[M_3(-COO)_3]_\infty$ SBUs were combined with ditopic BPDC, a framework $Cd_3(BPDC)_3$ (termed JUC-48) was produced.[253] In particular, the two crystallographically independent Cd^{2+} are both coordinated in an octahedral environment by five carboxylate O and one solvent molecule. The distorted hexagonal channels show dimensions of 21.1 × 24.9 Å. The authors identified the helix as 3_1 by taking carboxylate C as points of extension but wrongly obtained a 3-c **etb** net. Following the deconstruction approach described in the publication, the net **eth** would logically be obtained, another (nonminimal transitivity) way of linking 3_1 helices, other than **eta** and **etb**. However, according to our approach, we better describe it as a **qsl** net with transitivity 4 10 and symmetry *Pbcn*. A very similar MOF, termed CZJ-3, Cd(CVB) (H_2CVB = (*E*)-4-(2-carboxyvinyl)benzoic acid) is produced through combination of LA helix type SBUs $[M_3(-COO)_3]_\infty$ with ditopic CVB (Figure 89, right).[254] CZJ-3 crystallizes in the chiral hexagonal space group $P6_522$, and the authors have not determined the topology of the framework. In analogy to JUC-48, we deconstructed the framework and found a (5,7)-c **dmj** net with transitivity 2 4 and symmetry $P6_522$. In this structure, there are

DOI: 10.1021/acs.chemrev.6b00346
Chem. Rev. XXXX, XXX, XXX−XXX

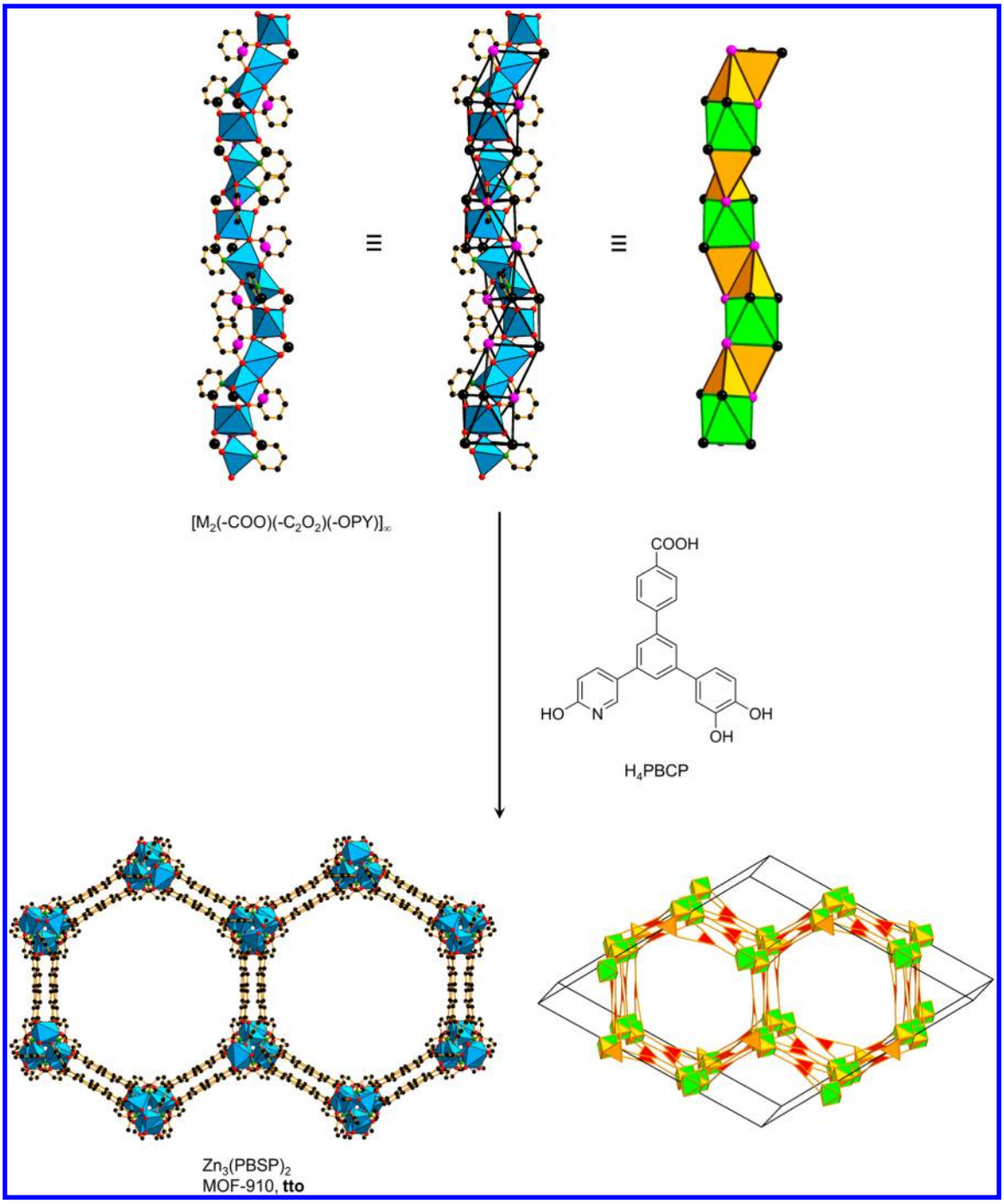

Figure 66. Single-crystal X-ray structure of MOF-910 and its underlying **tto** topology. The special nature of the trifunctional linker facilitates a helical SBU and renders MOF-910 into a double-walled framework. Color code: black, C; red, O; green, N; blue polyhedra, metal; pink, points of extension.

two rods per unit cell running along 1/3,2/3, **z** and 2/3,1/3, **z**, both with symmetry $\mathbf{p}3_22$ and this appears to be the (unique?) minimal transitivity way of inking diminished LA rods of the same hand into a periodic framework. In contrast, in the **qsl** net rods of opposite hands are linked. Linking such $\mathbf{p}3_12$ and $\mathbf{p}3_22$ rods is possible with minimal transitivity and symmetry $R\bar{3}m$ (net **qsm**, transitivity 2 5), but apparently the greater freedom of the orthorhombic topology, **qsl**, is required by the crystal.

13.3. MOFs with Face-Shared Diminished (Missing Vertex) Pentagonal Bipyramids

The structure of MOF-76, Tb(BTC), was reported in 2005.[6] It contains $[M(-COO)_3]_\infty$ SBUs, in which each Tb^{3+} center is seven-coordinated by six carboxylate O and one water molecule. The topology has been determined as **rnb** in 2012,[4] but this description is no longer appropriate as it considers the metal centers as 6-c nodes. If we consider carboxylate C as points of extension, somewhat similar to La(BTB), also without dissecting the square representing the open metal site, we obtain a rod composed of edge-sharing polyhedra which may be considered as pentagonal bipyramids missing one equatorial vertex ("diminished"). This polyhedron has six vertices and one quadrangular and six triangular faces. Joining of such rods with triangular linkers then results in a 4-nodal (3,5,7)-c **msx** net (Figure 90). This net has transitivity 4 9 and symmetry $P4_322$.

DOI: 10.1021/acs.chemrev.6b00346
Chem. Rev. XXXX, XXX, XXX−XXX

Table 1. Rod MOFs Discussed in This Review, Together with the Composition of Their SBUs and the Underlying Net Topologies, Including Transitivity (T)

SBU	linker	name	formula	net	*T*	ref
simple helices						
$[M_3(POO_2)_3(-N)_3]_\infty$	H_4BPBMP	STA-16	Co_2(BPBMP)	**etb**	1 2	88
$[M_3(COO)_3(-PY)_3]_\infty$	BIPY, HOCA		$Zn_2(HOCA)_4$(BIPY)	**etb**	1 2	90
$[M_3(-TZ)_3Cl_3]_\infty$	H_2BDT		Mn_2(BDT)Cl_2	**etb**	1 2	89
$[M_4(OH)_2(L-ASP)_2(-COO)_2]_\infty$	H_2L-ASP		$Ni_5(OH)_2$(L-ASP)$_4$	**srs**	1 1	93
$[M(-COO)_2]_\infty$	H_2MTETBDC		Pb(MTETBDC)	**ths**	1 2	96
$[M(-COO)_2]_\infty$	H_2TMBD		Pb(TMBD)	**etm**	2 4	97
$[M(OH)_2(-COO)]_\infty$	H_4BTEC	MIL-120	$Al_4(OH)_8$(BTEC)	**raa**	2 5	100
$[M(OH)(-COO)_2]_\infty$	H_4BTEC	MIL-118A	$Al_2(OH)_2$(BTEC)	**rab**	2 5	101
$[M(OH)(-COO)]_\infty$	H_4BTEC	BCF-4	$Be_4(OH)_4$(BTEC)	**rab**	2 5	102
zigzag ladders						
$[MX(-COO)_2]_\infty$	H_2BDC	MOF-71	Co(BDC) (DMF)	**sra**	1 3	6
$[MX(-COO)_2]_\infty$	H_2BDC	MIL-68	V(OH) (BDC)	**rad**	3 6	114
$[MX(-COO)_2]_\infty$	H_2BPODC	CAU-8	Al(OH) (BPODC)	**cua**	2 5	116
$[M(-COO)_2]_\infty$	H_2BDC		Tb(BDC) (NO_3)	**irl**	1 3	28
$[M(-COO)_2]_\infty$	H_2BDC		UO_2(BDC)	**rac**	1 4	123
$[M(-COO)_2]_\infty$	H_2TDC		UO_2(TDC)	**rae**	2 5	123
$[M_2(-COO)_2(-PY)_2]_\infty$	HINA		Li(INA)	**sra**	1 3	113
$[M_3(OH)_4(-OCCN)_2(-NCN)_2]_\infty$	H_2PXT		$Co_3(OH)_4$(HPXT)$_2$	**umr**	1 3	128
$[M_2(OH)_2(-COO)_4]_\infty$	H_4BTEC	MIL-60	$V_2(OH)_2$(BTEC)	**fry**	2 5	129
$[M_2(OH)_2(-COO)_4]_\infty$	H_4TBAPy	ROD-7	$In_2(OH)_2$(TBAPy)	**frz**	3 6	134
$[M_2(OH)_2(-COO)_4]_\infty$	H_3BTTB	437-MOF	$In_3(OH)_3$(BTTB)$_2$	**dum**	2 4	136
$[M_2(-COO)_4]_\infty$	H_4TBAPy	ROD-6	Mn_2(TBAPy)	**lrk**	3 7	137
$[M_2(-COO)_4]_\infty$	H_4TBAPy	ROD-8	Cd_2(TBAPy)	**lrl**	3 7	137
$[M_2(OH)_2(-COO)_4]_\infty$	H_4BPTTC	MIL-119	$In_2(OH)_2$(BPTTC)	**frx**	3 6	138
$[M_3(-COO)_6]_\infty$	H_3NTBPC	FIR-5	Mg_3(NTBPC)$_2$	**hyp**	4 8	139
linked tetrahedra						
$[M(-PZ)_2]_\infty$	H_2BDP		Co(BDP)	**snp**	1 3	141
$[M(-COO)_2]_\infty$	H_2NDC		Mn(NDC)	**snp**	1 3	140
$[M(-O)(-OH)_2(-COO)]_\infty$	H_4TOB		Co(H_2TOB)	**rkf**	1 4	152
$[M_2(-OH)_2(-COO)_2]_\infty$	H_6TOHDC		Zn(H_4TOHDC)	**whw**	1 4	153
$[M(-COO)_2]_\infty$	H_4ATC	MOF-77	Zn_2(ATC)	**ssm**	2 7	6
$[M(-PZ)_2]_\infty$	H_3BTP		Zn_3(BTP)$_2$	**ccg**	4 10	39
$[M(-COO)(-COOH)]_\infty$	H_4BTEC		Li_2(H_2BTEC)	**zbn**	2 7	154
$[M_3(H_2O)(-PZ)_8]_\infty$	H_3BTP		$Zn_9(H_2O)_3$(BTP)$_8$	**ltw**	2 6	39
linked octahedra						
$[M(-COO)_3]_\infty$	H_2SUC	MIL-17	Pr_2(SUC)$_3$	**oab**	2 6	155
$[M(-COO)_3]_\infty$	H_2ADC	MIL-83	Eu_2(ADC)$_3$	**swk**	1 4	160
$[M(-COO)_3]_\infty$	H_2HFIPBB	ITQMOF-2	Ln_2(HFIPBB)$_3$	**bvh**	2 7	164
$[M(-COO)_3]_\infty$	H_2HFIPBB	RPF-4	La_2(HFIPBB)$_3$	**fga**	3 11	165
$[M(-PZ)_3]_\infty$	H_2BDP		Fe_2(BDP)$_3$	**sct**	2 8	166
$[M(-TZ)_3]_\infty$	H_2BDT		$Fe_2(H_{0.67}BDT)_3$	**yzh**	2 8	159
$[M(-PO_2OH)_2(-POO_2)]_\infty$	H_4PBMP		Zr_2H_4(PBMP)$_3$	**wnf**	1 4	169
$[M(-COO)_3]_\infty$	H_2*m*BDC		Eu_2(*m*BDC)$_3$	**rn-1**	3 10	171
$[M(-COO)_3]_\infty$	NH_2−H_2*m*BDC		$Pr_2(NH_2$-*m*BDC)$_3$	**rn-2**	3 10	172
$[M(-COO)_2(-PY)_2]_\infty$	HPBA	MCF-44	Fe(PBA)$_2$	**hlz**	2 4	173
$[M(-COO)_2(-PY)_2]_\infty$	H*m*PBA	MCF-34	Mn(*m*PBA)$_2$	**zhl**	2 8	177
$[M(-COO)_3]_\infty$	H_3BTTN	UTSA-30	Yb(BTTN)	**hyb**	2 4	29
$[M(-COO)_3]_\infty$	H_3NTBPC	FIR-8	Ce(NTBPC)	**hyc**	4 9	178
$[M(-COO)_3]_\infty$	H_3CMPDB		Er(CMPDB)	**hyd**	4 9	179
$[M(-COO)_3]_\infty$	H_6L		Ln_2L	**rn-3**	7 19	181
$[M(-COO)_3]_\infty$	H_4DDPP		Eu(HDDPP)	**rn-4**	5 13	182
linked trigonal prism						
$[M(-COO)_3]_\infty$	H_2*m*PYDC		Er_2(PYDC)$_3$	**ttw**	1 3	161
$[M(-COO)_3]_\infty$	H_2ADIP	GWMOF-6	Pr_2(ADIP)$_3$	**rn-5**	3 8	186
$[M_2(-COO)_6]_\infty$	H_2CHDC		Nd_2(CHDC)$_3$	**zbf**	2 6	188
$[M_2(-COO)_6]_\infty$	H_2BDC		Cd_3(BDC)$_3$	**zbc**	3 7	189
$[M_2(-COO)_6]_\infty$	H_2BPDC		Ln_2(BPDC)$_3$	**rn-6**	3 9	190
$[M_2Cl(-COO)_6]_\infty$	H_2-1,4-NDC		Ln_2Cl(1,4-NDC)$_3$	**zbh**	2 7	193

DOI: 10.1021/acs.chemrev.6b00346
Chem. Rev. XXXX, XXX, XXX−XXX

Table 1. continued

SBU	linker	name	formula	net	*T*	ref
$[NaM(-COO)_3]_\infty$	H_2BPODC		$NaTb(BPODC)_2$	**zbd**	2 6	194
$[M_2(-COO)_6]_\infty$	H_3BTB	MIL-103	Tb(BTB)	**tpr**	2 4	195
$[M_2(-COO)_6]_\infty$	H_3NTB		Tb(NTB)	**zbi**	4 8	202
linked square pyramid						
$[M_2(-COO)_6]_\infty$	H_2ADIP	GWMOF-3	$Pr_2(ADIP)_3$	**zbl**	2 5	186
$[M(-COO)_3(HCOOH)]_\infty$	H_2BPDC		$Ln_2(BPDC)_3(HCOOH)_2$	**zbo**	3 9	203
$[M_2(-COO)_6]_\infty$	H_2PDC	MOF-80	$Tb_2(PDC)_3$	**rn-7**	3 10	6
$[M(-COO)_3]_\infty$	H_3BCMTPA	MIL-112	La(BCMTPA)		–	209
$[M_2(-COO)_6]_\infty$	H_3CPIA		La(CPIA)	**rn-8**	4 8	210
$[M(-COO)_3]_\infty$	H_3BPT		Yb(BPT)	**zcd**	6 13	211
$[M_3(\text{-}PO_2OH)_3]_\infty$	H_6TTTP		$Al(H_3TTTP)$	**zbq**	6 13	212
$[M(-COO)_2(-PY)]_\infty$	H_2*m*PYDC		Mg(*m*PYDC)	**zbp**	4 8	214
linked tetragonal prism						
$[M_2O_2(-COO)_4]_\infty$	H_2BDC	MIL-140A	ZrO(BDC)	**gui**	3 6	215
$[M_2O(-COO)_4]_\infty$	H_2*m*BDC		$In_2O(mBDC)_2$	**svq**	1 4	218
$[M_2(OH)_2(-SOO_2)_4]_\infty$	H_2NDS	LnPF-1	Ln(OH) (NDS)	**fee**	1 3	219
$[M_3(OH)_2(-COO)_4(-PY)_2]_\infty$	H_2*o*PYDC	CUK-1	$Co_3(OH)_2(oPYDC)_2$	**fee**	1 3	220
$[M(-SOO_2)_4]_\infty$	V–H_4TPPS		Sm(V-HTPPS)	**zbs**	2 4	223
$[M_3(OH)_2(-O)_8]_\infty$	H_2DOCBD		$Co_3(OH)_2(DOCBD)_2$	–	–	226
mixed polyhedra						
$[M_2(-COO)_4M(-COO)_2]_\infty$	H_3BPT		$Cd_3(BPT)_2$	**zbu**	4 9	227
$[M_2(-COO)_4M(-COO)_2]_\infty$	H_3BPT		$Cd_3(BPT)_2$	**zbv**	6 13	227
$[M(-COO)_2M(-COO)_2(-C_2O_2)_2]_\infty$	H_2TDC, H_2OX		$Dy_2(TDC)_2(OX)$	**zbt**	2 6	228
$[M_3(-COO)_6M(-COO)_2]_\infty$	H_2HPDC	MOF-79	$Cd_2(HPDC)_2$	**rn-9**	2 8	6
$[Na_3(-COO)_7M_3(-COO)_5]_\infty$	H_2*m*BDC	MOF-CJ2	$NaZn(mBDC)_2$	**zbw**	2 8	229
$[M_3(-COO)_8M_6(-COO)_{10}]_\infty$	H_2BDC	MOF-73	$Mn_3(BDC)_3$	**zbx**	3 12	6
$[M(-COO)_3M_2(-COO)_3]_\infty$	H_2BDC		Fe(BDC)	**zce**	3 10	231
$[M_2(-COO)(-C_2O_2)(-OPY)]_\infty$	H_3PBSP	MOF-910	$Zn_3(PBSP)_2$	**tto**	6 16	
linked triangles - helical ribbon						
$[M(OH)(-COO)_2]_\infty$	H_2TDC	NOTT-401	Sc(OH) (TDC)	**yfm**	1 4	232
$[M(OH)(-COO)_2]_\infty$	H_4BPTC	NOTT-400	$Sc_2(OH)_2(BPTC)$	**nti**	3 7	232
$[M(-PZ)_2]_\infty$	H_2BPZ		Cd(BPZ)	**wjp**	1 4	147
$[M(OH)(-COO)_2]_\infty$	H_2BCIm		In(OH) (BCIm) (NO_3)	**sbq**	10 25	40
$[CaM(-COO)_4]_\infty$	OH-H_2*m*BDC		$PbCa(OH\text{-}mBDC)_2$	**zba**	2 6	237
$[M(-COO)_2]_\infty$	H_2BDC		Co(BDC)	**zbz**	2 6	238
linked quadrangles						
$[M_2(-COO)_2(-CNS)_2]_\infty$	H_2MNA	CUK-2	$Co_2(MNA)_2$	**pcl**	1 4	220
$[M_4(OH)_2(-COO)_6]_\infty$	H_3TPTC		$Cd_4(OH)_2(TPTC)_2$	**shf**	4 8	239
$[M_2(-COO)_6]_\infty$	H_2TDC		$Ln_2(TDC)_3$	**zbb**	3 6	240
$[M_5(OH)_4(-COO)_6]_\infty$	H_2DMBDC		$Zn_5(OH)_4(DMBDC)_3$	**zca**	3 8	150
other rods						
$[M_5(OH)_9(-SOO_2)_6]_\infty$	H_2NDS	LnPF-3	$Ln_5(OH)_9(NDS)_3$	–	–	221
$[(UO_2)_3O(OH)_2(-COO)_3]_\infty$	H_4BTEC		$(UO_2)_{12}O_4(OH)_8(BTEC)_3$	**zcc**	2 4	241
$[M(-COO)_3]_\infty$	H_3BTC	MIL-45	$KFe_3(BTC)_3$	**zcb**	6 16	243
$[M_6(-COO)_9(COO)_2$						
$M_3(-COO)_6(COO)_2]_\infty$	H_3BTC		$[NH_2(CH_3)_2]Fe_5(BTC)_3(OAc)_2$	**rn-10**	10 16	244
$[M_{13}(OH)_{27}(-COO)_6]_\infty$	NH_2–H_2BDC	CAU-6	$Al_{13}(OH)_{27}(NH_2\text{–}BDC)_3Cl_6$	**can**	1 3	245
aperiodic helices						
BC helix						
$[M(-COO)_2]_\infty$	H_4BIPA-TC		Ca_2(BIPA-TC)	**hqx**	3 9	247
$[M(-PZ)(-COO)]_\infty$	H_2DMPMB	ROD-1	Cd(DMPMB)	**wuy**	1 6	
$[NaM(-COO)_4]_\infty$	Zn–H_8OCPP	LnMPF-1	Na_2Ln_2(Zn-OCPP)	**hqy**	4 10	248
LA helix						
$[M(-COO)_3]_\infty$	H_3BTC	CAU-17	Bi(BTC)	**rn-11**	54 135	30
$[M_3(\text{-}O)_3(-COO)_3]_\infty$	H_4DOBDC	MOF-74	Zn_2(DOBDC)	**msf**	4 9	6
$[M_3(-O)_3(-COO)_3]_\infty$	H_4DOBPDC	IRMOF-74	Mg_2(DOBPDC)	**msg**	5 11	71
$[M_3(\text{-}O)_3(-COO)_3]_\infty$	H_4*m*DOBDC		Co_2(*m*DOBDC)	**msh**	4 10	251
$[M_3(-O)_3(-COO)_3]_\infty$	H_4*m*DOBPDC		Zn_2(*m*DOBPDC)	**msi**	5 11	252
$[M_3(-COO)_3]_\infty$	H_2BPDC	JUC-48	$Cd_3(BPDC)_3$	**qsl**	4 10	253
$[M_3(-COO)_3]_\infty$	H_2CVB	CZJ-3	Cd(CVB)	**dmj**	2 4	254

DOI: 10.1021/acs.chemrev.6b00346
Chem. Rev. XXXX, XXX, XXX–XXX

Table 1. continued

SBU	linker	name	formula	net	*T*	ref
diminished pentagonal bipyramid						
$[M(-COO)_3]_\infty$	H_3BTC	MOF-76	Tb(BTC)	**msx**	4 9	6
$[M(-COO)_3]_\infty$	H_3BTB		La(BTB)	**tpr**	2 4	199
$[M(-COO)_3]_\infty$	H_3BTB		La(BTB)	**awd**	4 9	199
$[M_3(-COO)_3]_\infty$	H_3BTN	PCP-1	La(BTN)	–	–	200
(1,3,4) helix						
$[M_2(-COO)_6]_\infty$	H_2DMS		$Ln_2(DMS)_3$	**fni**	1 3	162
$[M_2(-COO)_6]_\infty$	H_2DMS		$Ln_2(DMS)_3$	**yan**	1 4	162

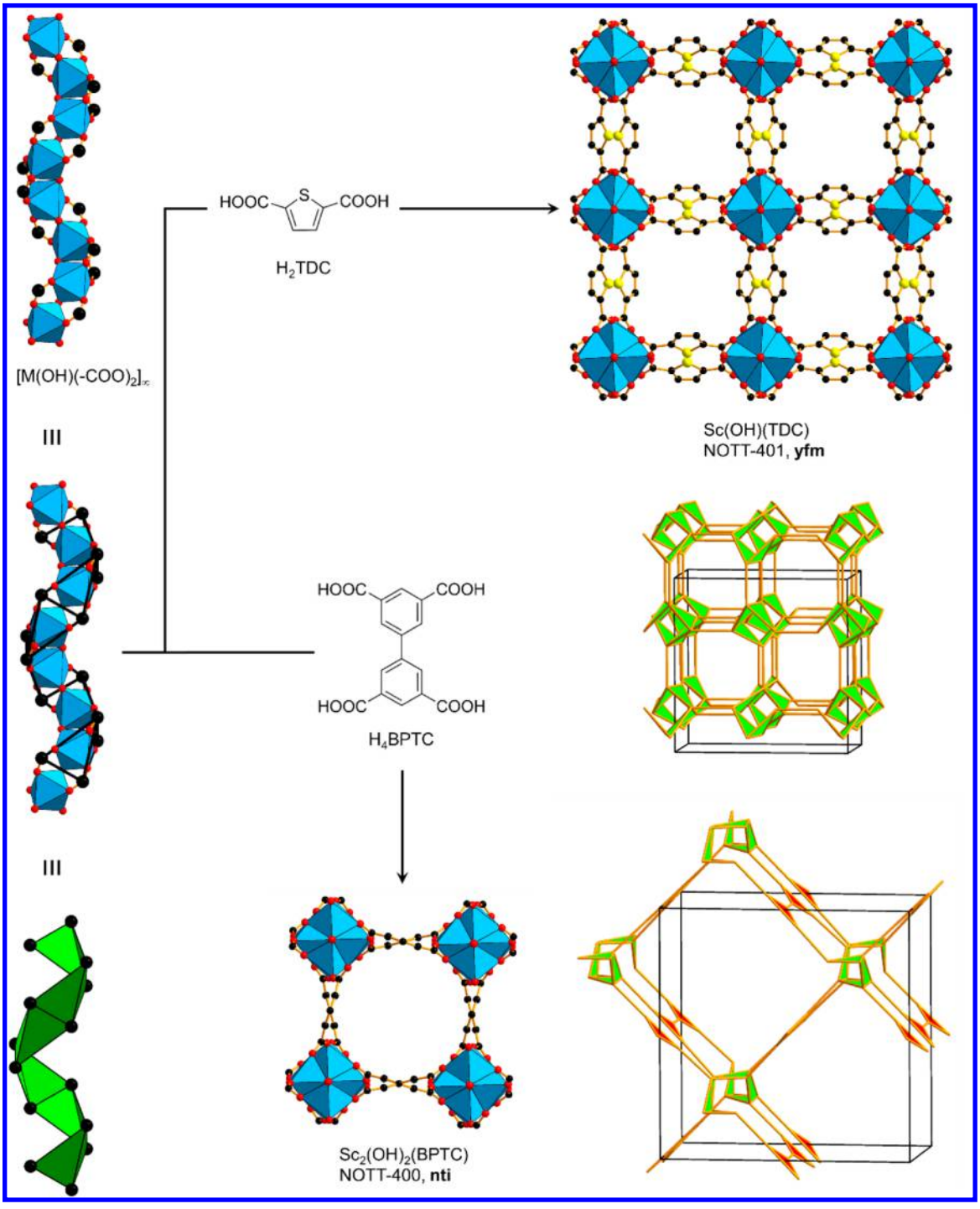

Figure 67. Structural diversity when linking $[M(OH)(-COO)_2]_\infty$ helical ribbon SBUs with ditopic or tetratopic carboxylates. The resulting nets show either 5-c **yfm** or (3,5)-c **nti** topology.[232] Color code: black, C; red, O; yellow, S; blue polyhedra, metal.

DOI: 10.1021/acs.chemrev.6b00346
Chem. Rev. XXXX, XXX, XXX−XXX

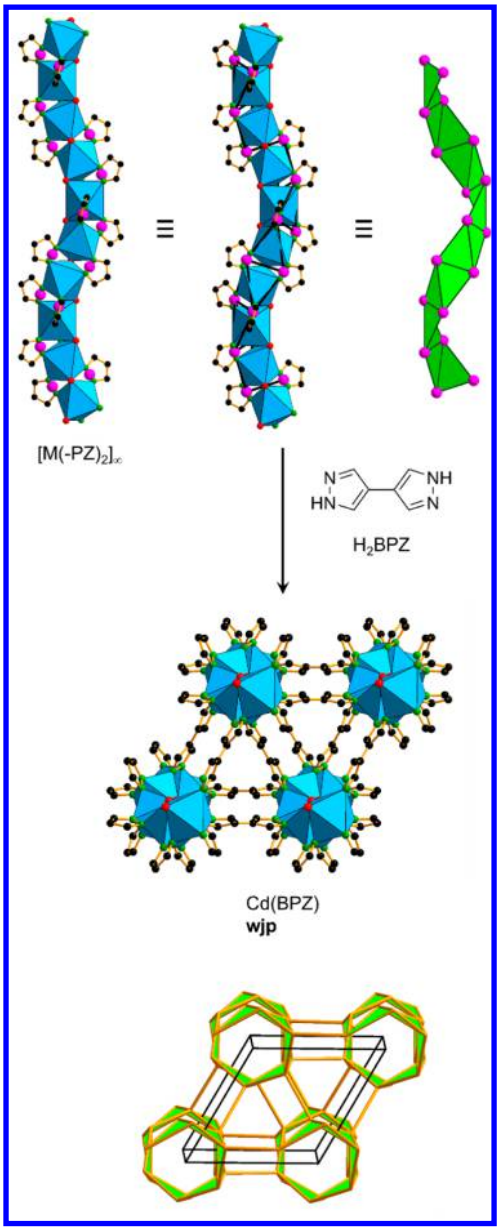

Figure 68. Hexagonal helical ribbon SBUs of formula $[M(-PZ)_2]_\infty$ that have the framework Cd(BPZ), crystallizing in $P6_122$. The underlying topology is 5-c **wjp**.[147] Color code: black, C; green, N; blue polyhedra, metal; pink, points of extension.

This topology has been encountered quite frequently in many isostructural compounds, when lanthanide salts are reacted with H_3BTC.[255−264]

Another series of frameworks can be described similarly, with La(BTB) as the parent compound.[199,265] In the rod SBU of formula $[M(-COO)_3]_\infty$, each La^{3+} is nine-coordinated by eight oxygen from six carboxylate groups and one solvent (water) molecule. Figure 91 (right) shows such SBUs, deconstructed into triangular face-sharing trigonal prisms that when combined with the triangular BTB linker, produced a framework with an underlying binodal (3,5)-c **tpr** net. It contains two kinds of vertices and four kinds of edge with transitivity 2 4 and symmetry $P\bar{6}m2$. However, we believe that the dissection of square faces, of such trigonal prismatic SBUs is more appropriate which transforms the 5-c node into a 6-c and 7-c node, respectively. The square face that contains the open metal site is not dissected in order to keep the structural information, similar to MOF-74. This different deconstruction then leads to a 4-nodal (3,6,7)-c **awd** net (Figure 91, left). It shows transitivity 4 9 and symmetry $R32$. Notably all reported crystals of this group have the same chiral $R32$ symmetry rather than the higher symmetry, $P\bar{6}m2$, of the simpler deconstruction.

Another framework that could potentially fall into this category is La(BTN) (H_3BTN = 6,6′,6″-(benzene-1,3,5-triyl)tris(2-naphthoic acid) as shown in Figure 92.[200] The SBU is composed of face-sharing diminished pentagonal bipyramids that have the same composition as those in La(BTB), however with a highly distorted configuration. Subjecting this net to Systre turns the SBU into a rod composed of face-sharing octahedra with one edge missing and we therefore do not describe this topology in detail.

13.4. MOF Based on Helices of the Erickson Notation (1,3,4)

In the terminology of Erickson,[53] the BC helix is (1,2,3). The next chiral 3^6 cylinder tiling is (1,3,4), which we identify in the MOF described here. The framework is $Ln_2(DMS)_3$ (Ln = Tb, Dy, Ho, Er, Yb, H_2DMS = 2,3-dimethylsuccinic acid), where the $[M_2(-COO)_6]_\infty$ SBU is composed of Ln^{3+} which are eight-coordinated. They are exclusively surrounded by carboxylate oxygen.[162] The authors described the topology appropriately, by considering the carboxylate C as points of extension, leading to a uninodal 5-c **fni** net (Figure 93, left). This net contains chiral 4^4 cylinder tilings and has transitivity 1 3 and symmetry $I4_122$. If we dissect all the quadrangles by joining the shorter diagonal, this compound does not possess open metal sites, we obtain a 7-c **yan** net (Figure 93, right). This net contains now the chiral (1,3,4) 3^6 cylinder tiling and has transitivity 1 4 and again symmetry $I4_122$.

14. RULES FOR THE DECONSTRUCTION AND ANALYSIS OF MOF STRUCTURES

Rules for deconstruction of MOF structures have been discussed before,[4] but here we call attention to points especially relevant for rod MOF structures. In many cases, this deconstruction can be done automatically by a program such as TOPOS;[27] however, we prefer to do it by inspection of the crystal structure. Normally this procedure takes less than an hour, which is not much time to spend on a compound especially since it has taken typically thousands of hours to be synthesized and characterized.

First: identify the points of extension. These mark the interface between the organic and inorganic components of the structure. For example, in carboxylates, the carboxylate C atom. Sometimes a fictive atom as detailed in section 1.3.

Second: identify the metal SBUs. Metal atoms in an SBU are joined to others in the same SBU by M−X−M links (here X is normally an O or N atom) or share a point of extension with other M atoms in the same SBU. The smallest such group are the components of the same SBU.

Third: identify the branch points of the organic linkers.[5]

If the metal SBUs are finite and have a well-defined center then the task of deconstructing the MOF is almost over. If the linkers are ditopic, simply record the links between SBU centers. Otherwise record the links between the centers of the metal SBUs and the branch points of the linker and the links (if any) between branch points of the linkers. Submitting this information to Systre[33] will provide the symmetry of the net and an optimal embedding and identification if the net is known to RCSR.

With rod structures, the procedure is more complicated. We have now to identify the shape of the metal SBUs as defined by the pattern of points of extension. Even for finite SBUs this is

DOI: 10.1021/acs.chemrev.6b00346
Chem. Rev. XXXX, XXX, XXX−XXX

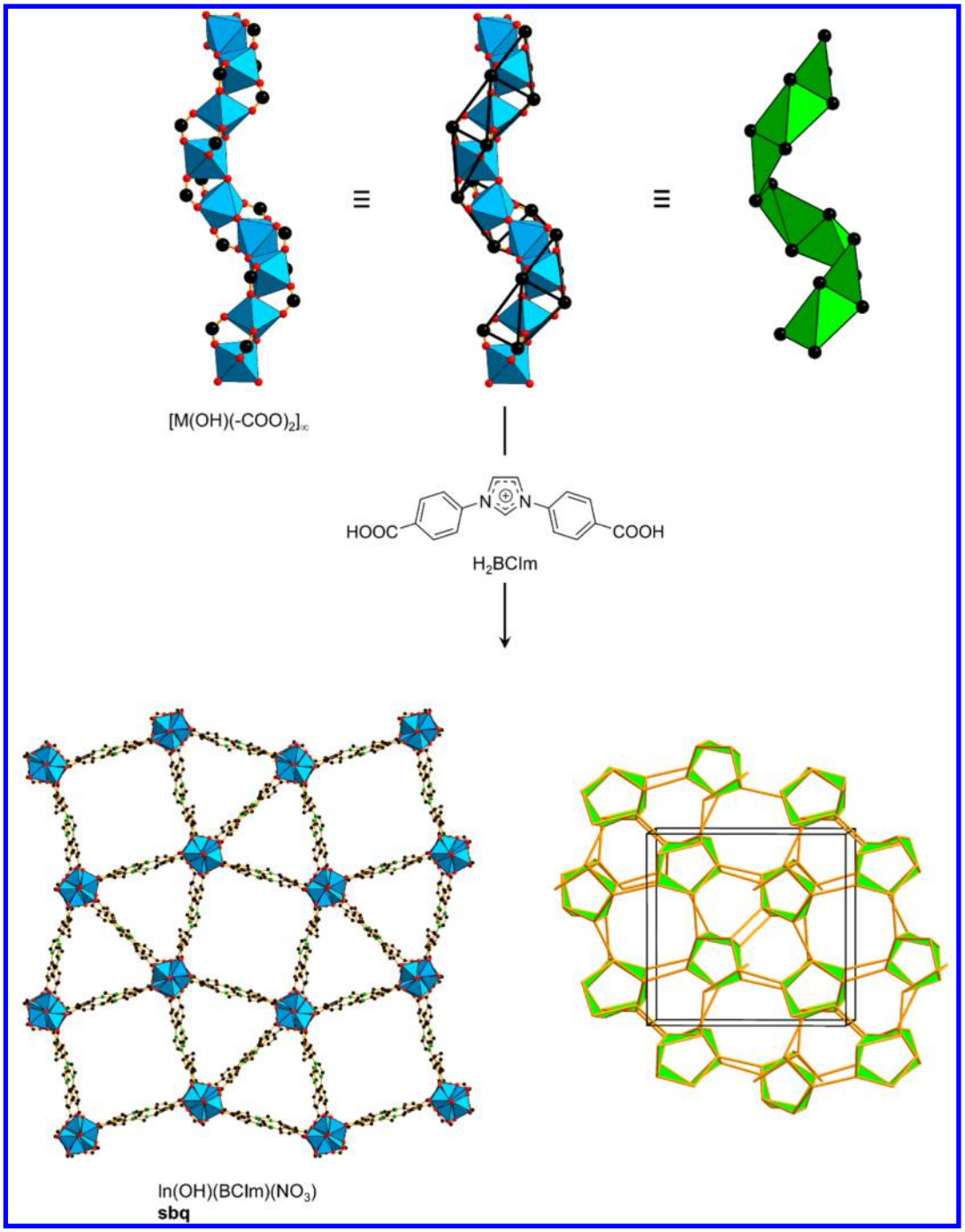

Figure 69. Pentagonal helical ribbon SBUs of formula $[M(OH)(-COO)_2]_\infty$ that have the framework $In(OH)(BCIm)(NO_3)$. The underlying topology is **sbq** with minimal transitivity 10 25.[40,236] Color code: black, C; red, O; green, N; blue polyhedra, metal.

not always obvious. In Figure 94, we show a carboxylate SBU containing 24 carboxylate C atoms (black).[266] As shown in the figure, the pattern of the C atoms could be taken as either a rhombicuboctahedron, 3.4^3, or as a sub cube, $3^4.4$, depending on the range of C···C distances used. One could use an objective criterion,[31] but actually all we need for a finite SBU is the location of the center. But this example has a twist. When the underlying net of the crystal structure is processed by Systre, it is found to have a higher symmetry than the crystal structure and the shape of the coordination figure (used in the augmented version of the net) is actually a truncated octahedron, 4.6^2, as also shown in Figure 94. Of course in this example the determination of the underlying net remains unambiguous.

Turning now to rod SBUs, we again define the shape of the rod as the pattern of points of extension. For organic linkers that are tritopic or larger we replace the branch points by coordination figures as in many examples in this review. The linkages of these nodes (vertices of the shapes) are submitted to Systre as before.

In many cases, such as the many MOF structures based on zigzag ladder SBUs, one again gets one clearly preferred deconstruction. Sometimes two possibilities present themselves as in the MOFs isoreticular to La(BTB) of section 13.3. In that

DOI: 10.1021/acs.chemrev.6b00346
Chem. Rev. XXXX, XXX, XXX−XXX

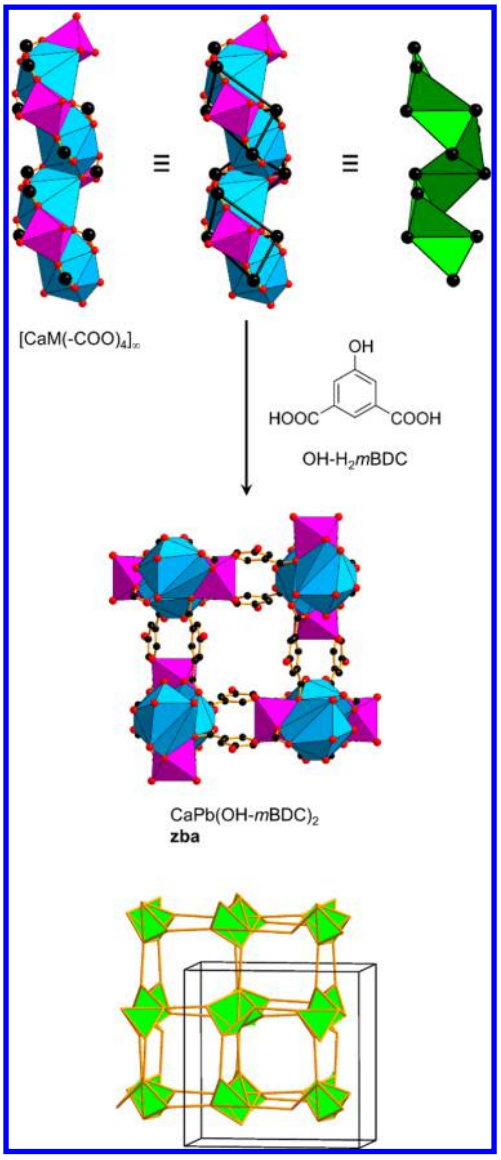

Figure 70. Heterometallic, tetragonal helical ribbon SBU of formula $[CaM(-COO)_4]_\infty$ that has the framework $CaPb(OH\text{-}mBDC)_2$. The underlying topology is a binodal (4,6)-c **zba** net.[237] Color code: black, C; red, O; blue polyhedra, metal, pink polyhedra, Ca.

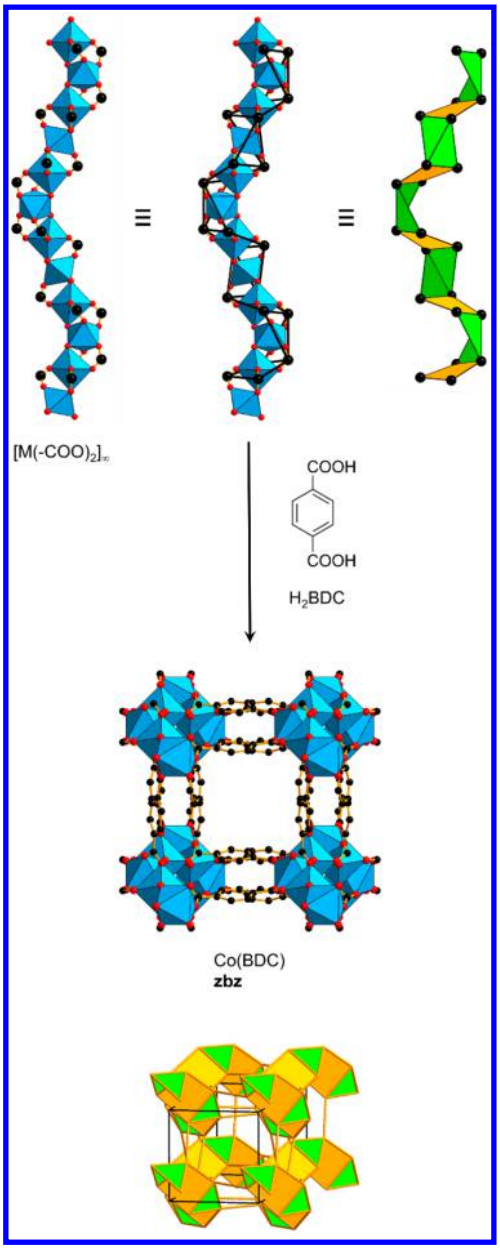

Figure 71. Crystal structure of Co(BDC) and the underlying (4,5)-c **zbz** net. The triangular and quadrangular SBUs form a 4-fold helix.[238] Color code: black, C; red, O; blue polyhedra, metal.

case, we chose the net with the lower intrinsic symmetry as that matched the symmetry of all the reported materials.

In many rod MOFs, there are two or more points of extension close to each other on one end of a linker. This geometry occurs in the large family of MOFs related to MOF-74 and to MOFs formed from linkers containing (*meta*) 1,3-benzenedicarboxylate. When both points of extension are on the same rod, we often join them in determining the rod pattern. This procedure is different from that used in deconstructing finite SBUs because then we never directly link points of extension on the same linker. Consider again as an example HKUST-1 with a BTC linker (section 1.3). We do not take the C···C carboxylate distances on the same linker as links of the pattern. But in contrast, in the case of CAU-17 (section 13.2) with Bi rods joined by BTC linkers, two of the three carboxylate C atoms are on the same rod, and clearly a link between them is part of the pattern of the rod SBU (they are among the shorter C···C distances). Conversely in MOF-76, again with a BTC linker, the C···C distances corresponding to the *meta* carboxylates are greater than others on the rod and therefore not used in the deconstruction (section 13.3, Figure 90).

We use these last examples to emphasize that sometimes there may be two, or even more, ways of deconstructing the structures of rod MOFs. In these cases, one should resist the impulse to single out one as the unique "right" one.

15. CONCLUDING REMARKS

In this review, we have focused on the geometrical structures of rod MOFs. In every case, it is possible to derive an underlying net, many of which are in accord with the minimum transitivity principle.[5] We hope this will encourage those interested in synthesis to likewise analyze their creations. After all, the most important property of a chemical compound is how its atoms are arranged and connected into shapes.

We recognize a relatively small number of rod shapes (e.g., helices, ribbons, ladders, and cylinder tilings), which should form

DOI: 10.1021/acs.chemrev.6b00346
Chem. Rev. XXXX, XXX, XXX−XXX

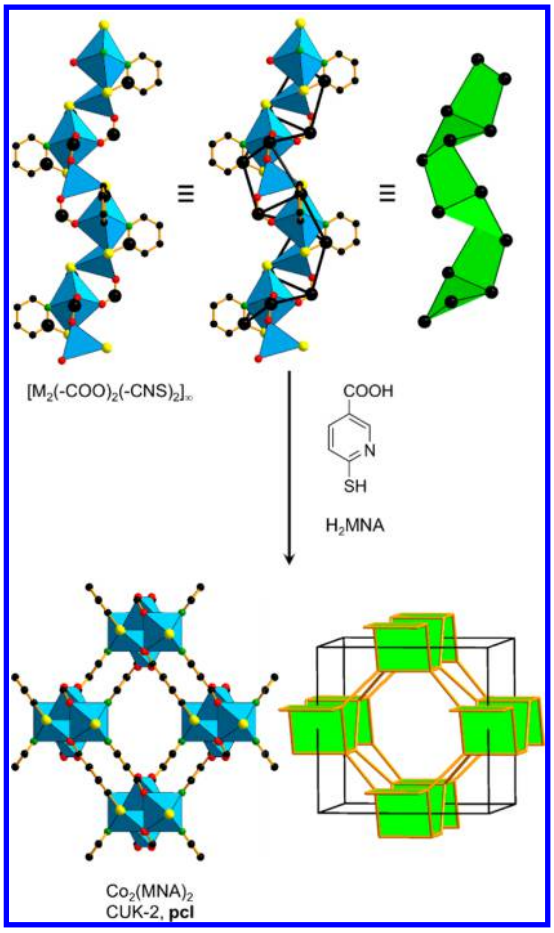

Figure 72. Crystal structure of CUK-2 built of cross-linked double-crankshaft chains, leading to an overall 4-c **pcl** net.[220] Color code: black, C; red, O; green, N; yellow, S; blue polyhedra, metal.

an essential part of the library of shapes for the reticular chemistry of rod MOFs, a field still in its infancy. Such components should also provide necessary input data for future computer compilations and evaluations of hypothetical MOFs. Of course the synthetic chemist must develop strategies for how to target specific SBUs in the laboratory, a topic beyond the scope of this review.

We remark that we have not encountered a rod MOF with more than one kind of rod, indeed CAU-17 is a rare example of a MOF (the only one in this review) in which all rods are not related by symmetry. This suggests that a fertile area of exploration awaits the intrepid chemist, who will attempt to link more than one kind of rod into the same structure much as is currently being done with MOFs with multiple finite SBUs.[267−275]

Table 1 shows all the rod MOFs discussed in this contribution, showing different topologies or are chemically different.

ASSOCIATED CONTENT

Supporting Information

The Supporting Information is available free of charge on the ACS Publications website at DOI: 10.1021/acs.chemrev.6b00346.

CIF file of $Pn\bar{3}n$ symmetry (CIF)

Additional Systre output files for nets with maximum symmetry embeddings (PDF)

AUTHOR INFORMATION

Corresponding Author

*E-mail: mokeeffe@asu.edu.

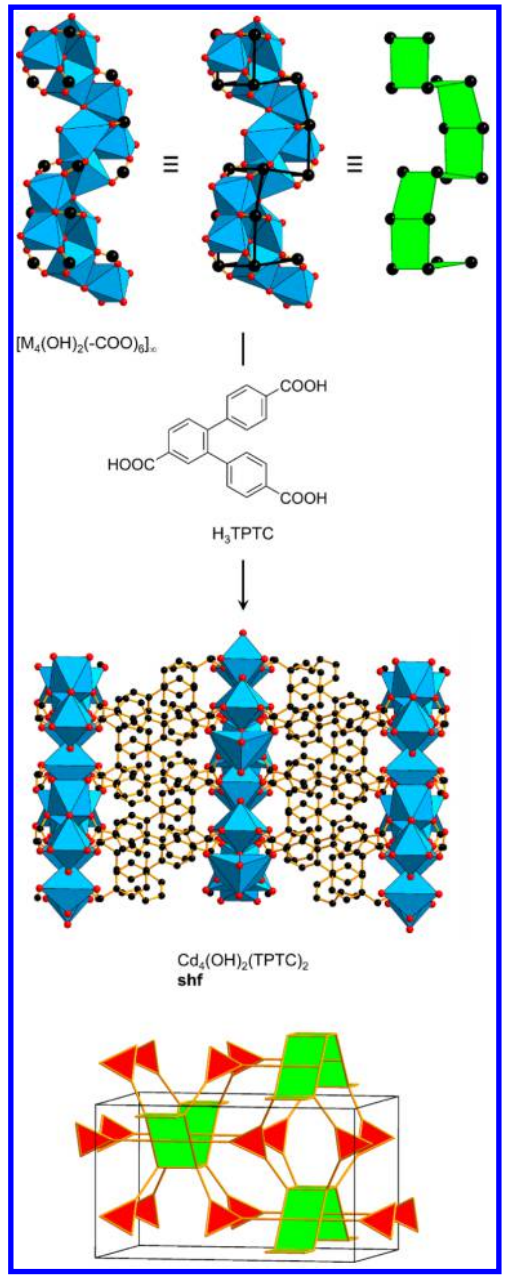

Figure 73. Crystal structure of $Cd_4(OH)_2(TPTC)_2$ built of double-crankshaft chains linked through tritopic linkers into an overall (3,4)-c **shf** net.[239] Color code: black, C; red, O; blue polyhedra, metal.

Notes

The authors declare no competing financial interest.

Biographies

Alexander Schoedel was born in Munich, Germany, and obtained his Diploma degree (M.S. equiv) from the Ludwig Maximilians University, Munich (2009) with Prof. Thomas Bein. He received his Ph.D. from the University of South Florida (2014) with Prof. Michael J. Zaworotko and has since been working as a DFG Postdoctoral Scholar at the University of California, Berkeley, with Prof. Omar M. Yaghi. He is currently an Assistant Professor in the Department of Chemistry at Florida Institute of Technology, Melbourne, USA. His research interests concern reticular chemistry of metal−organic frameworks and related materials, topological crystal chemistry, as well as clean energy applications.

Mian Li (born in Shantou, 1982) studied in Nanjing University and now works at Shantou University. His current research interests include

DOI: 10.1021/acs.chemrev.6b00346
Chem. Rev. XXXX, XXX, XXX−XXX

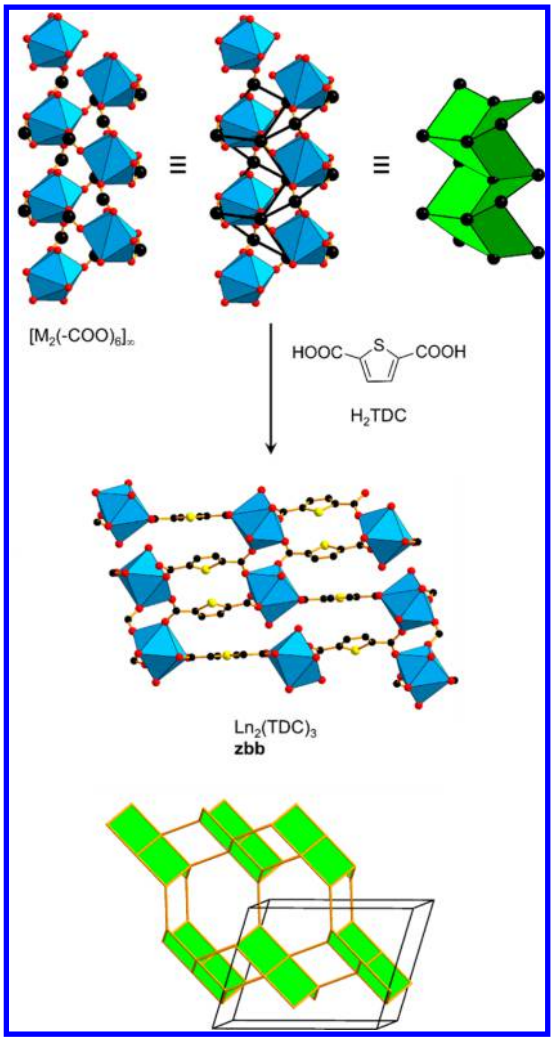

Figure 74. Crystal structure of $Ln_2(TDC)_3$ formed by double ladder SBUs, leading to an overall trinodal (4,5)-c **zbb** net.[191,240] Color code: black, C; red, O; yellow, S; blue polyhedra, metal.

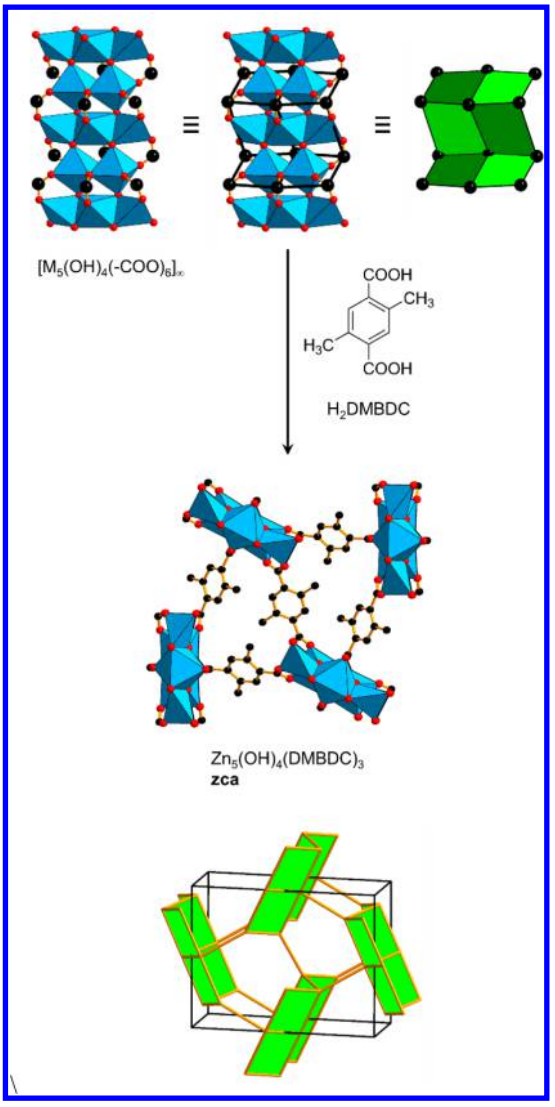

Figure 75. Crystal structure of $Zn_5(OH)_4(DMBDC)_3$, formed by a $[M_5(OH)_4(-COO)_6]_\infty$ SBU. The linking of such double ladder SBUs facilitate a trinodal (4,5)-c **zca** net.[150] Color code: black, C; red, O; blue polyhedra, metal.

chemical topology, luminescent compounds involving Cu−Cu interaction, and host−guest chemistry in biological metal−organic frameworks.

Dan Li was born in Chaozhou, Guangdong, China, in 1964. He received his B.Sc. from Sun Yat-Sen University in 1984 and then served as a teaching assistant at Shantou University. He pursued his Ph.D. at The University of Hong Kong with Prof. Chi-Ming Che from 1988−1993. In April 1993, he returned to Shantou University after the completion of his doctoral degree. He worked as Professor in Chemistry, Director of Research Institute for Biomedical and Advanced Materials, and Vice President of Shantou University. He moved to Jinan University in Guangzhou as the Founding Dean of College of Chemistry and Materials Science in 2016. He was a recipient of the National Science Found for Distinguished Young Scholars of China in 2009. He has been admitted as a Fellow of The Royal Society of Chemistry (FRSC) since 2014. His research interest includes supramolecular coordination chemistry, photoluminescence, porosity, chirality, and especially the design, synthesis, and properties of luminescent d10 transition-metal coordination compounds, including MOFs.

Michael O'Keeffe was born in 1934 in England where he attended Bristol University (B. Sc.; Ph. D., D. Sc.). He is currently Regents' Professor Emeritus at Arizona State University, where he has been since 1963, and Visiting Scholar at University of California, Berkeley. His research concerns the taxonomy of real and hypothetical chemical structures, particularly those with translational symmetry, and reticular chemistry.

Omar M. Yaghi was born in Amman, Jordan, in 1965. He received his Ph.D. from the University of Illinois-Urbana (1990) with Prof. Walter G. Klemperer. He was an NSF Postdoctoral Fellow at Harvard University (1990−1992) with Professor Richard H. Holm. He has been on the faculties of Arizona State University (1992−1998), University of Michigan (1999−2006), and University of California, Los Angeles (2007−2012). His current position is the James and Neeltje Tretter Professor of Chemistry, University of California, Berkeley, and Faculty Scientist at Lawrence Berkeley National Laboratory. His work encompasses the synthesis, structure, and properties of inorganic compounds and the design and construction of new crystalline materials. He has shown that organic and inorganic molecules can be stitched together into extended porous structures called metal−organic frameworks, zeolitic imidazolate frameworks, and covalent organic frameworks.

DOI: 10.1021/acs.chemrev.6b00346
Chem. Rev. XXXX, XXX, XXX−XXX

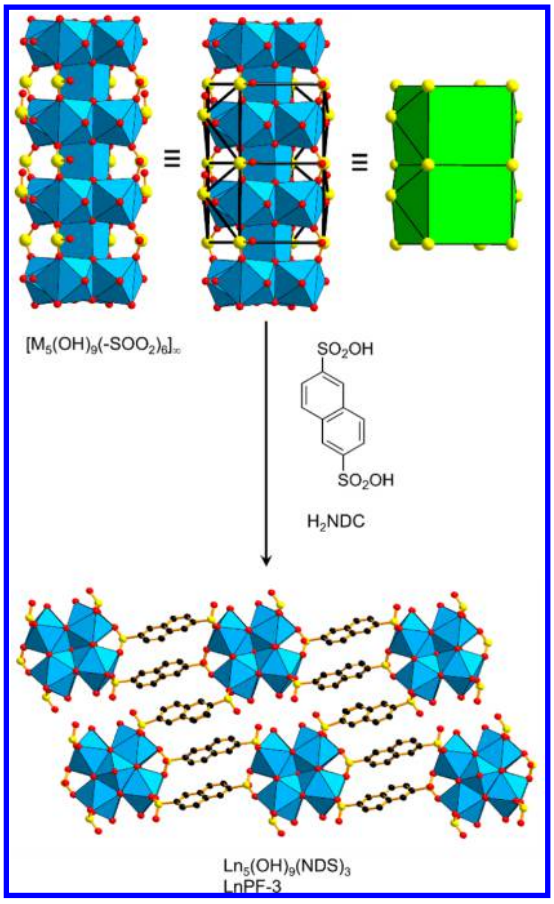

Figure 76. Structure of LnPF-3. The rod SBU is deconstructed into linked bicapped tetragonal prisms.[221] Color code: black, C; red, O; yellow, S; blue polyhedra, metal.

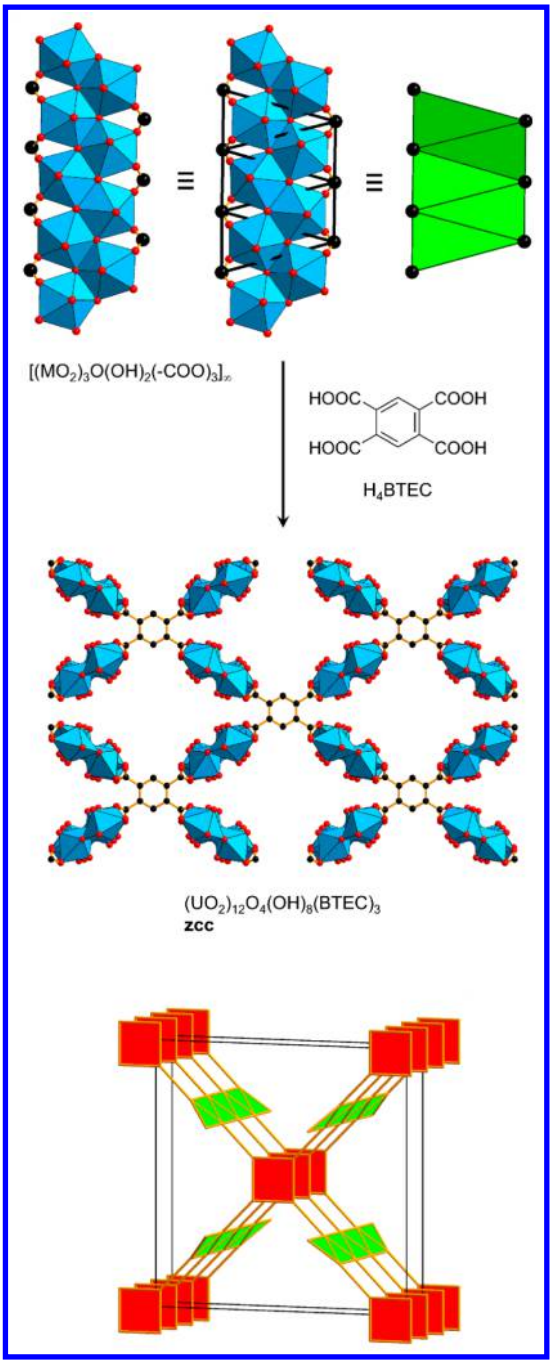

Figure 77. Crystal structure of $(UO_2)_{12}O_4(OH)_8(BTEC)_3$. Rod SBU composed of edge-sharing triangles is linked with square nodes into a (3,4)-c **zcc** net.[241] Color code: black, C; red, O; blue polyhedra, metal.

ACKNOWLEDGMENTS

Funding of MOF research in the Omar Yaghi group is supported by BASF SE (Ludwigshafen, Germany), U.S. Department of Defense, Defense Threat Reduction Agency (HDTRA 1-12-1-0053), U.S. Department of Energy, Office of Science, Office of Basic Energy Sciences, Energy Frontier Research Center grant (DE-SC0001015). Michael O'Keeffe's research is supported by the US National Science Foundation, grant DMR 1104798. Funding of MOF research in the Dan Li group is supported by the National Basic Research Program of China (973 Program, 2012CB821706 and 2013CB834803) and the National Natural Science Foundation of China (91222202 and 21171114). A.S. gratefully acknowledges the German Research Foundation (DFG, SCHO 1639/1-1) for financial support. We thank Ms. Noelle Catarineu for fruitful discussions on MOF-910.

REFERENCES

(1) Democritus ca. 460 BC-370 BC
(2) Furukawa, H.; Cordova, K. E.; O'Keeffe, M.; Yaghi, O. M. The Chemistry and Applications of Metal-Organic Frameworks. *Science* **2013**, *341*, 1230444.
(3) Yaghi, O. M.; O'Keeffe, M.; Ockwig, N. W.; Chae, H. K.; Eddaoudi, M.; Kim, J. Reticular synthesis and the design of new materials. *Nature* **2003**, *423*, 705−714.
(4) O'Keeffe, M.; Yaghi, O. M. Deconstructing the Crystal Structures of Metal−Organic Frameworks and Related Materials into Their Underlying Nets. *Chem. Rev.* **2012**, *112*, 675−702.
(5) Li, M.; Li, D.; O'Keeffe, M.; Yaghi, O. M. Topological Analysis of Metal−Organic Frameworks with Polytopic Linkers and/or Multiple Building Units and the Minimal Transitivity Principle. *Chem. Rev.* **2014**, *114*, 1343−1370.
(6) Rosi, N. L.; Kim, J.; Eddaoudi, M.; Chen, B.; O'Keeffe, M.; Yaghi, O. M. Rod Packings and Metal−Organic Frameworks Constructed from Rod-Shaped Secondary Building Units. *J. Am. Chem. Soc.* **2005**, *127*, 1504−1518.
(7) Wilmer, C. E.; Leaf, M.; Lee, C. Y.; Farha, O. K.; Hauser, B. G.; Hupp, J. T.; Snurr, R. Q. Large-scale screening of hypothetical metal−organic frameworks. *Nat. Chem.* **2011**, *4*, 83−89.
(8) Martin, R. L.; Simon, C. M.; Smit, B.; Haranczyk, M. In silico Design of Porous Polymer Networks: High-Throughput Screening for Methane Storage Materials. *J. Am. Chem. Soc.* **2014**, *136*, 5006−5022.
(9) Lin, L.-C.; Berger, A. H.; Martin, R. L.; Kim, J.; Swisher, J. A.; Jariwala, K.; Rycroft, C. H.; Bhown, A. S.; Deem, M. W.; Haranczyk, M.;

DOI: 10.1021/acs.chemrev.6b00346
Chem. Rev. XXXX, XXX, XXX−XXX

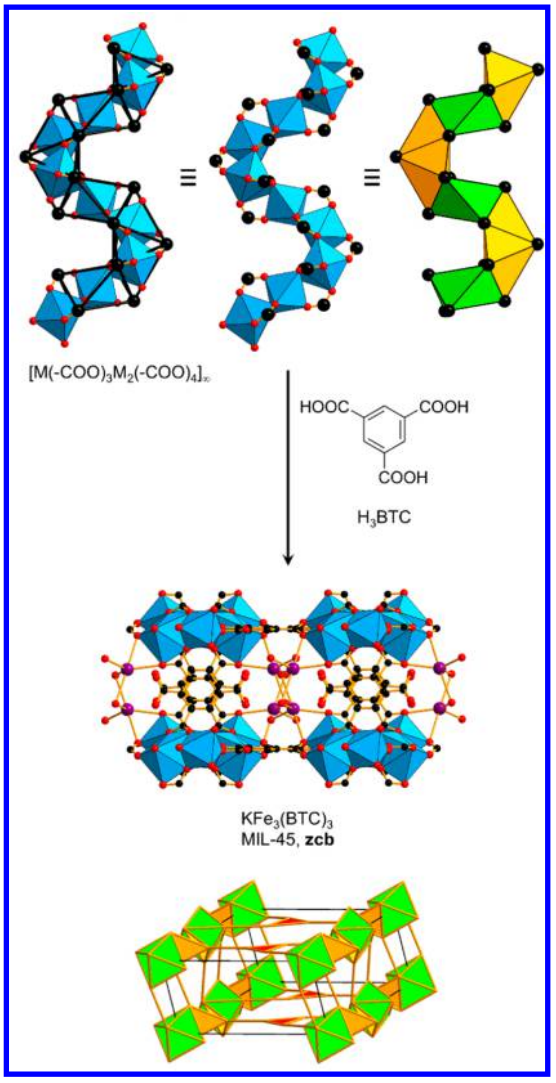

Figure 78. Crystal structures and net topology of MIL-45. The rod SBUs is formed by face-sharing octahedra and tetrahedra.[243] Color code: black, C; red, O; blue polyhedra, metal; purple, K.

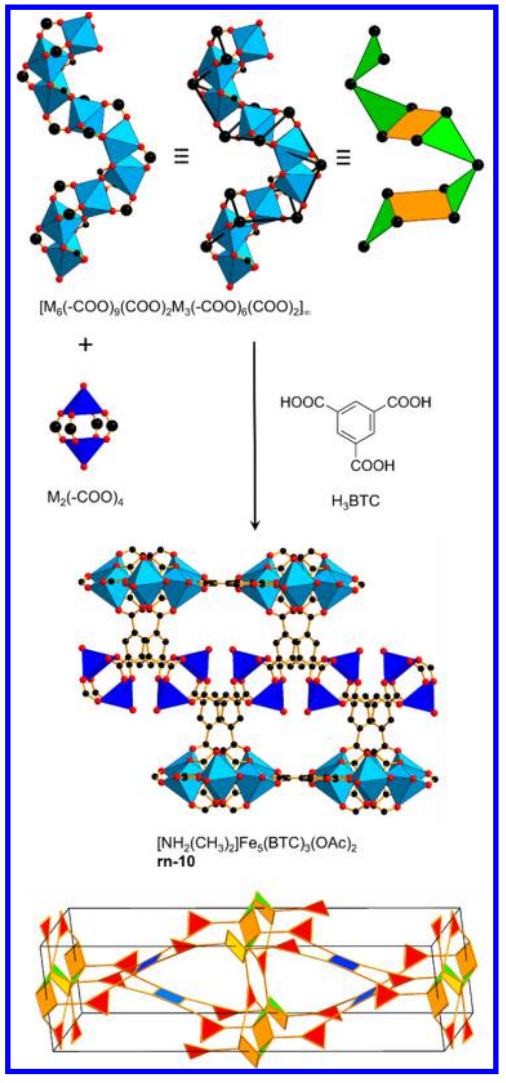

Figure 79. Crystal structure and topology of $[NH_2(CH_3)_2]$-$Fe_5(BTC)_3(OAc)_2$. The complicated net is 10-nodal with 16 kinds of edges.[244] Color code: black, C; red, O; blue polyhedra, metal.

et al. In silico screening of carbon-capture materials. *Nat. Mater.* **2012**, *11*, 633−641.
(10) Boyd, P. G.; Woo, T. K. A generalized method for constructing hypothetical nanoporous materials of any net topology from graph theory. *CrystEngComm* **2016**, *18*, 3777−3792.
(11) Addicoat, M. A.; Coupry, D. E.; Heine, T. AuToGraFS: Automatic Topological Generator for Framework Structures. *J. Phys. Chem. A* **2014**, *118*, 9607−9614.
(12) Chung, Y. G.; Camp, J.; Haranczyk, M.; Sikora, B. J.; Bury, W.; Krungleviciute, V.; Yildirim, T.; Farha, O. K.; Sholl, D. S.; Snurr, R. Q. Computation-Ready, Experimental Metal−Organic Frameworks: A Tool To Enable High-Throughput Screening of Nanoporous Crystals. *Chem. Mater.* **2014**, *26*, 6185−6192.
(13) Martin, R. L.; Haranczyk, M. Exploring frontiers of high surface area metal-organic frameworks. *Chem. Sci.* **2013**, *4*, 1781−1785.
(14) Martin, R. L.; Haranczyk, M. Insights into Multi-Objective Design of Metal−Organic Frameworks. *Cryst. Growth Des.* **2013**, *13*, 4208−4212.
(15) Martin, R. L.; Haranczyk, M. Construction and Characterization of Structure Models of Crystalline Porous Polymers. *Cryst. Growth Des.* **2014**, *14*, 2431−2440.
(16) Martin, R. L.; Haranczyk, M. Optimization-Based Design of Metal−Organic Framework Materials. *J. Chem. Theory Comput.* **2013**, *9*, 2816−2825.
(17) Simon, C. M.; Kim, J.; Gomez-Gualdron, D. A.; Camp, J. S.; Chung, Y. G.; Martin, R. L.; Mercado, R.; Deem, M. W.; Gunter, D.; Haranczyk, M.; et al. The materials genome in action: identifying the performance limits for methane storage. *Energy Environ. Sci.* **2015**, *8*, 1190−1199.
(18) Witman, M.; Ling, S.; Anderson, S.; Tong, L.; Stylianou, K. C.; Slater, B.; Smit, B.; Haranczyk, M. In silico design and screening of hypothetical MOF-74 analogs and their experimental synthesis. *Chem. Sci.* **2016**, *7*, 6263−6272.
(19) Delgado-Friedrichs, O.; O'Keeffe, M. Crystal nets as graphs: Terminology and definitions. *J. Solid State Chem.* **2005**, *178*, 2480−2485.
(20) O'Keeffe, M.; Peskov, M. A.; Ramsden, S. J.; Yaghi, O. M. The Reticular Chemistry Structure Resource (RCSR) Database of, and Symbols for, Crystal Nets. *Acc. Chem. Res.* **2008**, *41*, 1782−1789.
(21) Delgado-Friedrichs, O.; O'Keeffe, M.; Yaghi, O. M. Taxonomy of periodic nets and the design of materials. *Phys. Chem. Chem. Phys.* **2007**, *9*, 1035−1043.
(22) Chui, S. S.-Y.; Lo, S. M.-F.; Charmant, J. P. H.; Orpen, A. G.; Williams, I. D. A Chemically Functionalizable Nanoporous Material $[Cu_3(TMA)_2(H_2O)_3]_n$. *Science* **1999**, *283*, 1148−1150.
(23) Barthelet, K.; Marrot, J.; Riou, D.; Férey, G. A Breathing Hybrid Organic−Inorganic Solid with Very Large Pores and High Magnetic Characteristics. *Angew. Chem., Int. Ed.* **2002**, *41*, 281−284.

DOI: 10.1021/acs.chemrev.6b00346
Chem. Rev. XXXX, XXX, XXX−XXX

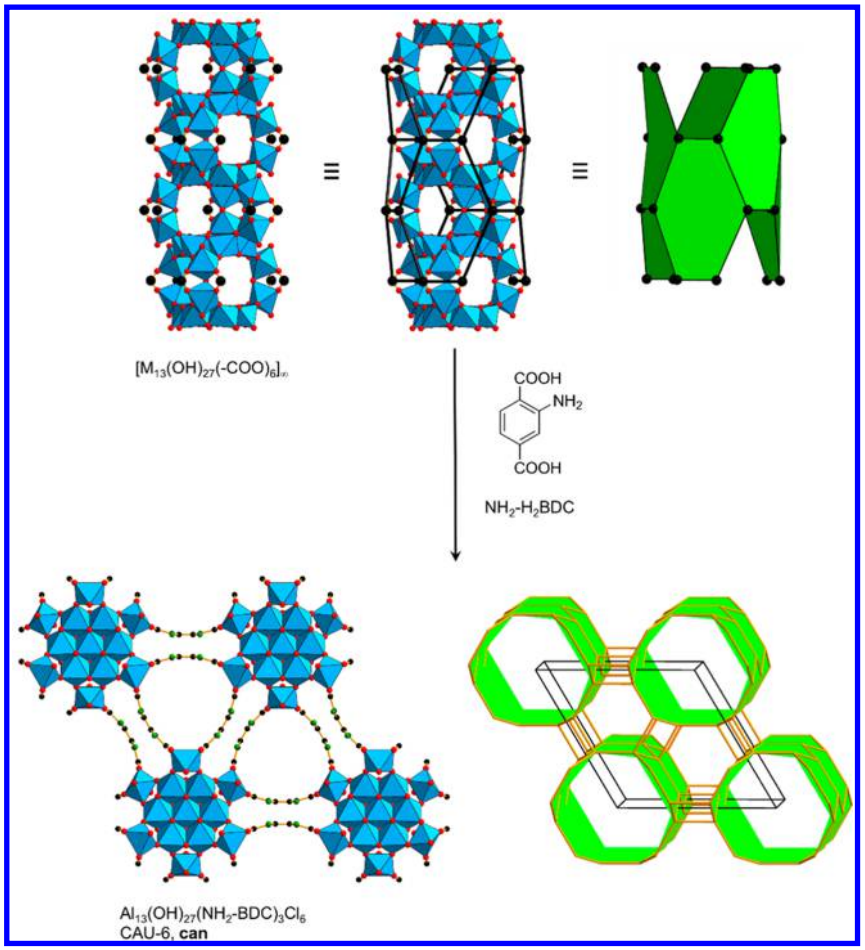

Figure 80. Linking of column-shaped SBUs with linear linkers to produce CAU-6, $Al_{13}(OH)_{27}(NH_2{-}BDC)_3Cl_6$. It crystallizes as a zeolitic 4-c **can** net.[245] Color code: black, C; red, O; green, N; blue polyhedra, metal.

(24) Serre, C.; Millange, F.; Thouvenot, C.; Noguès, M.; Marsolier, G.; Louër, D.; Férey, G. Very Large Breathing Effect in the First Nanoporous Chromium(III)-Based Solids: MIL-53 or $Cr^{III}(OH)\cdot\{O_2C{-}C_6H_4{-}CO_2\}\cdot\{HO_2C{-}C_6H_4{-}CO_2H\}_x\cdot H_2O_y$. *J. Am. Chem. Soc.* **2002**, *124*, 13519−13526.
(25) Kongpatpanich, K.; Horike, S.; Sugimoto, M.; Fukushima, T.; Umeyama, D.; Tsutsumi, Y.; Kitagawa, S. Synthesis and Porous Properties of Chromium Azolate Porous Coordination Polymers. *Inorg. Chem.* **2014**, *53*, 9870−9875.
(26) Alexandrov, E. V.; Blatov, V. A.; Kochetkov, A. V.; Proserpio, D. M. Underlying nets in three-periodic coordination polymers: topology, taxonomy and prediction from a computer-aided analysis of the Cambridge Structural Database. *CrystEngComm* **2011**, *13*, 3947−3958.
(27) Blatov, V. A.; Shevchenko, A. P.; Proserpio, D. M. Applied Topological Analysis of Crystal Structures with the Program Package ToposPro. *Cryst. Growth Des.* **2014**, *14*, 3576−3586.
(28) Reineke, T. M.; Eddaoudi, M.; O'Keeffe, M.; Yaghi, O. M. A Microporous Lanthanide−Organic Framework. *Angew. Chem., Int. Ed.* **1999**, *38*, 2590−2594.
(29) He, Y.; Xiang, S.; Zhang, Z.; Xiong, S.; Fronczek, F. R.; Krishna, R.; O'Keeffe, M.; Chen, B. A microporous lanthanide-tricarboxylate framework with the potential for purification of natural gas. *Chem. Commun.* **2012**, *48*, 10856−10858.
(30) Inge, A. K.; Köppen, M.; Su, J.; Feyand, M.; Xu, H.; Zou, X.; O'Keeffe, M.; Stock, N. Unprecedented Topological Complexity in a Metal−Organic Framework Constructed from Simple Building Units. *J. Am. Chem. Soc.* **2016**, *138*, 1970−1976.
(31) Brunner, G. A definition of coordination and its relevance in the structure types AlB_2 and NiAs. *Acta Crystallogr., Sect. A: Cryst. Phys., Diffr., Theor. Gen. Crystallogr.* **1977**, *33*, 226−227.
(32) Alvarez, S. Distortion Pathways of Transition Metal Coordination Polyhedra Induced by Chelating Topology. *Chem. Rev.* **2015**, *115*, 13447−13483.
(33) Delgado-Friedrichs, O.; O'Keeffe, M. Identification of and symmetry computation for crystal nets. *Acta Crystallogr., Sect. A: Found. Crystallogr.* **2003**, *59*, 351−360.
(34) Andersson, S.; O'Keeffe, M. Body-centred cubic cylinder packing and the garnet structure. *Nature* **1977**, *267*, 605−606.
(35) O'Keeffe, M.; Andersson, S. Rod packings and crystal chemistry. *Acta Crystallogr., Sect. A: Cryst. Phys., Diffr., Theor. Gen. Crystallogr.* **1977**, *33*, 914−923.
(36) O'Keeffe, M. Cubic cylinder packings. *Acta Crystallogr., Sect. A: Found. Crystallogr.* **1992**, *48*, 879−884.
(37) O'Keeffe, M.; Plevert, J.; Teshima, Y.; Watanabe, Y.; Ogama, T. The invariant cubic rod (cylinder) packings: symmetries and coordinates. *Acta Crystallogr., Sect. A: Found. Crystallogr.* **2001**, *57*, 110−111.
(38) O'Keeffe, M.; Plevert, J.; Ogawa, T. Homogeneous cubic cylinder packings revisited. *Acta Crystallogr., Sect. A: Found. Crystallogr.* **2002**, *58*, 125−132.
(39) Colombo, V.; Galli, S.; Choi, H. J.; Han, G. D.; Maspero, A.; Palmisano, G.; Masciocchi, N.; Long, J. R. High thermal and chemical stability in pyrazolate-bridged metal−organic frameworks with exposed metal sites. *Chem. Sci.* **2011**, *2*, 1311−1319.
(40) Li, M.; Li, D.; O'Keeffe, M.; Su, Z.-M. Pentagonal helices in a periodic metal-organic framework. Crystals as computers for discovering structures of minimal transitivity. *Chem. Commun.* **2015**, *51*, 12228−12230.

DOI: 10.1021/acs.chemrev.6b00346
Chem. Rev. XXXX, XXX, XXX−XXX

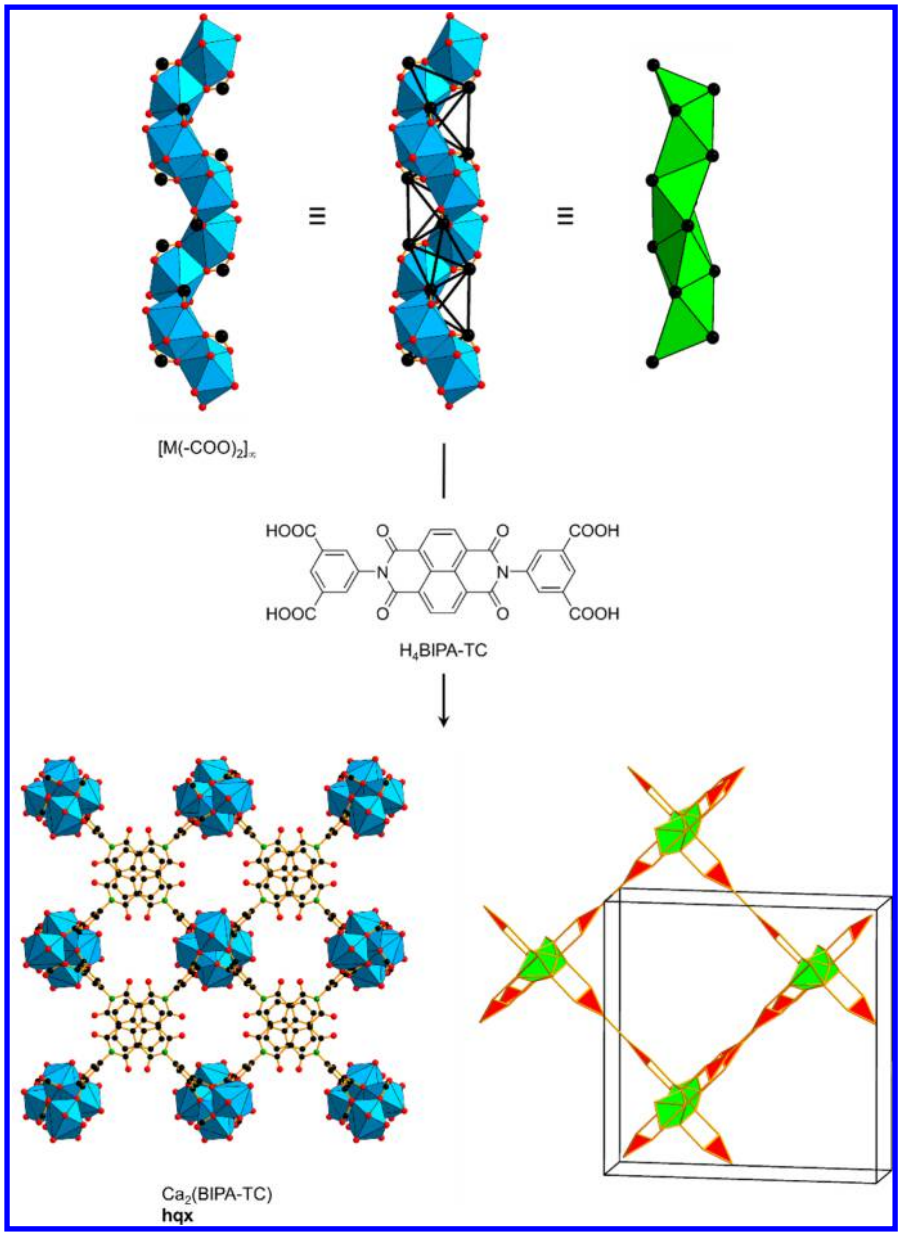

Figure 81. Crystal structure of Ca_2(BIPA-TC) and the underlying **hqx** net. The face-sharing tetrahedra rod SBUs are running [001].[247] Color code: black, C; red, O; green, N; blue polyhedra, metal.

(41) The reader is warned that in the program Systre (available at gavrog.org), commonly used to analyze the symmetry and identity of nets, the term ladder is used in a different sense from that here.
(42) Koch, E.; Fischer, W. Types of sphere packings for crystallographic point groups, rod groups and layer groups. *Z. Kristallogr.* **1978**, *148*, 107−152.
(43) Boerdijk, A. H. Some remarks concerning close-packing of equal spheres. *Philips Res. Rep.* **1952**, *7*, 303−313.
(44) Bernal, J. D. The Bakerian Lecture, 1962. The Structure of Liquids. *Proc. R. Soc. London, Ser. A* **1964**, *280*, 299−322.
(45) Nelson, D. R. Order, frustration, and defects in liquids and glasses. *Phys. Rev. B: Condens. Matter Mater. Phys.* **1983**, *28*, 5515−5535.
(46) Zheng, C.; Hoffmann, R.; Nelson, D. R. A helical face-sharing tetrahedron chain from irrational twist, stella quadrangula, and related matters. *J. Am. Chem. Soc.* **1990**, *112*, 3784−3791.
(47) Nyman, H.; Carroll, C. E.; Hyde, B. G. Rectilinear rods of face-sharing tetrahedra and the structure of *β*-Mn. *Z. Kristallogr.* **1991**, *196*, 39−46.
(48) Lidin, S.; Andersson, S. Regular Polyhedra Helices. *Z. Anorg. Allg. Chem.* **1996**, *622*, 164−166.
(49) Sadoc, J. F.; Rivier, N. Boerdijk-Coxeter helix and biological helices. *Eur. Phys. J. B* **1999**, *12*, 309−318.
(50) Lord, E. A. Helical Structures: The Geometry of Protein Helices and Nanotubes. *Struct. Chem.* **2002**, *13*, 305−314.
(51) Lord, E. A.; Ranganathan, S. The *γ*-brass structure and the Boerdijk−Coxeter helix. *J. Non-Cryst. Solids* **2004**, *334*−*335*, 121−125.
(52) Zhu, Y.; He, J.; Shang, C.; Miao, X.; Huang, J.; Liu, Z.; Chen, H.; Han, Y. Chiral Gold Nanowires with Boerdijk−Coxeter−Bernal Structure. *J. Am. Chem. Soc.* **2014**, *136*, 12746−12752.
(53) Erickson, R. O. Tubular Packing of Spheres in Biological Fine Structure. *Science* **1973**, *181*, 705−716.
(54) Dresselhaus, M. S.; Dresselhaus, G.; Eklund, P. C. *Science of Fullerenes and Carbon Nanotubes*; Academic Press: San Diego, 1996.
(55) Dietzel, P. D. C.; Morita, Y.; Blom, R.; Fjellvåg, H. An In Situ High-Temperature Single-Crystal Investigation of a Dehydrated Metal−Organic Framework Compound and Field-Induced Magnetization of One-Dimensional Metal−Oxygen Chains. *Angew. Chem., Int. Ed.* **2005**, *44*, 6354−6358.
(56) Dietzel, P. D. C.; Johnsen, R. E.; Blom, R.; Fjellvåg, H. Structural Changes and Coordinatively Unsaturated Metal Atoms on Dehydration

DOI: 10.1021/acs.chemrev.6b00346
Chem. Rev. XXXX, XXX, XXX−XXX

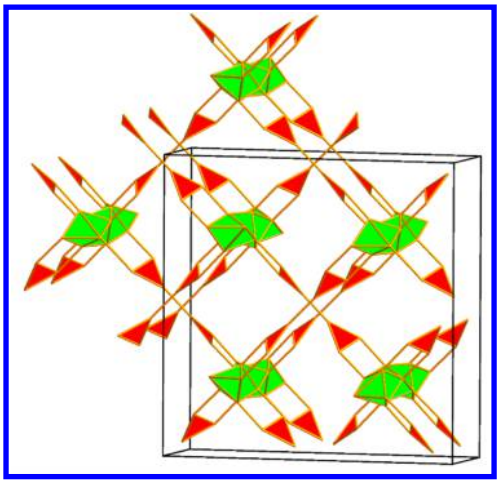

Figure 82. In the net **hqx**, the 3-c nodes are sufficiently widely spaced to allow a second copy of the structure with opposite hand to interpenetrate. The ideal symmetry of the pair of nets is $I4_1/acd$.

of Honeycomb Analogous Microporous Metal−Organic Frameworks. *Chem. - Eur. J.* **2008**, *14*, 2389−2397.
(57) Caskey, S. R.; Wong-Foy, A. G.; Matzger, A. J. Dramatic Tuning of Carbon Dioxide Uptake via Metal Substitution in a Coordination Polymer with Cylindrical Pores. *J. Am. Chem. Soc.* **2008**, *130*, 10870−10871.
(58) Bloch, E. D.; Hudson, M. R.; Mason, J. A.; Chavan, S.; Crocellà, V.; Howe, J. D.; Lee, K.; Dzubak, A. L.; Queen, W. L.; Zadrozny, J. M.; et al. Reversible CO Binding Enables Tunable CO/H_2 and CO/N_2 Separations in Metal−Organic Frameworks with Exposed Divalent Metal Cations. *J. Am. Chem. Soc.* **2014**, *136*, 10752−10761.
(59) Wang, L. J.; Deng, H.; Furukawa, H.; Gándara, F.; Cordova, K. E.; Peri, D.; Yaghi, O. M. Synthesis and Characterization of Metal−Organic Framework-74 Containing 2, 4, 6, 8, and 10 Different Metals. *Inorg. Chem.* **2014**, *53*, 5881−5883.
(60) Rowsell, J. L. C.; Yaghi, O. M. Effects of Functionalization, Catenation, and Variation of the Metal Oxide and Organic Linking Units on the Low-Pressure Hydrogen Adsorption Properties of Metal−Organic Frameworks. *J. Am. Chem. Soc.* **2006**, *128*, 1304−1315.
(61) Lee, K.; Isley, W. C.; Dzubak, A. L.; Verma, P.; Stoneburner, S. J.; Lin, L.-C.; Howe, J. D.; Bloch, E. D.; Reed, D. A.; Hudson, M. R.; et al. Design of a Metal−Organic Framework with Enhanced Back Bonding for Separation of N_2 and CH_4. *J. Am. Chem. Soc.* **2014**, *136*, 698−704.
(62) Banerjee, D.; Cairns, A. J.; Liu, J.; Motkuri, R. K.; Nune, S. K.; Fernandez, C. A.; Krishna, R.; Strachan, D. M.; Thallapally, P. K. Potential of Metal−Organic Frameworks for Separation of Xenon and Krypton. *Acc. Chem. Res.* **2015**, *48*, 211−219.
(63) Valvekens, P.; Vandichel, M.; Waroquier, M.; Van Speybroeck, V.; De Vos, D. Metal-dioxidoterephthalate MOFs of the MOF-74 type: Microporous basic catalysts with well-defined active sites. *J. Catal.* **2014**, *317*, 1−10.
(64) Phang, W. J.; Lee, W. R.; Yoo, K.; Ryu, D. W.; Kim, B.; Hong, C. S. pH-Dependent Proton Conducting Behavior in a Metal−Organic Framework Material. *Angew. Chem., Int. Ed.* **2014**, *53*, 8383−8387.
(65) Rudenko, A. N.; Bendt, S.; Keil, F. J. Multiscale Modeling of Water in Mg-MOF-74: From Electronic Structure Calculations to Adsorption Isotherms. *J. Phys. Chem. C* **2014**, *118*, 16218−16227.
(66) Hu, Q.; Yu, J.; Liu, M.; Liu, A.; Dou, Z.; Yang, Y. A Low Cytotoxic Cationic Metal−Organic Framework Carrier for Controllable Drug Release. *J. Med. Chem.* **2014**, *57*, 5679−5685.
(67) Ji, H.; Park, J.; Cho, M.; Jung, Y. Assessments of Semilocal Density Functionals and Corrections for Carbon Dioxide Adsorption on Metal−Organic Frameworks. *ChemPhysChem* **2014**, *15*, 3157−3165.
(68) In crystallography, a screw N_n implies rotation by $360/N$ degrees followed by a translation n/N of the lattice vector parallel to the rod. Noncrystallographers use the notation N/m which implies rotation by $360m/N$ degrees followed by a translation $1/N$ of the translation vector.

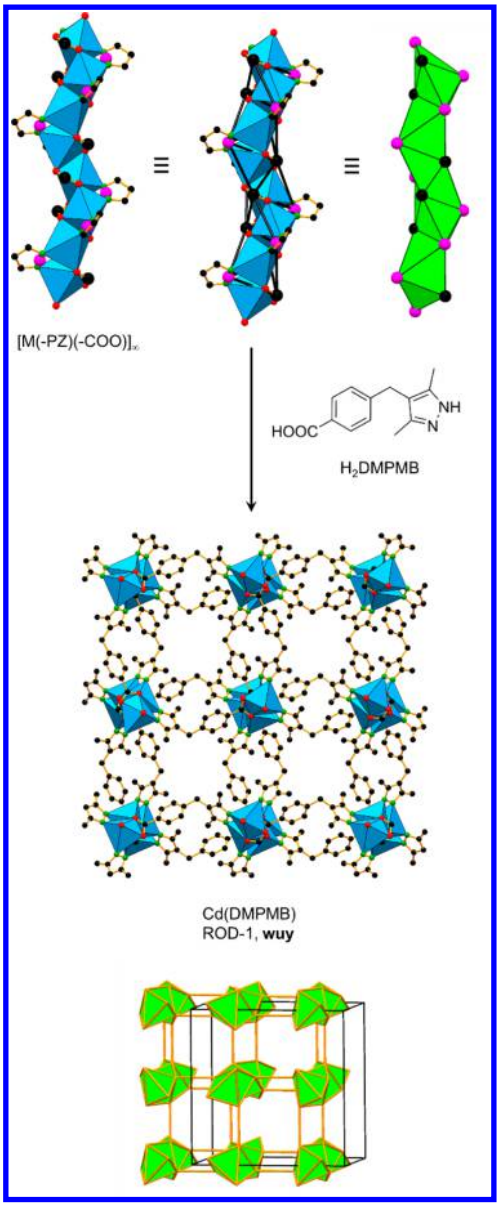

Figure 83. Single crystal structure of ROD-1. The flexible linker facilitates connections between the BC helices. The underlying topology is a uninodal 7-c **wuy** net. Color code: black, C; red, O; green, N; blue polyhedra, metal; pink, points of extension.

To convert from one notation to the other if N,n are coprime note that $nm(\mathrm{mod}N) = 1$, thus $7_3 = (7,5)$. If N,n are not coprime first divided by the greatest common denominator. Thus 6_2 corresponds to two 3_1 = two (3,1), a "double helix".

(69) Lidin, S.; Fredrickson, D. A Higher Dimensional Description of the Structure of β-Mn. *Symmetry* **2012**, *4*, 537−544.
(70) Rosi, N. L.; Eddaoudi, M.; Kim, J.; O'Keeffe, M.; Yaghi, O. M. Infinite Secondary Building Units and Forbidden Catenation in Metal-Organic Frameworks. *Angew. Chem., Int. Ed.* **2002**, *41*, 284−287.
(71) Deng, H.; Grunder, S.; Cordova, K. E.; Valente, C.; Furukawa, H.; Hmadeh, M.; Gandara, F.; Whalley, A. C.; Liu, Z.; Asahina, S.; et al. Large-pore apertures in a series of metal-organic frameworks. *Science* **2012**, *336*, 1018−1023.
(72) Llewellyn, P. L.; Maurin, G.; Devic, T.; Loera-Serna, S.; Rosenbach, N.; Serre, C.; Bourrelly, S.; Horcajada, P.; Filinchuk, Y.; Férey, G. Prediction of the Conditions for Breathing of Metal Organic Framework Materials Using a Combination of X-ray Powder Diffraction, Microcalorimetry, and Molecular Simulation. *J. Am. Chem. Soc.* **2008**, *130*, 12808−12814.

DOI: 10.1021/acs.chemrev.6b00346
Chem. Rev. XXXX, XXX, XXX−XXX

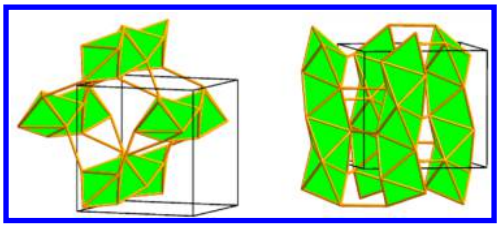

Figure 84. 7-c Net **lll** with transitivity 1 6 and symmetry $I4_122$. This is the unique minimal transitivity way to join BC helices, all of the same hand.

(73) Millange, F.; Guillou, N.; Walton, R. I.; Greneche, J.-M.; Margiolaki, I.; Ferey, G. Effect of the nature of the metal on the breathing steps in MOFs with dynamic frameworks. *Chem. Commun.* **2008**, 4732−4734.

(74) Coombes, D. S.; Corà, F.; Mellot-Draznieks, C.; Bell, R. G. Sorption-Induced Breathing in the Flexible Metal Organic Framework CrMIL-53: Force-Field Simulations and Electronic Structure Analysis. *J. Phys. Chem. C* **2009**, *113*, 544−552.

(75) Coudert, F.-X.; Mellot-Draznieks, C.; Fuchs, A. H.; Boutin, A. Prediction of Breathing and Gate-Opening Transitions Upon Binary Mixture Adsorption in Metal−Organic Frameworks. *J. Am. Chem. Soc.* **2009**, *131*, 11329−11331.

(76) Dubbeldam, D.; Krishna, R.; Snurr, R. Q. Method for Analyzing Structural Changes of Flexible Metal−Organic Frameworks Induced by Adsorbates. *J. Phys. Chem. C* **2009**, *113*, 19317−19327.

(77) Watanabe, S.; Sugiyama, H.; Adachi, H.; Tanaka, H.; Miyahara, M. T. Free energy analysis for adsorption-induced lattice transition of flexible coordination framework. *J. Chem. Phys.* **2009**, *130*, 164707.

(78) Horike, S.; Shimomura, S.; Kitagawa, S. Soft porous crystals. *Nat. Chem.* **2009**, *1*, 695−704.

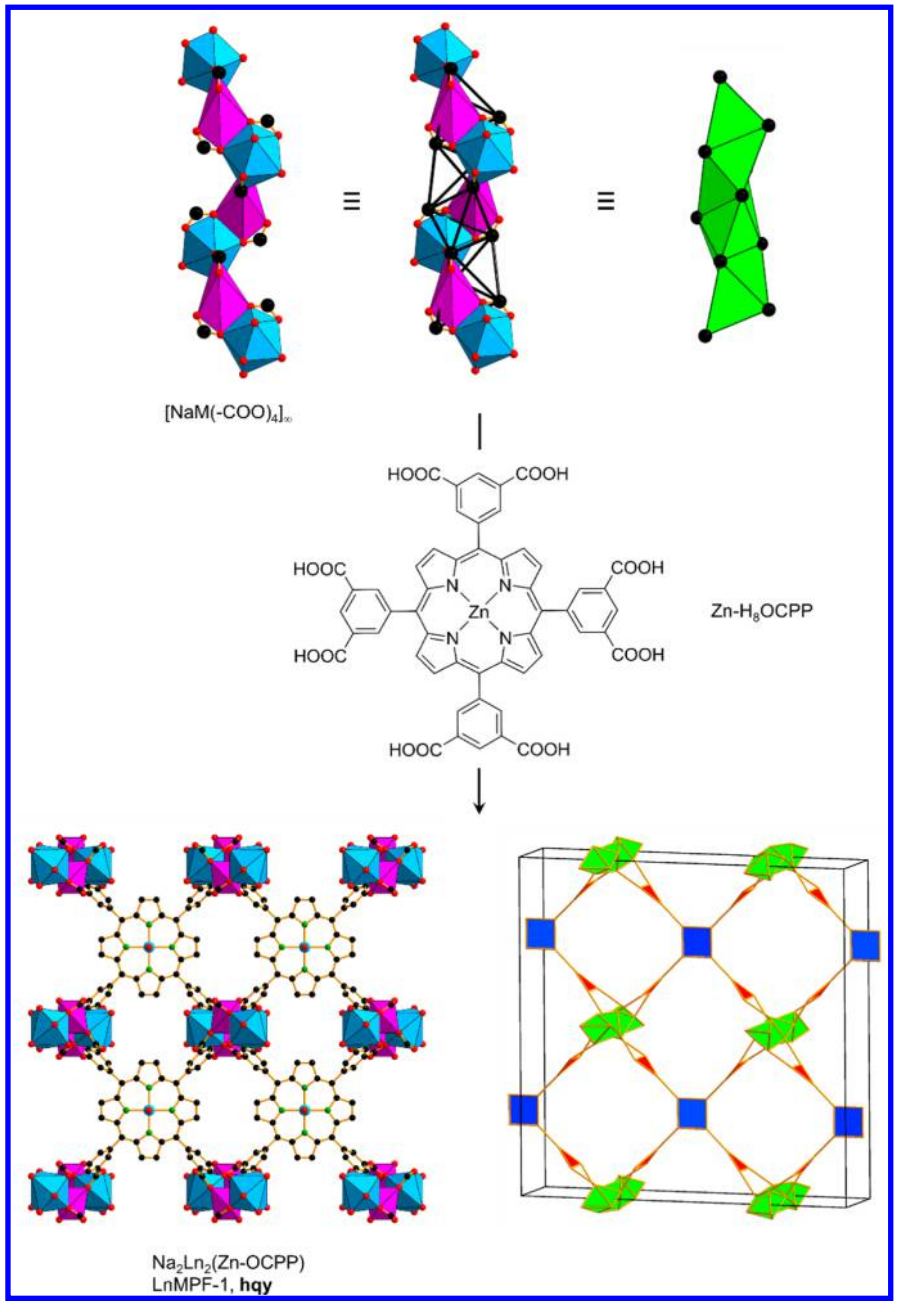

Figure 85. Single crystal X-ray structure of LnMPF-1. The underlying net is derived from a BC-helix, **hqy**.[248] Color code: black, C; red, O; green, N; blue polyhedra, metal; pink polyhedra, Na.

DOI: 10.1021/acs.chemrev.6b00346
Chem. Rev. XXXX, XXX, XXX−XXX

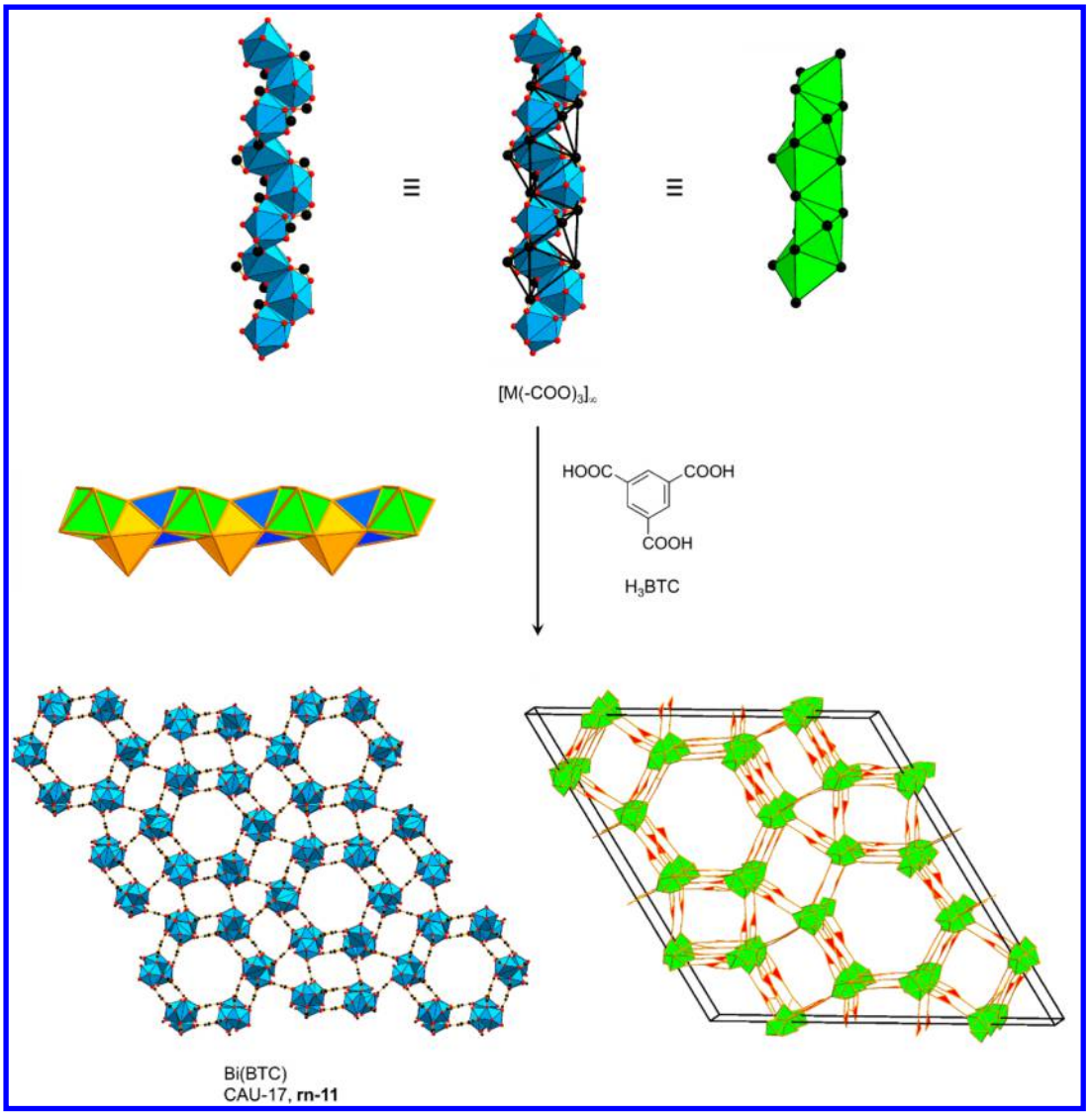

Figure 86. Single crystal structure of CAU-17.[30] The highly complex net shows a transitivity of 54 135. The LA helix composed of octahedra is also shown in different colors. Color code: black, C; red, O; blue polyhedra, metal.

(79) Neimark, A. V.; Coudert, F.-X.; Boutin, A.; Fuchs, A. H. Stress-Based Model for the Breathing of Metal−Organic Frameworks. *J. Phys. Chem. Lett.* **2010**, *1*, 445−449.
(80) Zang, J.; Nair, S.; Sholl, D. S. Osmotic ensemble methods for predicting adsorption-induced structural transitions in nanoporous materials using molecular simulations. *J. Chem. Phys.* **2011**, *134*, 184103.
(81) Triguero, C.; Coudert, F.-X.; Boutin, A.; Fuchs, A. H.; Neimark, A. V. Mechanism of Breathing Transitions in Metal−Organic Frameworks. *J. Phys. Chem. Lett.* **2011**, *2*, 2033−2037.
(82) Grosch, J. S.; Paesani, F. Molecular-Level Characterization of the Breathing Behavior of the Jungle-Gym-type DMOF-1 Metal−Organic Framework. *J. Am. Chem. Soc.* **2012**, *134*, 4207−4215.
(83) Ortiz, A. U.; Boutin, A.; Fuchs, A. H.; Coudert, F.-X. Anisotropic Elastic Properties of Flexible Metal-Organic Frameworks: How Soft are Soft Porous Crystals? *Phys. Rev. Lett.* **2012**, *109*, 195502.
(84) Vanduyfhuys, L.; Verstraelen, T.; Vandichel, M.; Waroquier, M.; Van Speybroeck, V. Ab Initio Parametrized Force Field for the Flexible Metal−Organic Framework MIL-53(Al). *J. Chem. Theory Comput.* **2012**, *8*, 3217−3231.
(85) Ghysels, A.; Vanduyfhuys, L.; Vandichel, M.; Waroquier, M.; Van Speybroeck, V.; Smit, B. On the Thermodynamics of Framework Breathing: A Free Energy Model for Gas Adsorption in MIL-53. *J. Phys. Chem. C* **2013**, *117*, 11540−11554.
(86) Chen, L.; Mowat, J. P. S.; Fairen-Jimenez, D.; Morrison, C. A.; Thompson, S. P.; Wright, P. A.; Düren, T. Elucidating the Breathing of the Metal−Organic Framework MIL-53(Sc) with ab Initio Molecular Dynamics Simulations and in Situ X-ray Powder Diffraction Experiments. *J. Am. Chem. Soc.* **2013**, *135*, 15763−15773.
(87) Sarkisov, L.; Martin, R. L.; Haranczyk, M.; Smit, B. On the Flexibility of Metal−Organic Frameworks. *J. Am. Chem. Soc.* **2014**, *136*, 2228−2231.
(88) Wharmby, M. T.; Mowat, J. P.; Thompson, S. P.; Wright, P. A. Extending the pore size of crystalline metal phosphonates toward the mesoporous regime by isoreticular synthesis. *J. Am. Chem. Soc.* **2011**, *133*, 1266−1269.
(89) Dincă, M.; Yu, A. F.; Long, J. R. Microporous Metal−Organic Frameworks Incorporating 1,4-Benzeneditetrazolate: Syntheses, Structures, and Hydrogen Storage Properties. *J. Am. Chem. Soc.* **2006**, *128*, 8904−8913.
(90) Liu, G. L.; Qin, Y. J.; Jing, L.; Wei, G. Y.; Li, H. Two novel MOF-74 analogs exhibiting unique luminescent selectivity. *Chem. Commun.* **2013**, *49*, 1699−1701.
(91) Groves, J. A.; Miller, S. R.; Warrender, S. J.; Mellot-Draznieks, C.; Lightfoot, P.; Wright, P. A. The first route to large pore metal phosphonates. *Chem. Commun.* **2006**, 3305−3307.
(92) Miller, S. R.; Pearce, G. M.; Wright, P. A.; Bonino, F.; Chavan, S.; Bordiga, S.; Margiolaki, I.; Guillou, N.; Férey, G.; Bourrelly, S.; et al.

DOI: 10.1021/acs.chemrev.6b00346
Chem. Rev. XXXX, XXX, XXX−XXX

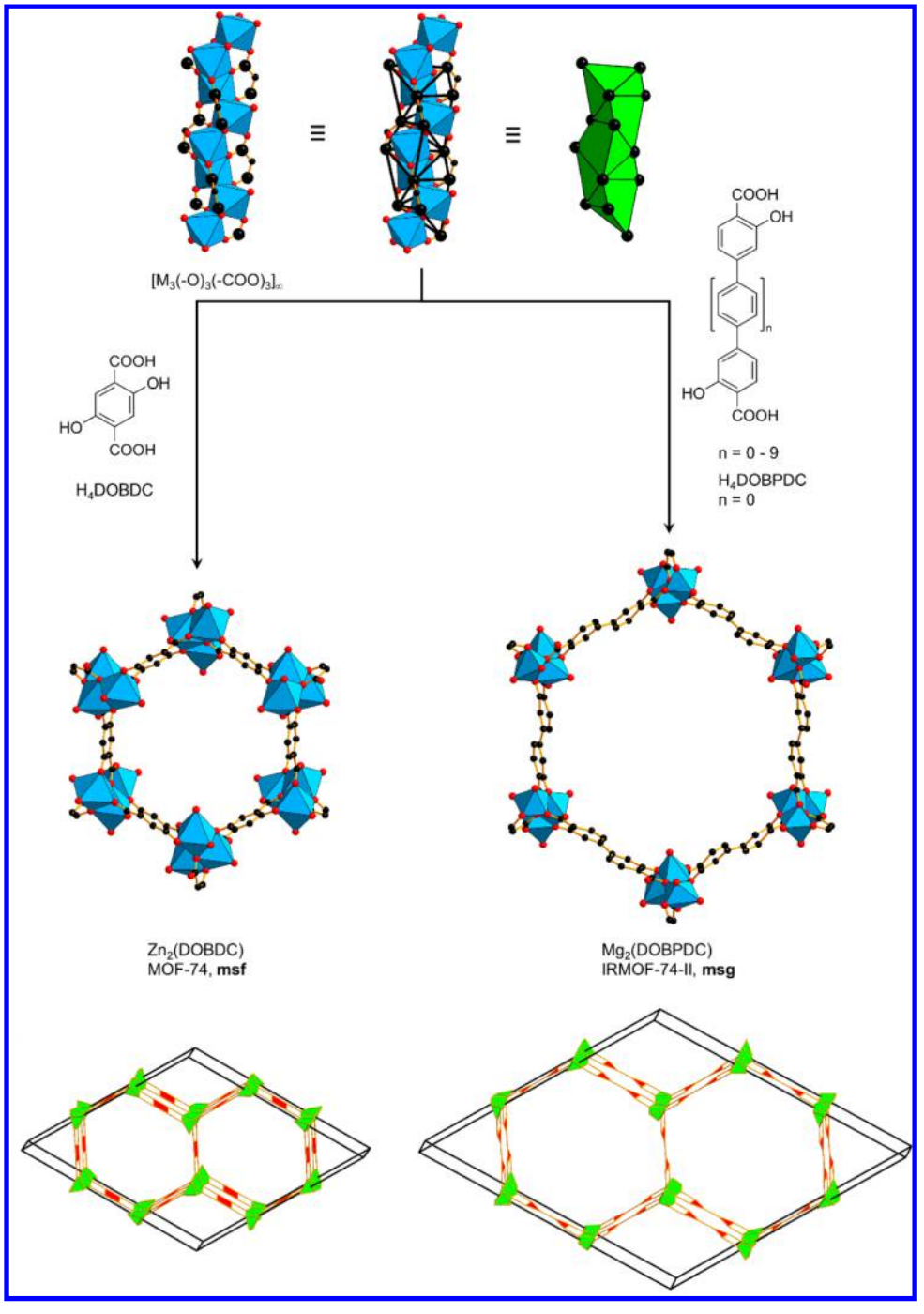

Figure 87. Deconstruction of the parent MOF-74 (left) and expanded variants (right) into their underlying nets. The SBU is derived from a LA helix, as a rod of square pyramids sharing triangular faces. The resulting nets are 4-nodal **msf** and 5-nodal **msg**.[6,71] Color code: black, C; red, O; blue polyhedra, metal.

Structural Transformations and Adsorption of Fuel-Related Gases of a Structurally Responsive Nickel Phosphonate Metal−Organic Framework, Ni-STA-12. *J. Am. Chem. Soc.* **2008**, *130*, 15967−15981.

(93) Anokhina, E. V.; Go, Y. B.; Lee, Y.; Vogt, T.; Jacobson, A. J. Chiral Three-Dimensional Microporous Nickel Aspartate with Extended Ni−O−Ni Bonding. *J. Am. Chem. Soc.* **2006**, *128*, 9957−9962.

(94) Lu, W.; Wei, Z.; Gu, Z.-Y.; Liu, T.-F.; Park, J.; Park, J.; Tian, J.; Zhang, M.; Zhang, Q.; Gentle, T., III; et al. Tuning the structure and function of metal-organic frameworks via linker design. *Chem. Soc. Rev.* **2014**, *43*, 5561−5593.

(95) Anokhina, E. V.; Jacobson, A. J. $[Ni_2O(l\text{-}Asp)(H_2O)_2]\cdot 4H_2O$: A Homochiral 1D Helical Chain Hybrid Compound with Extended Ni−O−Ni Bonding. *J. Am. Chem. Soc.* **2004**, *126*, 3044−3045.

(96) He, J.; Zeller, M.; Hunter, A. D.; Xu, Z. White light emission and second harmonic generation from secondary group participation (SGP) in a coordination network. *J. Am. Chem. Soc.* **2012**, *134*, 1553−1559.

(97) Zhou, X.-P.; Xu, Z.; Zeller, M.; Hunter, A. D. Reversible uptake of $HgCl_2$ in a porous coordination polymer based on the dual functions of carboxylate and thioether. *Chem. Commun.* **2009**, 5439−5441.

(98) Zhao, M.; Ou, S.; Wu, C.-D. Porous Metal−Organic Frameworks for Heterogeneous Biomimetic Catalysis. *Acc. Chem. Res.* **2014**, *47*, 1199−1207.

(99) Walsh, A.; Payne, D. J.; Egdell, R. G.; Watson, G. W. Stereochemistry of post-transition metal oxides: revision of the classical lone pair model. *Chem. Soc. Rev.* **2011**, *40*, 4455−4463.

DOI: 10.1021/acs.chemrev.6b00346
Chem. Rev. XXXX, XXX, XXX−XXX

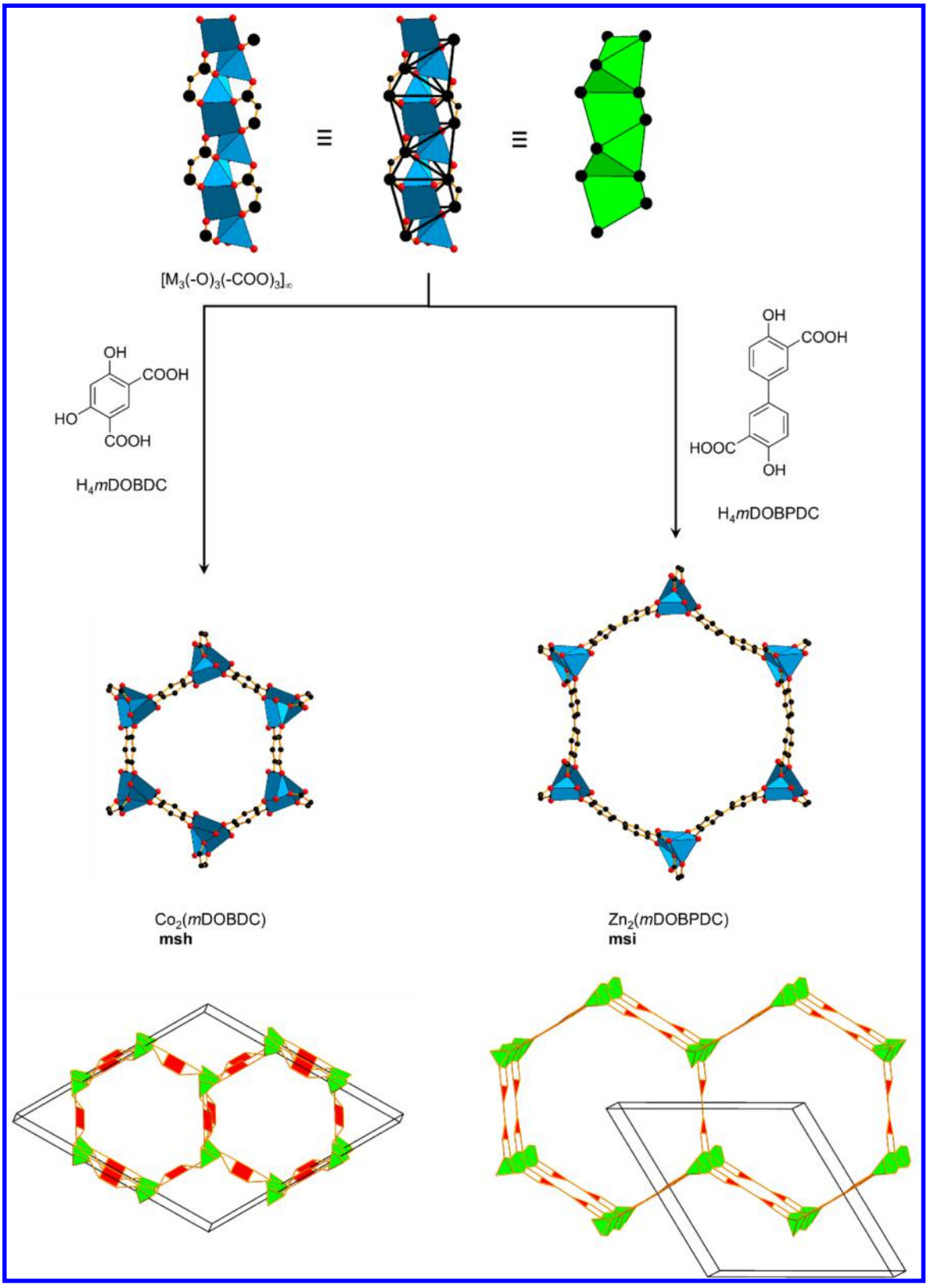

Figure 88. Deconstruction of MOF-74 isomers (left) and its expanded variant. The SBU is again derived from a LA helix; however, the connectivity is different, yielding 4-nodal **msh** and 5-nodal **msi** nets.[2S1,2S2] Color code: black, C; red, O; blue polyhedra, metal.

(100) Volkringer, C.; Loiseau, T.; Haouas, M.; Taulelle, F.; Popov, D.; Burghammer, M.; Riekel, C.; Zlotea, C.; Cuevas, F.; Latroche, M.; et al. Occurrence of Uncommon Infinite Chains Consisting of Edge-Sharing Octahedra in a Porous Metal Organic Framework-Type Aluminum Pyromellitate $Al_4(OH)_8[C_{10}O_8H_2]$ (MIL-120): Synthesis, Structure, and Gas Sorption Properties. *Chem. Mater.* **2009**, *21*, 5783−5791.

(101) Volkringer, C.; Loiseau, T.; Guillou, N.; Férey, G.; Haouas, M.; Taulelle, F.; Audebrand, N.; Margiolaki, I.; Popov, D.; Burghammer, M.; et al. Structural Transitions and Flexibility during Dehydration−

DOI: 10.1021/acs.chemrev.6b00346
Chem. Rev. XXXX, XXX, XXX−XXX

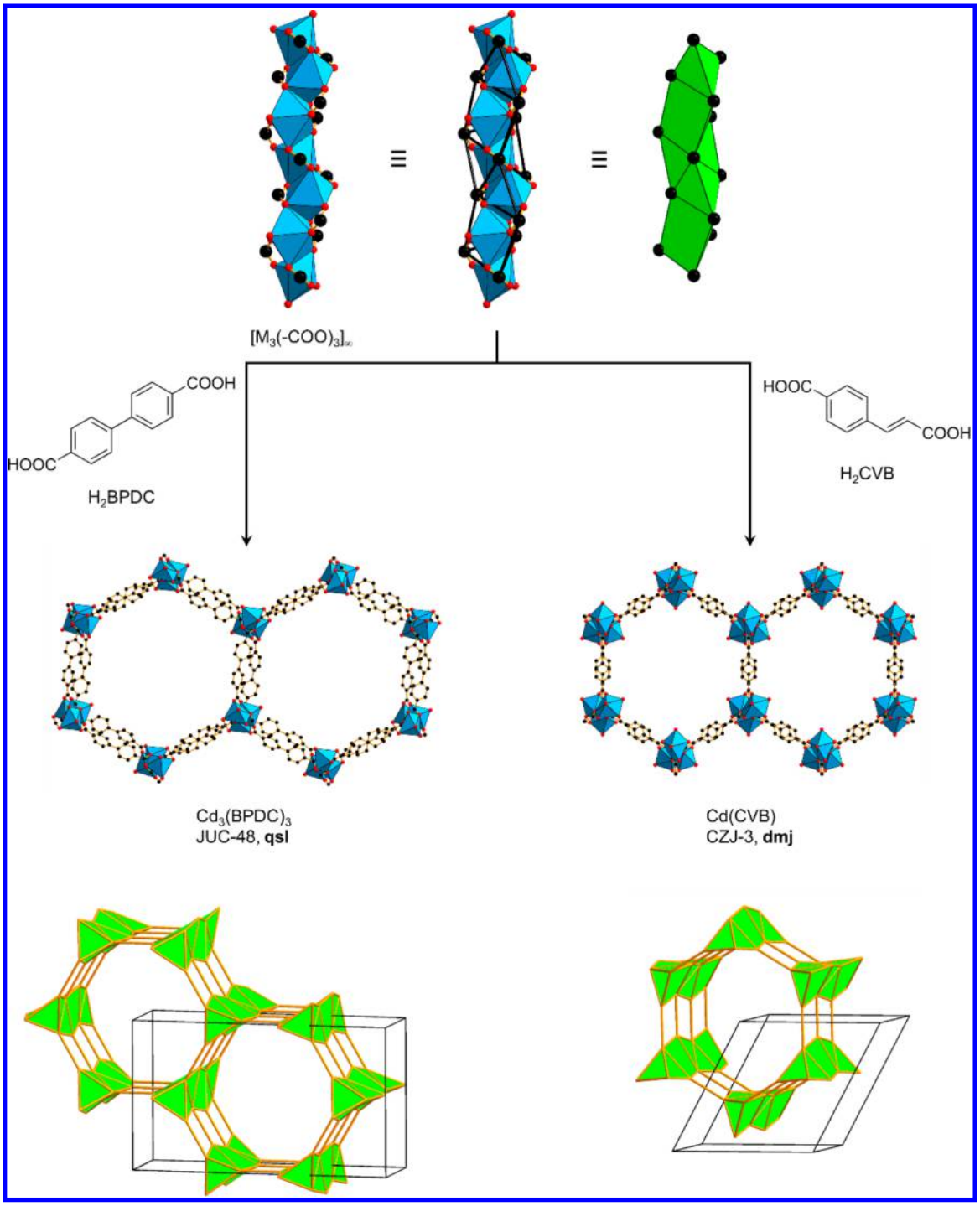

Figure 89. Crystal structures and deconstruction of JUC-48 (left) and CZJ-3 (left). The SBU is a LA helix, with different connectivity depending on the linker, leading to **qsl** and **dmj** nets.[253,254] Color code: black, C; red, O; blue polyhedra, metal.

Rehydration Process in the MOF-type Aluminum Pyromellitate $Al_2(OH)_2[C_{10}O_8H_2]$ (MIL-118). *Cryst. Growth Des.* **2009**, *9*, 2927−2936.

(102) Kang, M.; Luo, D.; Lin, Z.; Thiele, G.; Dehnen, S. Crystalline beryllium carboxylate frameworks containing inorganic chains of BeO_4 tetrahedra. *CrystEngComm* **2013**, *15*, 1845.

(103) Anokhina, E. V.; Vougo-Zanda, M.; Wang, X.; Jacobson, A. J. In(OH)BDC·0.75BDCH_2 (BDC = Benzenedicarboxylate), a Hybrid Inorganic−Organic Vernier Structure. *J. Am. Chem. Soc.* **2005**, *127*, 15000−15001.

(104) Comotti, A.; Bracco, S.; Sozzani, P.; Horike, S.; Matsuda, R.; Chen, J.; Takata, M.; Kubota, Y.; Kitagawa, S. Nanochannels of Two Distinct Cross-Sections in a Porous Al-Based Coordination Polymer. *J. Am. Chem. Soc.* **2008**, *130*, 13664−13672.

(105) Bloch, E. D.; Britt, D.; Lee, C.; Doonan, C. J.; Uribe-Romo, F. J.; Furukawa, H.; Long, J. R.; Yaghi, O. M. Metal Insertion in a Microporous Metal−Organic Framework Lined with 2,2′-Bipyridine. *J. Am. Chem. Soc.* **2010**, *132*, 14382−14384.

(106) Liu, Y.; Chen, Y.-P.; Liu, T.-F.; Yakovenko, A. A.; Raiff, A. M.; Zhou, H.-C. Selective gas adsorption and unique phase transition properties in a stable magnesium metal-organic framework constructed from infinite metal chains. *CrystEngComm* **2013**, *15*, 9688.

(107) Alvarez, E.; Guillou, N.; Martineau, C.; Bueken, B.; Van de Voorde, B.; Le Guillouzer, C.; Fabry, P.; Nouar, F.; Taulelle, F.; de Vos,

DOI: 10.1021/acs.chemrev.6b00346
Chem. Rev. XXXX, XXX, XXX−XXX

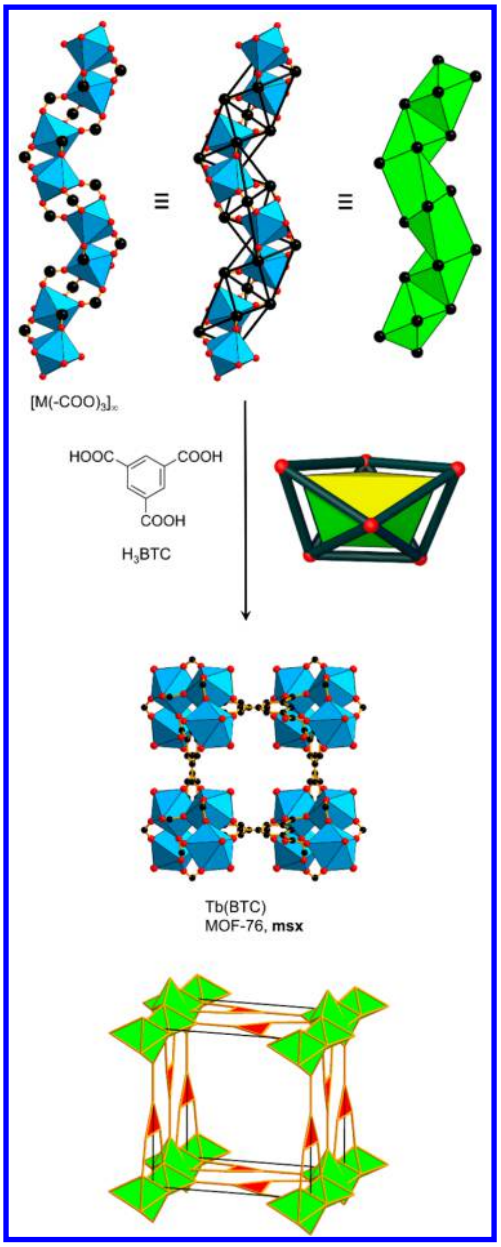

Figure 90. Single crystal structure of MOF-76 and its underlying 4-nodal (3,3,5,7)-c **msx** net.[6] The tiling of the diminished pentagonal bipyramid is highlighted. Color code: black, C; red, O; blue polyhedra, metal.

D.; et al. The Structure of the Aluminum Fumarate Metal−Organic Framework A520. *Angew. Chem., Int. Ed.* **2015**, *54*, 3664−3668.
(108) Evans, O. R.; Manke, D. R.; Lin, W. Homochiral Metal−Organic Frameworks Based on Transition Metal Bisphosphonates. *Chem. Mater.* **2002**, *14*, 3866−3874.
(109) Zhang, X.-M.; Hou, J.-J.; Zhang, W.-X.; Chen, X.-M. Two Mixed-Valence Vanadium(III,IV) Phosphonoacetates with 16-Ring Channels: $H_2(DABCO)[V^{IV}O(H_2O)V^{III}(OH)(O_3PCH_2CO_2)_2]\cdot 2.5H_2O$ and $H_2(PIP)[V^{IV}O(H_2O)V^{III}(OH)(O_3PCH_2CO_2)_2]\cdot 2.5H_2O$. *Inorg. Chem.* **2006**, *45*, 8120−8125.
(110) Demessence, A.; Long, J. R. Selective Gas Adsorption in the Flexible Metal−Organic Frameworks Cu(BDTri)L (L = DMF, DEF). *Chem. - Eur. J.* **2010**, *16*, 5902−5908.
(111) Colombo, V.; Montoro, C.; Maspero, A.; Palmisano, G.; Masciocchi, N.; Galli, S.; Barea, E.; Navarro, J. A. Tuning the adsorption properties of isoreticular pyrazolate-based metal-organic frameworks through ligand modification. *J. Am. Chem. Soc.* **2012**, *134*, 12830−12843.
(112) Zhang, X.-M.; Hao, Z.-M.; Zhang, W.-X.; Chen, X.-M. Dehydration-Induced Conversion from a Single-Chain Magnet into a Metamagnet in a Homometallic Nanoporous Metal−Organic Framework. *Angew. Chem., Int. Ed.* **2007**, *46*, 3456−3459.
(113) Abrahams, B. F.; Grannas, M. J.; Hudson, T. A.; Robson, R. A Simple Lithium(I) Salt with a Microporous Structure and Its Gas Sorption Properties. *Angew. Chem., Int. Ed.* **2010**, *49*, 1087−1089.
(114) Barthelet, K.; Marrot, J.; Férey, G.; Riou, D. $V^{III}(OH)\{O_2C\text{-}C_6H_4\text{-}CO_2\}.(HO_2C\text{-}C_6H_4\text{-}CO_2H)_x(DMF)_y(H_2O)_z$ (or MIL-68), a new vanadocarboxylate with a large pore hybrid topology: reticular synthesis with infinite inorganic building blocks? *Chem. Commun.* **2004**, 520−521.
(115) Volkringer, C.; Meddouri, M.; Loiseau, T.; Guillou, N.; Marrot, J.; Férey, G.; Haouas, M.; Taulelle, F.; Audebrand, N.; Latroche, M. The Kagomé Topology of the Gallium and Indium Metal-Organic Framework Types with a MIL-68 Structure: Synthesis, XRD, Solid-State NMR Characterizations, and Hydrogen Adsorption. *Inorg. Chem.* **2008**, *47*, 11892−11901.
(116) Reinsch, H.; Kruger, M.; Marrot, J.; Stock, N. First keto-functionalized microporous Al-based metal-organic framework: $[Al(OH)(O_2C\text{-}C_6H_4\text{-}CO\text{-}C_6H_4\text{-}CO_2)]$. *Inorg. Chem.* **2013**, *52*, 1854−1859.
(117) Blake, A. J.; Champness, N. R.; Easun, T. L.; Allan, D. R.; Nowell, H.; George, M. W.; Jia, J.; Sun, X. Z. Photoreactivity examined through incorporation in metal-organic frameworks. *Nat. Chem.* **2010**, *2*, 688−694.
(118) Wang, S.-N.; Yang, Y.; Bai, J.; Li, Y.-Z.; Scheer, M.; Pan, Y.; You, X.-Z. An unprecedented nanoporous and fluorescent supramolecular framework with an $SrAl_2$ topology controllably synthesized from a flexible ditopic acid. *Chem. Commun.* **2007**, 4416−4418.
(119) Dai, F.; Sun, D.; Sun, D. Three 3D Lanthanide−Organic Frameworks Based on Novel Flexible Multicarboxylates: From ssa to rtl Topologies. *Cryst. Growth Des.* **2011**, *11*, 5670−5675.
(120) Fang, M.; Li, J. J.; Shi, P. F.; Zhao, B.; Cheng, P. Structures, luminescence, and slow magnetic relaxation of eight 3D lanthanide-organic frameworks. *Dalton Trans.* **2013**, *42*, 6553−6563.
(121) Liang, J.; Shimizu, G. K. H. Crystalline Zinc Diphosphonate Metal−Organic Framework with Three-Dimensional Microporosity. *Inorg. Chem.* **2007**, *46*, 10449−10451.
(122) Iremonger, S. S.; Liang, J.; Vaidhyanathan, R.; Martens, I.; Shimizu, G. K.; Daff, T. D.; Aghaji, M. Z.; Yeganegi, S.; Woo, T. K. Phosphonate monoesters as carboxylate-like linkers for metal organic frameworks. *J. Am. Chem. Soc.* **2011**, *133*, 20048−20051.
(123) Thuéry, P.; Harrowfield, J. Uranyl−Organic Frameworks with Polycarboxylates: Unusual Effects of a Coordinating Solvent. *Cryst. Growth Des.* **2014**, *14*, 1314−1323.
(124) Wang, K.-X.; Chen, J.-S. Extended Structures and Physicochemical Properties of Uranyl−Organic Compounds. *Acc. Chem. Res.* **2011**, *44*, 531−540.
(125) Andrews, M. B.; Cahill, C. L. Uranyl Bearing Hybrid Materials: Synthesis, Speciation, and Solid-State Structures. *Chem. Rev.* **2013**, *113*, 1121−1136.
(126) Loiseau, T.; Mihalcea, I.; Henry, N.; Volkringer, C. The crystal chemistry of uranium carboxylates. *Coord. Chem. Rev.* **2014**, *266−267*, 69−109.
(127) Abrahams, B. F.; Dharma, A. D.; Grannas, M. J.; Hudson, T. A.; Maynard-Casely, H. E.; Oliver, G. R.; Robson, R.; White, K. F. Isomeric ionic lithium isonicotinate three-dimensional networks and single-crystal-to-single-crystal rearrangements generating microporous materials. *Inorg. Chem.* **2014**, *53*, 4956−4969.
(128) Zhang, X. H.; Hao, Z. M.; Zhang, X. M. Spin canting and metamagnetism in the first hybrid cobalt-hypoxanthine open framework with umr topology. *Chem. - Eur. J.* **2011**, *17*, 5588−5594.
(129) Barthelet, K.; Riou, D.; Nogues, M.; Férey, G. Synthesis, Structure, and Magnetic Properties of Two New Vanadocarboxylates with Three-Dimensional Hybrid Frameworks. *Inorg. Chem.* **2003**, *42*, 1739−1743.

DOI: 10.1021/acs.chemrev.6b00346
Chem. Rev. XXXX, XXX, XXX−XXX

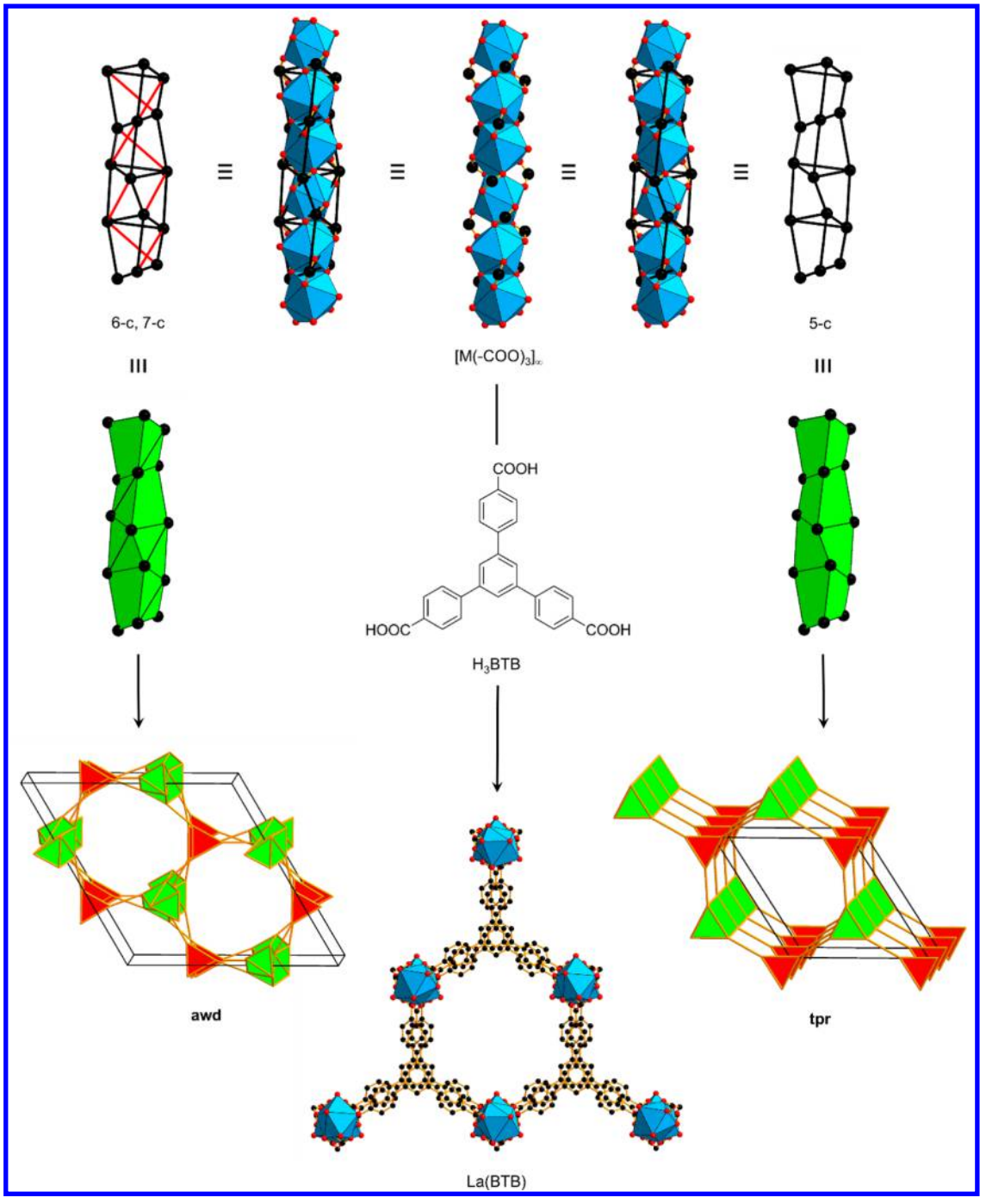

Figure 91. Deconstruction of La(BTB) composed of rods with linked trigonal prisms (right), leading to a **tpr** net or higher coordination **awd** net (left).[199,265] Color code: black, C; red, O; blue polyhedra, metal.

(130) Sanselme, M.; Grenéche, J. M.; Riou-Cavellec, M.; Férey, G. $[Fe_2(C_{10}O_8H_2)]$: An antiferromagnetic 3D iron(II) carboxylate built from ferromagnetic edge-sharing octahedral chains (MIL-62). *Chem. Commun.* **2002**, 2172−2173.

(131) Sanselme, M.; Riou-Cavellec, M.; Férey, G. A new three-dimensional iron fluoride pyromellitate $K(H_3O)[Fe_2F_2(C_{10}O_8H_2)]\cdot 3.5H_2O$. *Solid State Sci.* **2002**, *4*, 1419−1424.

(132) Volkringer, C.; Loiseau, T.; Guillou, N.; Férey, G.; Elkaïm, E. Syntheses and structures of the MOF-type series of metal 1,4,5,8,-naphthalenetetracarboxylates $M_2(OH)_2[C_{14}O_8H_4]$ (Al, Ga, In) with infinite trans-connected M−OH−M chains (MIL-122). *Solid State Sci.* **2009**, *11*, 1507−1512.

(133) Fateeva, A.; Chater, P. A.; Ireland, C. P.; Tahir, A. A.; Khimyak, Y. Z.; Wiper, P. V.; Darwent, J. R.; Rosseinsky, M. J. A water-stable porphyrin-based metal-organic framework active for visible-light photocatalysis. *Angew. Chem., Int. Ed.* **2012**, *51*, 7440−7444.

(134) Stylianou, K. C.; Heck, R.; Chong, S. Y.; Bacsa, J.; Jones, J. T. A.; Khimyak, Y. Z.; Bradshaw, D.; Rosseinsky, M. J. A Guest-Responsive Fluorescent 3D Microporous Metal−Organic Framework Derived from a Long-Lifetime Pyrene Core. *J. Am. Chem. Soc.* **2010**, *132*, 4119−4130.

(135) Li, R. J.; Li, M.; Zhou, X. P.; Li, D.; O'Keeffe, M. A highly stable MOF with a rod SBU and a tetracarboxylate linker: unusual topology and CO_2 adsorption behaviour under ambient conditions. *Chem. Commun.* **2014**, *50*, 4047−4049.

(136) Du, M.; Chen, M.; Yang, X.-G.; Wen, J.; Wang, X.; Fang, S.-M.; Liu, C.-S. A channel-type mesoporous In(iii)−carboxylate coordination framework with high physicochemical stability for use as an electrode material in supercapacitors. *J. Mater. Chem. A* **2014**, *2*, 9828−9834.

DOI: 10.1021/acs.chemrev.6b00346
Chem. Rev. XXXX, XXX, XXX−XXX

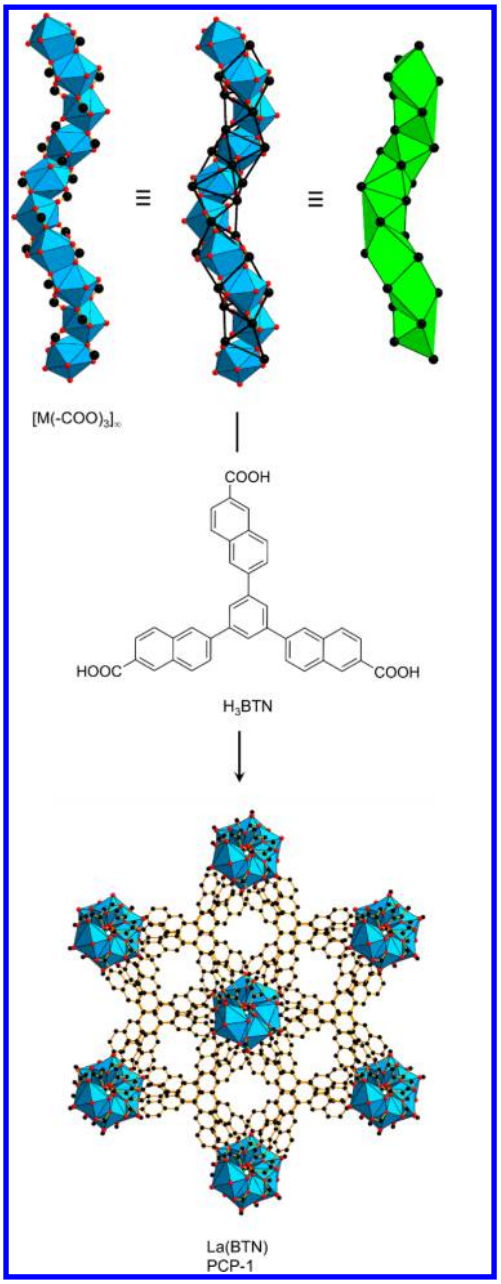

Figure 92. Crystal structure and rod SBU of La(BTN).[200] Color code: black, C; red, O; blue polyhedra, metal.

(137) Li, R.-J.; Li, M.; Zhou, X.-P.; Ng, S. W.; O'Keeffe, M.; Li, D. ROD-8, a rod MOF with a pyrene-cored tetracarboxylate linker: framework disorder, derived nets and selective gas adsorption. *CrystEngComm* **2014**, *16*, 6291.

(138) Volkringer, C.; Loiseau, T.; Férey, G. Two metal-organic frameworks with infinite indium hydroxide chains connected through tetradentate carboxylate linkers. *Solid State Sci.* **2009**, *11*, 29−35.

(139) He, Y.-P.; Tan, Y.-X.; Zhang, J. Stable Mg-Metal−Organic Framework (MOF) and Unstable Zn-MOF Based on Nanosized Tris((4-carboxyl)phenylduryl)amine Ligand. *Cryst. Growth Des.* **2013**, *13*, 6−9.

(140) Moon, H. R.; Kobayashi, N.; Suh, M. P. Porous Metal−Organic Framework with Coordinatively Unsaturated MnII Sites:Sorption Properties for Various Gases. *Inorg. Chem.* **2006**, *45*, 8672−8676.

(141) Choi, H. J.; Dincă, M.; Long, J. R. Broadly Hysteretic H_2 Adsorption in the Microporous Metal−Organic Framework Co(1,4-benzenedipyrazolate). *J. Am. Chem. Soc.* **2008**, *130*, 7848−7850.

(142) Choi, H. J.; Dinca, M.; Dailly, A.; Long, J. R. Hydrogen storage in water-stable metal-organic frameworks incorporating 1,3- and 1,4-benzenedipyrazolate. *Energy Environ. Sci.* **2010**, *3*, 117−123.

(143) Lu, Y.; Tonigold, M.; Bredenkötter, B.; Volkmer, D.; Hitzbleck, J.; Langstein, G. A Cobalt(II)-containing Metal-Organic Framework Showing Catalytic Activity in Oxidation Reactions. *Z. Anorg. Allg. Chem.* **2008**, *634*, 2411−2417.

(144) Galli, S.; Masciocchi, N.; Colombo, V.; Maspero, A.; Palmisano, G.; López-Garzón, F. J.; Domingo-García, M.; Fernández-Morales, I.; Barea, E.; Navarro, J. A. R. Adsorption of Harmful Organic Vapors by Flexible Hydrophobic Bis-pyrazolate Based MOFs. *Chem. Mater.* **2010**, *22*, 1664−1672.

(145) Tabacaru, A.; Pettinari, C.; Masciocchi, N.; Galli, S.; Marchetti, F.; Angjellari, M. Pro-porous coordination polymers of the 1,4-bis((3,5-dimethyl-1H-pyrazol-4-yl)-methyl)benzene ligand with late transition metals. *Inorg. Chem.* **2011**, *50*, 11506−11513.

(146) Tonigold, M.; Lu, Y.; Mavrandonakis, A.; Puls, A.; Staudt, R.; Mollmer, J.; Sauer, J.; Volkmer, D. Pyrazolate-based cobalt(II)-containing metal-organic frameworks in heterogeneous catalytic oxidation reactions: elucidating the role of entatic states for biomimetic oxidation processes. *Chem. - Eur. J.* **2011**, *17*, 8671−8695.

(147) Pettinari, C.; Tabacaru, A.; Boldog, I.; Domasevitch, K. V.; Galli, S.; Masciocchi, N. Novel coordination frameworks incorporating the 4,4′-bipyrazolyl ditopic ligand. *Inorg. Chem.* **2012**, *51*, 5235−5245.

(148) Tăbăcaru, A.; Pettinari, C.; Timokhin, I.; Marchetti, F.; Carrasco-Marín, F.; Maldonado-Hódar, F. J.; Galli, S.; Masciocchi, N. Enlarging an Isoreticular Family: 3,3′,5,5′-Tetramethyl-4,4′-bipyrazolato-Based Porous Coordination Polymers. *Cryst. Growth Des.* **2013**, *13*, 3087−3097.

(149) Wade, C. R.; Corrales-Sanchez, T.; Narayan, T. C.; Dincă, M. Postsynthetic tuning of hydrophilicity in pyrazolate MOFs to modulate water adsorption properties. *Energy Environ. Sci.* **2013**, *6*, 2172−2177.

(150) Wang, F.-K.; Song, X.-X.; Yang, S.-Y.; Huang, R.-B.; Zheng, L.-S. Influence of hydrothermal synthesis temperature on the structures of two 3D coordination polymers. *Inorg. Chem. Commun.* **2007**, *10*, 1198−1201.

(151) He, C.-T.; Tian, J.-Y.; Liu, S.-Y.; Ouyang, G.; Zhang, J.-P.; Chen, X.-M. A porous coordination framework for highly sensitive and selective solid-phase microextraction of non-polar volatile organic compounds. *Chem. Sci.* **2013**, *4*, 351−356.

(152) Feller, R. K.; Cheetham, A. K. Fe(III), Mn(II), Co(II), and Ni(II) 3,4,5-trihydroxybenzoate (gallate) dihydrates; a new family of hybrid framework materials. *Solid State Sci.* **2006**, *8*, 1121−1125.

(153) Abrahams, B. F.; Moylan, M.; Orchard, S. D.; Robson, R. Zinc Saccharate: A Robust, 3D Coordination Network with Two Types of Isolated, Parallel Channels, One Hydrophilic and the Other Hydrophobic. *Angew. Chem., Int. Ed.* **2003**, *42*, 1848−1851.

(154) Aliev, S. B.; Samsonenko, D. G.; Rakhmanova, M. I.; Dybtsev, D. N.; Fedin, V. P. Syntheses and Structural Characterization of Lithium Carboxylate Frameworks and Guest-Dependent Photoluminescence Study. *Cryst. Growth Des.* **2014**, *14*, 4355−4363.

(155) Serpaggi, F.; Férey, G. Hybrid open frameworks (MIL-n): synthesis and crystal structure of MIL-17 — a rare-earth dicarboxylate with a relatively open framework, $[Pr(H_2O)]_2[O_2C(CH_2)_2CO_2]_3{\cdot}H_2O$. *Microporous Mesoporous Mater.* **1999**, *32*, 311−318.

(156) Perles, J.; Iglesias, M.; Ruiz-Valero, C.; Snejko, N. Rare-earths as catalytic centres in organo-inorganic polymeric frameworks. *J. Mater. Chem.* **2004**, *14*, 2683−2689.

(157) Manna, S. C.; Zangrando, E.; Bencini, A.; Benelli, C.; Chaudhuri, N. R. Syntheses, Crystal Structures, and Magnetic Properties of $[Ln^{III2}(Succinate)_3(H_2O)_2]{\cdot}0.5H_2O$ [Ln = Pr, Nd, Sm, Eu, Gd, and Dy] Polymeric Networks: Unusual Ferromagnetic Coupling in Gd Derivative. *Inorg. Chem.* **2006**, *45*, 9114−9122.

(158) Bondar, O. A.; Lukashuk, L. V.; Lysenko, A. B.; Krautscheid, H.; Rusanov, E. B.; Chernega, A. N.; Domasevitch, K. V. New microporous copper(II) coordination polymers based upon bifunctional 1,2,4-triazole/tetrazolate bridges. *CrystEngComm* **2008**, *10*, 1216−1226.

(159) Yan, Z.; Li, M.; Gao, H. L.; Huang, X. C.; Li, D. High-spin versus spin-crossover versus low-spin: geometry intervention in cooperativity

DOI: 10.1021/acs.chemrev.6b00346
Chem. Rev. XXXX, XXX, XXX−XXX

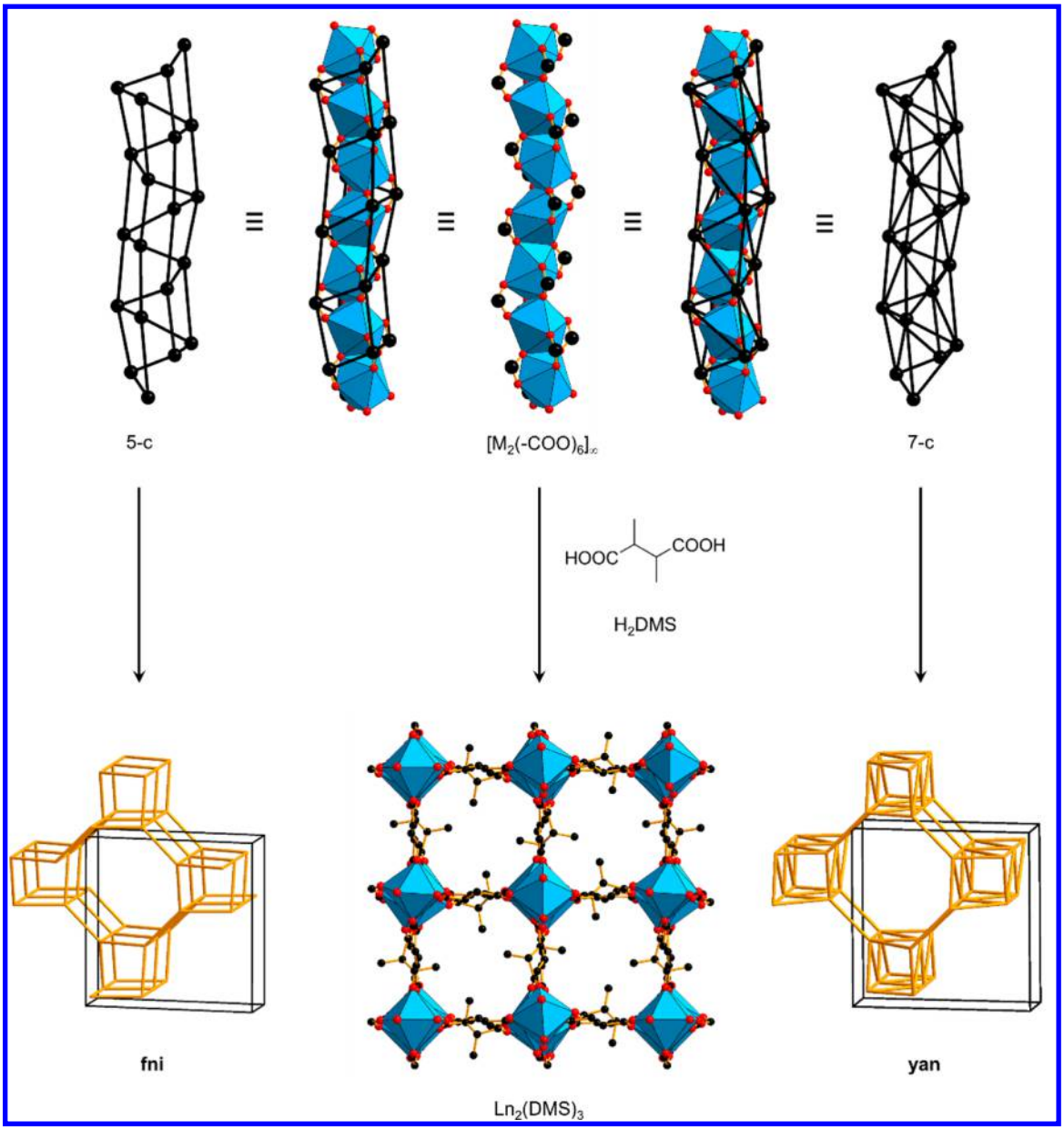

Figure 93. Crystal structure and deconstruction of $Ln_2(DMS)_3$ composed of either 5-c rods (**fni**) or 7-c rods (**yan**).[162] Color code: black, C; red, O; blue polyhedra, metal.

in a 3D polymorphic iron(II)-tetrazole MOFs system. *Chem. Commun.* **2012**, *48*, 3960−3962.

(160) Millange, F.; Serre, C.; Marrot, J.; Gardant, N.; Pellé, F.; Férey, G. Synthesis, structure and properties of a three-dimensional porous rare-earth carboxylate MIL-83(Eu): $Eu_2(O_2C\text{-}C_{10}H_{14}\text{-}CO_2)_3$. *J. Mater. Chem.* **2004**, *14*, 642−645.

(161) Jia, J.; Lin, X.; Blake, A. J.; Champness, N. R.; Hubberstey, P.; Shao, L.; Walker, G.; Wilson, C.; Schröder, M. Triggered Ligand Release Coupled to Framework Rearrangement: Generating Crystalline Porous Coordination Materials. *Inorg. Chem.* **2006**, *45*, 8838−8840.

(162) Gomez, G. E.; Bernini, M. C.; Brusau, E. V.; Narda, G. E.; Massad, W. A.; Labrador, A. Two Sets of Metal Organic Frameworks along the Lanthanide Series Constructed by 2,3-Dimethylsuccinate: Structures, Topologies, and Strong Emission without Ligand Sensitization. *Cryst. Growth Des.* **2013**, *13*, 5249−5260.

(163) Saines, P. J.; Steinmann, M.; Tan, J.-C.; Yeung, H. H. M.; Cheetham, A. K. Structural diversity and luminescent properties of lanthanide 2,2- and 2,3-dimethylsuccinate frameworks. *CrystEngComm* **2013**, *15*, 100−110.

(164) Harbuzaru, B. V.; Corma, A.; Rey, F.; Atienzar, P.; Jordá, J. L.; García, H.; Ananias, D.; Carlos, L. D.; Rocha, J. Metal−Organic Nanoporous Structures with Anisotropic Photoluminescence and Magnetic Properties and Their Use as Sensors. *Angew. Chem., Int. Ed.* **2008**, *47*, 1080−1083.

(165) Gándara, F.; Andrés, A. d.; Gómez-Lor, B.; Gutiérrez-Puebla, E.; Iglesias, M.; Monge, M. A.; Proserpio, D. M.; Snejko, N. A Rare-Earth MOF Series: Fascinating Structure, Efficient Light Emitters, and Promising Catalysts. *Cryst. Growth Des.* **2008**, *8*, 378−380.

(166) Herm, Z. R.; Wiers, B. M.; Mason, J. A.; van Baten, J. M.; Hudson, M. R.; Zajdel, P.; Brown, C. M.; Masciocchi, N.; Krishna, R.; Long, J. R. Separation of hexane isomers in a metal-organic framework with triangular channels. *Science* **2013**, *340*, 960−964.

(167) Mowat, J. P.; Miller, S. R.; Griffin, J. M.; Seymour, V. R.; Ashbrook, S. E.; Thompson, S. P.; Fairen-Jimenez, D.; Banu, A. M.; Duren, T.; Wright, P. A. Structural chemistry, monoclinic-to-orthorhombic phase transition, and CO_2 adsorption behavior of the small pore scandium terephthalate, $Sc_2(O_2CC_6H_4CO_2)_3$, and its nitro-

DOI: 10.1021/acs.chemrev.6b00346
Chem. Rev. XXXX, XXX, XXX−XXX

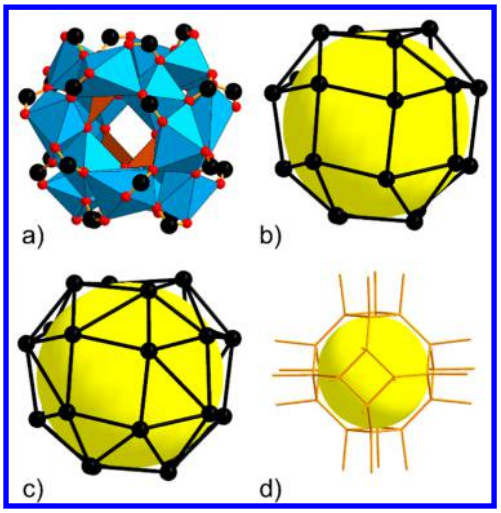

Figure 94. (a) 24-c SBU; (b) the pattern of carboxylate C atoms as a 4.4^3 polyhedron; (c) the same atoms as a $3^4.4$ polyhedron; and (d) part of the augmented net (**ddy-a**) underlying a crystal structure with the SBU in (a).[266] Color code: black, C; red, O; orange polyhedra, P; blue polyhedra, metal.

and amino-functionalized derivatives. *Inorg. Chem.* **2011**, *50*, 10844−10858.
(168) Graham, A. J.; Banu, A. M.; Duren, T.; Greenaway, A.; McKellar, S. C.; Mowat, J. P.; Ward, K.; Wright, P. A.; Moggach, S. A. Stabilization of scandium terephthalate MOFs against reversible amorphization and structural phase transition by guest uptake at extreme pressure. *J. Am. Chem. Soc.* **2014**, *136*, 8606−8613.
(169) Taddei, M.; Costantino, F.; Vivani, R. Synthesis and Crystal Structure from X-ray Powder Diffraction Data of Two Zirconium Diphosphonates Containing Piperazine Groups. *Inorg. Chem.* **2010**, *49*, 9664−9670.
(170) Lin, J.-M.; Guan, Y.-F.; Wang, D.-Y.; Dong, W.; Wang, X.-T.; Gao, S. Syntheses, structures and properties of seven isomorphous 1D Ln3+complexes Ln(BTA) $(HCOO)(H_2O)_3$ (H_2BTA = bis(tetrazoly)-amine, Ln = Pr, Gd, Eu, Tb, Dy, Er, Yb) and two 3D Ln^{3+} complexes $Ln(HCOO)_3$ (Ln = Pr, Nd). *Dalton Trans.* **2008**, 6165−6169.
(171) Wang, G.; Song, T.; Fan, Y.; Xu, J.; Wang, M.; Wang, L.; Zhang, L.; Wang, L. A porous lanthanide metal−organic framework with luminescent property, nitrogen gas adsorption and high thermal stability. *Inorg. Chem. Commun.* **2010**, *13*, 95−97.
(172) Qiu, Y.; Deng, H.; Yang, S.; Mou, J.; Daiguebonne, C.; Kerbellec, N.; Guillou, O.; Batten, S. R. Syntheses, Crystal Structures, and Gas Storage Studies in New Three-Dimensional 5-Aminoisophthalate Praseodymium Polymeric Complexes. *Inorg. Chem.* **2009**, *48*, 3976−3981.
(173) Zhou, H.; Li, M.; Li, D.; Zhang, J.; Chen, X. Thermal expansion behaviors of Mn(II)-pyridylbenzoate frameworks based on metal-carboxylate chains. *Sci. China: Chem.* **2014**, *57*, 365−370.
(174) Xiong, R.-G.; Wilson, S. R.; Lin, W. Bis(isonicotinato)iron(II): a rare, neutral three-dimensional iron coordination polymer. *J. Chem. Soc., Dalton Trans.* **1998**, 4089−4090.
(175) Wei, Q.; Nieuwenhuyzen, M.; Meunier, F.; Hardacre, C.; James, S. L. Guest sorption and desorption in the metal-organic framework $[Co(INA)_2]$ (INA = isonicotinate) - evidence of intermediate phases during desorption. *Dalton Trans.* **2004**, 1807−1811.
(176) Liu, T.; Luo, D.; Xu, D.; Zeng, H.; Lin, Z. An open-framework rutile-type magnesium isonicotinate and its structural analogue with an anatase topology. *Dalton Trans.* **2013**, *42*, 368−371.
(177) Zhou, H. L.; Lin, R. B.; He, C. T.; Zhang, Y. B.; Feng, N.; Wang, Q.; Deng, F.; Zhang, J. P.; Chen, X. M. Direct visualization of a guest-triggered crystal deformation based on a flexible ultramicroporous framework. *Nat. Commun.* **2013**, *4*, 2534.
(178) He, Y. P.; Tan, Y. X.; Zhang, J. Gas sorption, second-order nonlinear optics, and luminescence properties of a series of lanthanide-organic frameworks based on nanosized tris((4-carboxyl)phenylduryl)-amine ligand. *Inorg. Chem.* **2013**, *52*, 12758−12762.
(179) Dang, S.; Zhang, J.-H.; Sun, Z.-M. Tunable emission based on lanthanide(III) metal−organic frameworks: an alternative approach to white light. *J. Mater. Chem.* **2012**, *22*, 8868−8873.
(180) Dang, S.; Min, X.; Yang, W.; Yi, F. Y.; You, H.; Sun, Z. M. Lanthanide metal-organic frameworks showing luminescence in the visible and near-infrared regions with potential for acetone sensing. *Chem. - Eur. J.* **2013**, *19*, 17172−17179.
(181) Dang, S.; Zhang, J. H.; Sun, Z. M.; Zhang, H. Luminescent lanthanide metal-organic frameworks with a large SHG response. *Chem. Commun.* **2012**, *48*, 11139−11141.
(182) Feng, X.; Li, R.; Wang, L.; Ng, S. W.; Qin, G.; Ma, L. A series of homonuclear lanthanide coordination polymers based on a fluorescent conjugated ligand: syntheses, luminescence and sensor for pollutant chromate anion. *CrystEngComm* **2015**, *17*, 7878−7887.
(183) Pan, L.; Zheng, N.; Wu, Y.; Han, S.; Yang, R.; Huang, X.; Li, J. Synthesis, Characterization and Structural Transformation of A Condensed Rare Earth Metal Coordination Polymer. *Inorg. Chem.* **2001**, *40*, 828−830.
(184) Zhang, X.; Ballem, M. A.; Hu, Z. J.; Bergman, P.; Uvdal, K. Nanoscale light-harvesting metal-organic frameworks. *Angew. Chem., Int. Ed.* **2011**, *50*, 5729−5733.
(185) Chen, B.; Wang, L.; Xiao, Y.; Fronczek, F. R.; Xue, M.; Cui, Y.; Qian, G. A Luminescent Metal−Organic Framework with Lewis Basic Pyridyl Sites for the Sensing of Metal Ions. *Angew. Chem., Int. Ed.* **2009**, *48*, 500−503.
(186) de Lill, D. T.; Gunning, N. S.; Cahill, C. L. Toward Templated Metal−Organic Frameworks: Synthesis, Structures, Thermal Properties, and Luminescence of Three Novel Lanthanide−Adipate Frameworks. *Inorg. Chem.* **2005**, *44*, 258−266.
(187) de Lill, D. T.; de Bettencourt-Dias, A.; Cahill, C. L. Exploring Lanthanide Luminescence in Metal-Organic Frameworks: Synthesis, Structure, and Guest-Sensitized Luminescence of a Mixed Europium/Terbium-Adipate Framework and a Terbium-Adipate Framework. *Inorg. Chem.* **2007**, *46*, 3960−3965.
(188) Lü, J.; Bi, W.-H.; Xiao, F.-X.; Batten, S. R.; Cao, R. Lanthanide Coordination Polymers Constructed from Infinite Rod-Shaped Secondary Building Units and Flexible Ligands. *Chem. - Asian J.* **2008**, *3*, 542−547.
(189) Zhang, J.; Bu, J. T.; Chen, S.; Wu, T.; Zheng, S.; Chen, Y.; Nieto, R. A.; Feng, P.; Bu, X. Urothermal Synthesis of Crystalline Porous Materials. *Angew. Chem., Int. Ed.* **2010**, *49*, 8876−8879.
(190) Guo, X.; Zhu, G.; Fang, Q.; Xue, M.; Tian, G.; Sun, J.; Li, X.; Qiu, S. Synthesis, Structure and Luminescent Properties of Rare Earth Coordination Polymers Constructed from Paddle-Wheel Building Blocks. *Inorg. Chem.* **2005**, *44*, 3850−3855.
(191) Huang, W.; Wu, D.; Zhou, P.; Yan, W.; Guo, D.; Duan, C.; Meng, Q. Luminescent and Magnetic Properties of Lanthanide-Thiophene-2,5-dicarboxylate Hybrid Materials. *Cryst. Growth Des.* **2009**, *9*, 1361−1369.
(192) He, H.; Ma, H.; Sun, D.; Zhang, L.; Wang, R.; Sun, D. Porous Lanthanide−Organic Frameworks: Control over Interpenetration, Gas Adsorption, and Catalyst Properties. *Cryst. Growth Des.* **2013**, *13*, 3154−3161.
(193) Tan, B.; Xie, Z. L.; Feng, M. L.; Hu, B.; Wu, Z. F.; Huang, X. Y. Ionothermal syntheses, crystal structures and properties of three-dimensional rare earth metal-organic frameworks with 1,4-naphthalenedicarboxylic acid. *Dalton Trans.* **2012**, *41*, 10576−10584.
(194) Lin, Y.-W.; Jian, B.-R.; Huang, S.-C.; Huang, C.-H.; Hsu, K.-F. Synthesis and Characterization of Three Ytterbium Coordination Polymers Featuring Various Cationic Species and a Luminescence Study of a Terbium Analogue With Open Channels. *Inorg. Chem.* **2010**, *49*, 2316−2324.
(195) Devic, T.; Serre, C.; Audebrand, N.; Marrot, J.; Férey, G. MIL-103, A 3-D Lanthanide-Based Metal Organic Framework with Large One-Dimensional Tunnels and A High Surface Area. *J. Am. Chem. Soc.* **2005**, *127*, 12788−12789.

DOI: 10.1021/acs.chemrev.6b00346
Chem. Rev. XXXX, XXX, XXX−XXX

(196) Devic, T.; Wagner, V.; Guillou, N.; Vimont, A.; Haouas, M.; Pascolini, M.; Serre, C.; Marrot, J.; Daturi, M.; Taulelle, F.; et al. Synthesis and characterization of a series of porous lanthanide tricarboxylates. *Microporous Mesoporous Mater.* **2011**, *140*, 25−33.
(197) Feyand, M.; Mugnaioli, E.; Vermoortele, F.; Bueken, B.; Dieterich, J. M.; Reimer, T.; Kolb, U.; de Vos, D.; Stock, N. Automated diffraction tomography for the structure elucidation of twinned, sub-micrometer crystals of a highly porous, catalytically active bismuth metal-organic framework. *Angew. Chem., Int. Ed.* **2012**, *51*, 10373−10376.
(198) Reinsch, H.; Krüger, M.; Wack, J.; Senker, J.; Salles, F.; Maurin, G.; Stock, N. A new aluminium-based microporous metal−organic framework: Al(BTB) (BTB = 1,3,5-benzenetrisbenzoate). *Microporous Mesoporous Mater.* **2012**, *157*, 50−55.
(199) Duan, J.; Higuchi, M.; Horike, S.; Foo, M. L.; Rao, K. P.; Inubushi, Y.; Fukushima, T.; Kitagawa, S. High CO_2/CH_4 and C_2 Hydrocarbons/CH_4 Selectivity in a Chemically Robust Porous Coordination Polymer. *Adv. Funct. Mater.* **2013**, *23*, 3525−3530.
(200) Duan, J.; Higuchi, M.; Krishna, R.; Kiyonaga, T.; Tsutsumi, Y.; Sato, Y.; Kubota, Y.; Takata, M.; Kitagawa, S. High $CO_2/N_2/O_2/CO$ separation in a chemically robust porous coordination polymer with low binding energy. *Chem. Sci.* **2014**, *5*, 660−666.
(201) He, Y.; Zhang, Z.; Xiang, S.; Fronczek, F. R.; Krishna, R.; Chen, B. A robust doubly interpenetrated metal-organic framework constructed from a novel aromatic tricarboxylate for highly selective separation of small hydrocarbons. *Chem. Commun.* **2012**, *48*, 6493−6495.
(202) Wu, P.; Wang, J.; Li, Y.; He, C.; Xie, Z.; Duan, C. Luminescent Sensing and Catalytic Performances of a Multifunctional Lanthanide-Organic Framework Comprising a Triphenylamine Moiety. *Adv. Funct. Mater.* **2011**, *21*, 2788−2794.
(203) Han, Y.-F.; Zhou, X.-H.; Zheng, Y.-X.; Shen, Z.; Song, Y.; You, X.-Z. Syntheses, structures, photoluminescence, and magnetic properties of nanoporous 3D lanthanide coordination polymers with 4,4′-biphenyldicarboxylate ligand. *CrystEngComm* **2008**, *10*, 1237−1242.
(204) Dimos, A.; Tsaousis, D.; Michaelides, A.; Skoulika, S.; Golhen, S.; Ouahab, L.; Didierjean, C.; Aubry, A. Microporous Rare Earth Coordination Polymers: Effect of Lanthanide Contraction on Crystal Architecture and Porosity. *Chem. Mater.* **2002**, *14*, 2616−2622.
(205) Kiritsis, V.; Michaelides, A.; Skoulika, S.; Golhen, S.; Ouahab, L. Assembly of a Porous Three-Dimensional Coordination Polymer: Crystal Structure of $\{[La_2(adipate)_3(H_2O)_4]6H_2O\}_n$. *Inorg. Chem.* **1998**, *37*, 3407−3410.
(206) Guillerm, V.; Weseliński, L. J.; Belmabkhout, Y.; Cairns, A. J.; D'Elia, V.; Wojtas, L.; Adil, K.; Eddaoudi, M. Discovery and introduction of a (3,18)-connected net as an ideal blueprint for the design of metal−organic frameworks. *Nat. Chem.* **2014**, *6*, 673−680.
(207) Roy, S.; Chakraborty, A.; Maji, T. K. Lanthanide−organic frameworks for gas storage and as magneto-luminescent materials. *Coord. Chem. Rev.* **2014**, *273*−*274*, 139−164.
(208) Li, B.; Chen, B. Porous Lanthanide Metal−Organic Frameworks for Gas Storage and Separation. *Struct. Bonding (Berlin, Ger.)* **2014**, *163*, 75−107.
(209) Devic, T.; David, O.; Valls, M.; Marrot, J.; Couty, F.; Férey, G. An Illustration of the Limit of the Metal Organic Framework's Isoreticular Principle Using a Semirigid Tritopic Linker Obtained by "Click" Chemistry. *J. Am. Chem. Soc.* **2007**, *129*, 12614−12615.
(210) Lama, P.; Aijaz, A.; Neogi, S.; Barbour, L. J.; Bharadwaj, P. K. Microporous La(III) Metal−Organic Framework Using a Semirigid Tricarboxylic Ligand: Synthesis, Single-Crystal to Single-Crystal Sorption Properties, and Gas Adsorption Studies. *Cryst. Growth Des.* **2010**, *10*, 3410−3417.
(211) Guo, Z.; Xu, H.; Su, S.; Cai, J.; Dang, S.; Xiang, S.; Qian, G.; Zhang, H.; O'Keeffe, M.; Chen, B. A robust near infrared luminescent ytterbium metal-organic framework for sensing of small molecules. *Chem. Commun.* **2011**, *47*, 5551−5553.
(212) Tang, S. F.; Cai, J. J.; Li, L. J.; Lv, X. X.; Wang, C.; Zhao, X. B. A highly porous three-dimensional aluminum phosphonate with hexagonal channels: synthesis, structure and adsorption properties. *Dalton Trans.* **2014**, *43*, 5970−5973.
(213) Mallick, A.; Saha, S.; Pachfule, P.; Roy, S.; Banerjee, R. Selective CO_2 and H_2 adsorption in a chiral magnesium-based metal organic framework (Mg-MOF) with open metal sites. *J. Mater. Chem.* **2010**, *20*, 9073−9080.
(214) Banerjee, D.; Finkelstein, J.; Smirnov, A.; Forster, P. M.; Borkowski, L. A.; Teat, S. J.; Parise, J. B. Synthesis and Structural Characterization of Magnesium Based Coordination Networks in Different Solvents. *Cryst. Growth Des.* **2011**, *11*, 2572−2579.
(215) Guillerm, V.; Ragon, F.; Dan-Hardi, M.; Devic, T.; Vishnuvarthan, M.; Campo, B.; Vimont, A.; Clet, G.; Yang, Q.; Maurin, G.; et al. A series of isoreticular, highly stable, porous zirconium oxide based metal-organic frameworks. *Angew. Chem., Int. Ed.* **2012**, *51*, 9267−9271.
(216) Cavka, J. H.; Jakobsen, S.; Olsbye, U.; Guillou, N.; Lamberti, C.; Bordiga, S.; Lillerud, K. P. A New Zirconium Inorganic Building Brick Forming Metal Organic Frameworks with Exceptional Stability. *J. Am. Chem. Soc.* **2008**, *130*, 13850−13851.
(217) Baburin, I. A.; Blatov, V. A.; Carlucci, L.; Ciani, G.; Proserpio, D. M. Interpenetrating metal-organic and inorganic 3D networks: a computer-aided systematic investigation. Part II [1]. Analysis of the Inorganic Crystal Structure Database (ICSD). *J. Solid State Chem.* **2005**, *178*, 2452−2474.
(218) Vougo-Zanda, M.; Wang, X.; Jacobson, A. J. Influence of Ligand Geometry on the Formation of In−O Chains in Metal-Oxide Organic Frameworks (MOOFs). *Inorg. Chem.* **2007**, *46*, 8819−8824.
(219) Snejko, N.; Cascales, C.; Gomez-Lor, B.; Gutiérrez-Puebla, E.; Iglesias, M.; Ruiz-Valero, C.; Monge, M. A. From rational octahedron design to reticulation serendipity. A thermally stable rare earth polymeric disulfonate family with CdI_2-like structure, bifunctional catalysis and optical properties. *Chem. Commun.* **2002**, 1366−1367.
(220) Humphrey, S. M.; Chang, J.-S.; Jhung, S. H.; Yoon, J. W.; Wood, P. T. Porous Cobalt(II)−Organic Frameworks with Corrugated Walls: Structurally Robust Gas-Sorption Materials. *Angew. Chem., Int. Ed.* **2007**, *46*, 272−275.
(221) Gándara, F.; García-Cortés, A.; Cascales, C.; Gómez-Lor, B.; Gutiérrez-Puebla, E.; Iglesias, M.; Monge, A.; Snejko, N. Rare Earth Arenedisulfonate Metal−Organic Frameworks: An Approach toward Polyhedral Diversity and Variety of Functional Compounds. *Inorg. Chem.* **2007**, *46*, 3475−3484.
(222) Li, X.-J.; Wang, X.-Y.; Gao, S.; Cao, R. Two Three-Dimensional Metal−Organic Frameworks Containing One-Dimensional Hydroxyl/Carboxylate Mixed Bridged Metal Chains: Syntheses, Crystal Structures, and Magnetic Properties. *Inorg. Chem.* **2006**, *45*, 1508−1516.
(223) Chen, W. T.; Yamada, Y.; Liu, G. N.; Kubota, A.; Ichikawa, T.; Kojima, Y.; Guo, G. C.; Fukuzumi, S. X-Ray crystal structure of [HSm{V(IV)O(TPPS)}]n and encapsulation of nitrogen molecules in 1-D channels. *Dalton Trans.* **2011**, *40*, 12826−12831.
(224) Chen, W.-T.; Hu, R.-H.; Wang, Y.-F.; Zhang, X.; Liu, J. A Tb−Zn tetra(4-sulfonatophenyl)porphyrin hybrid: Preparation, structure, photophysical and electrochemical properties. *J. Solid State Chem.* **2014**, *213*, 218−223.
(225) Chen, W.-T.; Luo, Z.-G.; Wang, Y.-F.; Zhang, X.; Fu, H.-R. Synthesis, structure, photophysical and electrochemical properties of a novel metalloporphyrin with a condensed three-dimensional porous open framework. *Inorg. Chim. Acta* **2014**, *414*, 1−7.
(226) Gutschke, S. O. H.; Molinier, M.; Powell, A. K.; Wood, P. T. Hydrothermal Synthesis of Microporous Transition Metal Squarates: Preparation and Structure of $[Co_3(\mu_3\text{-}OH)_2(C_4O_4)_2]\cdot 3H_2O$. *Angew. Chem., Int. Ed. Engl.* **1997**, *36*, 991−992.
(227) Li, L.; Wang, S.; Chen, T.; Sun, Z.; Luo, J.; Hong, M. Solvent-Dependent Formation of Cd(II) Coordination Polymers Based on a C_2-Symmetric Tricarboxylate Linker. *Cryst. Growth Des.* **2012**, *12*, 4109−4115.
(228) Xu, J.; Cheng, J.; Su, W.; Hong, M. Effect of Lanthanide Contraction on Crystal Structures of Three-Dimensional Lanthanide Based Metal−Organic Frameworks with Thiophene-2,5-Dicarboxylate and Oxalate. *Cryst. Growth Des.* **2011**, *11*, 2294−2301.

DOI: 10.1021/acs.chemrev.6b00346
Chem. Rev. XXXX, XXX, XXX−XXX

(229) He, J.; Yu, J.; Zhang, Y.; Pan, Q.; Xu, R. Synthesis, Structure, and Luminescent Property of a Heterometallic Metal−Organic Framework Constructed from Rod-Shaped Secondary Building Blocks. *Inorg. Chem.* **2005**, *44*, 9279−9282.
(230) Zhang, T.-z.; Lu, Y.; Li, Y.-g.; Zhang, Z.; Chen, W.-l.; Fu, H.; Wang, E.-b. Metal−organic frameworks constructed from three kinds of new Fe-containing secondary building units. *Inorg. Chim. Acta* **2012**, *384*, 219−224.
(231) Whitfield, T. R.; Wang, X.; Liu, L.; Jacobson, A. J. Metal-organic frameworks based on iron oxide octahedral chains connected by benzenedicarboxylate dianions. *Solid State Sci.* **2005**, *7*, 1096−1103.
(232) Ibarra, I. A.; Yang, S.; Lin, X.; Blake, A. J.; Rizkallah, P. J.; Nowell, H.; Allan, D. R.; Champness, N. R.; Hubberstey, P.; Schroder, M. Highly porous and robust scandium-based metal-organic frameworks for hydrogen storage. *Chem. Commun.* **2011**, *47*, 8304−8306.
(233) Reinsch, H.; van der Veen, M. A.; Gil, B.; Marszalek, B.; Verbiest, T.; de Vos, D.; Stock, N. Structures, Sorption Characteristics, and Nonlinear Optical Properties of a New Series of Highly Stable Aluminum MOFs. *Chem. Mater.* **2013**, *25*, 17−26.
(234) Qian, J.; Jiang, F.; Yuan, D.; Wu, M.; Zhang, S.; Zhang, L.; Hong, M. Highly selective carbon dioxide adsorption in a water-stable indium-organic framework material. *Chem. Commun.* **2012**, *48*, 9696−9698.
(235) Yang, S.; Sun, J.; Ramirez-Cuesta, A. J.; Callear, S. K.; David, W. I.; Anderson, D. P.; Newby, R.; Blake, A. J.; Parker, J. E.; Tang, C. C.; et al. Selectivity and direct visualization of carbon dioxide and sulfur dioxide in a decorated porous host. *Nat. Chem.* **2012**, *4*, 887−894.
(236) Song, B.-Q.; Wang, X.-L.; Zhang, Y.-T.; Wu, X.-S.; Liu, H.-S.; Shao, K.-Z.; Su, Z.-M. Periodic tiling of triangular and square nanotubes in a cationic metal-organic framework for selective anion exchange. *Chem. Commun.* **2015**, *51*, 9515−9518.
(237) Lin, J.-D.; Wu, S.-T.; Li, Z.-H.; Du, S.-W. A series of novel Pb(II) or Pb(II)/M(II) (M = Ca and Sr) hybrid inorganic-organic frameworks based on polycarboxylic acids with diverse Pb-O-M (M = Pb, Ca and Sr) inorganic connectivities. *CrystEngComm* **2010**, *12*, 4252−4262.
(238) Kang, Y.; Chen, S.; Wang, F.; Zhang, J.; Bu, X. Induction in urothermal synthesis of chiral porous materials from achiral precursors. *Chem. Commun.* **2011**, *47*, 4950−4952.
(239) Fang, S.-M.; Chen, M.; Yang, X.-G.; Wang, C.; Du, M.; Liu, C.-S. An unusual (4,10)-connected 3-D metal-organic framework based on non-planar tricarboxyl tecton and tetracadmium(ii) secondary building units. *CrystEngComm* **2012**, *14*, 5299−5304.
(240) Chen, Z.; Zhao, B.; Cheng, P.; Zhao, X.-Q.; Shi, W.; Song, Y. A Purely Lanthanide-Based Complex Exhibiting Ferromagnetic Coupling and Slow Magnetic Relaxation Behavior. *Inorg. Chem.* **2009**, *48*, 3493−3495.
(241) Mihalcea, I.; Henry, N.; Volkringer, C.; Loiseau, T. Uranyl−Pyromellitate Coordination Polymers: Toward Three-Dimensional Open Frameworks with Large Channel Systems. *Cryst. Growth Des.* **2012**, *12*, 526−535.
(242) Dalai, S.; Bera, M.; Rana, A.; Chowdhuri, D. S.; Zangrando, E. Combination of covalent and hydrogen bonding in the formation of 3D uranyl-carboxylate networks. *Inorg. Chim. Acta* **2010**, *363* (13), 3407−3412.
(243) Riou-Cavellec, M.; Albinet, C.; Livage, C.; Guillou, N.; Noguès, M.; Grenèche, J. M.; Férey, G. Ferromagnetism of the hybrid open framework $K[M_3(BTC)_3]\cdot 5H_2O$ (M = Fe, Co) or MIL-45. *Solid State Sci.* **2002**, *4*, 267−270.
(244) Li, Y.-W.; Zhao, J.-P.; Wang, L.-F.; Bu, X.-H. An Fe-based MOF constructed from paddle-wheel and rod-shaped SBUs involved in situ generated acetate. *CrystEngComm* **2011**, *13*, 6002.
(245) Reinsch, H.; Marszalek, B.; Wack, J.; Senker, J.; Gil, B.; Stock, N. A new Al-MOF based on a unique column-shaped inorganic building unit exhibiting strongly hydrophilic sorption behaviour. *Chem. Commun.* **2012**, *48*, 9486−9488.
(246) Seichter, W.; Mögel, H.-J.; Brand, P.; Salah, D. Crystal Structure and Formation of the Aluminium Hydroxide Chloride $[Al_{13}(OH)_{24}(H_2O)_{24}]Cl_{15}\cdot 13\ H_2O$. *Eur. J. Inorg. Chem.* **1998**, *1998*, 795−797.
(247) Han, L.; Qin, L.; Xu, L.; Zhou, Y.; Sun, J.; Zou, X. A novel photochromic calcium-based metal-organic framework derived from a naphthalene diimide chromophore. *Chem. Commun.* **2013**, *49*, 406−408.
(248) Tripuramallu, B. K.; Titi, H. M.; Roy, S.; Verma, R.; Goldberg, I. Ameliorated synthetic methodology for crystalline lanthanoid−metalloporphyrin open frameworks based on a multitopic octacarboxyporphyrin scaffold: structural, gas sorption and photophysical properties. *CrystEngComm* **2016**, *18*, 515−520.
(249) Fracaroli, A. M.; Furukawa, H.; Suzuki, M.; Dodd, M.; Okajima, S.; Gandara, F.; Reimer, J. A.; Yaghi, O. M. Metal-organic frameworks with precisely designed interior for carbon dioxide capture in the presence of water. *J. Am. Chem. Soc.* **2014**, *136*, 8863−8866.
(250) Bloch, E. D.; Queen, W. L.; Krishna, R.; Zadrozny, J. M.; Brown, C. M.; Long, J. R. Hydrocarbon Separations in a Metal-Organic Framework with Open Iron(II) Coordination Sites. *Science* **2012**, *335*, 1606−1610.
(251) Kapelewski, M. T.; Geier, S. J.; Hudson, M. R.; Stück, D.; Mason, J. A.; Nelson, J. N.; Xiao, D. J.; Hulvey, Z.; Gilmour, E.; FitzGerald, S. A.; et al. M2(m-dobdc) (M = Mg, Mn, Fe, Co, Ni) Metal−Organic Frameworks Exhibiting Increased Charge Density and Enhanced H2 Binding at the Open Metal Sites. *J. Am. Chem. Soc.* **2014**, *136*, 12119−12129.
(252) McDonald, T. M.; Lee, W. R.; Mason, J. A.; Wiers, B. M.; Hong, C. S.; Long, J. R. Capture of carbon dioxide from air and flue gas in the alkylamine-appended metal-organic framework mmen-Mg_2(dobpdc). *J. Am. Chem. Soc.* **2012**, *134*, 7056−7065.
(253) Fang, Q.-R.; Zhu, G.-S.; Jin, Z.; Ji, Y.-Y.; Ye, J.-W.; Xue, M.; Yang, H.; Wang, Y.; Qiu, S.-L. Mesoporous Metal−Organic Framework with Rare etb Topology for Hydrogen Storage and Dye Assembly. *Angew. Chem., Int. Ed.* **2007**, *46*, 6638−6642.
(254) Dong, M.-J.; Zhao, M.; Ou, S.; Zou, C.; Wu, C.-D. A Luminescent Dye@MOF Platform: Emission Fingerprint Relationships of Volatile Organic Molecules. *Angew. Chem., Int. Ed.* **2014**, *53*, 1575−1579.
(255) Guo, X.; Zhu, G.; Li, Z.; Sun, F.; Yang, Z.; Qiu, S. A lanthanide metal-organic framework with high thermal stability and available Lewis-acid metal sites. *Chem. Commun.* **2006**, 3172−3174.
(256) Yang, J.; Yue, Q.; Li, G.-D.; Cao, J.-J.; Li, G.-H.; Chen, J.-S. Structures, Photoluminescence, Up-Conversion, and Magnetism of 2D and 3D Rare-Earth Coordination Polymers with Multicarboxylate Linkages. *Inorg. Chem.* **2006**, *45*, 2857−2865.
(257) Chen, B.; Yang, Y.; Zapata, F.; Lin, G.; Qian, G.; Lobkovsky, E. B. Luminescent Open Metal Sites within a Metal−Organic Framework for Sensing Small Molecules. *Adv. Mater.* **2007**, *19*, 1693−1696.
(258) Chen, B.; Wang, L.; Zapata, F.; Qian, G.; Lobkovsky, E. B. A Luminescent Microporous Metal−Organic Framework for the Recognition and Sensing of Anions. *J. Am. Chem. Soc.* **2008**, *130*, 6718−6719.
(259) Luo, J.; Xu, H.; Liu, Y.; Zhao, Y.; Daemen, L. L.; Brown, C.; Timofeeva, T. V.; Ma, S.; Zhou, H.-C. Hydrogen Adsorption in a Highly Stable Porous Rare-Earth Metal-Organic Framework: Sorption Properties and Neutron Diffraction Studies. *J. Am. Chem. Soc.* **2008**, *130*, 9626−9627.
(260) Gustafsson, M.; Bartoszewicz, A.; Martín-Matute, B.; Sun, J.; Grins, J.; Zhao, T.; Li, Z.; Zhu, G.; Zou, X. A Family of Highly Stable Lanthanide Metal−Organic Frameworks: Structural Evolution and Catalytic Activity. *Chem. Mater.* **2010**, *22*, 3316−3322.
(261) Jiang, H.-L.; Tsumori, N.; Xu, Q. A Series of (6,6)-Connected Porous Lanthanide−Organic Framework Enantiomers with High Thermostability and Exposed Metal Sites: Scalable Syntheses, Structures, and Sorption Properties. *Inorg. Chem.* **2010**, *49*, 10001−10006.
(262) Li, Z.; Zhu, G.; Lu, G.; Qiu, S.; Yao, X. Ammonia Borane Confined by a Metal−Organic Framework for Chemical Hydrogen Storage: Enhancing Kinetics and Eliminating Ammonia. *J. Am. Chem. Soc.* **2010**, *132*, 1490−1491.
(263) Liu, K.; You, H.; Zheng, Y.; Jia, G.; Song, Y.; Huang, Y.; Yang, M.; Jia, J.; Guo, N.; Zhang, H. Facile and rapid fabrication of metal-organic

DOI: 10.1021/acs.chemrev.6b00346
Chem. Rev. XXXX, XXX, XXX−XXX

framework nanobelts and color-tunable photoluminescence properties. *J. Mater. Chem.* **2010**, *20*, 3272−3279.
(264) Xie, L.-H.; Wang, Y.; Liu, X.-M.; Lin, J.-B.; Zhang, J.-P.; Chen, X.-M. Crystallographic studies into the role of exposed rare earth metal ion for guest sorption. *CrystEngComm* **2011**, *13*, 5849−5857.
(265) Yao, Q.; Bermejo Gómez, A.; Su, J.; Pascanu, V.; Yun, Y.; Zheng, H.; Chen, H.; Liu, L.; Abdelhamid, H. N.; Martín-Matute, B.; et al. Series of Highly Stable Isoreticular Lanthanide Metal−Organic Frameworks with Expanding Pore Size and Tunable Luminescent Properties. *Chem. Mater.* **2015**, *27*, 5332−5339.
(266) Du, D.-Y.; Qin, J.-S.; Sun, Z.; Yan, L.-K.; O'Keeffe, M.; Su, Z.-M.; Li, S.-L.; Wang, X.-H.; Wang, X.-L.; Lan, Y.-Q. An unprecedented (3,4,24)-connected heteropolyoxozincate organic framework as heterogeneous crystalline Lewis acid catalyst for biodiesel production. *Sci. Rep.* **2013**, *3*, 2616.
(267) Guillerm, V.; Kim, D.; Eubank, J. F.; Luebke, R.; Liu, X.; Adil, K.; Lah, M. S.; Eddaoudi, M. A supermolecular building approach for the design and construction of metal-organic frameworks. *Chem. Soc. Rev.* **2014**, *43*, 6141−6172.
(268) Schoedel, A.; Zaworotko, M. J. $[M_3(\mu_3\text{-}O)(O_2CR)_6]$ and related trigonal prisms: versatile molecular building blocks for crystal engineering of metal-organic material platforms. *Chem. Sci.* **2014**, *5*, 1269−1282.
(269) Zhao, X.; Wang, X.; Wang, S.; Dou, J.; Cui, P.; Chen, Z.; Sun, D.; Wang, X.; Sun, D. Novel Metal−Organic Framework Based on Cubic and Trisoctahedral Supermolecular Building Blocks: Topological Analysis and Photoluminescent Property. *Cryst. Growth Des.* **2012**, *12*, 2736−2739.
(270) Nouar, F.; Eubank, J. F.; Bousquet, T.; Wojtas, L.; Zaworotko, M. J.; Eddaoudi, M. Supermolecular Building Blocks (SBBs) for the Design and Synthesis of Highly Porous Metal-Organic Frameworks. *J. Am. Chem. Soc.* **2008**, *130*, 1833−1835.
(271) Zheng, S.-T.; Wu, T.; Irfanoglu, B.; Zuo, F.; Feng, P.; Bu, X. Multicomponent Self-Assembly of a Nested Co24@Co48 Metal−Organic Polyhedral Framework. *Angew. Chem., Int. Ed.* **2011**, *50*, 8034−8037.
(272) Schoedel, A.; Cairns, A. J.; Belmabkhout, Y.; Wojtas, L.; Mohamed, M.; Zhang, Z.; Proserpio, D. M.; Eddaoudi, M.; Zaworotko, M. J. The asc Trinodal Platform: Two-Step Assembly of Triangular, Tetrahedral, and Trigonal-Prismatic Molecular Building Blocks. *Angew. Chem., Int. Ed.* **2013**, *52*, 2902−2905.
(273) Tu, B.; Pang, Q.; Ning, E.; Yan, W.; Qi, Y.; Wu, D.; Li, Q. Heterogeneity within a Mesoporous Metal−Organic Framework with Three Distinct Metal-Containing Building Units. *J. Am. Chem. Soc.* **2015**, *137*, 13456−13459.
(274) Wong-Foy, A. G.; Lebel, O.; Matzger, A. J. Porous Crystal Derived from a Tricarboxylate Linker with Two Distinct Binding Motifs. *J. Am. Chem. Soc.* **2007**, *129*, 15740−15741.
(275) Stoeck, U.; Senkovska, I.; Bon, V.; Krause, S.; Kaskel, S. Assembly of metal-organic polyhedra into highly porous frameworks for ethene delivery. *Chem. Commun.* **2015**, *51*, 1046−1049.
(276) Catarineu, N. R.; Schoedel, A.; Urban, P.; Morla, M. B.; Trickett, C. A.; Yaghi, O. M. Two Principles of Reticular Chemistry Uncovered in a Metal-Organic Framework of Heterotritopic Linkers and Infinite Secondary Building Units. *J. Am. Chem. Soc.* **2016**, DOI: 10.1021/jacs.6b07267.
(277) Xiao, Q.; Wu, Y.; Li, M.; O'Keeffe, M.; Li, D. A metal-organic framework with rod secondary building unit based on the Boerdijk-Coxeter helix. *Chem. Commun.* **2016**, DOI: 10.1039/C6CC04912E.

NOTE ADDED IN PROOF

Since this review was accepted a paper describing the preparation, structure, and properties of MOF-910 (section 9, Figure 66) has appeared.[276] A paper describing the preparation, structure, and properties of ROD-1 (section 13.1, Figure 83) has also appered.[277]

DOI: 10.1021/acs.chemrev.6b00346
Chem. Rev. XXXX, XXX, XXX−XXX